Developing biocompatible materials with improved angiogenic potential for surgical treatment of stress urinary incontinence and pelvic organ prolapse

By:

Naşide Mangır

A thesis submitted in partial fulfilment of the requirements for the degree of
Doctor of Philosophy

The University of Sheffield
Faculty of Engineering
Department of Materials Science and Engineering

March 2019

Table of Contents

1

Abstract

Stress urinary incontinence (SUI) and pelvic organ prolapse (POP) are two related conditions that significantly impair the quality of life. One in ten women will require primary surgery for SUI and POP. Surgical treatment of both conditions often necessitates the use of a surgical mesh material which is now known to be associated with serious complications in up to 40% of women in long term follow- up. Recently, the use of vaginal mesh products in urogyneacological procedures have been suspended in NHS hospitals in England. There appears to be an unmet and urgent need for better biomaterials to support the pelvic floor which are able to better integrate into tissues at the sites of implantation. The aim of this thesis was to develop a synthetic, degradable material for use in the female pelvic floor that can promote angiogenesis and that can integrate well into tissues.

As a first step, an in vivo assay has been developed and optimized to allow effective screening of constructed biomaterials. Biomaterials were processed with electrospinning of polylactic acid (PLA) which is a commonly used, degradable polymer for soft tissue applications. Electrospun PLA scaffolds were functionalized by incorporation of Vitamin C and Estradiol and were tested for their effects on stimulating new blood vessel formation and extracellular matrix production. As a final step, mesenchymal stem cells (MSCs) were also tested for their ability to promote angiogenesis. The final biomaterials were always tested for suitability of their biomechanical properties for applications in the pelvic floor.

Both Vitamin C and Estradiol could effectively be incorporated into the electrospun PLA scaffolds with desirable ultrastructural and mechanical properties. Vitamin C was released from the scaffolds over several weeks whereas Estradiol was released over months. Both drugs increased the angiogenic potential of scaffolds and extracellular matrix production. Estradiol releasing electrospun PLA scaffolds resulted in the most dramatic increase in new blood vessel formation. Also MSCs had a mild stimulatory effect on angiogenesis. Future work is underway to test the Estradiol releasing scaffolds in relevant animal models.

Presentations and Publications

Publications

Mangir, N; Dikici B; Chapple C; MacNeil, S, "Evaluating polypropylene mesh as a material used in surgical treatment of stress urinary incontinence and pelvic organ prolapse" accepted for publication in Nature Reviews Urology.

Mangir, N; Eke, G; Hasirci N; Chapple C; Hasirci, V; MacNeil, S, "An Estradiol releasing hydrogel to be used as a proangiogenic biomaterial for use as a tissue interposition graft in urogenital reconstruction," accepted for publication Neurourol. Urodyn., 2019.

N. Mangir, S. Roman, C. R. Chapple, and S. MacNeil, "Complications related to use of mesh implants in surgical treatment of stress urinary incontinence and pelvic organ prolapse: infection or inflammation?," World J. Urol., Feb. 2019.

S. Roman, **N. Mangir**, L. Hympanova, C. R. Chapple, J. Deprest, and S. MacNeil, "Use of a simple in vitro fatigue test to assess materials used in the surgical treatment of stress urinary incontinence and pelvic organ prolapse," Neurourol. Urodyn., Sep. 2018.

S. Shafaat, **N. Mangir**, S. R. Regureos, C. R. Chapple, and S. MacNeil, "Demonstration of improved tissue integration and angiogenesis with an elastic, estradiol releasing polyurethane material designed for use in pelvic floor repair," Neurourol. Urodyn., vol. 37, no. 2, 2018.

N. Mangir, C. J. Hillary, C. R. Chapple, and S. MacNeil, "Oestradiol-releasing Biodegradable Mesh Stimulates Collagen Production and Angiogenesis: An Approach to Improving Biomaterial Integration in Pelvic Floor Repair," Eur. Urol. Focus, 2017.

G. Eke, N. **Mangir, N**. Hasirci, S. MacNeil, and V. Hasirci, "Development of a UV crosslinked biodegradable hydrogel containing adipose derived stem cells to promote vascularization for skin wounds and tissue engineering," Biomaterials, vol. 129, 2017.

S. Roman, **N. Mangir**, J. Bissoli, C. R. Chapple, and S. MacNeil, "Biodegradable scaffolds designed to mimic fascia-like properties for the treatment of pelvic organ prolapse and stress urinary incontinence," J. Biomater. Appl., vol. 30, no. 10, pp. 1578–1588, May 2016.

N. Mangır, A. J. Bullock, S. Roman, N. Osman, C. Chapple, and S. MacNeil, "Production of ascorbic acid releasing biomaterials for pelvic floor repair," Acta Biomater., vol. 29, pp. 188–197, Jan. 2016.

Book Chapter

N. Mangir, C. R. Chapple, and S. MacNeil, "Synthetic Materials Used in the Surgical Treatment of Pelvic Organ Prolapse: Problems of Currently Used Material and Designing the Ideal Material". Pelvic Floor Disorders DOI: 10.5772/intechopen.69095 ISBN: 978-1-78923-245-Copyright year: 2018

Presentations

- Oral Presentation_ COST ReST Meeting – Biomaterials, Biomechanics of the Lower Pelvic Floor and Surgical Interventions, Holiday Inn Royal Victoria Hotel, 27- 28 Nov 2016 Sheffield UK "Developing Pelvic Floor Support Materials For Women With Stress Urinary Incontinence & Pelvic Organ Prolapse"

- Invited speaker- EPSRC funded GRCF workshop on Affordable Healthcare in Pakistan - Developing Biomedical Materials for Clinical Impact from 9-13th Jan 2017 Leopold Hotel, Sheffield "Developing Pelvic Floor Support Materials For Women With Stress Urinary Incontinence & Pelvic Organ Prolapse"

- The CUA/EAU International Exchange Programme - Department of Academic Urology Royal Hallamshire Hospital, Sheffield 20 Mar 2017 "Tissue engineering applications in urology"

- Poster Presentation- University of Sheffield, Medical School Research Day 16th June 2017 "An estradiol releasing, proangiogenic mesh can improve biomaterial integration in pelvic floor repair"

- Invited speaker_Society of Urological Surgery, "Take Home Messages_Functional Urology" 5-8 Nov 2016, Antalya, TURKEY

- Invited speaker_ Turkish Continence Society, 5th Congress on Functional and Female Urology, 5- 8th Oct 2017 Antalya "Applications of Tissue Engineering in Reconstructive Urology"

- Invited speaker_ Turkish Continence Society, 5th Congress on Functional and Female Urology, 5- 8th Oct 2017 Antalya "Take Home Messages_ Overactive Bladder"

Acknowledgements

This thesis represents a significant transformation in my academic development. During the five years I have spent in the Engineering Faculty I have worked with brilliant bioengineers, cell biologists, chemical and materials engineers which has given me a completely different perspective and a new approach to clinical problems. I am grateful to everyone who has been a part of this multidisciplinary environment.

A number of key people have made this possible for me. First and foremost, I would like express my most sincere gratitude to Prof Sheila MacNeil and Prof Christopher Chapple for establishing, leading and maintaining this research group over years despite all odds. If I had not seen their dedication and determination, I would not be able to survive to the end of this thesis.

I would also like to thank Dr Frederik Claeyssens for accepting to be my supervisor and for all his support during my studies.

I am grateful to all my friends and colleagues at the Kroto Research Institute for their help and assistance. In particular, I would like to thank Dr. Anthony Bullock, Dr. Sabiniano Roman, Dr. Ahtasham Raza, Dr. Giulia Gigliobianco, Dr. Gözde Eke, Dr. Julio Bissoli and Dr Christopher Hillary.

I would also like to extend my appreciation to my examiners Dr Gwendolen Reilly and Dr Vanessa Hearnden for all their useful feedback and guidance during my first and second year reporting. Additionally, I would like express my gratitude to Prof Alicia El- Haj and Mr Dan Wood for acting as my PhD viva examiners. It was a true pleasure to discuss my work with them.

I must also acknowledge the continuous support of Prof Levent Türkeri back home in İstanbul who has always inspired me as a gifted surgeon, an excellent clinician and a very good scientist.

Finally, I would like to thank The Urology Foundation and the Rosetrees trust for their generous financial support during my PhD studies.

Abbreviations

A2P	Ascorbate-2- Phosphate	**EDTA**	Ethylene Diaminetetraacetic Acid
AA	Ascorbic Acid	**FBR**	Foreign Body Response
ADSC	Adipose Derived Stem Cells	**FCS**	Foetal Calf Serum
AFS	Autologous Fascia Sling	**FDA**	Food And Drug Administration
ATFP	Arcus Tendineus Fascia Pelvis	**FGF**	Fibroblast Growth Factor
ATMP	Advanced Therapy Medicinal Product	**FITC**	Fluorescein Isothiocyanate
BMI	Body Mass Index	**GelMA**	Methacrylated Gelatin
CAM	Chorioallantoic Membrane	**H&E**	Haematoxylin And Eosin
CI	Confidence Interval	**HA**	Hyaluronic Acid
cmH$_2$O	Centimeters Water	**HAMA**	Methacrylated Hyaluronic Acid
DAPI	4′,6-Diamidino-2-Phenylindole Dihydrochloride	**HDF**	Human Dermal Fibroblasts
DCM	Dichloromethane	**IMS**	Industrial Methylated Spirits
DMEM	Dulbecco's Modified Eagles Medium	**ISD**	Intrinsic Sphincter Deficiency
DNA	Deoxyribonucleic Acid	**LCA**	Lens Cullinaris Agglutinine
DOA	Detrusor Overactivity	**LM**	Levator Muscles
E2	17-β-Estradiol	**MHRA**	Medicines And Healthcare Regulatory Agency
ECM	Extracellular Matrix	**MMP**	Metalloproteinases

EDD	Embryonic Development Day	**PU**	Polyurethane
MRI	Magnetic Resonance Imaging	**PUL**	Pubourethral Ligament
MSC	Mesenchymal Stem Cell	**PVS**	Pubovaginal Sling
MUI	Mixed Urinary Incontinence	**QoL**	Quality Of Life
MUS	Midurethral Sling	**SD**	Standard Deviation
N	Newtons	**SEM**	Scanning Electron Microscopy
NHS	National Health Service	**SIS**	Small Intestine Submucosa
Pa	Pascals	**SMA**	Smooth Muscle Actin
PBS	Phosphate Buffered Saline	**SUI**	Stress Urinary Incontinence
PCL	Polycaprolactone	**UI**	Urinary Incontinence
PCM	Pubococcygeus Muscles	**UK**	United Kingdom
PFMT	Pelvic Floor Muscle Repair	**USA**	United States Of America
PGA	Polyglycolic Acid	**UTS**	Ultimate Tensile Strength
PLA	Polylactic Acid	**UV**	Ultraviolet
PLGA	Polylactic-Co-Glycolic Acid	**VEGF**	Vascular Endothelial Growth Factor
PLLA	Poly- L-Lactic Acid	**YM**	Young's Modulus
POP	Pelvic Organ Prolapse	**2D**	Two Dimension
PPL	Polyproylene	**3D**	Three Dimension

List of Figures

List of Tables

Chapter 1. Introduction

Mangir, N; Dikici B; Chapple C; MacNeil, S, "Evaluating polypropylene mesh as a material used in surgical treatment of stress urinary incontinence and pelvic organ prolapse" accepted for publication in *Nature Reviews Urology*.

Mangir, N; Chapple C; MacNeil, S. Synthetic Materials Used in the Surgical Treatment of Pelvic Organ Prolapse: Problems of Currently Used Material and Designing the Ideal Material. Pelvic Floor Disorders DOI: 10.5772/intechopen.69095 ISBN: 978-1-78923-245- Copyright year: 2018

1.1 Stress Urinary Incontinence (SUI) and Pelvic Organ Prolapse (POP) in Women

1.1.1. Definitions

Stress urinary incontinence (SUI) is defined as a symptom as "the complaint of involuntary loss of urine on effort or physical exertion (e.g. sporting activities), or on sneezing or coughing" [1]. Synonymously SUI also refers to an objective indication of a disease or a health problem when it is used as a sign defined as 'observation of involuntary leakage from the urethra synchronous with effort or physical exertion or on sneezing or coughing'.

The POP is "the descent of one or more of the anterior vaginal wall, posterior vaginal wall, the uterus (cervix) or the apex of the vagina (vaginal vault or cuff scar after hysterectomy). The presence of any such sign should be correlated with relevant POP symptoms. Most commonly this correlation would occur at the level of the hymen or beyond" [1].

1.1.2. Prevalance

The prevalence of SUI in the population is studied in several large scale epidemiological studies. In a population based prevalence study involving women from four European countries and Canada, the overall prevalence of SUI was reported to be 6.4% (95% Confidence interval 5.9- 6.9). The prevalence increased with age from 0.1% in women aged <39 years old to 8% in women aged >60 years old [2]. In another large cross- sectional study conducted in USA, Sweden and UK 31.8% of the women had SUI symptoms 'at least sometimes' and 14.8% had SUI 'at least often' [3]. One of the largest population based evaluation of lower urinary tract symptoms to date was conducted in China, reporting a 18.9% prevalance of SUI in women >20 years old [4]. Worldwide a total of nearly 153 million women were predicted to have SUI by 2018, representing a 20% increase from 2008 to 2018 [5]. The variability in the prevalence rates of SUI can be due to the definition of SUI used, the population studied and the methodologies used in the studies (e.g. design and conduct of questionnaires).

Similarly the prevalence of POP increases with increasing age. In the UK, prolapse symptoms were reported by 8.4% of women in the community [6]. In the large, prospective (n=161 861) Women' s Health Initiative study conducted in 40 centres in the USA 41.1% of women with a uterus and 38% of women without a uterus had some form of POP on physical examination, respectively. The vast majority of these were cystoceles followed by uterine prolapse and rectocele [7].

1.1.3. Impact

SUI has a significant impact on the indivual patients suffering from the condition, family members and the health care systems. UI also poses a great economic burden for health care systems. In USA over 13 billion USD were spent in 1995 on treatment of SUI [8]. These costs include costs of diagnosis and treatment, however many patients find themselves in a position to pay for extra amounts for routine care of incontinence (primary care visits and towels/ pads) because healthcare providers often impose limits on the maximum number pads etc. In the UK the cost of SUI to the NHS is estimated to be £117M per year [9].

Urinary incontinence has significant impact on physical, psychological and social well- being of women. Regardless of the methodology used to measure patients with urinary incontinence consistently have lower quality of life scores when compared to continent women [10]. The type of UI effects the health related quality of life differently. Patients with urgency UI and mixed UI have significantly worse health related quality of life scores compared to patients with SUI [11]. Additionally depression, anxiety and stress levels are known to increase with increased severity of UI [12].

Despite its negative impact on the quality of life of women, less then 25% of women seek help for their UI [13]. In a population based cross- sectional study performed in Staffordshire, UK, only 17% of women sought professional help for their incontinence. UI is often quoted as a stigmatized condition however the relationship between help seeking behaviour and stigma associated with UI is not well studied.

POP can also effect a women' s quality of life, psychosocial and sexual well being. Validated disease specific questionnaires have been developed and used mainly to assess the effects of various treatments on the QoL of women with POP. A few studies have demonstrated an impairment of quality of life in women living with POP [14]. Although the relationship between POP and health related quality of life is not well studied, POP has been shown to have profound effects on the body image of women. Women with POP reported feelings of being 'less feminine', 'self-conscious' and 'isolated' [15]. As the perceived body image gets worse both the disease specific and the generalized quality of life decreases [16].

1.1.4. Risk factors

Childbirth (obstetric) injury is believed to be the principle factor causing pelvic floor disorders in female. Although epidemiological evidence shows a clear relationship between childbirth and pelvic floor disorders [7] the exact mechanisms of such an injury leading to POP is not yet known. The mechanisms investigated constitute direct injury to the nerves, muscles and connective tissues. The severity of the injury may vary between compression, stretching or tearing. The ability of the tissue remodelling after the injury and co- existing morbidities all decide the final outcome.

The levator ani muscle complex, particularly the pubococygeal muscle, is known to be injured during vaginal delivery in 20% of women [17] being more common in forceps assisted vaginal delivery [18]. Also levator defects were present in 55% of women seeking treatment for POP as opposed to 16% of controls. Therefore, although the long term effects of a levator injury during childbirth on development of POP is not completely elucidated in long term follow up studies, it is likely to be one of the contributing factors.

Injury to the nerves innervating the pelvic floor muscles, particularly the pudental nerve that arises from the S2- S4 nerve roots during childbirth has also been suggested as a mechanism resulting in injury to pelvic floor muscles. Neurophysiologic studies demonstrated significantly prolonged pudental nerve terminal motor latency and reduced anal pressure on voluntary contraction 2-3 days after vaginal delivery. Repeat measurements in the same patients 2 months after vaginal delivery showed shorter pudental nerve motor latency times suggesting a denervation injury of the pudental nerve after vaginal delivery with a subsequent reinnervation [19]. Also electromyographic studies demonstrated that in women with SUI and POP denervation of pubococcygeus muscle was significantly more compared to normal women [20].   The risk of pudental nerve denervation was found to be higher in difficult vaginal deliveries such as forceps deliveries, high birth weight and prolonged second stage of labour.

During and after pregnancy there is extensive connective tissue remodelling in the pelvic floor. The synthesis and degradation of main components of the extracellular matrix, mainly collagen and elastin, are changed and the connective tissue is remodelled. Defects in these biochemical processes are proposed as a mechanism for development of POP and SUI. The changes in connective tissues of women with SUI and POP are reviewed elsewhere and include: increased collagen turnover, decreased elastin synthesis and differential expression of candidate genes involved in structural proteins [21].

1.2. The pelvic floor support

1.2.1. Anatomical basis of pelvic floor support

Pelvic organs in women are kept in place by ligaments and other connective tissue components at three levels in the pelvis (Figure 1.1). Level I is formed by the cardinal and uterosacral ligaments providing apical support. The cardinal ligaments attach uterus and upper vagina to the pelvic side walls whereas uterosacral ligaments attach it to the sacral bone. Both ligaments are composed of thick and strong collagenous fibres extending vertically and posteriorly towards the sacrum indicating a function that does not necessarily involve flexibility but strength mostly in the vertical direction. Level II support comprises of fascia and connective tissues attaching the lateral walls of the vagina to the arcus tendinous fascia pelvis which supports the mid- vagina laterally. Biomechanically level II support structures are less fibrous than level I. Level III urogenital diaphragm and perineal body supporting lower part of the vagina and urethra [22].

The pelvic floor is the hammock- like structure made up of skeletal and smooth muscles surrounded by connective tissues and attached to pelvic bones. Its' main function is to counteract the forces generated by gravity and intra- abdominal pressure.

Figure 1.1. The three levels forming the female pelvic floor support (*Reproduced with permission from DeLancey, John OL. "Anatomie aspects of vaginal eversion after hysterectomy." American Journal of Obstetrics & Gynecology 166.6 (1992): 1717-1728.*)
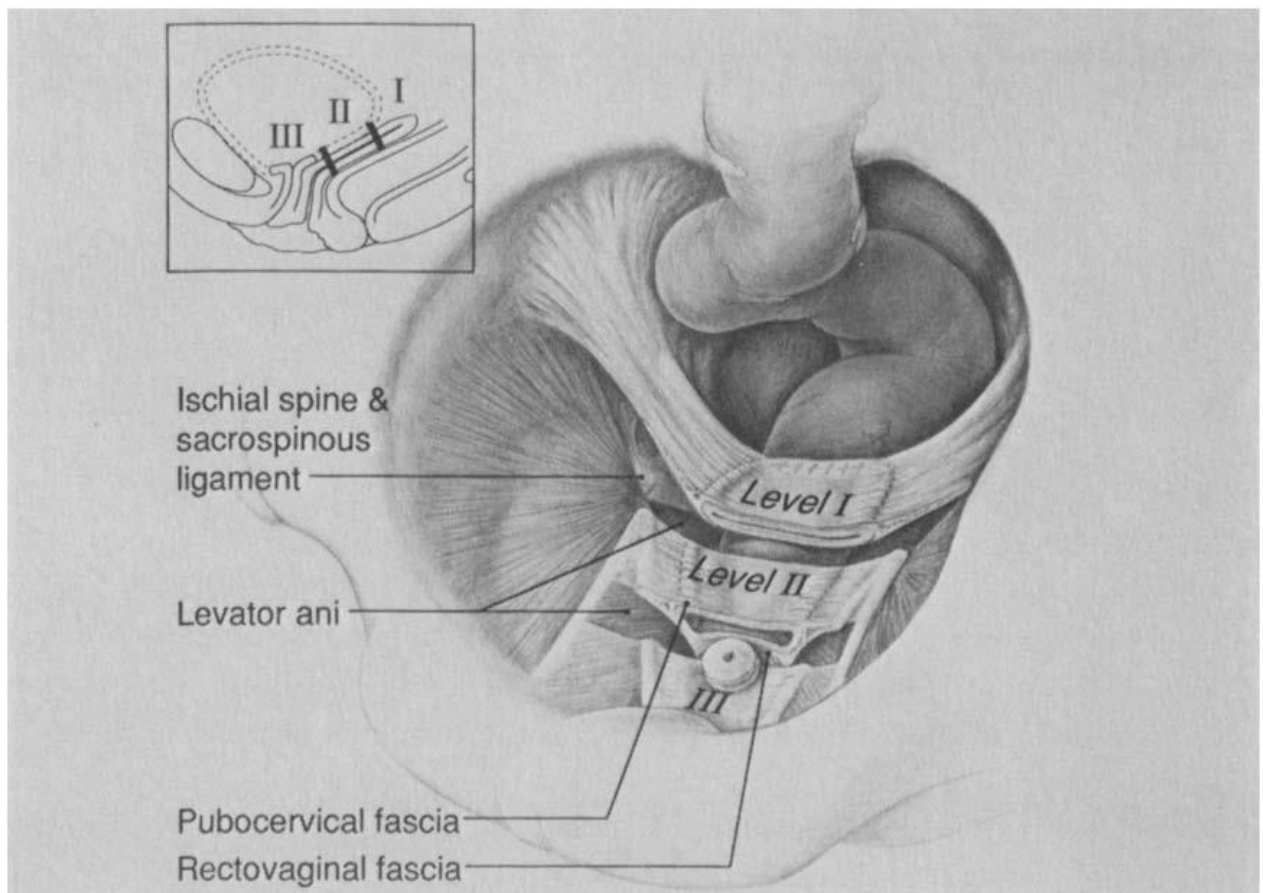
1.2.2. Biomechanical basis of pelvic floor support

Biomechanics is an interdisciplinary area that applies the principles of engineering and the methods of mechanics to biological systems. Mechanics is concerned with the description of motion and how forces create motion [23]. Biomechanics help us understand how the forces acting on structural elements of our bodies create motion that leads to normal development and functioning or to damage tissues in cases where there is an overload. When studying bioengineering of the pelvic floor, the biological constitution in relation to the mechanical forces acting on it needs to be considered and materials used in pelvic floor reconstruction needs to have defined characteristics of material deformation and load bearing as well as how it contributes to tissue remodelling once it is implanted in to the body. It is important that clinicians/ surgeons have a basic understanding of biomechanical principles so that they can define the biomechanics of the tissue to be replaced and select the best material to meet the specific needs.

The available knowledge on the biomechanical properties of the female pelvic floor mainly comes from mechanical testing of samples from the pelvic floor from human and animal samples. The availability of human samples for mechanical testing is limited due to challenges and ethical concerns related to obtaining large tissue samples. Therefore, in humans biopsy samples or cadaveric tissues are used to define the biomechanical features of the pelvic floor muscles and fascia [24]. Another method was to study whole pelvic floor samples of animals that contain all the muscles and the connective tissues of the pelvic floor (e.g. 'vaginal supportive tissue complex'). Such samples obtained from rats demonstrated that the ultimate failure in the testing protocol was due to a failure of paravaginal attachments [25]. Samples that only contain the connective tissues (e.g. fascia) have also been tested [26]. Disruption in the fascial structures is thought to be the main mechanism by which pelvic organ prolapse occurs [25].

Another factor limiting our ability to have robust definitions of mechanical properties of pelvic floor structures is the lack of standardized mechanical testing protocols for biological tissue samples. To obtain reproducible results when mechanically testing biological samples their unique organization, composition and *in vivo* functions need to be adapted to the mechanical testing protocols. Currently mechanical testing of samples from animal or human pelvic floor can mainly be tested by uniaxial and biaxial tensile testing. In uniaxial testing, the tissue to be tested is placed between two clamps (clamp-to-clamp testing) and a load is applied to the sample in one direction while observing the sample for elongation/ strain. Uniaxial testing is most commonly performed in these studies and it gives more reproducible results.

Biaxial testing has the advantage of allowing a more reflective measurement of the *in vivo* loading conditions by applying force from several different directions, not one single direction. However biaxial testing is more complex giving highly variable results [27]. In addition to this, the preconditioning of the biological samples to be tested, the temperature and the level of hydration of the tissues can also potentially affect the test results. With these limitations, the mechanical characteristics of healthy vaginal tissue in women have been measured to be as follows: the ultimate tensile strength 0.79±0.05 MPa, maximum elongation 1.68±0.11 mm and elastic modulus 6.65±1.48 MPa [28].

From a biomechanical point of view, the pelvic floor is a complex structure composed of active and passive soft tissue components attached to the pelvic bones (Figure 1.2). Passive components of the pelvic floor cannot by themselves generate any force however they can resist force when applied to them. These are all together called the pelvic floor connective tissues including the fascia. The active components of the pelvic floor are able to independently generate force which are mainly the muscular structures such as the levator ani muscles and the sphincteric muscles [29]. Muscular structures are mainly striated muscles and smooth muscles. Striated muscles of the pelvic floor (levator ani complex, coccygeus muscle, external urethral sphincters and external anal sphincters) have a major contribution to the biomechanical properties and they play a role in voluntary control of urinary and anal continence. The smooth muscles (the smooth muscles in the vaginal wall and internal urethral and anal sphincters) are essential in maintenance of continence.

Figure 1.2. The main normal support structures forming the female pelvic floor. The sections go from surface to deep down in the pelvic cavity as you go from section 1 to 4. The uterus, bladder and rectum are removed when necessary for demonstration purposes.
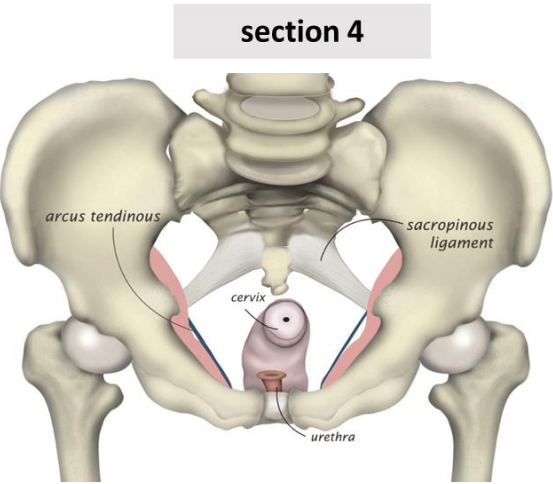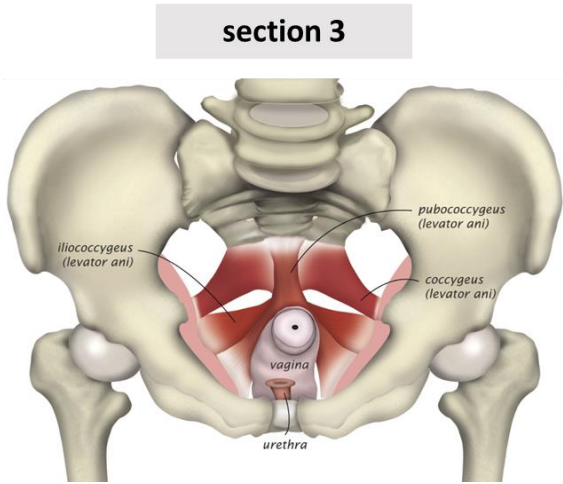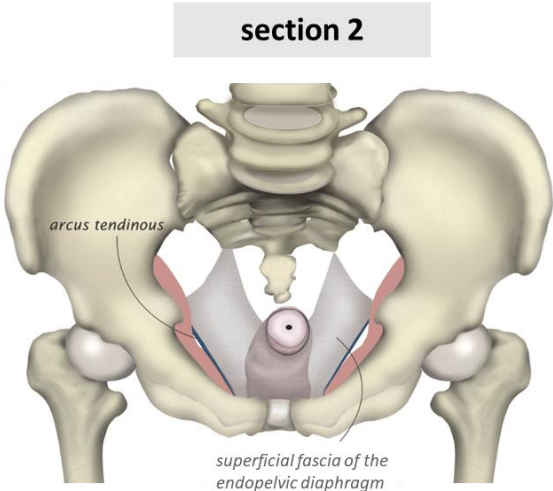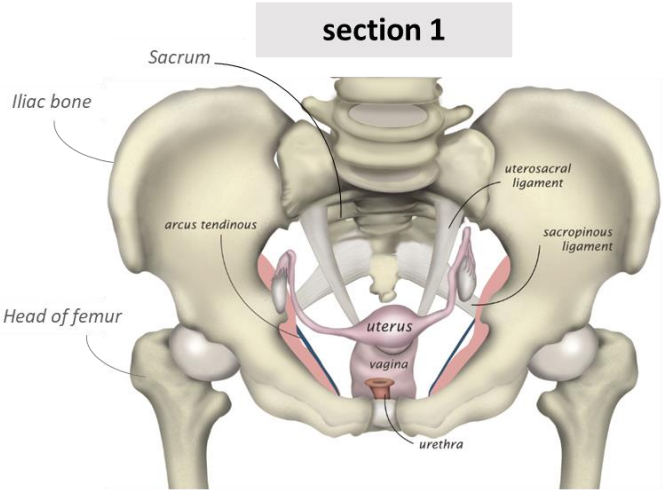
The connective tissues of the pelvic floor are an interconnected network of supportive tissues including the ligaments, endopelvic fascia and the perineal membrane. They are composed of different combinations of extracellular matrix proteins, mainly collagen, elastin and smooth muscle, together with blood vessels and nerves. Collagen generally exists in the fibrillar form which appears as bundles in cross sectional images. The collagen fibre alignment of the fascia is known to directly influence the mechanical properties, with the more aligned the fibres towards a particular direction the stiffer the fascia is in that direction (the lower the elasticity/ the less distensible) [30]. Another ECM protein is elastin which is an important element in those tissues and organs which exhibit resistance and recoil properties. Elastin gives elasticity to the structures meaning the structure is stretched when the force is applied and recoil occurs when the force is removed. Abnormalities in the homeostasis of the ECM tissues of the pelvic floor and their inability to maintain pelvic floor support have been implied in the pathogenesis of pelvic floor diseases [31], [32].

When defining the biomechanical properties of the pelvic floor it is important to make the measurements on specific groups of patients, such as postmenopausal women or women with birth trauma. Estimations of the *in vivo* situation in healthy and diseased subjects has been made using computer based modelling methods [29]. Computational models of the pelvic floor have the potential to reliably define the normal biomechanical behaviour in the female pelvic floor and can predict the mechanisms leading to damage to pelvic floor structures (e.g. birth trauma) and pelvic floor disorders. Anatomical, mechanical and biochemical data pertinent to pelvic floor muscles and soft tissues are combined mathematically to create computational models. Anatomical models demonstrating detailed 3D anatomy of the pelvic floor can now be reliably produced thanks to magnetic resonance imaging [33]. The remaining considerable challenge seems to be how to integrate the functionality of the muscles and other soft tissues into these models. The hope they offer is that once an accurate biomechanical model is created, population based data can be applied to these models before they are used clinically to predict individual patient/ disease outcomes.

1.3. The mechanisms underlying the development of SUI and POP

Both SUI and POP are thought to result from anatomical and/ or functional defects in the pelvic floor support structures. The anatomical and functional basis of SUI has been more fully investigated than POP.

1.3.1. SUI

The mechanisms of female continence are not completely elucidated. It is probably multifactorial and complex involving a coordinated functioning of the central and peripheral nervous systems, bladder, urethra and the pelvic floor. Urinary incontinence is a problem of the storage phase of the voiding cycle and mechanically it occurs when the pressure in the bladder, intravesical pressure, overcomes the urethral resistance. During normal bladder filling the intravesical pressure remains low despite increasing volumes of urine collected inside the bladder. This is due to the viscoelastic properties of the bladder wall (the smooth muscle and the connective tissues) called bladder compliance. At the same time spinal reflex pathways neurologically inhibit bladder smooth muscle contraction. As a result urine is stored inside the bladder at low pressures. Abnormalities in bladder wall, smooth muscle or innervation can lead to detrusor overactivity incontinence. In case of stress UI intravesical pressure exceeds that of the outflow pressure when a patient coughs, laughs or strains increasing the intravesical pressure. This is thought to be due to a decrease in normal urethral resistance.

SUI started being systematically evaluated after 1961 when Green devised a classification system for SUI based on the radiographic appearance of the bladder neck and urethra. He identified two types of SUI: type 1 with a loss of posterior urethro- vesical angle and type 2 with a rotational descent of the urethra. With the use of urodynamic studies, which at the time were reserved to diagnose neurogenic incontinence, McGuire added a type 3 SUI where a low urethral closure pressure and open bladder neck led to SUI. Type 3 SUI is also named as intrinsic sphincter deficiency. With the addition of urodynamic stuies, SUI started to being seen as a functional event rather than purely an anatomical defect. The treatment decisions also started to be made based on this classification. Types 1 and 2 would be good candidates for a retropubic urethropexy procedures which restore the retropubic position of the urethra whereas type 3 SUI would best be treated with an autologous fascia sling surgery as many patients would have undergone an unsuccessful retropubic urethropexy procedure.

Urethral support and urethral hypermobility

The female urethra has an important role in continence. The urethral mucosa and submucoca, urethral smooth muscle and periurethral striated muscles all contribute to the generation of urethral resistance.

Historically, SUI was first thought to result from a structural defect in the urethral support structures. The female urethra rests on the anterior vaginal wall which constitutes the majority of its structural support. Initial theories on the pathophysiology of female SUI emphasized that a loss of the retropubic position of the bladder neck and the urethra would lead to SUI. Enhorning' s theory of 'pressure transmission' stated that the maintanence of the retropubic position of the urethra during states of increased intraabdominal pressure would lead to transmission of the abdominal pressure on to the urethra facilitating urethral compression when straining. This theory was confirmed by the success of operations aiming to restore a retropubic position of the urethra (retropubic urethrapexy operations).

Intrinsic Sphincter deficiency

The intrinsic urethral sphincter is formed by the circularly oriented outer fibers of the urethral smooth muscle and the detrusor muscle in the bladder base. The intrinsic sphinter mechanism contributes to the formation of urethral resistance at rest. Clinically ISD defines a clinical condition where the female urethra cannot maintain a watertight seal even at rest. This could be a result of laxity in the ISD mechanism or the urethral wall itself can be rigid, fixed or scarred. The causes of ISD can be multifactorial involving neurologic, muscular and connective tissue dysfunction.   ISD can also be demonstrated urodynamically with lower urethral closure pressures (<20 cmH$_2$O) and lower vesical leak point pressures (<60 cmH$_2$O).

 Although the dichotomy of urethral hypermobility and ISD is still used and constitutes a useful framework when starting to evaluate SUI, recently more modern theories have provided unified concepts in understanding the pathophysiology of SUI. Two important theories form the basis of the modern understanding of SUI. The 'integral theory' suggested that urethral closure occurs by the synergistic action of three components of the pelvic floor. In the presence of sufficient tension in the pubourethral ligament (PUL), increases in intraabdominal pressure lead to contraction of the pubococcygeus muscles (PCM) anteriorly and the levator muscles (LM) posteriorly closing the bladder outlet [34]. Overall it is the laxity in the anterior vaginal wall that causes SUI. Modern synthetic mid- urethral sling surgeries use this principle stating that the placement of the surgical mesh in the position of PUL form a backboard against which the urethra can be compressed [35]. This theory takes into account structural elements of the urethral support structures as they are dynamically acting to maintain continence.

Similarly the 'hammock hypothesis' (Figure 1.3) proposed that the bladder neck and urethra normally rest on a hammock of musculofascial structures that enables compression of the urethra in cases of increased intraabdominal pressures maintaining the continence [36]. The main problem proposed by this model is the structural weakness of the hammock rather than the hypermobility of the urethra.

All these theories on the pathophysiology of SUI can be seen to have developed together with surgical techniques trying to understand how each technique worked. As a result, the surgical treatments evolved from urethral compression to restoration of the urethra back to its retropubic position and to creating a hammock-like structure where the urethra can be compressed when intraabdominal pressure increases. Additionally, over the years the focus has shifted from the bladder neck to the mid- urethra.

Figure 1.3. Illustration explaining the hammock hypothesis (DeLancey, John O.L. Structural support of the urethra as it relates to stress urinary incontinence: The hammock hypothesis. American Journal of Obstetrics & Gynecology , Volume 170 , Issue 6 , 1713 - 1723)
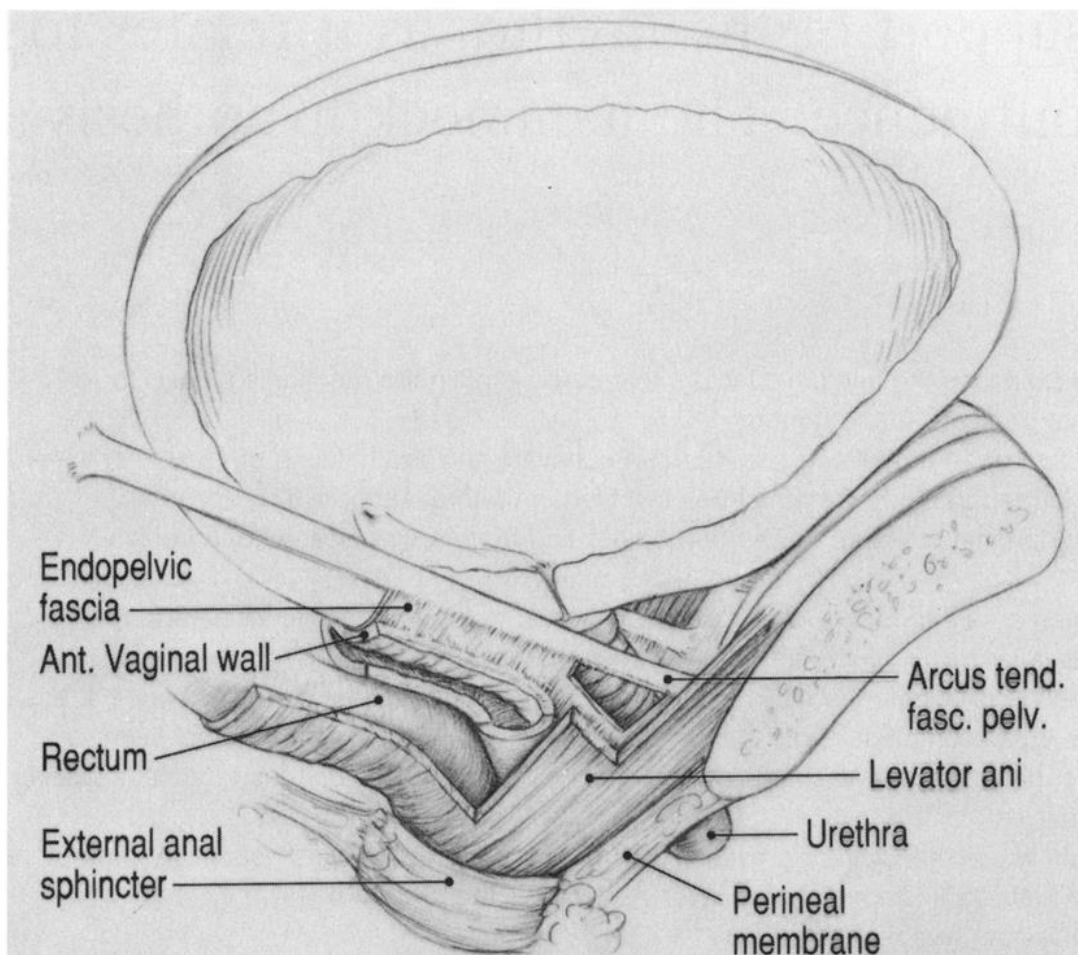
1.3.2. POP

In contrast to SUI, POP has mainly been studied as a structural disease. It is likely that there is a functional component because there appears to be major differences in patient defined and physician defined treatment outcomes in POP. Current surgical treatments for POP are based on identification and repair of anatomical defects that broadly occur at three levels in the pelvis. Level I cardinal- uterosacral ligaments providing apical support, level II arcus tendinous fascia pelvis supporting middle part of vagina laterally and level III urogenital diaphragm and perineal body supporting lower part of the vagina [22]. This anatomical description provides the basis of pelvic floor support structures that guides the reconstructive surgeon. After the level of the defect is identified it can be repaired by either an abdominal or a vaginal approach.

1.4. Treatment of SUI and POP

1.4.1. Non- surgical treatment of SUI

Traditionally non- surgical therapies are tried as a first line treatment for management of SUI as they usually are associated with least harm to the patient. The main conservative treatment option for women with SUI is pelvic floor muscle training (PFMT). Pelvic floor muscle training was first introduced by a gyneacologist, Arnold Kegel, in 1940s. He proposed that women with SUI showed evidence of weakness in the muscles surrounding the bladder neck and vagina [37]. PFMT improves SUI by strengthening the pelvic floor and improving urethral stabiliy. PFMT is not only used in the treatment of SUI but also to prevent SUI in childbearing women or in men before undergoing radical prostatectomy.

There is roboust clinical evidence to support the use of PFMT in women with SUI as a first line treatment to improve urinary incontinence and quality of life in women with SUI [38]. However there is high variability in the administration of PFMT to women. Supervised treatment regimes in the form of physiotherapy and schedules with different intensities have been used with greater benefit compared to purely self- motivated exercises done by the patient. The main limitation of PFMT is the difficulty in maintaining the initial short term benefits in the longer term follow up. It has been reported in a 15 year follow up study that long- term adherence to treatment with PFMT was poor and half of patients eventually went for a surgical treatment [39].

1.4.2. Surgical treatment of SUI

The estimated life- time risk of surgery for either SUI or POP in women was found to be 20% by the age of 80 [40]. Surgical treatment for SUI also reduces the money spent on the use of protective pads and towels from £3.84 to £1.36 per month [41].

The surgical treatment of SUI started developing in the early 20th century on three main lines. Firstly, SUI was thought to be a result of the loss of the normal retropubic position of the urethra. Hence surgical techniques aimed at repositioning the urethra back to its high retropubic position. Marshall- Marchetti- Krantz and Burch colposuspension operations where the urethra is secured and fixed in the retropubic area are based on this principle [42]. The invention and widespread clinical and surgical use of camera systems to look inside the viscus organs allowed cystoscopic assessment of bladder and urethra. This led to recognition of the internal urethral sphincter mechanism in the development of SUI. Vaginal plication operations such as the Kelly plication procedure, were described to strengthen the urethral sphincter [43]. Thirdly, the widespread use of urodynamic studies resulted in the definition of intrinsic sphincter deficiency which paved the way for the 'pubovaginal sling' operations.

The modern autologous fascia sling (AFS) surgeries as described by McGuire [44] and the integral theory for female SUI formed the basis for the modern synthetic mesh sling surgeries. The placement of the surgical mesh in the position of PUL in a tension free manner would induce fibrosis and form a collagenous 'neoligament' to replace the PUL forming a backboard where the urethra can be compressed [35]. Additionally, the integral theory stated that the placement of the fascia sling to the bladder neck was responsible for occurrence of storage symptoms after AFS surgeries. Therefore, Ulmsten when defining the synthetic sling surgeries suggested an alternative site for placement of the sling, the mid- urethra. The laxity of PUL was demonstrated by urodynamic (urethral pressure profile) studies identifying the mid- urethra as the most critical location to place the mesh. Importantly, the mid- urethra concept was validated by pre and post- operative urethral pressure measurements demonstrating improvement in urethral closure pressures after the mid- urethral sling surgeries.

1.4.3. Surgical treatment of POP

Historically the treatment of POP relied on pessaries until the 19th century. Advancements in the surgical sciences with widespread use of anaesthesia, new suture materials and antibiotics led to POP started to being treated surgically. Vaginal hysterectomy was first performed to treat uterine prolapse in 1861 by Samual Choppin. Also obliterative procedures that are still being used today for selected cases, such as Le Fort' s operation (colpocleisis) was also described in second half of the 19th century [45].

Modern surgical treatments of POP can be grouped as anterior compartment repairs, apical repairs and posterior compartment repairs all of which are based on identification and repair of anatomical defects. These repairs can be native tissue repairs or augmented repairs where biological or synthetic soft tissue support prostheses are used to reinforce the repairs. Additionally, the repairs can be performed via a vaginal route (transvaginally) or an abdominal route (transabdominally).

Anterior compartment repairs involve prolapse of bladder and/ or urethra. The two most commonly performed operations for anterior compartment repair are anterior colporrhaphy (mostly performed transvaginally) for midline defects and paravaginal repair procedures (mostly performed transabdominally) for lateral defects. In both procedures the defective pelvic fascia is repaired and sutured to stronger adjacent fascia. Nevertheless, the recurrence rates in anterior compartment repair are high which necessitate augmentation of the repair site. The first prosthetic material used to augment an anterior colporrhaphy procedure was performed in the mid-20th century to prevent recurrence of prolapse [46].

Apical compartment repairs when performed transabdominally involve sacrocolpo(hystero)pexy operations. Transvaginal approach to fix the vaginal vault to stronger ligaments in the pelvic floor are also used involving uterosacral ligament suspension, sacrospinous ligament suspension and illiococcygeus fixation. The posterior vaginal wall prolapse involves rectoceles which is mainly treated by posterior colporrhaphy procedures. Posterior colporrhaphy is when the rectovaginal fascia is plicated in the midline.

1.5. Biomaterials used in surgical treatment of SUI and POP

1.5.1.Biological materials

The first biological graft used in 1907 to treat SUI was the autologous gracilis muscle [42]. This was followed by use of the pyrimidalis muscle which is a triangular shaped muscle attaching to the pubic symphyses ineriorly and the superior margins attach to the linea alba. The use of pyrimidalis muscle allowed harvesting the muscle flap through the same incision avoiding another incision on the inner thigh (to harvest the gracilis muscle). Muscle flaps were taken down and tied together around the bladder neck forming the basis of the first sling surgeries. Later on not the muscle but rectus fascia alone started to be used as a sling material. The advantage of using fascia alone was that the fascia being an avascular and thin structure could be used as a graft rather than a flap making it easier to transpose from one part of the body to another. Another source of autologous fascia was the fascia lata (fascia of the thigh muscles).

Despite improvements and refinements made to the surgical technique, autologous fascia sling procedures were still associated with significant donor site morbidity. An alternative to autologous fascia grafts was obtaining fascia from allogeneic (cadaveric fascia lata, cadaveric de- cellularized dermis) or xenogeneic sources (porcine sources of de-cellularized extracellular matrix such as dermis and small intestinal submucosa). Allogeneic and xenogeneic sources of ECM can be transplanted after de-cellularization without a significant immune response to them. This is due to the conservation of ECM components (such as fibrillar collagen and collagen IV) during evolution from the early metazoan ancestor (early multicellular organisms) to human [47].

The surgical outcomes of using allogeneic or xenogeneic ECM products in soft tissue reconstruction have been reported to be variable due to differences in the source materials and processing methods for decellularization and sterilization. For treatment of SUI, biological sling materials have been compared with synthetic slings in 12 clinical trials, the meta-analysis of which demonstrated equal efficacy in the short term with shorter operative times, less perioperative complications and some evidence of less voiding dysfunction with the use of synthetic materials [48]. Additionally on comparison of different biological slings (porcine dermis, lyophilised dura mater, fascia lata, vaginal wall, autologous dermis and rectus fascia) autologous rectus fascia was found to be associated with better participant reported improvement rates within the first year over other biological materials.

In the case of pelvic organ prolapse repair, a meta- analysis comparing biological grafts with native tissue repairs showed no evidence of a benefit with regards to awareness of prolapse 1-3 years after surgery and prevention in recurrence of the prolapse in women treated with biological grafts [49]. Therefore prolapse repair with biological grafts is not any better than repair using native tissue repairs. The use of synthetic materials was proposed to reduce recurrence rates of vaginal POP repair procedures however this is now questioned. In a recent randomized controlled trial in the UK, the PROSPECT study, women were randomly allocated to vaginal prolapse repair with mesh versus biological graft. In one year follow up neither mesh nor the biological graft improved clinical outcomes for patients compared to native tissue repairs [50]. Also to be considered is the important potential risk of transmission of viral (e.g. Human immunodeficiency virus) and prion diseases and more commonly Hepatitis B and C with allografts. All can be reduced by the use of strict tissue banking protocols.

1.5.2. Synthetic materials

The flow of events show that a prosthetic material would first be used in hernia repair and then be transferred to the pelvic floor. The first metallic prosthesis used to treat SUI was a 'tantalum' plate implanted transvaginally, on top of Kelly plication sutures, to induce a fibrotic reaction [51]. The main idea here was to form a fixed plane at the posterior part of the proximal urethra. No significant adverse events were reported in 8 months follow up. Tantalum mesh was then inserted transvaginally to treat cystocele [46]. The logic behind was explained by the authors as follows: 'although there are numerous recognized procedures for the correction of cystoceles, there is still a significant rate of recurrence; therefore, a trial use of tantalum mesh was considered justifiable'. In four of 10 patients exposure of the tantalum mesh was reported.

Following the advancements in materials science and its application in hernia surgery, the first synthetic sling material, a 'gauze hammock' made of polyethylene ((Mersilene®) mesh), was used to treat SUI in 1968 [52]. Moir placed the Mersilene mesh hammock to the bladder neck and proximal urethra in a tensionless manner and secured the edges of the mesh to the rectus fascia. He reported more than 80% success rate in 71 patients at up to 5 years follow up. Although no long term follow up data was ever presented tissue damage with dense scarring was reported. A few years later, polyethylene was further improved and PPL (Marlex®) mesh [53], considered inert and resistant to infection, was used to treat SUI in a modified gauze hammock operation where mesh is placed to the bladder neck and attached to the Cooper's ligament. With most patients followed up for 5 years they reported 5% erosion rate [54].

The plastic mesh sling surgeries started to be widely performed only after Ulmsten and Petros described the Integral theory of SUI and performed the first intravaginal mesh- sling surgery in 1995. Transvaginal POP meshes gained widespread use after the success of MUS surgeries.

1.5. Clinical outcomes of mesh repairs for SUI and POP

Currently tension free vaginal tape procedures for SUI have long term subjective cure rates of up to 93% [55]. Nevertheless mesh related complications still occur in at least 4% of patients [56]. Professional societies and regulatory agencies are stating that the benefits of these operations outweigh the risks and that many women would be left without effective treatments if the use of mesh was to be banned.

POP repairs are now being performed in 2 main groups: transabdominal and transvaginal POP repair procedures, with most being performed via a vaginal route (transvaginally) [60]. The main sites of surgical implantation are demonstrated in Figure 1.4. The safety of mesh augmented transvaginal POP repair procedures is widely questioned with a mesh erosion rate of 8% in 1-3 year follow- up and can go up to 42% in longer term follow up [57]. There appears to be a consensus on lack of safety with transvaginal mesh implantation for POP. In contrast abdominal sacrocolpopexy procedures are performed with long term success rates of 97- 100% [58] and are considered the gold standard surgical treatment for advanced POP [59]. Mesh erosion still occurs in these operations in up to 6% in 2 years [60] and 10% of cases in 7 years follow up [61] however like synthetic mid- urethral slings the risks of mesh augmented abdominal POP repair procedures are considered to outweigh their risks.

Figure 1.4. Graphical demonstration of most common sites of surgical mesh implantation in the pelvic floor. (a) Transabdominal placement of PPL mesh to treat POP (sacrocolpopexy operations). (b) Transvaginal implantation of PPL mesh at the level of mid- urethra to treat SUI. (c) Transvaginal placement of PPL mesh for POP repair, 45° lateral view and 45° anterosuperior view. Many variations of these operations exist. Here fixation/ anchoring of the mesh to sacrospinous ligament and ATFP is demonstrated.
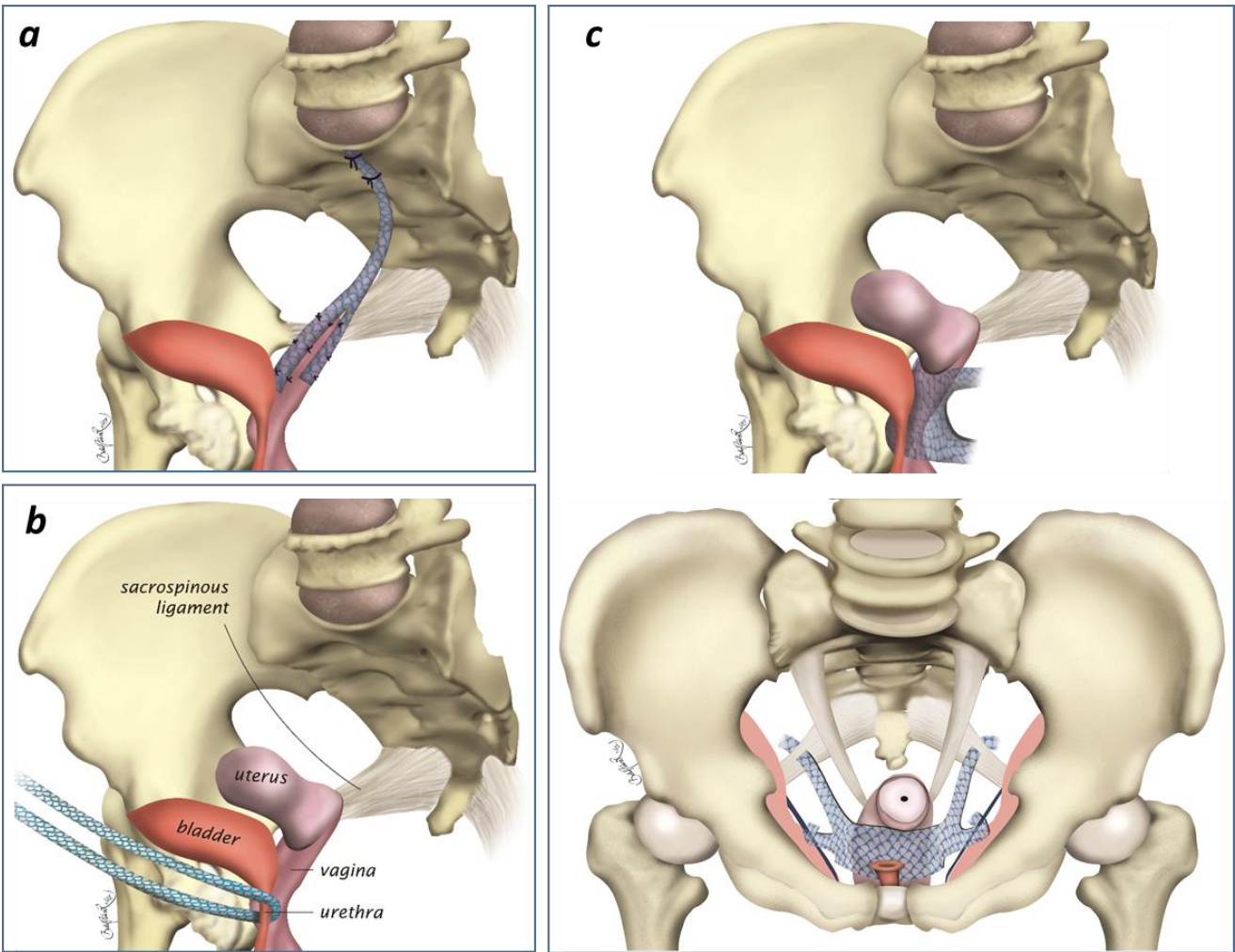
1.6. *Polypropylene mesh as a material*

The PPL vaginal meshes in current clinical use were never designed or tested specifically for use in the treatment of SUI and POP. Instead they were developed for use as a soft tissue prosthetic material in the context of abdominal hernia repair. Based on the available clinical data on its biocompatibility, the PPL mesh was cleared for use in the female pelvic floor after demonstration of the similarity of their textile properties to the existing abdominal hernia products via a 510(k) loophole. Therefore, it will be useful to review the context in which the PPL mesh developed.

Three main classes of materials have been used for biomedical applications: metals, ceramics and plastics. Plastics (plasticos: capable of being moulded in Greek) are synthetic, high molecular weight materials that became available for surgical applications after 1940s. Plastics provide unique material advantages over metals and ceramics that make them desirable for many biomedical applications. They have a more advanced performance-to-weight ratio compared to metals and they can easily be micro fabricated into small and complex structures. Additionally, plastics are versatile materials that can be made into an ivory hard object with desired rigidity and strength, a flexible rubbery mass or a porous spongy structure. Each of these could be degradable and non- degradable.

1.6.1.Synthesis and degradation of polypropylene

PPL ($[C_3H_6]_n$) is a thermoplastic (that can be processed and re-processed when heated), polymer synthesized from propylene monomers by addition polymerization. The resultant material is a series of long and flexible linear chains that can be oriented and crystallized. After the raw material of PPL is synthesized, it is melted and processed by a technique called 'extrusion' to form the usable end product. Extrusion is the process of injecting a stream of molten polymer through a die of constant section. The extrusion process forms continuous filaments which are then twisted, knitted and interlocked to form the specific pattern. After knitting, the mesh is cleaned of the residuals and stabilized. The finished mesh is than cut into shape and sterilized by autoclaving/high pressure steam. The extrusion process is graphically demonstrated in Figure 1.5 together with a more modern polymer production method called electrospinning. This comparison can give the reader a better understanding of how different polymer processing technologies can lead to a significant difference in the final product and tissue response to it. A complete comparison is provided in Table 1.

Figure 1.5. Demonstration of the industrial process used to produce the monofilament polypropylene (extrusion) as compared to the process of electrospinning. The polymer extrusion process to produce the monofilament PPL mesh. the end product of the extrusion process gross view and electron microscopic view can be seen in the upper raw. The electrospinning producing micro-nano sized fibrous mats are seen in the lower raw. (yellow and white scale bars represent 200 and 10 μm, respectively)
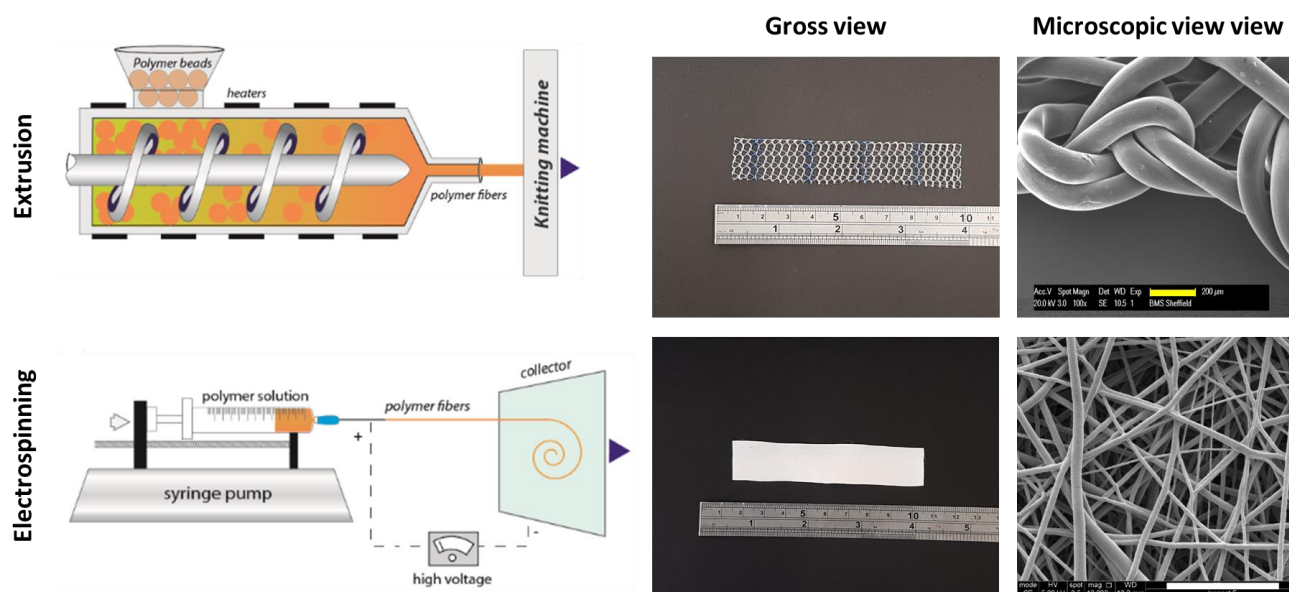
Table 2.1. Comparison of two methods of manufacturing polymers: the extrusion process to produce the surgical mesh and the electrospinning process

	Extruded mesh	**Electrospun mesh**
Raw material	Polymer beads	Polymer beads
Additives	Yes	No
Liquifying process	Heating	Dissolving
Manufacturing principle	Extrusion	Electrical field
Post process	Knitting	None
Sterilization	Autoclave	GMP produced
Pore size	>70 μm	1-10 μm
Fibre size	300-500 μm	1-10 μm
Tissue integration	Poor	Excellent
Level of technology	Industrialized process	Tissue engineering process

During polymer synthesis a variety of additives are used up to 30% of their total weight, although they are generally much less in medical grade raw materials [62]. Additives are essential ingredients that are used to adjust the polymer properties so that they can become suitable for industrial processing. Additives can also be used for property enhancement and to neutralize the effects of other additives. For example the PPL needs to be thermally stabilized by additives to survive melt processing [63]. Thus the quality of finished PPL surgical mesh depends on the quality of the raw materials and additives.

The manufacturers rely on suppliers of raw materials and components to obtain polymer resins. The device manufacturers need to implement supplier qualification procedures that include audits, incoming raw material and component specifications and quality metrics. This is only required for devices classified as 'high- risk' by the FDA. Thus the raw materials supplied to manufacturers for PPL mesh production were not strictly controlled by the FDA until January 2016, when these vaginal mesh implants were re- classified from class II to III. This means the purity, product quality and consistency, molecular weight and additives in the PPL mesh can be variable [64].

The polypropylene material was traditionally considered as being 'inert'. Although PPL completely degrades over many years, its' inertness is now questioned after repeated demonstrations of surface degradation on the PPL fibres [65], [66]. Synthetic polymers degrade by bulk hydrolysis (bulk erosion) and/ or surface erosion after implantation [67]. Bulk erosion leads to rapid break down of the material and a decrease in mechanical properties whereas surface erosion affects the performance of the material in the long term without changing its bulk [68]. PPL does not undergo bulk degradation as it is hydrophobic meaning it is not susceptible to hydrolysis.

However, PPL can undergo surface degradation after implantation. The biochemical environment of the human body represents an aggressive medium with a set temperature (37° C), pH (7.4 in blood) and salt concentration [69]. This environment can cause PPL degradation by oxidation [70]. Furthermore, this can be considerably facilitated by the presence of static or cyclic mechanical forces. A focal site of surface cracking, abrasion or wear can induce generation of macroradicals originating from chain rupture leading to increased brittleness and deterioration in strength. Data has demonstrated that PPL mesh extracted from pelvic floor of women shows surface fissures and cracking due to oxidative degradation [71]. Tissue sections of mesh explants also showed signs of PPL degradation [65]. Thus PPL mesh is resistant to hydrolytic degradation however it undergoes significant chemical and mechanical changes in human body and cannot be considered inert.

1.6.2. Mechanical properties of polypropylene mesh

In addition to biochemical properties, plastics have unique mechanical properties that are very much time dependent, often non- linear and that affect their performance in the long term. When a controlled force (stress) is applied to a plastic it causes a change in its size (strain) which is initially proportionate to the force applied (linear elasticity) (Figure 1.6). This proportionality is lost at some point and the stress- strain curve becomes non- linear. In the linear region the material turns back to its exact original size/ shape after the force is removed (elastic region). The end of elastic region is marked by the 'yield point' in the stress- strain curve. The yield strength of a material is the strength after which a material begins to plastically deform where permanent and irreversible disfigurement of the material occurs (the plastic region) and after the yield point the material does not come back to its original state when the force is removed.

Figure 1.6. Defining basic mechanical properties of a material by uniaxial mechanical testing. The tensiometer setup is demonstrated in (A). The load- elongation curve produced by this test is demonstrated in (B) together with the change in appearance of the sample loaded to the tensiometer.
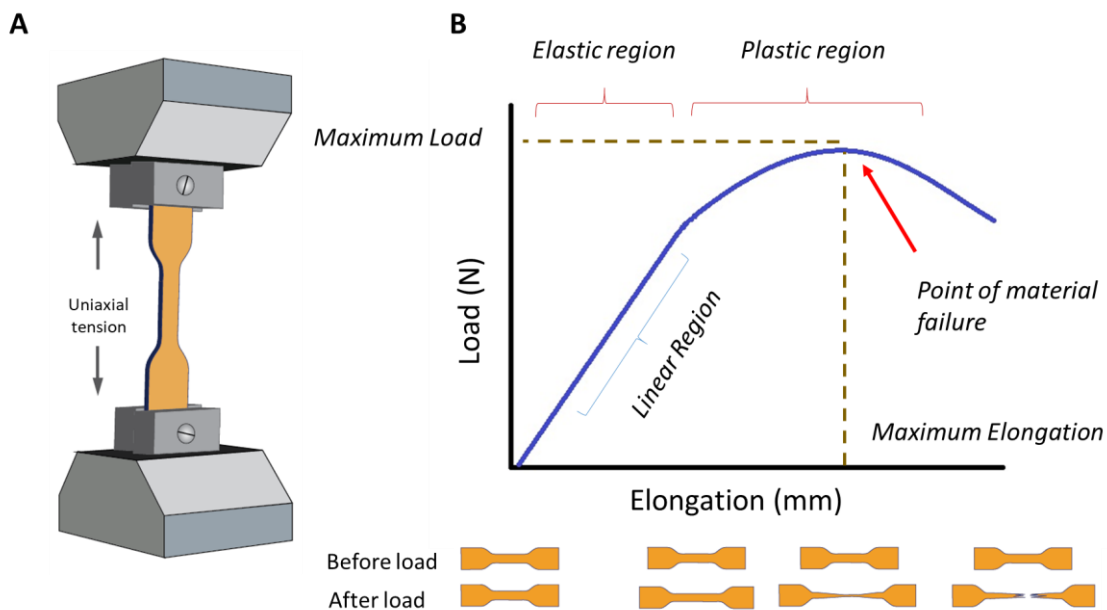
The biomechanical integration of the implant with the host tissues is fundamental to its long term efficacy. The mechanical properties of the material are required to be comparable to that of the tissue of implantation. Assuming that the mechanical properties of the PPL mesh is stable *in vivo* over years, the mesh material can be characterized mechanically. Defining the engineering requirements for pelvic implants is rather difficult due to the complexity of the anatomical structures and the variability of the forces/ loading conditions acting on them in health and disease. The uniaxial testing of the PPL mesh show that the PPL mesh is 5- 10 times stronger than those of the healthy paravaginal tissues [72]. Thus the PPL mesh is probably far too strong to be used in the pelvic floor.

1.6.3. In- service failure of polypropylene mesh

Plastic biological implants, can fail in service mechanically and/ or biochemically. Mechanical failure of an implanted biomaterial often results from an inaccurate estimation of the static and dynamic loads/ forces the material will undergo at the site of implantation during its lifetime. Defining the *in vivo* loading conditions and boundary conditions play a key role in the mechanical compatibility of the material and the tissue. For example, if the mesh is mainly bearing load, it needs to be tested in a certain direction by uniaxial testing whereas if it is working like an abdominal wall mesh it is better tested by its biaxial mechanical properties. It has been demonstrated that the same materials when tested by uni and biaxial mechanical tests can show significantly different mechanical properties [73]. Thus when defining the mechanical requirements of the mesh it has to be defined for a specific surgical application.

Another possible mechanism for the failure of the PPL mesh can be due to cyclic stress that the mesh undergoes over weeks and months. When designing the mesh implant if the yield strength of the material is not calculated correctly, the material can start undergoing plastic deformation a little each time in response to a force more than its yield strength and this when repeated over time causes the material to 'strain harden' [74]. Strain hardening indicates that the material will increase in stiffness over time resulting mechanical properties different to its original state.

1.6.4. Initial design of the polypropylene mesh and improvements made to the initial design

Ventral hernia occurs due to a defect in the fascia covering abdominal muscles and surgical treatments aim to repair the structural defect. Prosthetic materials have been used to treat large tissue defects that could not be closed with primary suture repairs or to reduce the chances of recurrence. It is attributed to Theodore Billroth (1829-1894) that "If we could artificially produce tissues of the density and toughness of fascia the secret of the radical cure of hernia would be discovered" [75].

The first prosthetic material used in hernia repair was made of silver, followed by tantalum (Figure 1.7). Tantalum wire mesh became quite popular at that time due to its inertness and ability to withstand infection however metals were inherently not suitable for soft tissue repairs as they were stiff and could fragment. After the plastics revolution materials made of nylon (polyamide) and dacron (polyester [polyethylene terephthalate (PET)]) started to be used [76]. Although the plastic meshes offered significant advantages over metallic meshes with their ductility and strength, the initial meshes were actually textile fabrics made of plastics which were boiled for sterilization before implantation. These plastics induced a dense fibrotic reaction and the infection rates were high.

It was only after Usher, who is a hernia surgeon, started to design a fit- for- purpose material that the surgical mesh gained widespread acceptance. He used a high density polyethylene and used a new manufacturing method to 'extrude' it as a monofilament with a thread count of 42 by 42 to the inch [77]. He optimized the porosity, stretch-ability and tensile strength of the new mesh to allow fibroplasia while keeping the necessary tensile strength. He then characterized the tissue response to the mesh in animal studies [78]. In 1962 Usher introduced an improved version of Marlex mesh made of polypropylene (PPL). PPL had improved material properties with higher heat resistance allowing sterilization with less compromise, it had high tensile strength with good flexibility and excellent resistance to infection [79]. PPL than became the standard of the modern mesh materials [80].

Figure 1.7. Milestones in development of the polypropylene mesh (PPL) as a material used in pelvic floor repair. (only mesh augmented incisional hernia repair procedures as they are related to mesh positioning are included here).

PELVIC RECONSTRUCTIVE SURGERY

HERNIA SURGERY*

First 'sling' surgery for SUI. Sling formed by gracilis muscle [42] — 1902 — First prosthetic mesh (made of Silver) used in hernia repair [81]

1907

First autologous fascia sling for SUI Sling formed by fascia lata [82]

Cystometry used in evaluation of bladder dysfunction [83]

1933

First rectus fascia 'sling' for SUI [86]

1939
First tantalum plate implantation for SUI [51] — 1940 — Tantalum gauze fabric introduced for hernia repair [84, 85]
1942

1947

Tantalum mesh first used in transvaginal POP repair [46]

First non-metallic (Dacron) mesh used in a group of hernia patients [76]

1955
First abdominal sacrocolpopexy using a synthetic material [88] — 1956
1958 — First woven, plastic mesh (made of Polyethylene) developed by Usher [87]

1962

First PPL (Marlex) used in SUI modified gauze hammock operation [53]

First PPL monofilament mesh (Marlex) introduced by Usher [79]

1970

Type III SUI defined & modern autologous fascia sling surgeries described [44]

1978
1979 — Onlay hernia repair described [89]

Integral theory for SUI put forward Tension free & mid-urethra concepts [34]

Sublay mesh repair described [90]

DeLancey's three levels of vaginal support

1989
1990
1992
Hammock hypothesis for SUI [36] — 1994 — Amid classification of mesh material based on filament structure and porosity [92]
1995
1996
First intravaginal mesh sling surgery for SUI [91] — 1997
1998

2002 — First lightweight mesh introduced
2004

First mesh product cleared for SUI (ProteGen Sling)- recalled in 1999 [93]

2016

First mesh product for POP approved by FDA (Gyneacare) [93]

First mesh kit approved by FDA (Apogee®, Perigee®) [93]

☐ Developments in material properties
☐ Developments in surgical technique
☐ Developments in disease understanding

50

Over the next few years heavy weight meshes were replaced by medium to light weight meshes that reduced the bulk of the foreign material leading to less inflammation, foreign body reaction, fibrosis and the associated pain sensation [94]. Also the pore sizes were made larger (macropororus). The first study to demonstrate a relationship between the material properties and side effects associated with the mesh when used in hernia repair was published by Amid [92]. In this study the porosity of the mesh was suggested as the main determinant of biocompatibility of a mesh implant. Later on, animal studies comparing heavy and light weight meshes showed that light weight PPL mesh displayed a marked reduction in fibrosis and foreign body reaction compared to heavy weight PPL [95]. Also clinical studies comparing heavy and light- weight mesh materials implanted for inguinal hernia repairs demonstrated less pain and less sensation than of a foreign material with lighter meshes [96]. Thus the current PPL mesh has evolved over the years from a metal wire to fabrics of plastic and eventually to the current mesh with a range of bulk densities and pore sizes.

When surgical mesh was first introduced it offered clear advantages over the previous prosthetic material made of metals. However, it also came with a new set of complications that were predominantly related to the use of plastics such as mesh contraction and colonization/ infection of the mesh. Modifications to the surgical technique of implantation were then made to avoid these complications (Figure 1.8). For example, the 'inlay repairs' where the mesh is placed in- between the edges of the fascia defect were replaced with 'onlay repairs' where the mesh was placed on top of the repaired fascia defect in a tension- free manner. Onlay repairs involved extensive subcutaneous tissue dissection and also a large area of the mesh implant stayed very close to skin increasing the chances of wound complications such as infection and seroma formation. To overcome this a 'sublay (retrorectus) technique' was introduced where the mesh is put underneath a thick muscle tissue (retro- rectus) in- between two fascial layers. Placement of the mesh onto a well vascularized wound bed and away from the skin were key factors in the success of this technique [97]. The ideal location of mesh in ventral hernia repair remains debatable and different methods are indicated for each specific case however it is certain that the surgical technique of implantation is a factor that has contributed to mesh related complications in hernia repair surgeries [98].

Figure 1.8. Graphical demonstration of mesh positioning in relation to muscle and fascia in incisional hernia repair. (A) A cross section of anterior abdominal wall with a fascia defect causing herniation of the intestine. (B) Inlay mesh implantation where the mesh fills in the gap created by the fascia defect. (C) Mesh onlay repairs where the mesh is on top of the fascia repair to reinforce it. (D) In the sublay technique the mesh is placed on a well vascularized wound bed underneath the muscle and it is in- between two strong fascial layers. (E) The mesh underlay procedures are mainly used in laparoscopic hernia repair procedures, in this case a mesh with anti- adhesive properties would be preferable instead of a polypropylene mesh to prevent attachment of intra-abdominal organs.
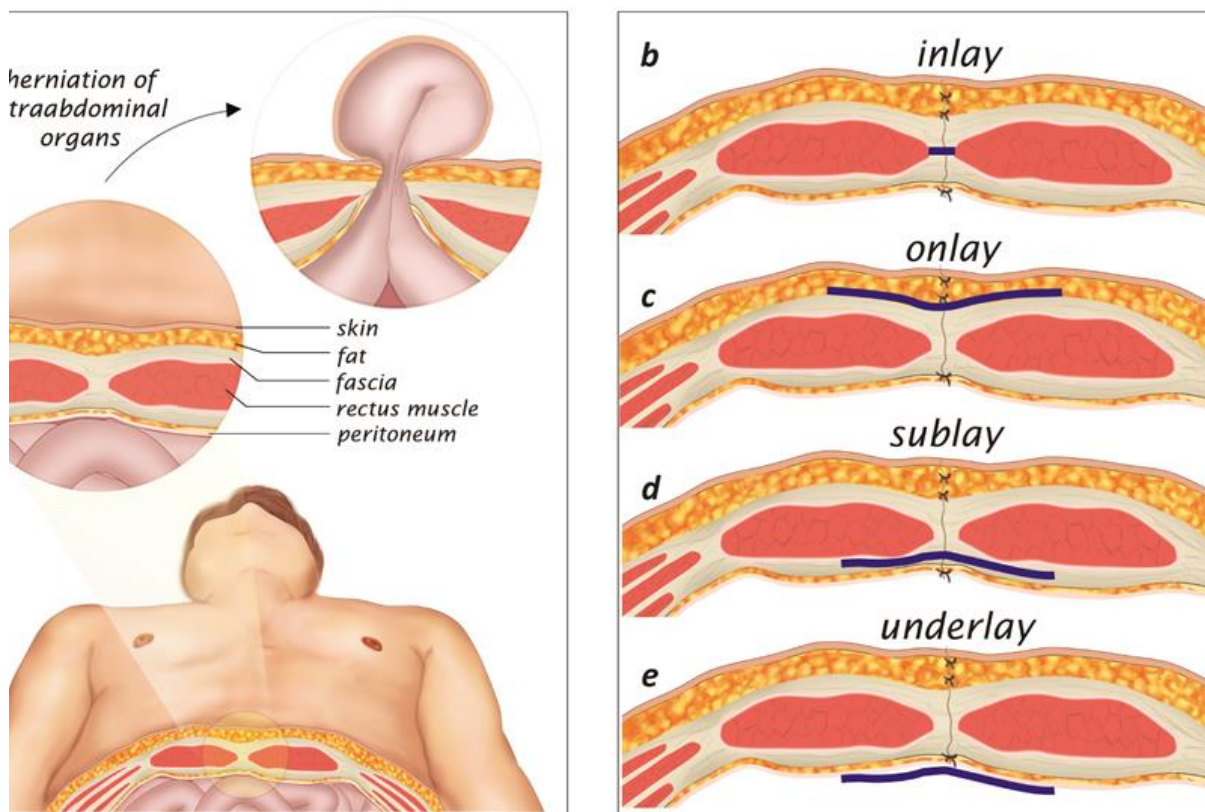
Just like new materials necessitated new surgical approaches, developments in the surgical technologies also required modifications in material properties in hernia surgery. For example, recent widespread use of laparoscopy led to an 'underlay' repair technique where the mesh is placed on the inside surface of the abdominal wall in direct contact with intraabdominal organs. The mesh in these cases needed to have additional anti- adhesive properties, such as Teflon based materials, to prevent adhesion of intraabdominal organs [99]. Thus the material properties and surgical technique developed hand to hand over many years to obtain best outcomes for hernia repairs.

1.6.5. Why did the polypropylene mesh fail in the pelvic floor?

The PPL mesh failed in the pelvic floor both biologically and mechanically. The biological response to PPL has mainly been studied histologically in the context of hernia surgery. Experimental studies to evaluate the tissue response to PPL in vaginal surgery started in 2007 [100], showing that graft related complications (exposure and contraction) occurred more when the mesh is implanted to vagina rather than in the abdominal wall [101]. In transvaginal mesh implantation the material traverses a clean contaminant area and it is very hard not to get the mesh contaminated during insertion. Minutes after mesh is inserted into body a 'race for the surface' begins and if the host cells cannot win the mesh gets contaminated which can remain dormant without causing obvious problems for a long time. Also after mesh implantation an inflammatory reaction begins which leads to tissue remodelling or a persistent inflammatory response. In the background of chronic inflammation, colonization and mechanical failure events leading to chronic pain, mesh contraction and erosion can occur [102]. We cannot currently predict which patients will be affected more by mesh complications.

Mechanically, the PPL mesh is now thought to be incompatible with the female pelvic floor. Essentially the PPL mesh is too strong and not elastic enough to be used in the pelvic floor [103], [104]. Other factors that have contributed to emergence of the vaginal mesh issue as a public health problem are listed in Tables 2 and 3.

Table 1.2. Problems that have occurred during development of meshes for pelvic floor repair

1. Lack of necessary regulations for approval of medical devices
a. Devices granted approval with no/ limited clinical data
2. Lack of understanding of female pelvic floor disorders
a. The female pelvic floor is structurally and functionally complex
b. Pelvic floor biomechanics not well studied
c. Targets for surgical treatment generally poorly defined, particularly in transvaginal POP repairs
3. Problems related to the material
a. Surgical mesh not designed for use in pelvic floor
b. Limitations in available technologies and materials at the time
c. Polypropylene considered inert however it undergoes surface degradation
4. Factors related to surgical technique
a. Proximity of large areas of mesh implant to skin wound
b. Implantation of mesh on to a poorly vascularized wound bed
5. Lack of relevant animal models of efficacy

Table 1.3. Problems that have occurred after the mesh was made available for widespread clinical use.

1. Lack of implementation of post marketing surveillance
2. Poor patient selection
a. Poorly defined disease subgroups
b. 'One size fits all' approach
3. Factors related to operating surgeon
a. Poor subspecialty training on management of all aspects of SUI and POP
b. Minimally invasive operations perceived as 'easy to do'
4. Extensive marketing

1.6.6. Current approaches to improve the polypropylene mesh

Efforts to make further improvements to the current surgical mesh are still ongoing. It is now widely accepted that the new generation, light- weight, macroporous meshes with high porosities are desirable to ensure a better mesh remodelling and reduce complications such as fibrosis, pain and mesh failure. The knit pattern and geometry of the mesh can also be modified to obtain desired mechanical properties [105].   Another approach to enhance the biocompatibility of PPL is to apply a bioactive coating onto it with more biocompatible substances, such as natural extracellular matrix [106]. Titanium coated light weight polypropylene meshes was also used in a pilot patient group to improve the biocompatibility of the PPL mesh [107].

There has also been research on degradable and hybrid degradable/ nondegradable mesh materials. The main idea behind a degradable mesh was that it would be absorbed after a period of time by which time the patients' own tissues would have at least partially recovered or regenerated and this would avoid the long term complications of permanent mesh like infection and fistula formation. The concept of using biodegradable scaffolds or support – often combined with patient cells to help regenerate tissues is well accepted in the world of tissue engineering and regenerative medicine [108] but has not yet been trialled clinically with respect to POP although there are materials in development.

1.7. Tissue engineering to construct biomaterials for pelvic floor

Advances in materials science and tissue engineering are finally being applied to designing novel materials specifically for use in the pelvic floor. The first tissue engineered approach to construct an autologous fascia equivalent for POP repair was reported in 2010. In this study human vaginal fibroblasts were seeded on a PLGA knitted mesh before implantation into nude mice for 12 weeks and a well- organized new fascia with a high collagen I/III ratio was demonstrated [109]. A stronger tissue engineered material was also constructed from knitted silk mesh seeded with adipose derived MSCs in 2013 [110]. A gelatine coated- polyamide knit mesh seeded with endometrial MSCs that was designed for POP repair was also shown to reduce inflammatory cell infiltration and increase neovascularization in a rat model in 2013 [111].

1.7.1. Previous work from Sheffield group: Choice of material and manufacturing technique

Our own group in Sheffield has also been developing biomaterials and tissue engineered substitutes to be used in pelvic floor repair over the last 8 years.

With respect to choice of materials we think it is important to be able to consider a range of degradable and non- degradable materials. The Sheffield group has mainly produced work on a biodegradable material, Poly-L-lactic acid (PLA) and a nondegradable polymer of polyurethane. PLA is known to have good biocompatibility and is commonly used in drug delivery applications [112]. Another promising material was polyurethanes with increased elasticity that can withstand cyclic mechanical distension *in vitro* [113]. The electrospun polyurethanes, together with electrospun ureidopyrimidinone- polycarbonate scaffolds, led to a better host response compared to ultra- lightweight PPL meshes after implantation in to sheep vagina for 6 months [114]. Electrospun materials and ultra- lightweight PPL were similar in this model with regards to graft related complications, passive mechanical properties and their effects on vaginal contractility.

Electrospinning is a widely used technique in tissue engineering that allows fabrication of scaffolds with micro/ nano sized fibres with different compositions and configurations. This technique can effectively be used to build scaffolds with several layers of different polymers in order to achieve desired biomechanical properties [115]. For example, transversely, obliquely and irregularly aligned fibres can be electrospun in a tri-layer structure with ultrastructural and biomechanical properties similar to native fascia [30]. Also we have shown that PLA scaffolds with random fibres have mechanical properties close to those of healthy paravaginal tissue [116] while showing successful integration into native tissues in short term [117].

PLA as a material

Polylactide (PLA) is a biodegradable polyester synthesized from the monomer 'lactic acid' which is made by bacterial fermentation of carbohydrates such as corn and potatoes. PLA has several chiral forms such as poly (L-lactic acid) (PLLA), poly (D-lactic acid) (PDLA) and poly (D,F-lactic acid) (PDLLA). PLLA is most commonly used and studied in biomedical applications. Higher molecular weight PLLA can take more than 5 years to degrade. PLA is highly biocompatible and as a degradable polymer it is commonly used as a drug delivery material [112].

Polymers have the obvious advantage of being strong enough and ductile especially for soft tissue regeneration. The word polymer refers to huge macromolecules made of repeating structural units called monomers ('polus': many and 'meres': parts in Greek). For instance, polysaccharides are made of single sugar units or polypropylene is a polymer made of 'propylene' monomers. Polymers can be natural or synthetic. Natural polymers can be derived from plants or animal sources and they share similar features with the extracellular matrix of humans. Therefore, natural polymers are recognized, metabolized and degraded by the tissues. Additionally, natural polymers are known to be stimulate less immunological reactions and toxicity compared to synthetic polymers. Commonly used natural polymers are chitosan, hyaluronic acid, gelatin and cellulose. The main limitations of natural polymers are variability in the material properties depending on the source of isolation, the risk of contamination with microorganisms, poor mechanical strength and unpredictable degradation pattern.

Synthetic materials have the main advantages of being available 'off the shelf' and being synthesized at reproducible quality and purity. Additionally, synthetic materials can be produced into various shapes and surface properties. The material properties of synthetic polymers are continuously being improved in the last half of the century to tailor the degradation times and improve the tissue response to these materials. The chemical properties of the material are the main determinant of its' biocompatibility. However, it appears that numerous issues related to the biochemistry of the materials have not been identified and addressed in *in vitro* and *in vivo* experiments before they are translated into clinical practice. This is especially true for biomaterials whose material properties change over time after implantation leading to a significantly different host response in the long term [118].

Polymers most commonly used for soft tissue regeneration are PolyLactic Acid (PLA), PolyGlycolic Acid (PGA) and PolyCaproLactone (PCL). All these polymers are approved by FDA for a variety of application mostly in suture materials. Basic physical properties of these polymers are listed in Table 4.

Table 1.4. A summary of the physical properties of the polymers most commonly used in scaffolds for soft tissue regeneration (* polymers used in this thesis).

Polymer	Degradation time	T_g (°C)	T_m (°C)	Tensile modulus
PLLA*	>2 years	60- 65	175	2.7 GPa
PGA	6- 12 months	35-40	>200	6 GPa
PCL	>2 years	54	55- 60	0.4 GPa
PU*	12-18 months	-35	180	1.31- 2.07 GPa
PPL	Non-degradable	-10	165	800- 1300 MPa

1.7.2. Design requirements for materials to be used in pelvic floor reconstruction

The PPL vaginal meshes in current clinical use were never designed or tested specifically for use in pelvic floor. The best available material was empirically used in pelvic floor based on an assumption that if it worked well in the abdomen to reinforce hernia repairs it would work equally well to support vaginal prolapse repairs. It is now being recognized that this approach was inherently flawed as the microbial flora, pH, vascular supply and physiological mechanical requirements of the pelvic floor are different from that of the abdomen.

The search for an ideal graft material to be used in pelvic floor continues since mid- twentieth century. An ideal graft has been defined arbitrarily as being biocompatible, noncarcinogenic, nonimmunogenic, able to provide structural support until tissue healing is completed, pliable, sterilizable, readily available, inexpensive and have a minimal risk of infection. Additionally, any material used to support the pelvic floor needs to have defined characteristics of material deformation and load bearing as well as how it contributes to tissue remodelling once it is implanted in to the body.

Biocompatibility is the ability of the biomaterial to perform with an appropriate host response that is defined for a particular clinical application [119]. This definition is often criticized for not providing any insights on how to assess biocompatibility or how to improve it . A tissue response is expected to any biomaterial once in contact with the host and what is needed is a mutually acceptable co- existence of the biomaterial and the host tissues while the biomaterial exerts its desired function. There are very many different ways the materials and tissues can interact. Classically, any synthetic material implanted in the body will trigger an inflammatory reaction sequentially involving acute inflammation, chronic inflammation, a foreign body reaction and wound healing/ scar formation. Under normal circumstances all available biomedical implants will generate a similar foreign body reaction that leads to formation of a fibrotic capsulation reaction with a thin (50 to 200 μm), tough, collagenous and avascular tissue around the implant material [120]. The fibrous capsule often defined as a desirable outcome from a clinicians point of view when the implant performs desired functions without causing any adverse reactions. However, in some cases, such as pain and deformation seen in capsular contracture of breast implants, foreign body reaction is considered an undesirable outcome that can necessitates excision of the implant.

Current understanding of biocompatibility defines a host response to the biomaterial that is more similar to normal wound healing where a healthy, vascularized tissue is formed in the biomaterial- tissue interface rather than the fibrous capsule. This could be achieved by reducing the capsule formation and increasing the vascularity around the implantation site [121]. Although the exact relationship between angiogenesis and foreign body reaction and biocompatibility of an implant material is not clearly defined, it was recently proposed that blood vessel density was directly correlated with the biocompatibility of an implant [122]. Therefore, a controlled increase in the angiogenesis in the surrounding tissues could be a strategy to increase the biocompatibility of the biomaterial.

1.7.3. Angiogenic properties of tissue engineered materials

The growth of new blood vessels into a tissue engineered substitute is crucial to improve its' tissue integration and to obtain a successful long term clinical outcome. It has been estimated that a distance of less than 200 µM from the supplying capillary is the critical distance for diffusion of oxygen and nutrients to any new tissue introduced into the body. Because of this the survival of any 3- dimensional tissue graft relies on rapid development of new blood vessels to supply not only the centre but also the margins of the graft [123]. A specific consideration should be given to clinical scenarios where the wound bed accommodating the biomaterial is already poorly vascularized, such as pelvic floor tissues of postmenopausal women with SUI and POP [124]. Clinical studies have demonstrated that post- menopausal women and women with co-morbidities that can have a negative impact vascular supply to tissues (e.g. diabetes, smoking, previous surgeries) were more likely to experience vaginal mesh related complications [125].

All attempts to design tissue engineered repair materials need to include an understanding of angiogenesis. Angiogenesis is the sprouting of capillaries from pre-existing blood vessels *in vivo*. This process involves a complex interaction between endothelial and non- endothelial cells as well as many enzymes, growth factors and adhesion molecules. Several strategies to promote angiogenesis of tissue engineered constructs have been described [126], these include: (1) engineering a scaffold that allows easy attachment and proliferation of endothelial cells, (2) designing the microstructure to aid the formation of capillaries, (3) providing angiogenic growth factors into the microenvironment within the biomaterial either directly by incorporating a growth factor into the scaffold material or indirectly by seeding a cell source that is able to synthesize angiogenic factors onto the material such as stem cells or genetically modified cells.

Accordingly, strategies for the introduction of clinically acceptable agents that would stimulate neovascularisation and new extracellular matrix production by the patient's endogenous cells have been assessed in the current work. To this end, effective pharmacological functionalization of electrospun PLA scaffolds by incorporating clinically acceptable bioactive factors such as vitamin C and Estradiol without compromising structural and mechanical properties are being assessed [127]. Estradiol and ascorbic acid were selected as a) both are already in use clinically which will make their regulatory approval less challenging, b) within the group it has been demonstrated that both can increase extracellular matrix (ECM) production as they are released from PLA scaffolds without compromising mechanical properties of these materials. To the best of our knowledge neither of these drugs has ever been investigated regarding their effects on the intrinsic angiogenic potential of a tissue engineered biomaterial.

1.8. Aims and Objectives

Aim: The aim of this project is to develop biocompatible synthetic materials for pelvic floor repair that can promote angiogenesis and improve tissue regeneration.

The specific objectives to accomplish this are;

1. To establish an *in vivo* bioassay to study the angiogenic potential of tissue engineered materials
   a. To explore the feasibility of running an *ex ovo* version of the traditional chick chorionic allantoic membrane (CAM) assay.
   b. To evaluate embryo survival rates in *ex ovo* cultures
   c. To find the best way of obtaining high quality images for image analysis
   d. To explore the best way of visualizing all macro and microvessels of the CAM
   e. To assess if any added value can be obtained from the *ex ovo* cultures of the chick embryo
2. To evaluate the chick aortic ring assay as an organ culture assay to study endothelial cell sprouting
3. To construct electrospun PLA scaffolds that release Vitamin C
   a. To determine the release characteristics of Vitamin C from the scaffolds
   b. To characterize the Vitamin C releasing scaffolds with regards to their ultrastructure and mechanical properties
   c. To assess how the scaffolds, affect proliferation and extracellular matrix production of cells (either fibroblasts or adipose derived stem cells) grown on these scaffolds
   d. To assess the angiogenic potential of Vitamin C releasing scaffolds on an *ex-ovo* CAM model.
   e. To assess the initial tissue response to the materials

4. To construct electrospun PLA scaffolds that release Estradiol
   a. To determine the release characteristics of Estradiol from the scaffolds
   b. To characterize the Estradiol releasing scaffolds with regards to their ultrastructure and mechanical properties
   c. To assess how the scaffolds, affect proliferation and extracellular matrix production of cells (either fibroblasts or adipose derived stem cells) grown on these scaffolds
   d. To assess the angiogenic potential of Estradiol releasing scaffolds on an *ex-ovo* CAM model.
   e. To evaluate the effect of Estradiol on the microvasculature of the CAM
   f. To assess the initial tissue response to the materials
5. To analyse if stem cells can provide any added benefit when added to scaffolds to promote angiogenesis
   a. To find an appropriate cell carrier to keep the stem cells on the CAM
   b. To find the most effective concentration of stem cells to promote angiogenesis in a chick aortic ring assay

Chapter 2. Materials and Methods

2.1. Cells

Two cell types were used in the experiments included in the current doctoral studies: human dermal fibroblasts and human adipose derived stem cells. Both cell types were isolated from a regular supply of donated skin and subcutaneous fat of patients undergoing breast reduction and abdominoplasty. All patients had given informed written consent and all procedures were covered under a research tissue bank license by the Human Tissue Authority (number 08/H1308/39).

2.1.1. Fibroblasts

After donated skin was received in the laboratory a split thickness skin graft was taken using a Watson knife by a named technician under laminar hood. Skin grafts were then cut into 0.5X 0.5 cm squares and incubated overnight at 4°C in a solution of 0.4% trypsin plus 0.1% w/v D-glucose in phosphate buffered saline (PBS) to enable easy separation of epidermal and dermal layers. After trypsinisation skin grafts were taken into a Petri dish and epidermal layer was peeled off the dermis using a forceps and scalpel. Dermal layer was used for fibroblast isolation. After washing with PBS the dermal pieces were minced thoroughly using a scalpel. Minced dermis was incubated overnight at 37°C in a 10 mL solution of 0.05% collagenase A in media. Next day the collagenase was neutralized, the resulting suspension was centrifuged at 1300 rpm for 10 minutes and the precipitate was resuspended in fibroblast growth media in T25 flasks. Fibroblast growth media consisted of Dulbecco's Modified Eagles's Medium (DMEM) (Gibco Invitrogen, Paisley, UK) supplemented with 10% foetal calf serum (Advanced Protein products, Brierly Hill, UK), 1% penicillin/streptomycin and 0.5% Fungizone (Gibco Invitrogen, Paisley, UK). After the first passage HDFs were cultured in T75 flasks and incubated at 37°C in the presence of 5% CO_2 with fresh media changes every 3–4 days. Regular inspections under inverted microscope were undertaken daily to visualize cell morphology of the growing cells and exclude any infections. For the experiments HDFs between passages 4- 9 were used.

Passaging was performed using incubating the cells with 4 ml of trypsin/ EDTA solution (Sigma- Aldrich, Dorset, UK) per flask for 4 minutes. Thereafter, the trypsin was neutralized with media, cells counted using a haemocytometer and the cell suspension was centrifuged at 1000 rpm. The pellet was than divided into 3-4 new T75 flasks at a density of 100.000 to 1.000.000 cells per flask.

2.1.2. Adipose derived stem cells

All ADSC isolation and characterization experiments were performed in collaboration with Dr Sabiniano Roman. Small lumps of human subcutaneous fat was placed in Petri dishes containing 10 mL of PBS containing 1% penicillin/ streptomycin. Initially the fat tissue was minced in a Petri dish using a sterile scissors and collected into a 50 mL centrifuge tubes. An equal volume of 0.1% collagenase type A solution in HANKS buffer was than added into the centrifuge tubes and incubated in 37°C for 40 minutes while shaking the tube every 10 minutes to facilitate enzymatic digestion. The collagenase was then neutralized adding an equal amount of culture media and centrifugation performed at 1300 rpm for 8 min. The supernatant containing all the undigested fat tissue is discarded and the supernatant (stromal vascular fraction) was resuspended in culture media. After the supernatant was washed with media and centrifuged again, the pellet was resuspended and cells were seeded in T25 flasks containing 4 ml of DMEM medium. Flasks were incubated in at 37°C and 5% CO_2.

Next day the media was removed and flasks were washed with PBS removing all the non-adherent cells. Regular inspections under inverted microscope were undertaken daily to visualize cell morphology of the growing cells and exclude any infections. Once the growing cells reached to a confluence of 80% passaging was performed using 2 ml of Trypsin/ EDTA (Sigma- Aldrich, Dorset, UK) per flask for 4 minutes. After the first passage cells were seeded into T75 flasks and for the experiments ADSCs between passages 3- 6 were used.

Cryopreserved ADSCs were also used. Previously isolated and characterized ADSCs were resurrected from cryogenic frozen vials and were cultured in T75 flasks which were then incubated in at 37°C and 5% CO_2. Regular inspections under inverted microscope were undertaken daily to visualize cell morphology of the growing cells and exclude any infections. Once the growing cells reached to a confluence of 80% passaging was performed using 4 ml of Trypsin/ EDTA (Sigma- Aldrich, Dorset, UK) per flask for 4 minutes. ADSCs between passages 3- 6 were used in all experiments.

2.2. Scaffolds

Electrospun Poly- (L)-lactic acid (PLA) scaffolds were produced with electrospinning technique (Figure 2.1). Polymer solutions were made by dissolving 10% w/v PLA (Sigma-Aldrich, Dorset, UK) (density: 1.24 g/ cm^3, M$_w$ 55-90K) in Dichloromethane (DCM) overnight on a benchtop shaker. After homogeneous solutions of suitable viscosities for electrospinning are formed polymer solutions were loaded into 5 mL syringes each fitted with an 18 G blunt tipped stainless steel needle (I&J Fisnar Inc.). Four syringes were loaded onto a programmable syringe pump (Aladdin 1000) attached to a purpose built electrospinning rig in a fume cupboard. The collector was wrapped with an aluminum foil and the distance between the tip of the blunt needle and the collector was arranged to be 17 cm. A copper plate punctured at 4 locations to form a diamond shape was fitted over the needles for equal distribution of electrical current. A crocodile clip that was connected to the voltage generator was than attached to the copper plate. The opposite charged end of the voltage generator was connected to the rotating collector with use of another crocodile clip. The syringe driver was set at a constant rate of 40µl/ min.   The voltage generator was set at 15kV. During electrospinning the formation of Taylor' s cone was observed at all times and excessive polymer solution that accumulated at the tip of the blunt needle was continuously removed with use of a sterile nonconductive rod. At the end of electrospinning the resultant sheet of scaffold was removed off the rotating collector along with the aluminum foil.

Figure 2.1. The electrospinning setup
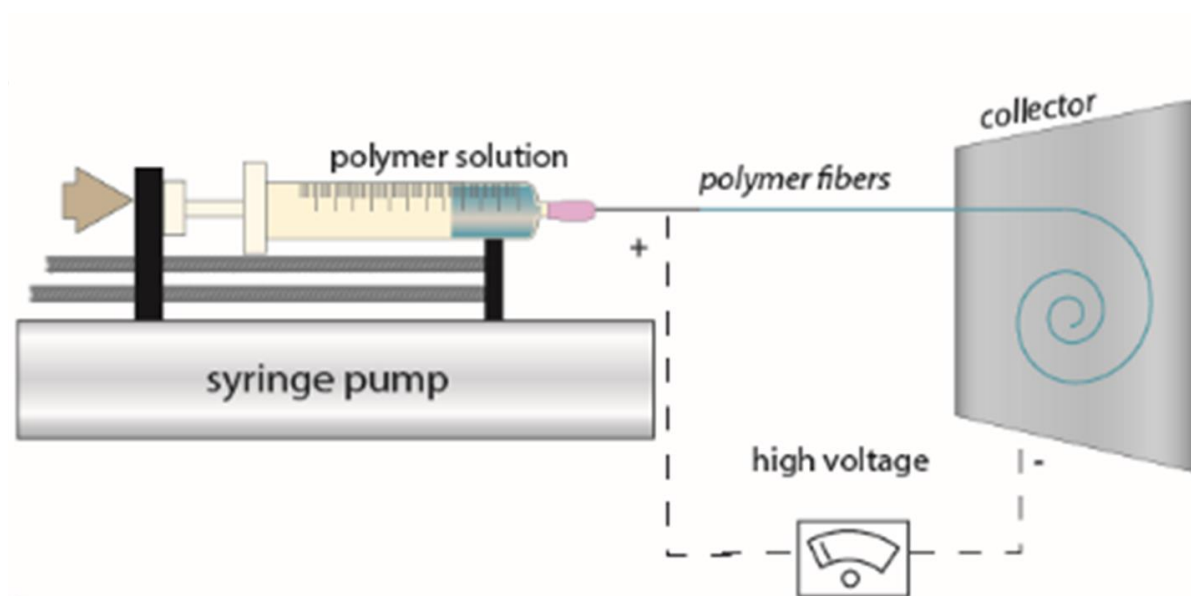
2.2.1. Preparation of drug releasing scaffolds

In addition to the standard electrospinning procedure described above, blend electrospinning and emulsion electrospinning techniques were used to form drug releasing scaffolds. A list of electrospun PLA scaffolds studied in this thesis is given in Table 2.1. In case of 17β Estradiol a homogeneous solution of the lipophilic Estradiol in DCM could be formed. Hence, a blend electrospinning technique where the drug is simply dissolved in polymer solution was used. However, in case of Vitamin C, the high hydrophilicity of the vitamin did not allow dissolution in DCM (Figure 2.2). Therefore, a stable emulsion of Vitamin C in polymer solution was formed before electrospinning.

Table 2.1. A list of biomaterials produced

Scaffold	Acronyms used	Technique of production	Ingredients
Electrospun PLA	PLA	Electrospinning	PLA
Estradiol releasing PLA	PLA Estradiol	Blend electrospinning	PLA, Estradiol
Emulsion electrospun PLA	Vehicle scaffold	Emulsion electrospinning	PLA, Span80, Water
Ascorbic Acid releasing PLA	PLA_AA	Emulsion electrospinning	PLA, Span80, AA in Water
Ascorbate-2 phosphate releasing PLA	PLA_A2P	Emulsion electrospinning	PLA, Span80, A2P in Water

Figure 2.2. Demonstration of preparation of stable emulsions from the polymer solution. In (A) phase separation of polymer solution when the water phase containing Vitamin C is added can be seen (red arrow). (B) is the stable emulsion obtained using the surfactant where water phase contains Vitamin C and oil phase contains PLA polymer. (C) control where only Vitamin C powder is mixed with polymer solution where the powder settles at the bottom and to the sides of the glass (blue arrow).
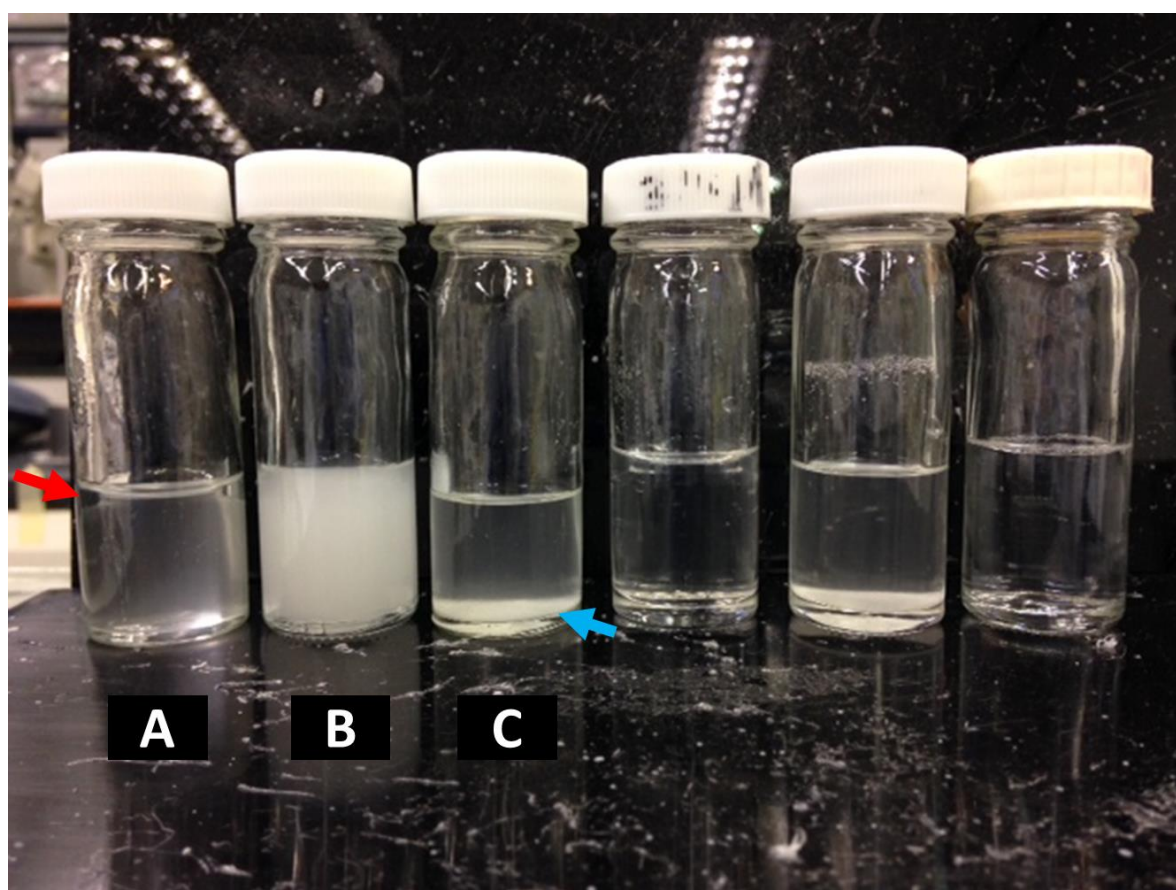
2.2.2. Emulsion electrospinning

After PLA polymer was dissolved in DCM as described above, 50 µl of surfactant, Span80 (Sigma- Aldrich), was added to the polymer solution while stirring at a rate of 250 RPM with the aid of a rotating magnet inside for 10 min. Two forms of Vitamin C were used: ascorbic acid (AA) and ascorbate-2 phosphate (A2P). Vitamin C was dissolved in 500 µl of distilled water and added drop wise into the polymer solution containing the surfactant while stirring at a rate of 1000 RPM. For control scaffolds (Vehicle scaffolds) distilled water without any drug was used to form an emulsion. The polymer solution was observed to turn into a milky, stable emulsion gradually. After a stable emulsion was formed all the emulsions were immediately electrospun. The resultant electrospun fibres are known to result in a core- shell morphology where the hydrophilic Vitamin C is in the core while the hydrophobic PLA polymer formed the shell (Figure 2.3).

Figure 2.3. Graphical demonstration of preparation of the emulsion electrospinning solutions. The hydrophilic Ascorbic Acid (AA) and Ascorbate- 2 – phosphate (A2P) dissolved in distilled water (dH$_2$O) were added into the polymer solution obtained by dissolving Polylactic acid (PLA) in dichloromethane (DCM). This emulsion forms a core- shell morphology upon electrospinning.
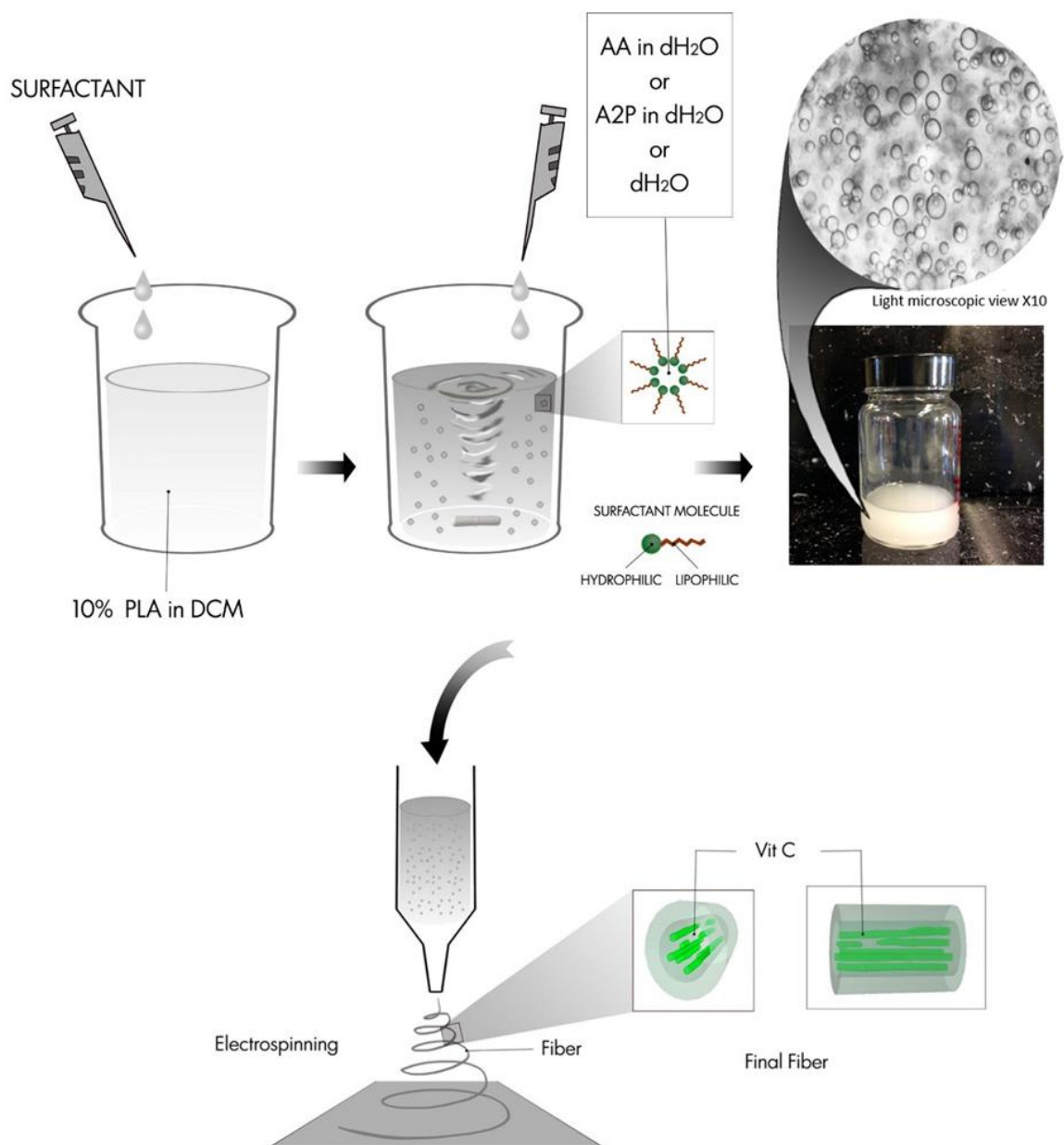
2.3. Characterization of scaffolds

2.3.1. Scanning electron microscopy

Scanning electron microscopy was performed to assess scaffold ultrastructure of plain scaffolds and to assess the deposited extracellular matrix on the cell seeded scaffolds.

On plain scaffolds, fibre diameters and pore sizes were examined on the SEM images of electrospun scaffolds. Dry samples of scaffolds were cut into 1x1 cm pieces and directly underwent gold sputtering (Edwards Sputter Coater S150B, Crawley, UK). Images were taken using a Phillips XL- 20 scanning electron microscope (Cambridge, UK).   The software ImageJ (National Institutes of Health) was used for measurements. For each experimental group three scaffold samples were examined with SEM.

For each piece of scaffold, four images were taken from the random sites within the scaffold. From each image taken, 10 fibres and 5 pores were randomly selected and the fibre diameter and pore sizes were measured. As a result, a total of 120 fibres and 60 pores were analysed per scaffold. A pore was defined as areas of void space bounded by fibres on all sides at or near the same depth of field.

For cell seeded scaffolds, the samples were fixed in 10% buffered formaldehyde solution for 10-15mins. After sequential incubation with 0.1M cacodylate buffer and glutaraldehyde in cacodylate buffer each for 20 minutes samples were washed in 0.1M cacodylate buffer twice for 15 min each wash. The samples were then incubated in osmium tetraoxide for 2 hours and in 0.1M cacodylate buffer for 15 min. Following these, samples were incubated in increasing concentrations of ethanol (75, 95, 100%) for 15 min each and were incubated for 30 min in 100% ethanol dried over anhydrous copper sulphate. Finally, the ethanol was removed and hexamethlydisalazine was added to the samples for 30 minutes and the samples were left to dry overnight. Dry samples were then mounted on 12.5 mm stubs and underwent gold sputtering with approximately 25 nm of gold (Edwards Sputter Coater S150B, Crawley, UK). Samples were imaged with a Phillips XL- 20 scanning electron microscope (Cambridge, UK).

2.3.2. Evaluation of the hydrophilicity of the scaffolds

The hydrophilicity of the scaffolds was mainly studied for Vitamin C releasing electrospun scaffolds as a significant change in hydrophilicity would be expected due to involvement of Vitamin C and the surfactant in the scaffolds. Hydrophilicity was studied by measurement of water contact angle and water uptake by the scaffolds.

Water contact angle measurement

Water contact angle measurement was performed by a contact angle goniometer (ramé- hart instrument co., NJ, USA). Scaffolds were cut into 1 cm x 1 cm squares and placed on the testing plate. Subsequently 0.03 mL of distilled water was carefully dropped onto the scaffolds and contact angles between water droplets and the scaffolds were measured immediately after dropping. Six samples were used at each test and average value was reported with standard deviation (±SD).

Water uptake measurement

Water uptake by scaffolds was assessed by incubating weighed 1x 1 cm pieces of each scaffold in 10 mL of PBS. Six samples for each group were weighed using a digital scale. Scaffolds were put in PBS and incubated at 37 °C for a total of 21 days. At days 1, 2, 3, 7, 14 and 21 scaffolds were carefully blotted with filter paper to remove surface water and weighed again. Water uptake of each scaffold was expressed as the percent increase in weight of the scaffold and calculated with the formula:

$(Weight_{wet} - Weight_{dry}) / Weight_{dry} \times 100$.

2.3.3. Mechanical testing

Uniaxial mechanical testing on scaffolds was performed using a BOSE tensiometer (BOSE Electroforce Test Instruments, MN). Samples were cut into 0.5x1 cm pieces and the thicknesses measured using a handheld micrometer thickness gauge. A small 22 N load cell was used in measurements. Samples were vertically placed between two grids and a ramp test was applied at a rate of 0.5 mm/ sec. The first failure point and plateau was used to calculate the ultimate tensile strength (UTS) and the displacement at this point (strain). The initial linear gradient of a plot of stress versus strain was taken as the Young's modulus (E).

2.4. Release of drugs from the scaffolds

2.4.1. Measurement of Vitamin C

Vitamin C was measured using two different methods: a spectrophotometric method and a UV- spectroscopic method. A spectrophotometric method was initially developed due to unavailability of other methods. As the UV- spectrophotometer become available in the Kroto S20 lab the release experiments were repeated. The UV spectroscopic method was less time consuming and allowed more accurate readings.

Spectrophotometric measurement of Vitamin C

A previously defined method called the 'Enzyme linked Ferric tripyridyltriazine spectrophotometric assay (EFTSA)' was used [128], [129]. In this assay the EFTSA solution which consists of acetate buffer, TPTZ (2,4,6-tripyridyl-s-triazine) and ferric chloride (FeCl3.6H20) is used to form a coloured ferrous tripyridyltriazine complex with reduction of ferric ion to ferrous ion by ascorbic acid at low pH. The absorbance of the ferrous tripyridyltriazine complex was read at 593 nm. Of the two forms of Vitamin C, ascorbic acid was directly measured with this method whereas A2P was first enzymatically converted to AA [130].

Briefly, after 2 parallel samples from each solution of Vitamin C were incubated for 5 min in 37°C water bath with or without 4 units/ mL of ascorbate oxidase (AO). Then in the presence of acetate buffer at pH 3.6, 8mM tripyridyltriazine (TPTZ) and 20mM Ferric chloride solutions were added. After 5 min incubation at room temperature, the absorbance was measured at 593 nm in a colorimetric plate reader (Bio- TEK, NorthStar Scientific Ltd, Leeds, UK). The difference between AO negative and positive readings were related to the presence of AA (Figure 2.4). For A2P measurement, samples were first incubated 15 min at room temperature with acid phosphatase (25 mg/mL in 0.1 M citric acid buffer at pH 4.8) to convert AA to A2P. The concentration of unknown solutions was determined with the aid of standard curves plotted for AA. The standard curves obtained with this method is demonstrated in Figure 2.4. Solutions of AA in both distilled water and PBS between 0.3 and 600 μM were studied. The lower limit of detection of AA (>6 μM) with this method was found to be lower when it was dissolved in distilled water compared to PBS (>60 μM). This is due to oxidation of AA with the metal ions present in PBS.

Figure 2.4. An example of running parallel samples with EFTSA method for detection of ascorbic acid (A). Standard curves obtained with this method in PBS and distilled water (B).
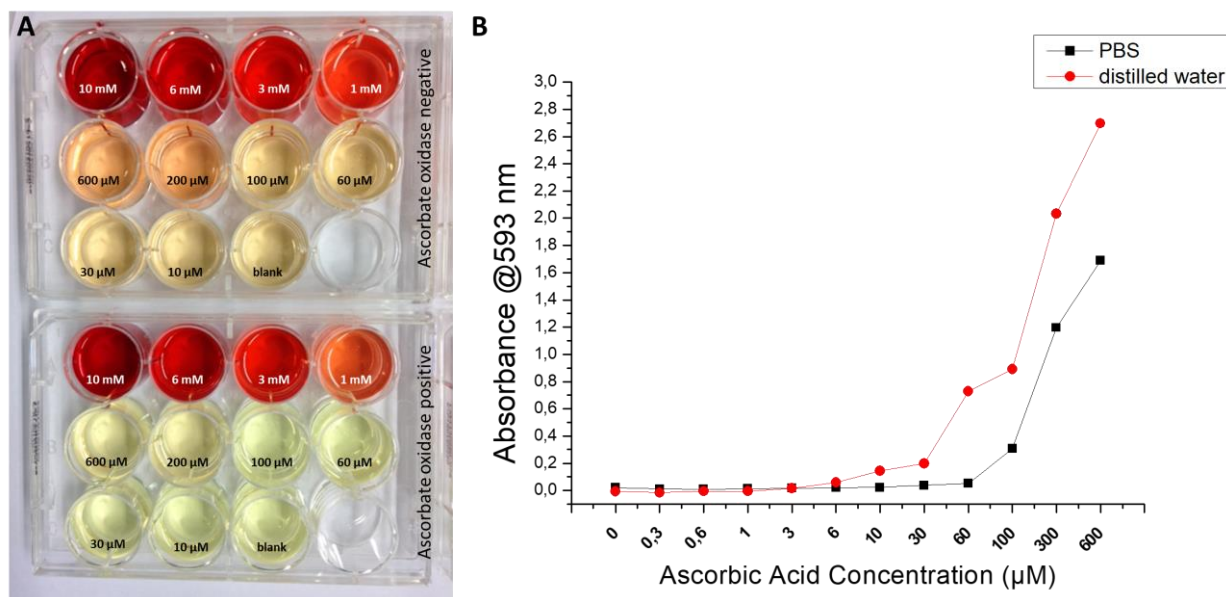
After construction of the standard curves, preliminary experiments were undertaken to detect AA released from scaffolds using the spectrophotometric method. For this scaffolds were cut into 3x3 cm square pieces and put into distilled water. On 8th, 24th, 48th and 72th hours samples were taken from distilled water and AA concentration was determined using the standard curve for the spectrophotometric assay. After the distilled water was either replaced or all the media was completely changed. The preliminary release curves obtained using the spectrophotometric method was demonstrated in Figure 2.5. The amount of AA detected in media continuously decreased after 3 days when it went down to undetectable levels. This demonstrated that AA was not only oxidized by the metal ions in media but also with the oxygen in the environment and incubator. A2P could be measured to increase consistently for 28 days when measured by sampling the media. A2P could not be measured after day 10 when replacing the media most probably due to released concentrations below the lower limit of detection of this test.

Figure 2.5. The release of AA and A2P from electrospun PLA scaffolds as measured by the spectrophotometric method.

Release of Ascorbic Acid (AA) from scaffolds
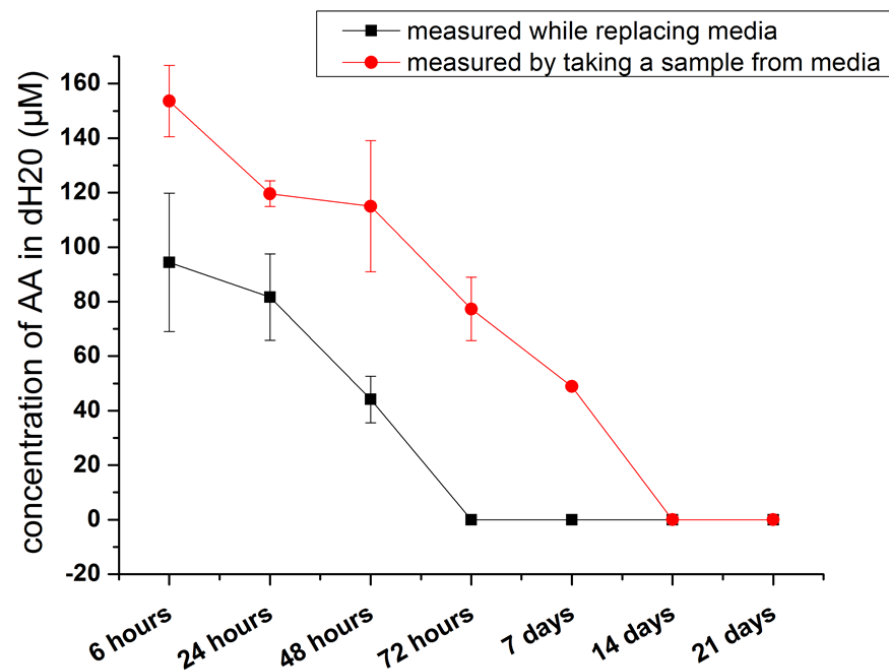
Release of Ascorbate-2 phosphate (A2P) from scaffolds
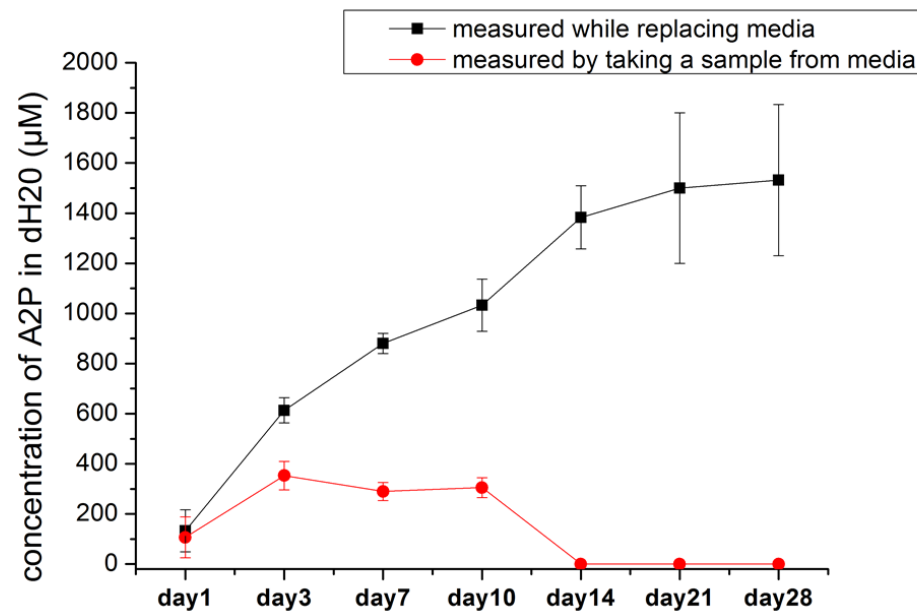
Therefore, AA could be detected as released from the electrospun PLA scaffolds using the spectrophotometric method however this had some important limitations. Firstly, the release could only be studied in distilled water to avoid interference with method of detection of AA with use of PBS. This is not ideal as the release studies are more relevant when performed in physiologically similar media and conditions. Secondly, even when distilled water was used, detection of AA, not A2P, was still very limited probably because AA oxidized immediately with oxygen in the air and became undetectable soon after it was released. Therefore, AA became undetectable after 72 hours whereas A2P was still detectable on day 28. Thirdly, the lower limit of detection for the spectrophotometric method was high (>30 µM) which precluded measurement of small changes in concentration. Thus the spectrophotometric method to measure AA release from the electrospun PLA scaffolds had significant limitations.

UV- spectrophotometric method

Vitamin C was also measured using a UV- spectrophotometer (Thermo Scientific^{TM} Evolution 220) at an absorbance wavelength of 252 nm. A calibration curve was constructed by measuring 8 concentrations of vitamin C (lowest: 10 nM and highest: 100 µM) prepared in distilled water (Figure 2.6). All solutions were freshly prepared and the absorbances were immediately measured. The lower limit of detection for Vitamin C with this method was 300 nM and upper limit of detection was 100 µM.

Figure 2.6. The standard curve for measurement of Ascorbic acid using UV- spectrophotometry.
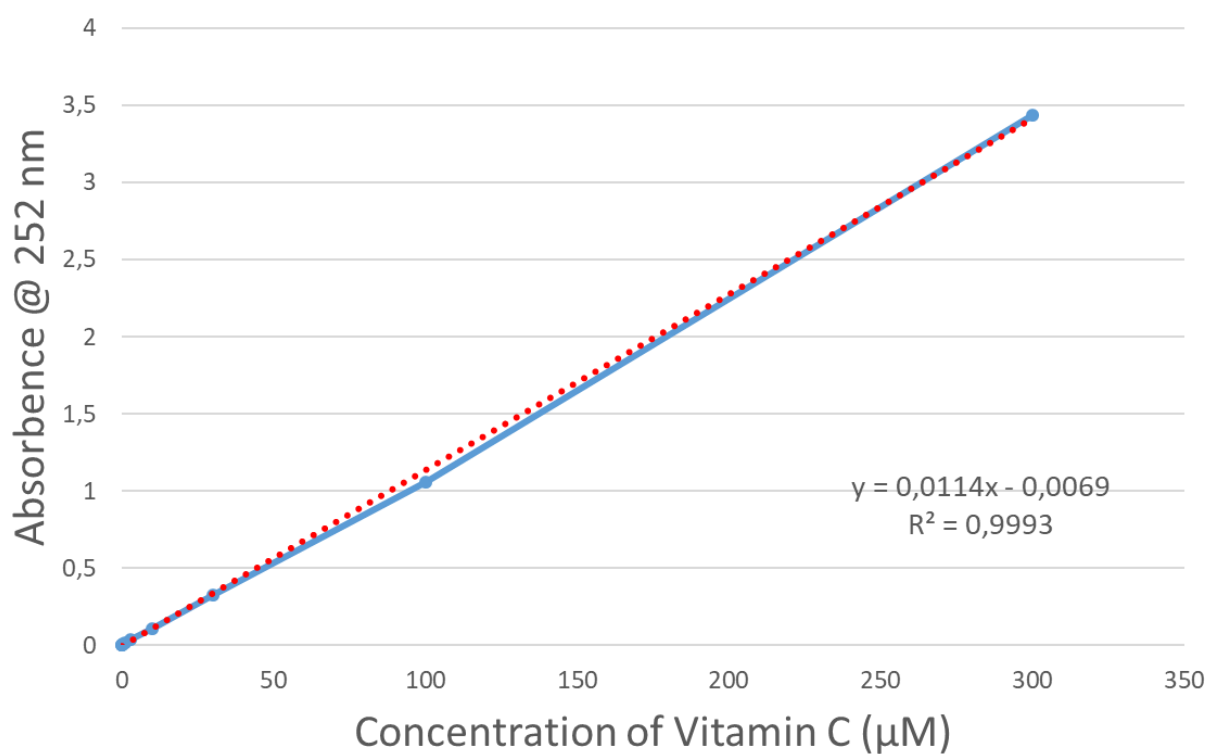
To detect release of Vitamin C from electrospun scaffolds a 1x1 cm piece of scaffold was placed in 4 mL of media and was kept in a dry incubator at 37°C. At 2, 4, 6, 8, 10 hours and daily afterwards a sample was removed from the media and the concentration measured. A vehicle scaffold with neither AA nor A2P was taken as a control. All the media was then removed and replaced with a fresh sample. These steps were repeated at each time point.

2.4.2. Measurement of Estradiol

Measurement of Estradiol was performed initially by a spectrofluoremeter and subsequently by UV- spectrophotometer. The release experiments for a duration of 6 months was initially started by Dr Christopher Hillary. The release of Estradiol from PLA scaffolds constructed within the current PhD studies was mainly studied using UV- spectrophotometer for a duration of 28 days.

Spectrofluorometric detection of Estradiol

A concentration ranges of Estradiol between 10 nM and 100 µM in PBS were measured using (Kontron SFM 25 spectralflurometer) at λ_{ex}277nm/λ_{em}310nm. Standard curves were constructed and used thereafter to determine an unknown concentration of the drug in solution during the release experiments (Figure 2.7).

UV- spectrophotometric detection of Estradiol

Estradiol was also detected using a UV- spectrophotometer (Thermo Scientific^{TM} Evolution 220) at an absorbance wavelength of 220 nm. Standard curves were constructed using a concentration of 10 nM and 100 µM in PBS and used to determine an unknown concentration of the drug in solution during the release experiments.

Figure 2.7. The standard curves for measurement of Estradiol using the spectralflurometer (A) and the UV- spectrophotometer (B).

y = 3,8347x + 2,5491
R² = 0,9992
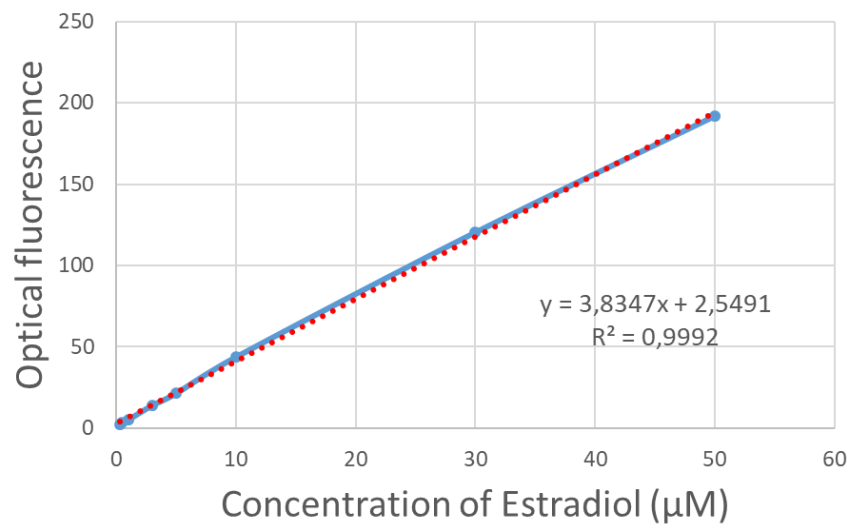
Lower limit of detection: 300 nM
Upper limit of detection: <100 µM

A

y = 0,0063x - 0,0009
R² = 0,9984
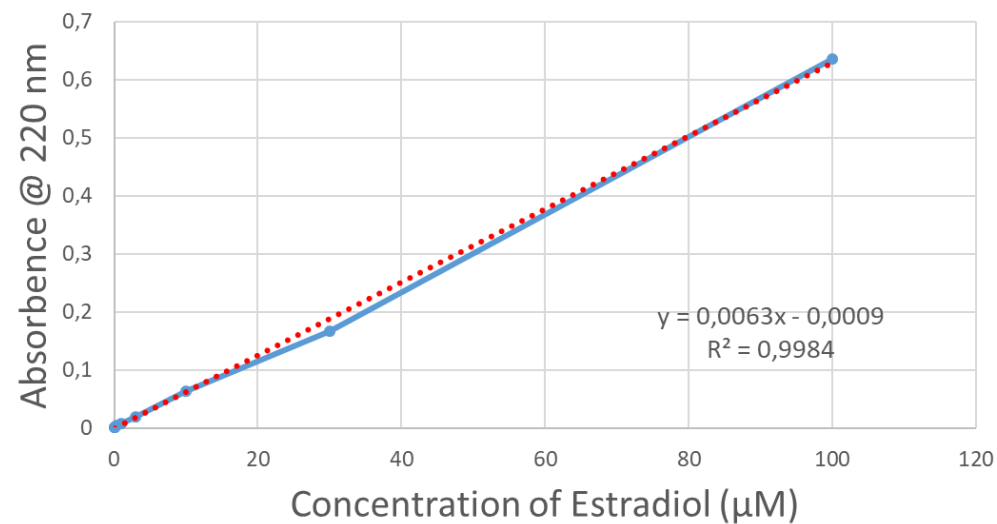
Lower limit of detection: 30 nM
Upper limit of detection: <300 µM

B

2.5. *In vitro* evaluation of scaffolds

2.5.1. Evaluation of metabolic activity by resazurin assay

In all experiments using cells in 2D or 3D cell metabolic activity was measured by a resazurin assay. A stock solution of resazurin sodium salt (Sigma-Aldrich, Dorset, UK) was first prepared by dissolving 0.124g wt/v of resazurin in 100mL of phosphate buffer saline (PBS). Dilutions of this stock solution in 1:20 was used for experiments. After the culture media was removed from each well the cells were washed with PBS and resazurin solution was added into each well. Cells were incubated for 60 min at 37°C in 5% CO_2 atmosphere. Then 100 µl of resazurin solution was pipetted out from each well and transferred into a 96 well plate. Absorbence was measured at 570 nm in a colorimetric plate reader (Bio- TEK, NorthStar Scientific Ltd, Leeds, UK). Culture wells without cells or cell free scaffolds in media were used as reagent blanks. Samples were then washed of the dye and either fixed with 3.7% formaldehyde or replaced with culture media if experiments were to be continued. Each measurement was performed in triplicates.

2.5.2. Measurement of total collagen with Sirius red staining

Total collagen production by the cells in 2D and 3D were measured using Sirius red staining (Figure 2.8). Sirius red is an elongated birefringent molecule that contains six salt-forming (-SO3H) sulfonic groups. It binds to a variety of molecules in tissues however when bound to collagen it attaches parallel to fibrillary collagen enhancing its natural birefringence. Birefringence refers to an optical property of a material that reflects the light in a manner that is dependent on the orientation of the molecule relative to the light hitting them. In other words optically anisotropic materials are referred to as being birefringent. The Sirius red staining relies on birefringent properties of the fibrillary collagen.

When the Sirius red stained tissues are examined under bright field microscope, all the proteins in the tissue would be visualized as Sirius red binds all. Visualizing Sirius red stained tissues under polarized light allows effective identification of collagen networks and appreciation of potential collagen alterations. Therefore, Sirius red stained samples need to be visualized under polarized light to show collagen specificity. The method used in these

studies relies on eluting the Sirius red that is first bound to all extracellular matrix elements produced by cells grown on the scaffolds. This is than measured using spectrophotometry.

Samples that were previously fixed in 3.7% formaldehyde were washed 3 times with PBS. Two mL of Sirius red stain (0.1% Direct Red 80 in saturated picric acid, Sigma- Aldrich) was added to each sample of monolayer cultured fibroblasts or fibroblasts grown on scaffolds. Samples were left to stain on a benchtop shaker for 16 hours. Afterwards excess stain was washed off with distilled water until the wash out water ran clear. Then specimens were left to dry under fume cupboard. Dry samples were pictured and weighed. The stain was then eluted with 2 ml 0.2 M NaOH: methanol 1:1 for 15 min. The absorbance was measured at 490 nm. Acellular scaffolds acted as controls for calculating collagen production. Results were expressed as Sirius Red stain per gram of PLA.

Figure 2.8. An example of how the Sirius Red staining was used to measure total collagen production of human dermal fibroblasts in tissue culture plastic (2D) and on scaffolds (3D). Yellow arrow shows a scaffold on which no collagen was produced and blue arrow shows an obvious collagen production on the scaffold stained by the Sirius red. In between a range of staining can be observed.
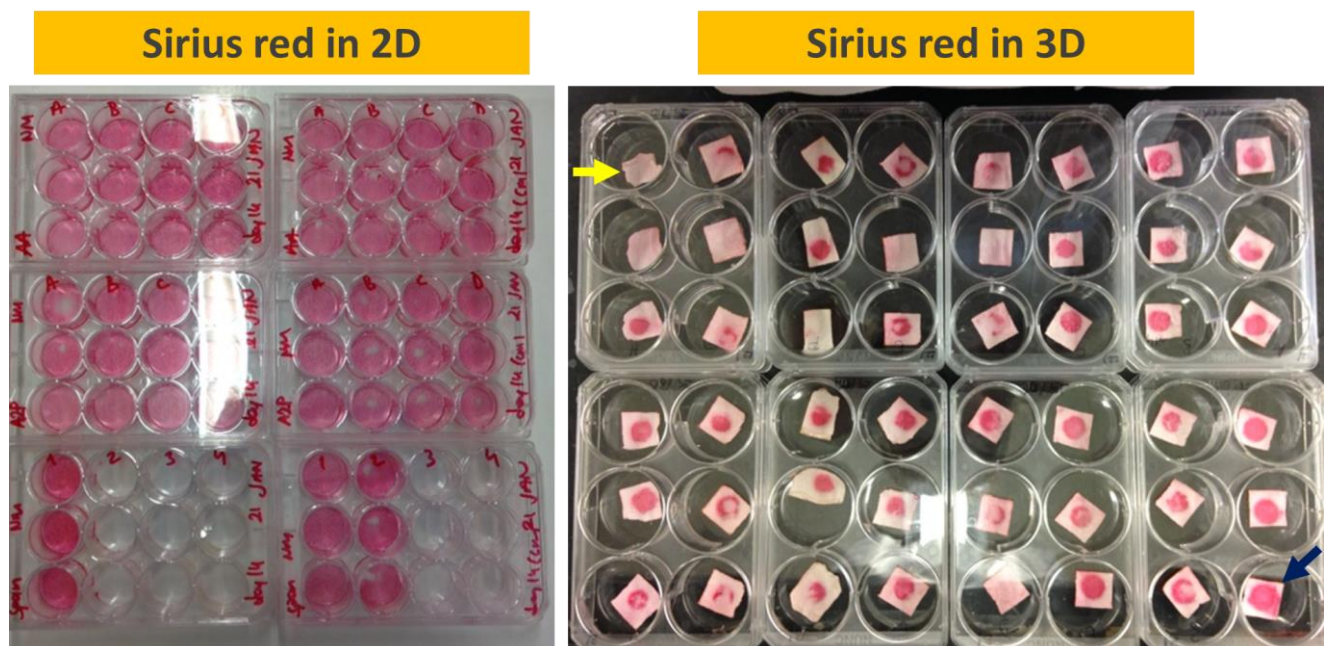
2.6. Evaluation of angiogenic properties of the scaffolds

The angiogenic potentials of the bioactive factors incorporated into the scaffolds were assessed using the chick aortic ring assay whereas the angiogenic potential of the final scaffolds were evaluated in a chick chorioallantoic membrane (CAM) assay. The aortic ring assay is an organ culture assay that allows studying a wide range of concentrations of bioactive factors whereas the CAM assay was used as an *in vivo* assay to test the angiogenic response to the final scaffolds as well as the initial tissue response to the biomaterial.

2.6.1. Chick aortic ring assay

2.6.1.1.Description of the methodology

<u>Incubation of fertilized eggs</u>

Pathogen-free fertilized white leghorn chicken eggs (Gallus gallus domesticus) were obtained from Henry Stewart Co. Ltd (UK). Care was consistent with the guidelines of the Home Office, UK. The fertilized eggs were incubated at 37°C in a humidified egg incubator for 12-14 days. Between embryonic development days (EDD) 12- 14 the eggs shells were cracked, embryos were taken out and sacrificed immediately by decapitation. A vertical incision on the chest wall was made on the midline and the heart of the chick was dissected out together with the aortic arches. The aortic arches, surrounding connective tissues and the heart of the chick embryo was placed in PBS. The remaining body parts were disposed of in line with Home Office requirements.

<u>Preparation of aortic rings for organ culture</u>

Under a dissection microscope placed inside a culture hood, the aortic arches were cleaned of the surrounding connective tissue using fine forceps and scalpel and the aortic arches were separated from the heart by cutting through the attachment of aortic roots at the ventricles of the heart. At the end of this procedure 3 aortic arches attached to a single common root and 2 other arches attached to another common root was obtained (Figure 2.9). Further dissection of the connective tissues around the aortic arches was performed until the collagenous outer wall of the aorta (the adventitia) was exposed completely. Thereafter each tubular branch of the aorta was cut into 1 mm rings under a stereomicroscope.

Figure 2.9. Dissection of aortic arches from the chick embryo. (A) The chest wall is opened to see the the heart and the aortic arches (arrows). (B) The aortic arches attached to the heart is next cut out. (C) The aortic arches of the chick embryo, dissected from all the surrounding connective tissues and ready to be sliced for the aortic ring assay. (scale bars 0.5 cm for all images)
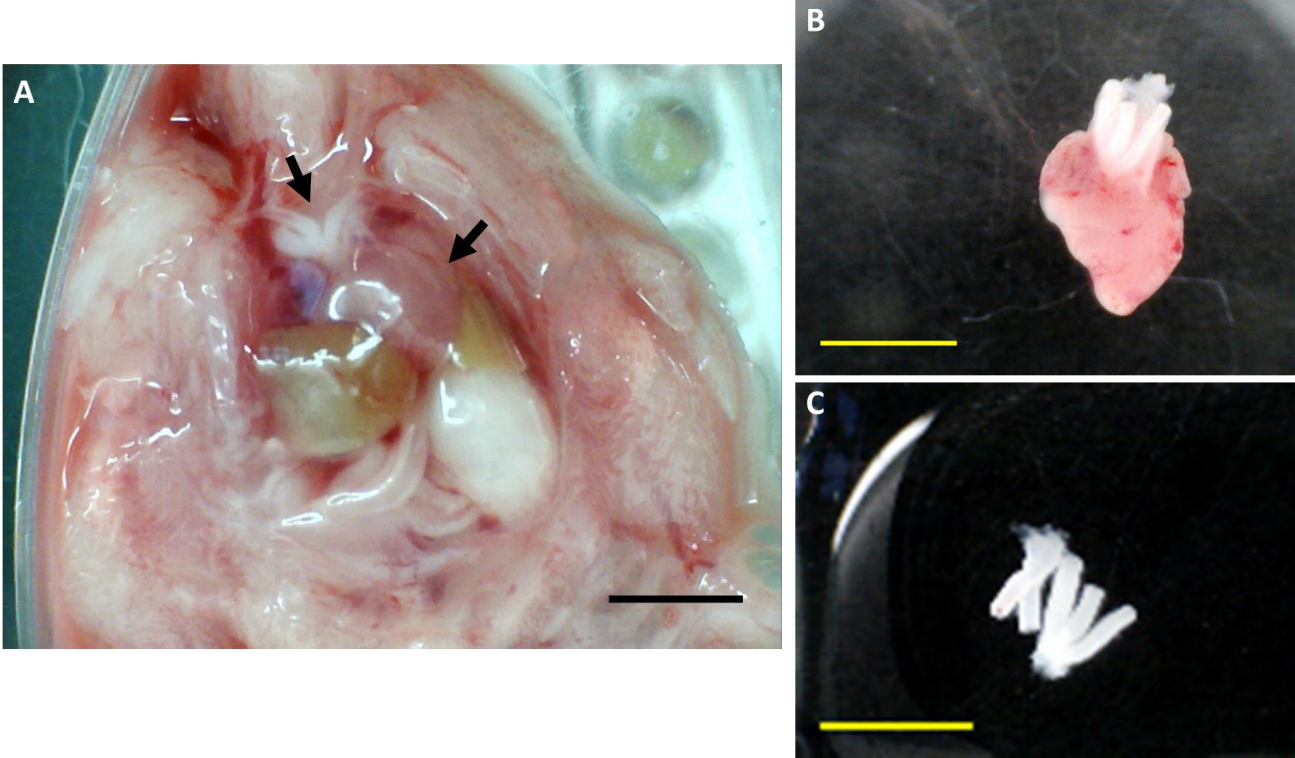
Culturing the aortic rings

Between 20- 25 aortic rings can be obtained from each embryo. Aortic rings were collected in PBS and immediately after the completion of the dissection aortic rings were embedded in 50 μL of Matrigel® (Basement Membrane Matrix, Corning®) in a 24 well plate. After 30 min of incubation in Matrigel allowing gelation of the Matrigel, MEM (supplemented with 2.5% FCS, 50 unit's/mL penicillin and 50 μg/mL streptomycin, GIBCO, Carlsbad, CA) (2 mL) was added into each well. The aortic rings were incubated in a cell culture incubator at 37°C and 5% CO_2 for 3- 5 days. Normal growth of endothelial cell sprouts in the chick aortic arch assay is shown in Figure 2.10.

If the experiments involved drug testing the required concentration of the drug was added into the culture media. In experiments where co- culture of aortic rings with different cell lines (e.g. ADSCs) was intended, a transparent tissue culture insert (Greiner Bio-One GmbH) was used to contain the desired component of co- culture. The endothelial sprouts were observed under an inverted microscope between days 3 and 5. The pictures taken at each time point and the longest sprout length for each sample was calculated. Endothelial cell sprouts had a typical appearance of long, micro tubular elongations originating from the inside of the aortic ring and forming endothelial cell lacunae as if they were forming blood vessel lumens between themselves (Figure 2.11). Endothelial cells were further characterized by immunofluorescence staining with Griffonia Simplicifolia Lectin I, isolectin B4 (Vector Laboratories, Burlingame, USA) that stained endothelial cells (Figure 2.12).

Figure 2.10. Normal growth of the endothelial cell sprouts from day 3 to day 5 in the chick aortic ring assay. The tubular endothelial cell sprouts can be seen in close view (red arrows) and the endothelial cell branches connect with each other to form a lumen (yellow arrow). (black scale bar: 1 mm; yellow scale bar: 0.2 mm)
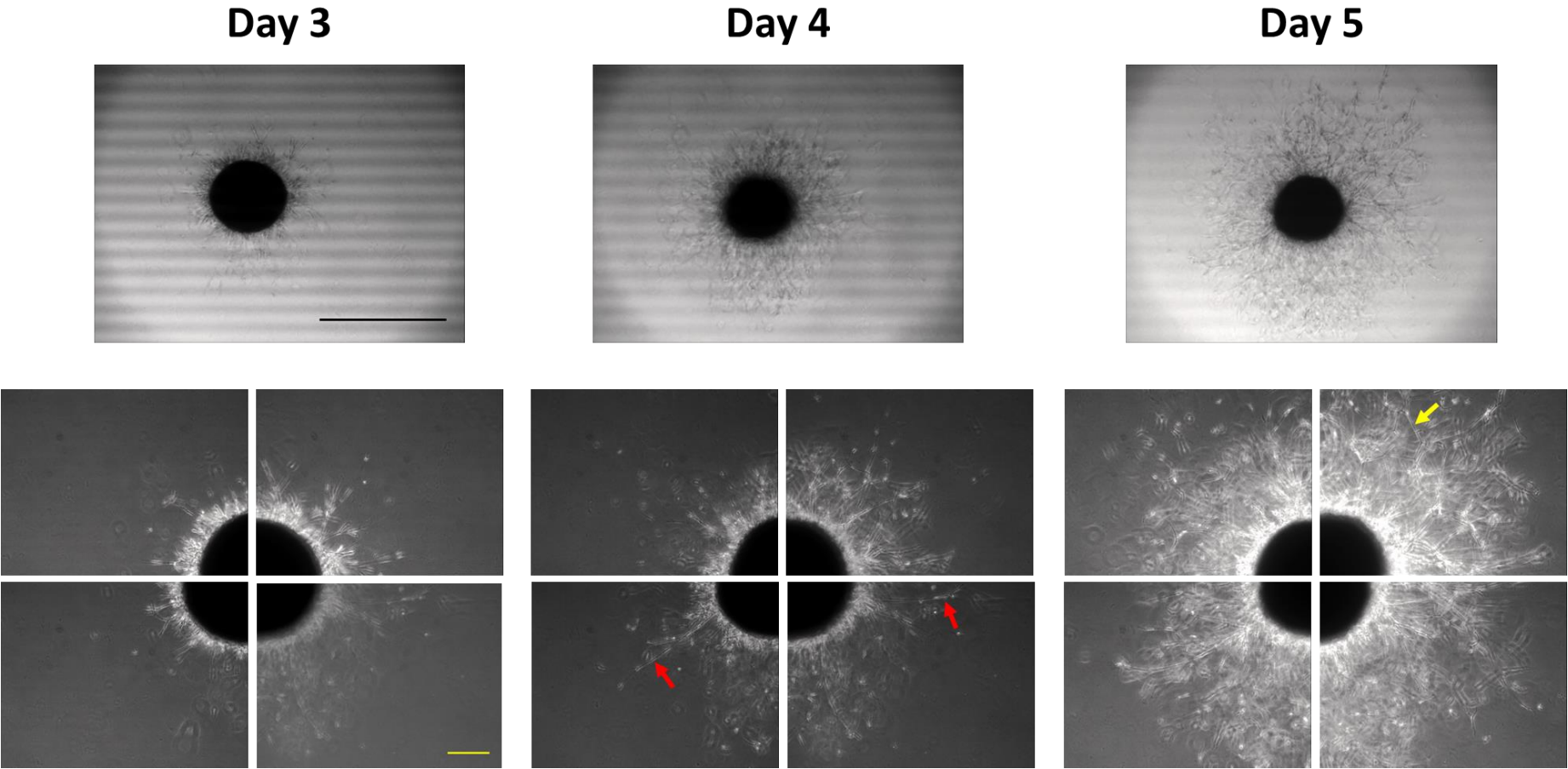
Figure 2.11. Observation of the endothelial cell sprouts in the chick aortic ring assay. Firstly, endothelial cell sprouts appearing like long microtubules appear on day 3 of organ culture assay (red arrows in A). The tubules than start branching (B) and the branches then connect with each other to form the typical vessel lumen- like structures (red arrows in C & D) that can only be fully seen adjusting the focus as they are on 3D matrix.
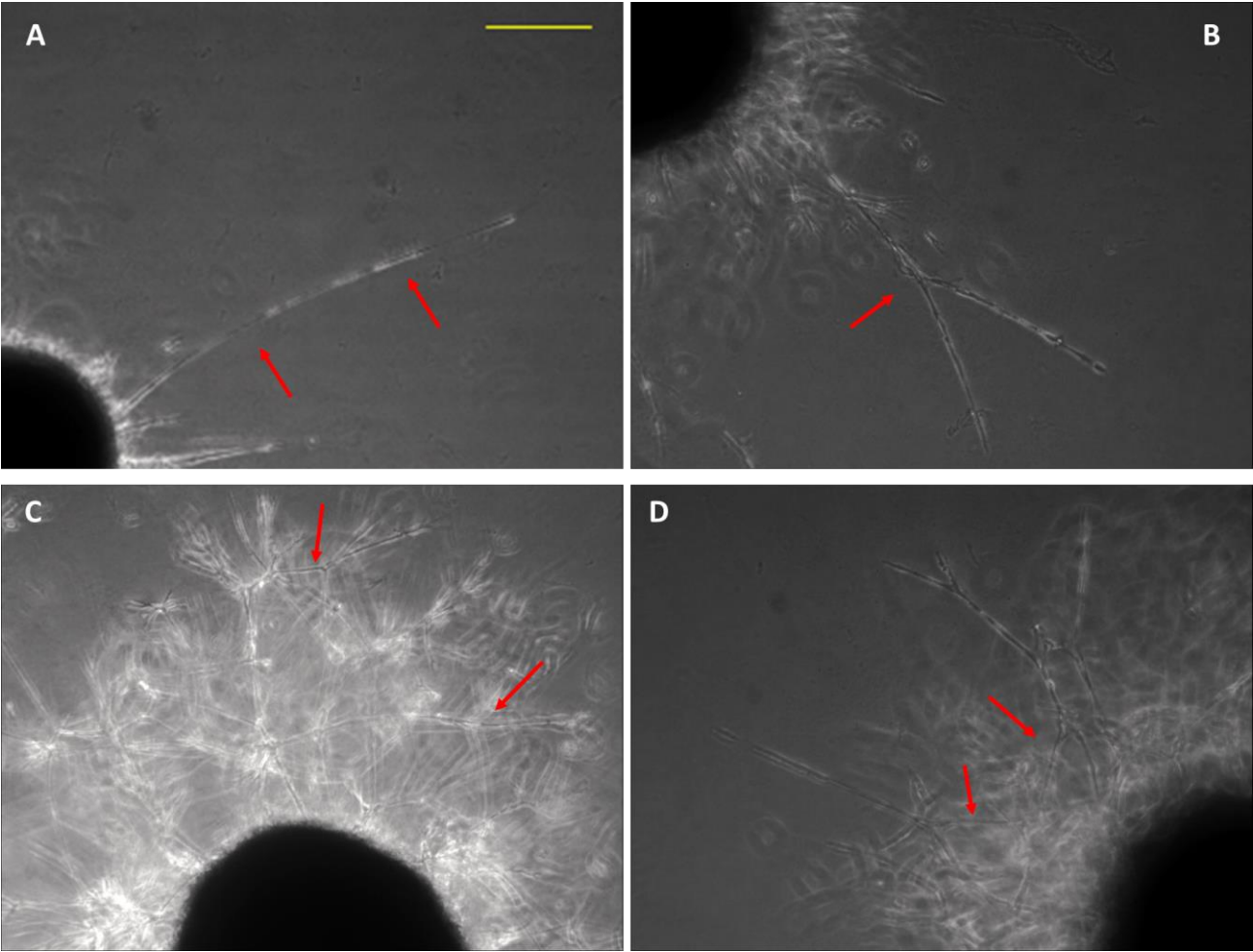
Figure 2.12. Characterization of the endothelial cell sprouts in the aortic ring assay. Staining with isolectin B4 (A) for endothelial cells, DAPI (B) for the cell nuclei and the combined images (C- D). Endothelial cell membranes appear green with isolectin B4 staining (A) and all cell nuclei appear blue with DAPI staining (B). Combining the two images allows visualization of endothelial sprouts. Error bar in A represents 200 μm and is applicable to all images.
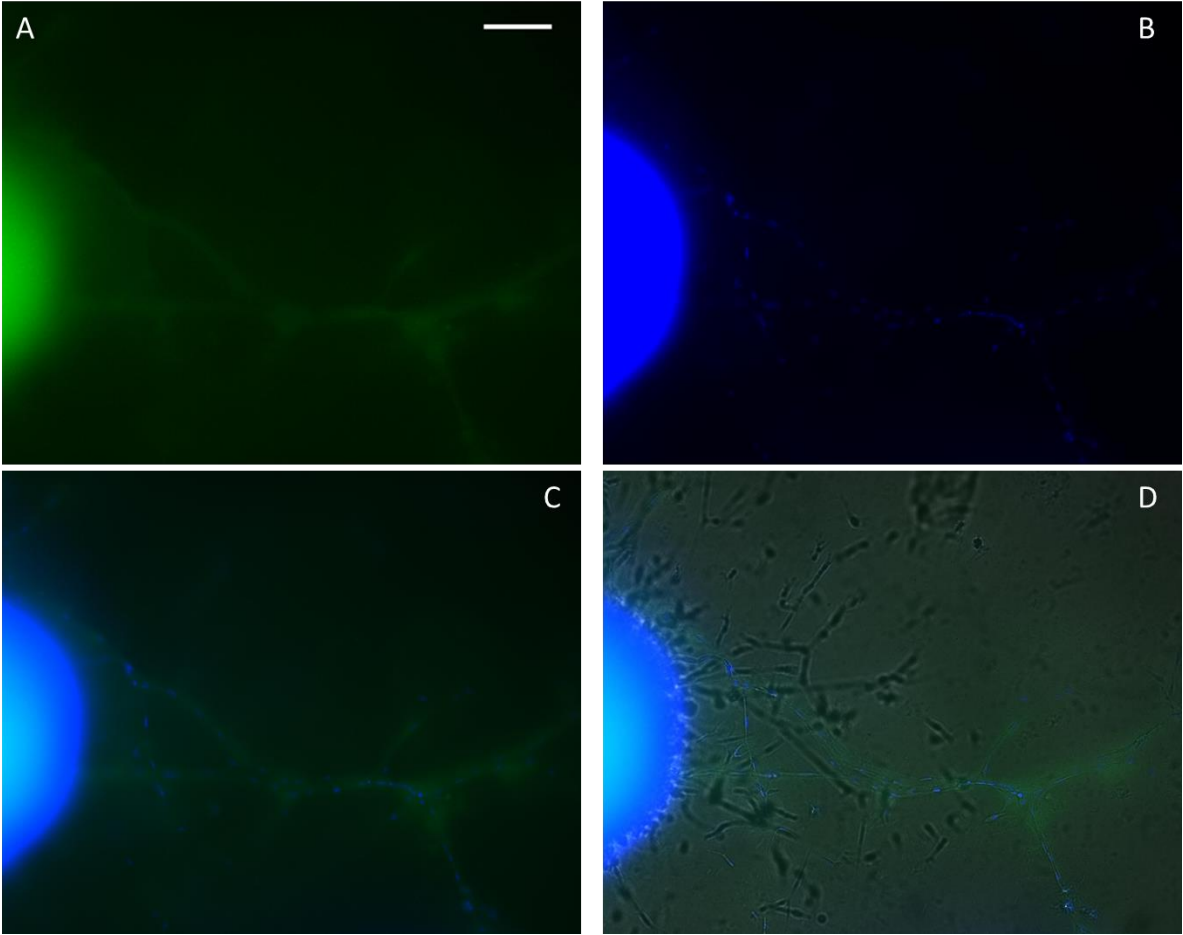
2.6.1.2. Optimizations in the chick aortic ring assay
Use of collagen as an extracellular matrix in the chick aortic ring assay

The endothelial cells need a 3D extracellular matrix to facilitate formation of the typical endothelial morphology in cell culture. For the aortic ring assay although classically Matrigel has been chosen as the ECM to embed the rings into [131], some literature suggested use of other ECM elements such as collagen and fibrin. Therefore, in the preliminary work, collagen type I was used as an ECM to grow the aortic rings in (Figure 2.13). This had led to extremely suboptimal results because with collagen matrix the endothelial cell sprouting was very difficult to observe under light microscopy. This could be for 2 reasons: i) the collagen matrix facilitated growth of fibroblastic/ dendritic cells along with endothelial cell sprouts making the endothelial cell sprouts invisible, ii) after day 3-4 days of the organ culture assay the collagen matrix started degrading resulting in formation of empty spaces in the matrix which also led to displacement of the aortic ring inside the gel. It appears that the ideal extracellular matrix to stimulate formation of endothelial cell sprouts and micro tubular structures should contain basement membrane proteins [132]. Therefore, use of collagen type I in aortic ring experiments was abandoned and Matrigel was used as a standard ECM for aortic ring assay.

Use of mouse aortic rings

The aortic ring assay was initially described and performed on the rodent aortic rings [133]. Using rodent tissues could have several advantages over using chick tissues. Firstly, the rodents are genetically more similar to humans and secondly the range of proteins and markers that could be used with mouse tissues are more widely available compared to those of chickens. Therefore, during the course of this PhD studies mouse aortic rings were obtained from freshly sacrificed mouse aortic tissues (biological Services, The University of Sheffield) and dissected under the microscope within 4 hours of scarification. The rings were cut into 1 mm thick slices and embedded in Matrigel as described above for the chick aortic ring assay. The maximum endothelial cell sprout growing from the mouse samples are shown in Figure 2.14. Out of 42 samples obtained from 2 different experiments measurable endothelial cell sprouts can be obtained only from 4 of the mouse aortic rings at 8 days of culture even with supplementation of media with fibroblast growth factor and vascular endothelial growth factor. Therefore, the mouse aortic ring was not as responsive as the chick aortic ring in the preliminary experiments. An obvious reason was that the embryonic tissues would have more regenerative capacity compared to adult tissues (aortic rings of the adult mice).

Figure 2.13. Using collagen as a matrix to grow chick aortic rings. Starting from day 3 the collagen matrix degrades leaving empty spaces around the aortic ring (red arrows) and pushing the ring to the side of the circular collagen collagen matrix.
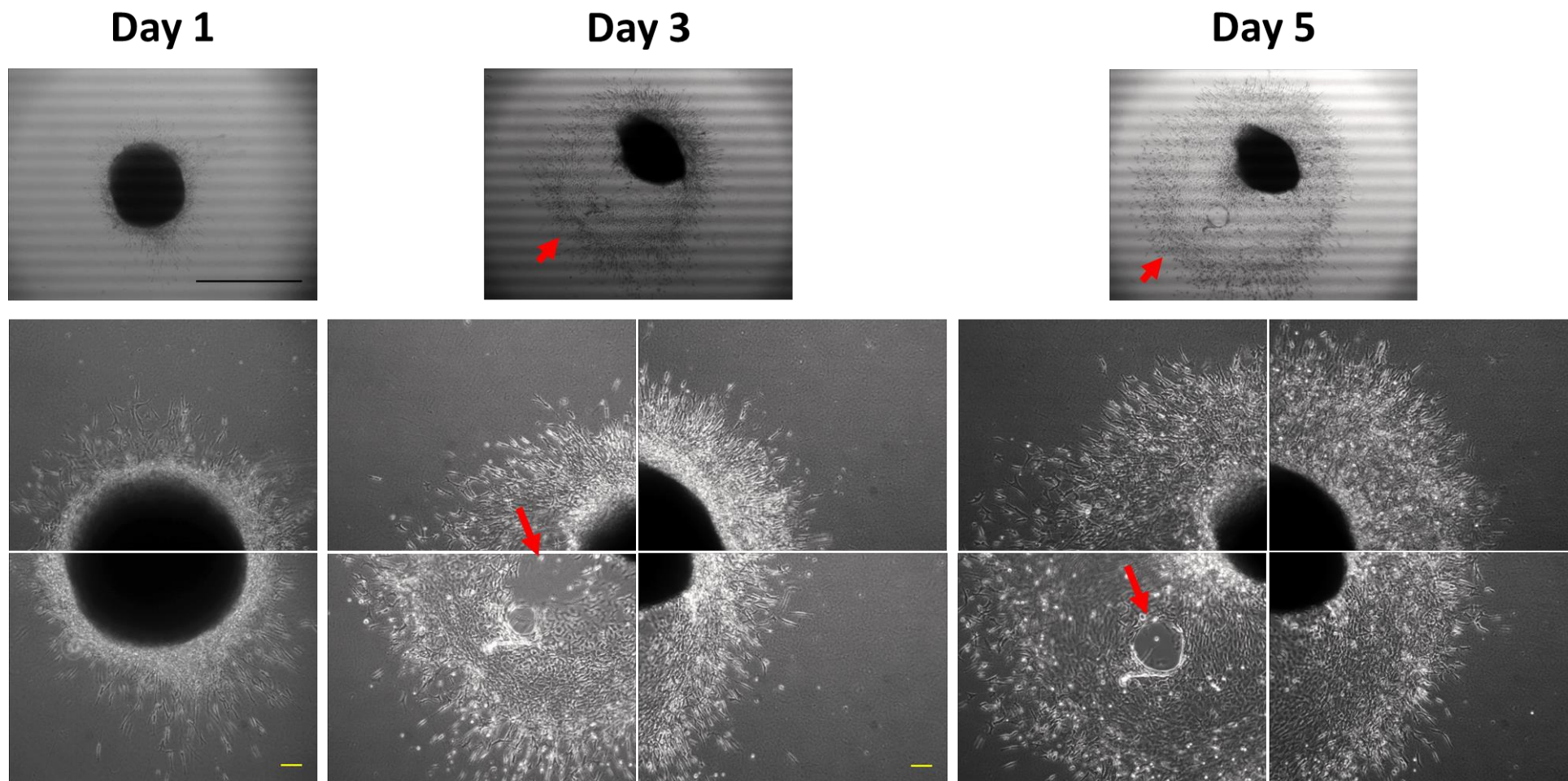
Figure 2.14. Preliminary findings of mouse aortic ring experiments. The most commonly encountered response at day 8 of organ culture with mouse aortic rings (A). Average response of the 4 samples where a measurable endothelial sprout could be observed (red arrow) (B). The maximum response as obtained by supplementation of the culture media with fibroblast growth factor (C) (Scale bar 0.2 mm).

The chick embryo metatarsal assay

Another organ culture assay that could have been used is the chick embryo metatarsal assay. Although this methodology had not been defined before, the mouse embryo metatarsal assay has been described previously [134]. The same methodology was used to create a culture of chick metatarsal/ phalangeal bones of the developing chick embryo on embryonic development days 12- 14. The preliminary results are shown in Figure 2.15. Although this assay was feasible the dissection of the surrounding connective tissues from the bones of chick metatarsal bones were difficult and required more delicate instruments. Furthermore, the phalanges were easier to dissect and could have given better results however this needed to be defined as a methodology first requiring further set of intense experiments. Therefore, this methodology was also abandoned.

Figure 2.15. The preliminary findings of the chick embryo metatarsal assay. The chick embryo metatarsal bones embedded in Matrigel can be seen in the upper row images. A closer view shows the endothelial cell sprouts growing from the periosteum on day 3 of the culture (red arrows) (Scale bars 0.2 mm).
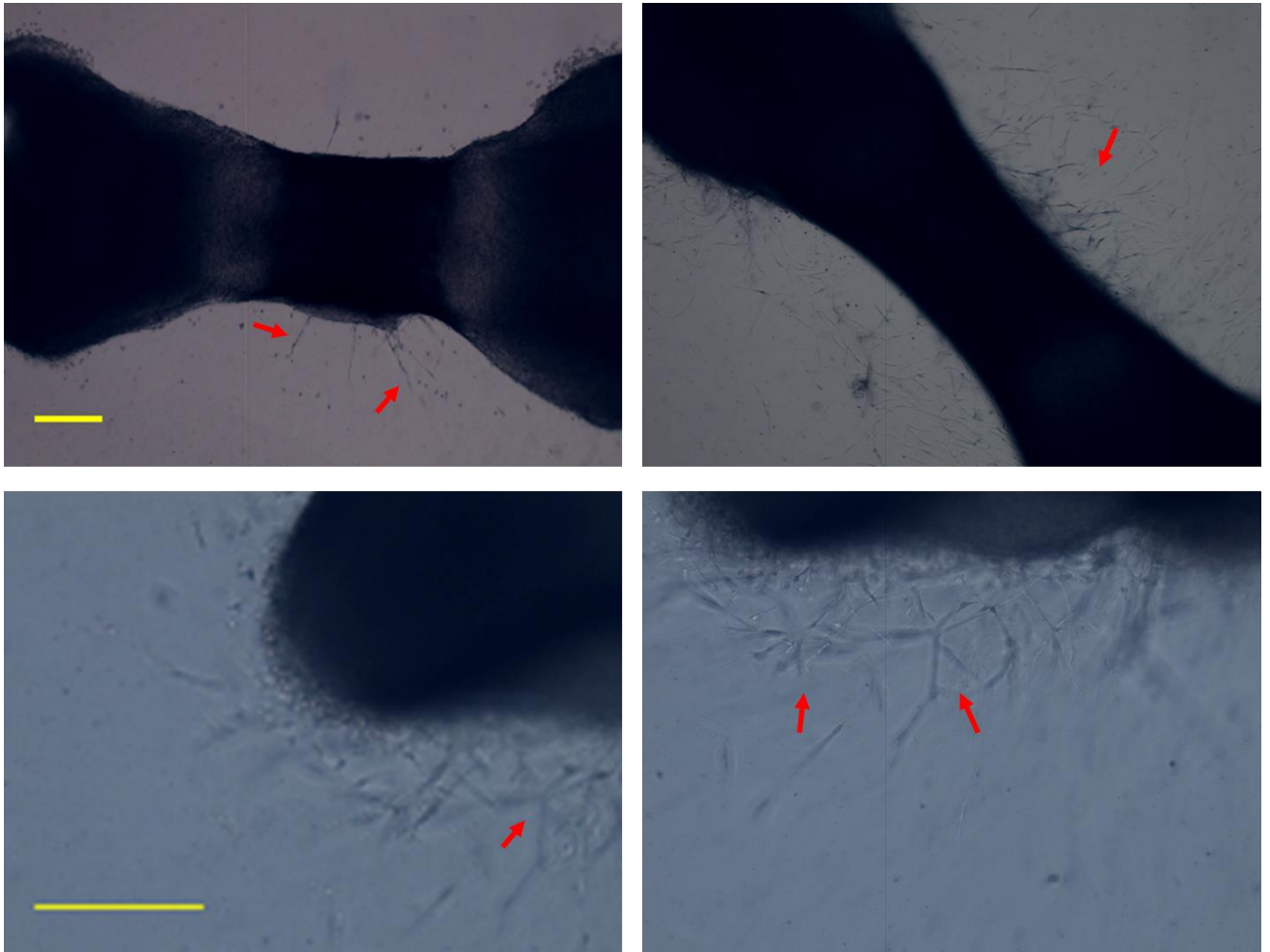
2.6.2. The chick chorioallantoic membrane assay

The CAM assay methodology is presented in the next chapter.

2.7. Statistical analysis

Statistical analysis was performed with SPSS v. 17.0. The differences between percentages were compared using Chi- square test. Differences between two group means were analysed with Student' s T test when the data was normally distributed and with Mann Whitney U test otherwise. Survival of the chick embryos were analysed with Kaplan Meier method. Correlation between two continuous variables was assessed by Pearson correlation test. A p value of <0,05 was considered statistically significant.

Chapter 3.
The *ex ovo* CAM assay

Mangir, N., Raza, A., Haycock, J. W., Chapple, C. & Macneil, S. An Improved In Vivo Methodology to Visualise Tumour Induced Changes in Vasculature Using the Chick Chorionic Allantoic Membrane Assay. *In Vivo* 32, 461–472 (2018)

Mangır N, Dikici S, Claeyssens F, MacNeil S. "Using ex ovo chick chorioallantoic membrane (CAM) assay to evaluate the biocompatibility and angiogenic response to biomaterials" under review in *ACS Biomaterials*.

3.1. Chapter Introduction

The chorioallantoic membrane (CAM) of the chick embryo forms by the fusion of the allantois of the developing chick embryo with the mesodermal layer of the chorion (Figure 3.1). It first appears as the allantoic vesicle on embryonic development day (EDD) 4 after which it enlarges rapidly until EDD 10 and fuses with the chorion [135] (Figure 3.2). The blood vessels located in the mesodermal layer of the CAM give rise to a capillary plexus that grows rapidly between EDD 8- 11 to mediate gas exchange with the environment. Therefore, the CAM is an extraembryonic membrane that functions as an organ for gas exchange between the embryo and the environment. It is rich in blood vessels and because it stays on top of the developing embryo it is easily accessible for experimental interventions.

Figure 3.1. Graphical demonstration of extraembryonic membranes of the chick embryo.
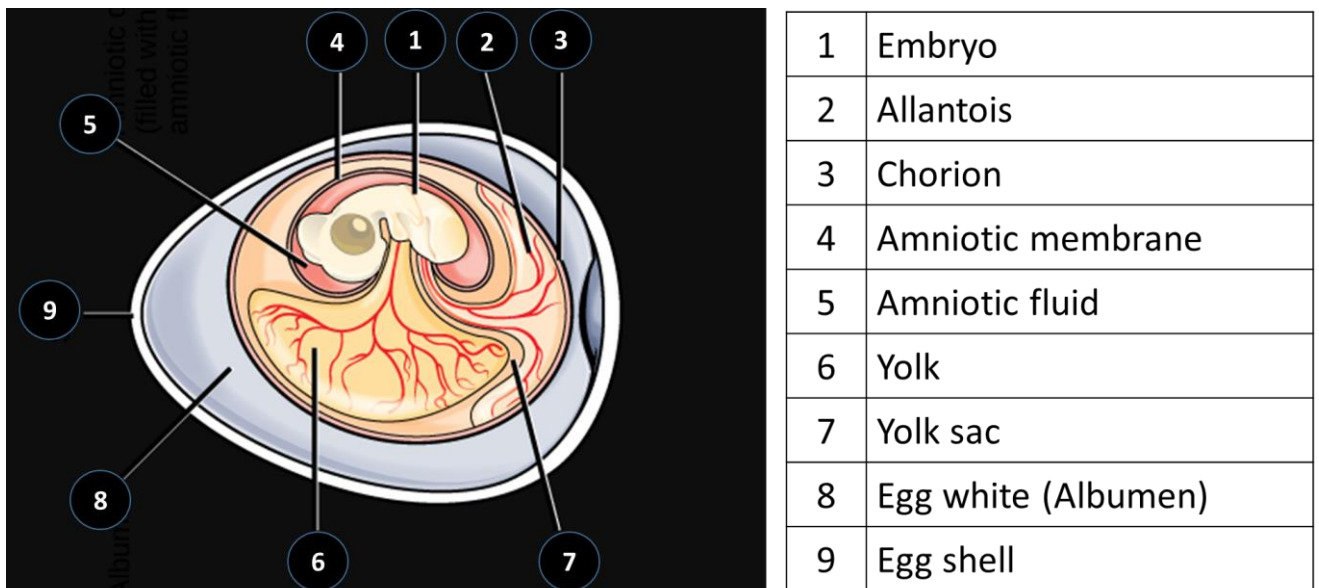
1	Embryo
2	Allantois
3	Chorion
4	Amniotic membrane
5	Amniotic fluid
6	Yolk
7	Yolk sac
8	Egg white (Albumen)
9	Egg shell

The CAM assay has been used as a well- established *in vivo* assay to study angiogenesis since the 1970s. The CAM model has indeed made fundamental contributions to understanding of tumour related angiogenesis. It was first demonstrated experimentally in the CAM assay that growth of solid neoplasms was always accompanied by neovascularization and that the formation of new blood vessels in this context was more vigorous and continuous than that observed in wounds and inflammation [136]. Today inhibition of angiogenesis is one of the main strategies used when developing targeted therapies for cancer. Additionally, cancer cell lines are commonly grown on the CAM to test the efficacy of anticancer drugs in pre- clinical studies.

The *in ovo* [137] and *ex ovo* culture methods have been used to grow chick embryos for use in research [135], [138]. The *in ovo* culture method was established first. In this method fertilized chicken eggs are placed in an incubator at 37°C with constant humidity to start embryogenesis. On day 3 of embryonic development 2-3 ml of albumen is removed from inside of the egg using a needle attached to a syringe. Removal of the albumen detached the CAM from the egg shell and increases the distance between the egg shell and the CAM allowing experimental intervention without damaging the vascular structures and embryo. After removal of the albumen, a small square window is opened on the egg shell which is than closed and sealed until further experimental interventions are done. The main advantage of this technique is that it allows a more physiological environment for development of the chick embryo. Also it is known that the egg shell itself is a source of calcium for the developing embryo which could be important when studying bone physiology. For example, when studying bone regeneration it may be a good idea to grow *in vivo* cultures to allow absorbance of calcium from the egg shell. It has also been suggested in earlier literature that the survival rates of *in ovo* cultures were higher however there is recent evidence against this suggestion.

The *ex ovo* method is where the embryo is grown outside of the egg shell for most of the embryonic life. This represents a useful modification of the classical *in ovo* CAM assay offering a few unique advantages. With use of the *ex ovo* CAM assay the growing embryo and the vascular structures can be better observed. Additionally, a larger area of the CAM can be used for experiments. The main concern with this technique is related to the survival and maintenance of the chick embryos outside of the egg shell [139]. There is literature to support both arguments suggesting a decreased [139] and unchanged [140]–[142] survival of *ex ovo* cultures.

Figure 3.2. The development of the CAM after first appearing on embryonic development day (EDD) 5 (black arrows) and growing up to cover the whole surface of the square weighing boat on EDD 9 (Black and red scale bars represent 1 cm and 5 mm, respectively).
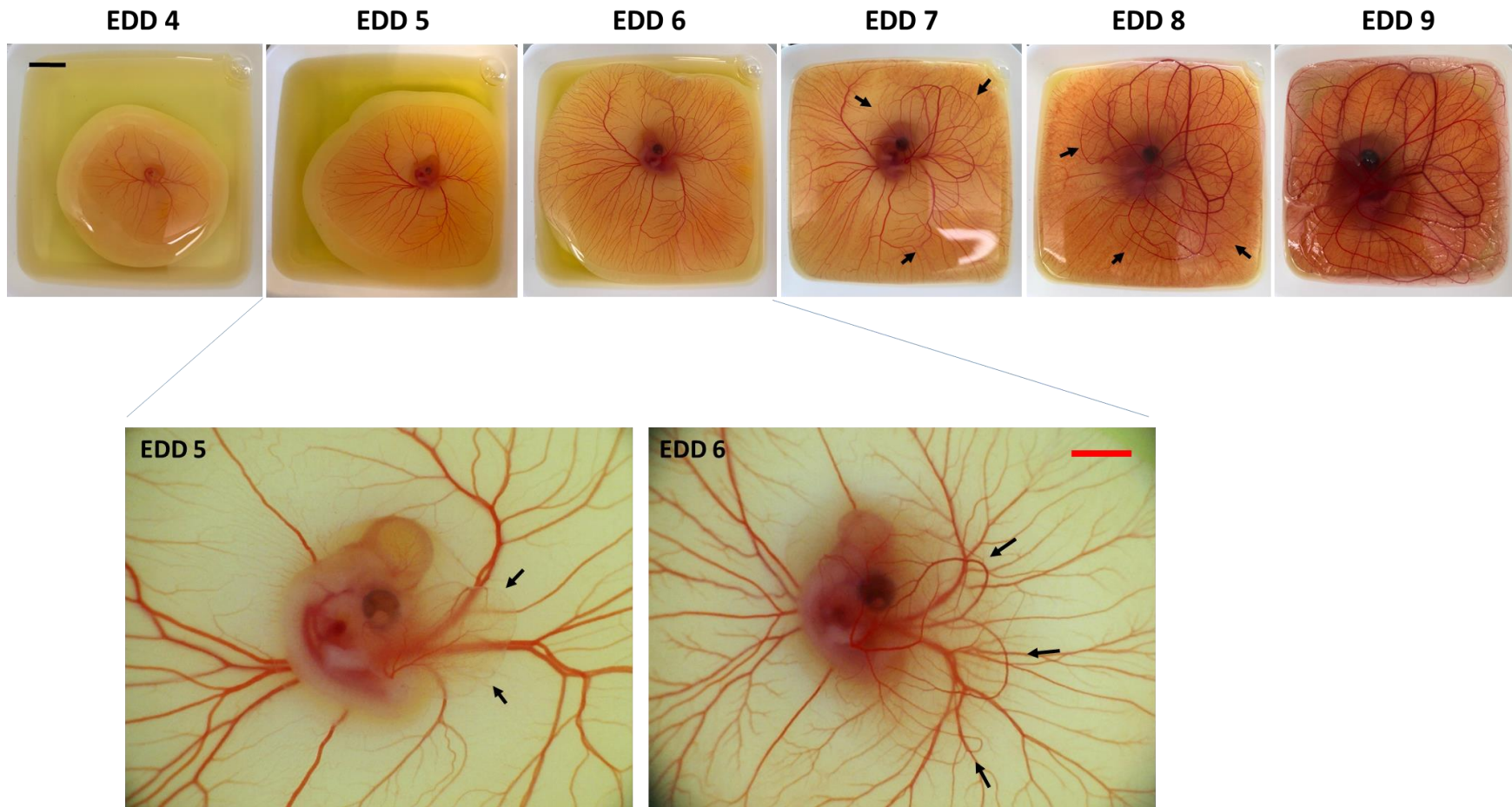
3.2. The *ex ovo* CAM assay protocol

3.2.1. Assay planning

All the experiments were planned beforehand as this is a 'bioassay'. The fertilized eggs that were laid on the same day of dispatch were received next day. The date of dispatch and the date received in the egg laboratory were recorded following the Home Office guidelines. After fertilized eggs were received they were stored at 10°C up to 10-12 days until the incubation is started.

The day of incubation of fertilized eggs started was embryonic development day (EDD) 0, followed by cracking the eggs on EDD 3, start of experimental intervention EDD 7 and sacrifice of the embryos on EDD 14 (Figure 3.3).

Practically, it was most convenient to receive 6 dozen of eggs at a time and to start incubation on a Friday (day 0), crack the eggs on a Monday (day 3), implant the test samples on the next Friday afternoon (day 7) and sacrifice the embryos on the third Friday (day 14). This allowed image acquisition during the weekdays when necessary.

Figure 3.3. The timeline of the *ex ovo* CAM assay. The incubation of the eggs starts at embryonic development day (EDD) 0, the *ex ovo* cultures start at EDD 3. The experimental intervention is done late on the EDD 7 and the angiogenic response can be evaluated anytime between EDD 10 and 14.
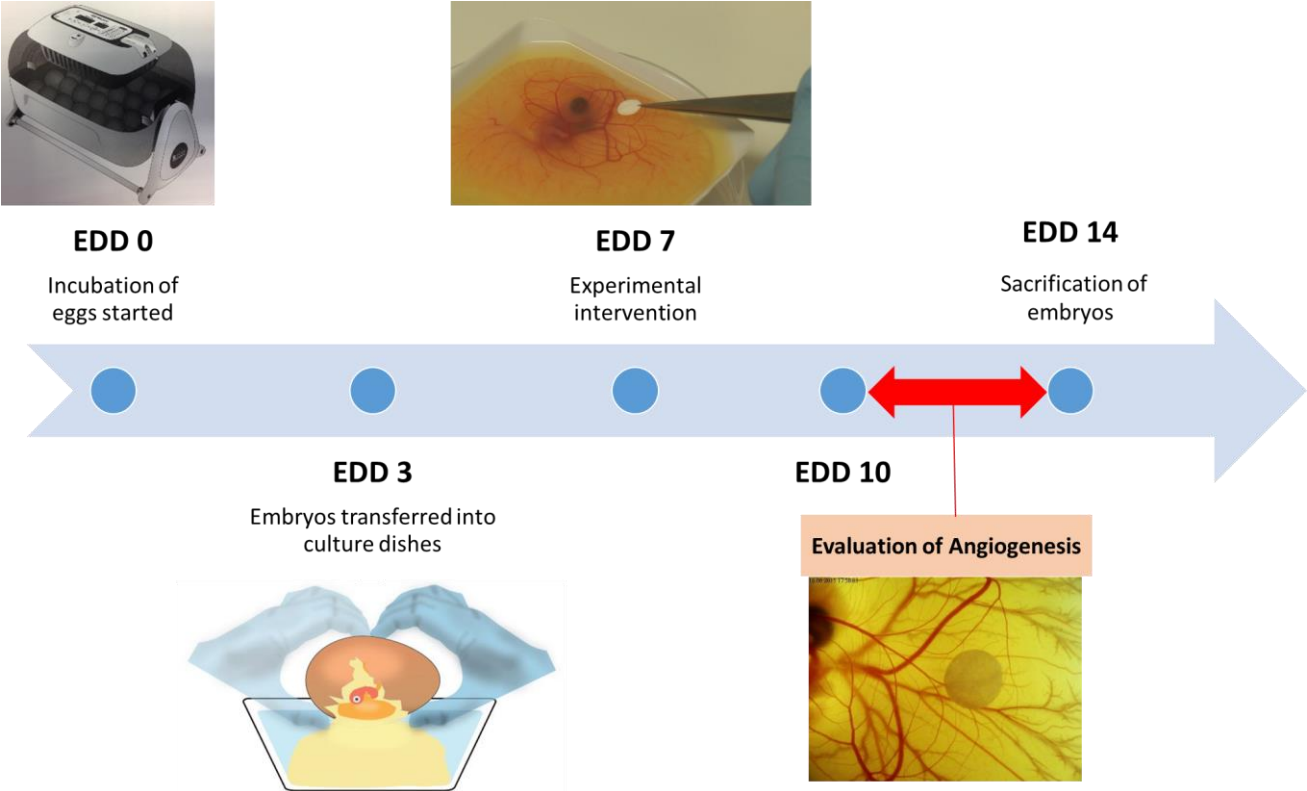
3.2.2. Incubation of fertilized eggs

The internal parts of a rotating egg incubator was cleaned by spraying IMS (70%) and left to dry inside the laminar flow cabinet. The fertilized eggs were removed from the fridge and the egg shells were wiped with tissue paper and 20% IMS under the laminar flow cabinet. The eggs were then placed in the rotating egg incubator lying on their horizontal axis. Eggs were incubated at 37- 38° C and 40- 60% humidity for 3 days.

3.2.3. Starting the *ex ovo* cultures

At EDD 3 the upper surface of the horizontally lying eggs were marked with a pen and the rotating incubator was put in a stationary state for at least 10 min. In the meanwhile, plastic weighing boats are dipped into 70% alcohol for disinfection and left to dry. Additionally, a 1% solution of Penicillin/ Streptomycin in PBS was prepared and 2 ml of the antibiotic solution is pipetted in each weighing boat (Figure 3.4). The eggs were taken out of the incubator and inside the laminar flow cabinet each egg was cracked from below (opposite to the marked line) by hitting it on a hard surface.

Figure 3.4. The preparation of the setup before cracking the eggs. The horizontally lying eggs are first marked on the top surface (insert). Inside the laminar hood, sterilized plastic weighing boats, antibiotic solution, Petri dishes, racks to hold the eggs, a beaker to use to collect the waste and a small heater to help keep the embryos warm.

The chick embryo was gently transferred into a plastic square weighing boat by separating the two halves of the egg shell (Figure 3.5). Successful embryo transfer was confirmed by observation of the beating heart in the developing embryo and an intact egg yolk. A sterile petri dish was covered as a lid on the weighing boat and the *ex ovo* cultures were put in a stationary sterile incubator 37- 38°C with 60% humidity immediately. Survival and normal development of the *ex ovo* cultures were checked daily afterwards. Any dead embryos were disposed of immediately following the Home Office procedures.

Figure 3.5. The start of *ex ovo* cultures on embryonic development day 3. The egg cracking technique is demonstrated with confirmation of a successful embryo transfer with intact egg yolk and the live embryo (5 & 6). Here a Petri dish is used instead of a weighing boat for better demonstration.
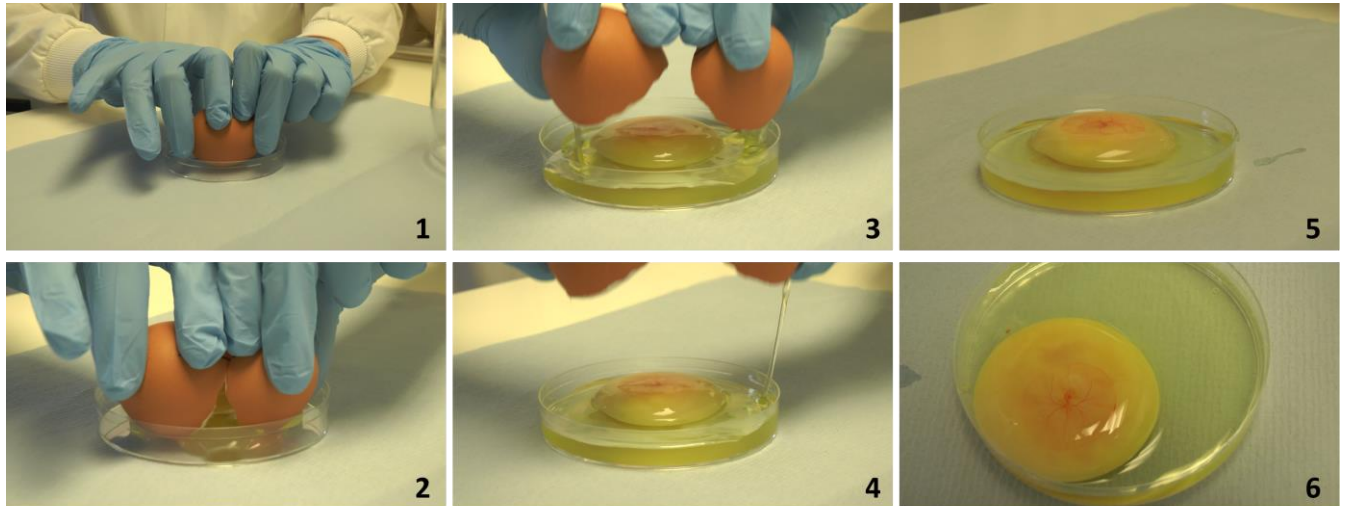
3.2.4. Start of experimental intervention

On EDD 7 the *ex ovo* cultures from incubator and placed in laminar flow cabinet. The biomaterials to be implanted were prepared beforehand. Scaffolds were cut into circular shapes with a diameter of 7- 10 mm using a laser cutter and sterilized for 40 min under UV radiation. Using a sterile forceps samples were placed in between two large vessels halfway between the embryo and the outer border of the CAM (Figure 3.6). It is important to delineate the borders of the CAM on EDD 7 and not to place the sample outside of the CAM to avoid growth of the CAM over the test sample (Figure 3.7). Daily checks of embryo survival and development continued.

Figure 3.6. Correct placement of the test sample on the CAM. The dashed arrows show the borders of the CAM which will grow further to cover all surface of the square weighing boat in a few days. Coloured circles show the preferred places for placement of the sample on the CAM.
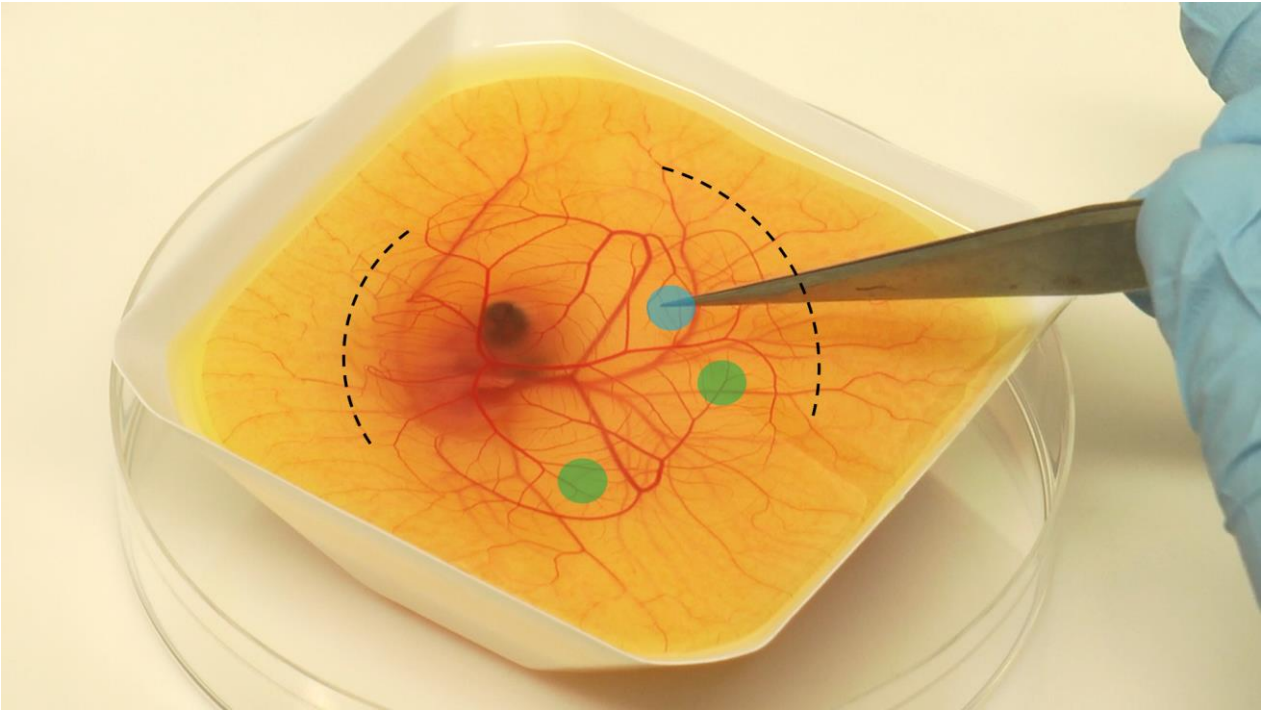
Figure 3.7. An example of correct and incorrect placement of the test samples on the CAM.
In embryonic development day (EDD) 7 the CAM does not completely cover the surface of
the square weighing boat leaving areas devoid of the CAM. The sample 1 is placed outside of
the CAM whereas sample 2 is placed correctly on the CAM the borders of which can be
followed by close inspection (arrows).   The area where sample 1 is placed is not the CAM
but the yolk sac. Following up this sample for 2 more days in the embryonic development it
could be observed that sample 1 blocks normal expansion of the CAM which is clearly seen
to accumulate behind the sample at EDD 9. Sample 2 grows and expands together with the
CAM. (Scale bars 10 mm for all images).
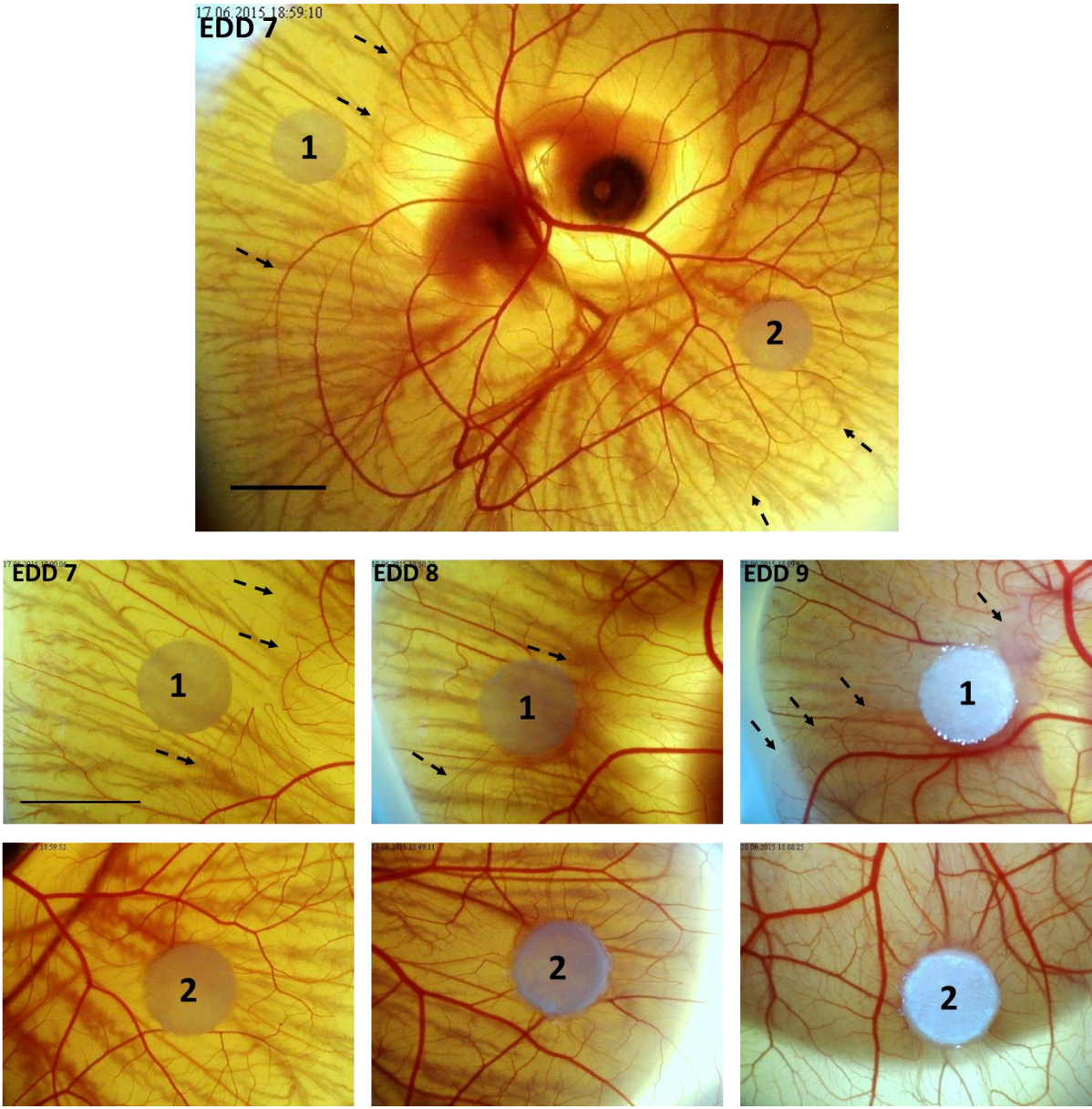
3.2.5. Evaluation of angiogenic response to scaffolds

Angiogenic responses to the scaffolds were evaluated between EDD 10- 14. In the case of ascorbic acid releasing scaffolds the angiogenic response was evaluated at EDD 11 whereas for Estradiol releasing scaffolds experiments were continued until EDD 14. This was because with ascorbic acid an anti- angiogenic dose of the drug was being demonstrated which was most evident at EDD 11, in preliminary studies.

A digital camera fixed at a constant height was used to take images (Figure 3.8). All samples were imaged while being trans illuminated with light coming from below. Additionally, two side lamps were also used when necessary. To obscure the unnecessary background due to presence of chick embryo body parts or egg yolk a 20% solution of oil in water emulsion was injected just beneath the test sample (Figure 3.9). For some samples, injection of the contrast underneath the test samples makes a significant difference (Figure 3.10). Standard procedures were consistently applied in all experiments to obtain standard, high quality images for subsequent image analysis.

Figure 3.8. The imaging unit used to take pictures of the CAM- biomaterial complex at the end of the experiments. The digital camera (yellow arrow) fixed at a constant height and a transillumination box (red arrow) are key to take high quality images consistently.
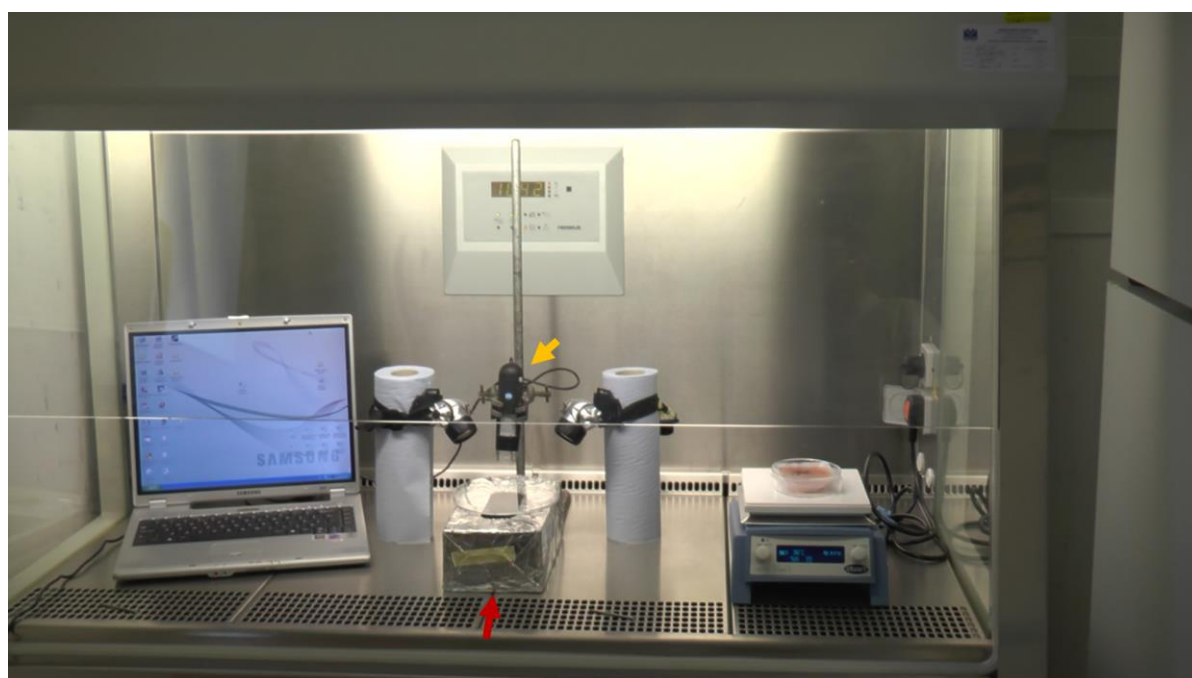
Figure 3.9. Demonstration of how an emulsion is injected underneath the CAM- biomaterial complex to obscure the unnecessary background. First the injectors containing the contrast agent is inserted between the two layers of the CAM (1-2). Than by rotating the petri dish the tip of the needle is brought underneath the area of interest containing the implanted scaffold and the contrast injection is started (3-4). After adequate amount of contrast is injected evenly the sample is ready for image acquisition (5-6).
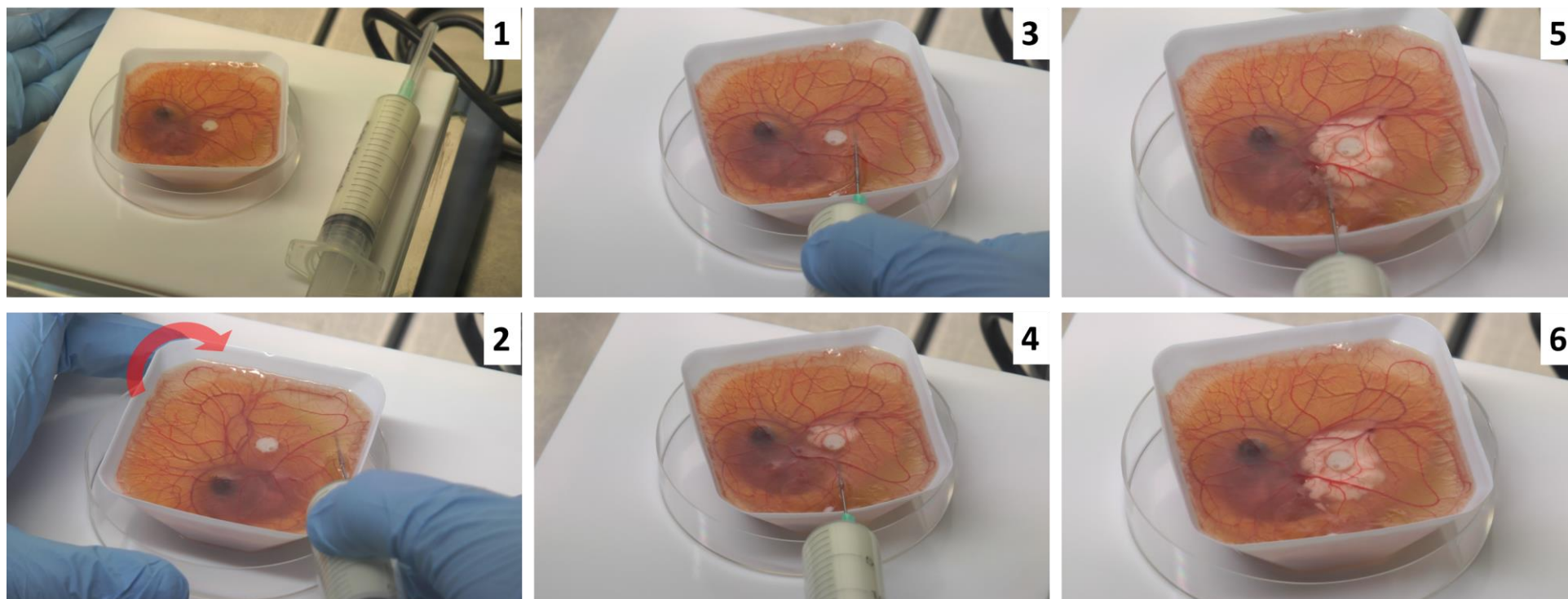
Figure 3.10. Comparison of images obtained before and after injection of the contrast. Here two contrast agents with different colours are compared. In the upper raw, a white contrast provides effective visualization of the blood vessels whereas in the lower raw the blue contrast obscures the small blood vessels. Error bars represent 400 μm.
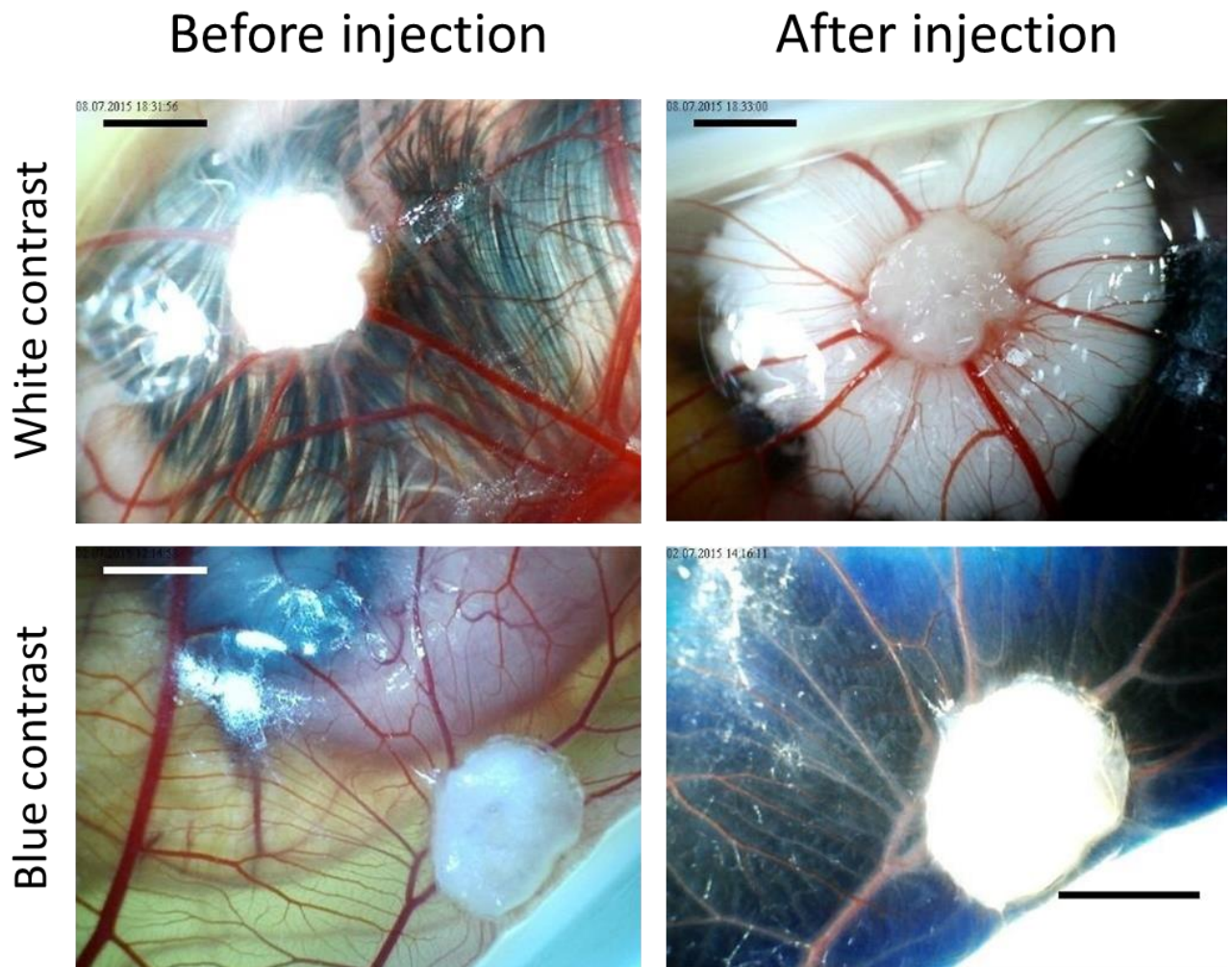
3.2.6. Sacrifice of chick embryos

The CAM is an extraembryonic structure and does not contain any nerve endings. However, nerve endings occur in the developing chick embryo starting from EDD 11. Therefore, this point was considered during all stages of experimental planning. Current experiments did not involve any noxious stimulus or intervention to the chick embryo and only implantation of biomaterials onto the CAM surface was performed. Therefore, no prior sedation or anaesthesia was performed during the experiments following the Home Office guidance statement 'a prior sedation or anaesthesia should be carried out before humane killing unless

to do so would be likely to cause greater distress than using the same method of killing without sedative or anaesthetic'.

On EDD 14 immediately after images were taken, the chick embryos were sacrificed by bleeding. The CAM- biomaterial complex was excised using tissue scissors and forceps with a margin of 1 cm. Samples were fixed in 3.7% formaldehyde for histologic examination.

3.3. Setting up control scaffolds for angiogenesis

The preliminary experiments on evaluating the angiogenic potential of a biomaterial proved to be challenging due to lack of data on what constitutes a pro- angiogenic material and what defines an anti- angiogenic material. Although there is data in the literature on the testing of certain drugs on the *ex ovo* CAM assay there was no data for biomaterials. A further complication when studying angiogenesis with biomaterials is that any foreign material placed on the CAM could potentially induce an antigenic reaction that can then be confused with an angiogenic response. Therefore, every material placed on the CAM needs to have its own set of controls.

3.3.1. A negative control for electrospun PLA scaffold

Incorporating antiangiogenic substances into the electrospun PLA scaffolds was chosen as a strategy to construct an anti- angiogenic PLA scaffold as a negative control for angiogenesis experiments. Among available options hydrocortisone releasing PLA scaffold was chosen as a negative control scaffold for several reasons: i) hydrocortisone has several derivatives that allow it to dissolve in water and oil phases, ii) it is known to have antiangiogenic properties, iii) its release can easily be demonstrated using the UV- spectrophotometer and iv) it is cheap and widely available.

Hydrocortisone (Sigma Aldrich, Dorset, UK) was dissolved in 500 µl of distilled water and an emulsion of hydrocortisone in 10% PLA solution was formed as described earlier in Chapter 2. Electrospun PLA scaffolds containing 0.01 gram of hydrocortisone per gram of PLA were constructed. Release of hydrocortisone was measured at an absorbance wavelength of 242 nm using UV- spectrophotometer. The calibration curve for hydrocortisone and release of

hydrocortisone from PLA scaffolds is demonstrated in Figure 3.11. Release of hydrocortisone from the scaffolds was only studied for 3 days.

Concentrations of hydrocortisone of up to 1 gram of hydrocortisone per gram of PLA can be used to observe more angiostatic effects by dissolving the lypophilic formulation of hydrocortisone in the polymer solution. However increased dosages reduced the embryo survival at EDD 10.

Figure 3.11.   The standard curve to determine the concentration of hydrocortisone in an unknown solution and the release of hydrocortisone from electrospun PLA scaffolds for 3 days.
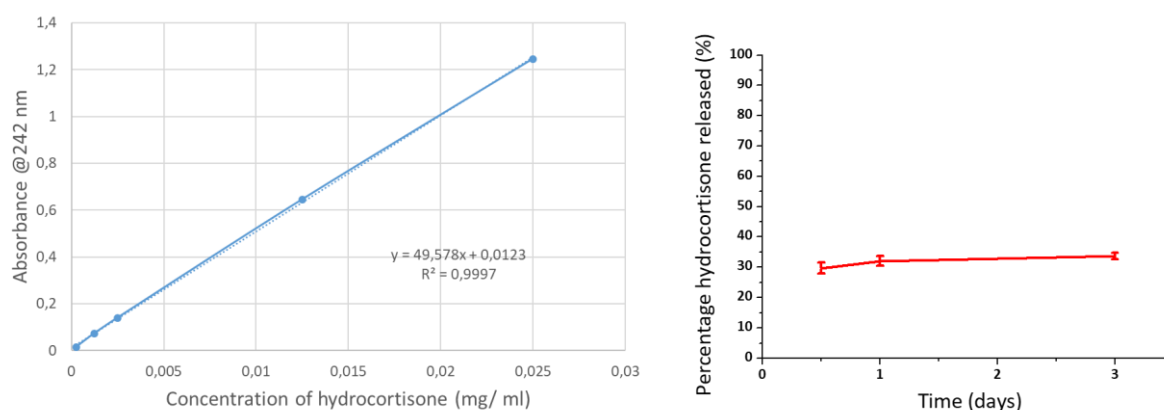
3.3.2. A positive control for electrospun PLA scaffold

Constructing a positive control where a pro- angiogenic drug is released from electrospun PLA scaffolds proved to be more difficult. Known pro- angiogenic substances such as VEGF, FGF and EGF were all protein structures that could not go into polymer solutions for electrospinning. A strategy to incorporate heparin into the PLA scaffolds by layer- by- layer coating was performed within the group previously [143] this was technically very challenging. Therefore, PLA scaffolds seeded with tumour cell lines were constructed with the idea that tumour cells would secrete pro- angiogenic factors.

To do this, the human melanoma cell line (C8161) available in the MacNeil lab (isolated from an abdominal wall metastasis from a recurrent malignant melanoma) was cultured in melanoma culture medium consisted of EMEM media (Sigma-Aldrich) supplemented with FSC (10%v/v), L-glutamine (2uM), Penicillin (100U/mL), streptomycin (100ug/mL) and Fungizone (0.625ug/mL). A total of 1 million C8161 cells were seeded on an electrospun poly (lactic acid) (PLA) scaffolds. After culturing *in vitro* overnight the scaffolds seeded with tumour cells were controlled for attachment and viability using the resazurin assay. Scaffolds seeded with tumour cells were then implanted on CAM at EDD 7 to constitute a positive control (Figure 3.12).

Figure 3.12. Demonstration of negative and positive controls to use when assessing the angiogenic potential of a biomaterial. An angiostatic effect is evaluated at embryonic development day (EDD) 10 whereas a proangiogenic response is best evaluated at EDD 14. Scaffolds constructed with an intention to act as positive controls have led to pathologic bleeding and probable hypercoagulation (arrows) eliminating use of this strategy to construct positive controls. (scale bars represent 200 µm)
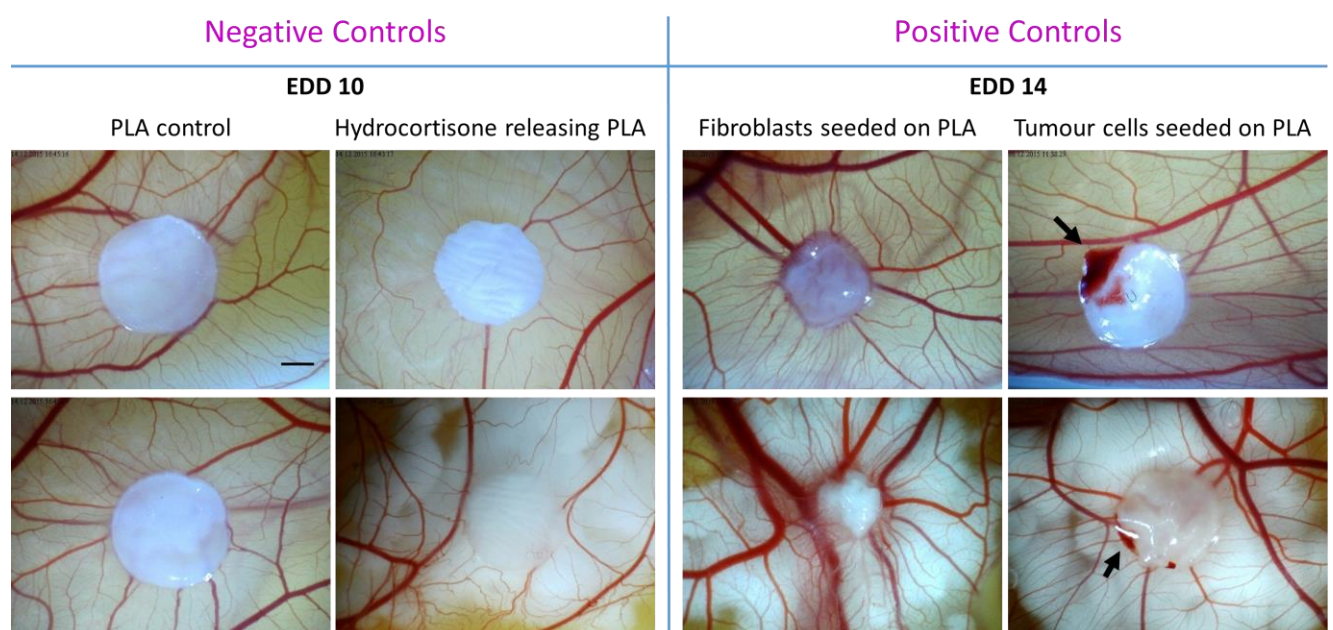
3.4. Evaluation of results

3.4.1. Evaluation of embryonic survival and development

Normal development of the *ex ovo* cultures are checked and recorded daily. The survival of the embryos, the presence of any developmental arrests and/ or presence of any infection were reported for each experimental group.

3.4.2. Evaluation of angiogenic response to biomaterials

The angiogenic response to biomaterials was analysed using digital images. A previously described methodology was used to calculate the 'vasculogenic index' [144]. All discernible vessels including capillaries, arterioles, venules that are within an imaginary circle drawn around the scaffold with a 1 mm margin were counted provided that they form an angle of less than 45° with a line radiating from the centre (Figure 3.13). Vessels branching within the annulus are counted as 1 vessel, whereas those branching outside the annulus are considered to be 2 vessels.

Figure 3.13. An example of how the 'vasculogenic index'is calculated. Original image and contrast injected image are shown together with demonstration of blood vessel counting. On the processed grayscale image (on the right hand side) all discernible vessels growing towards the scaffold in a spoke- wheel pattern are counted (Scale bar 2 mm)

Another method of quantification was also used when evaluating the angiogenic response to a transparent hydrogel. In this case transparency of the hydrogel allowed observation of blood vessels underneath the biomaterial itself. In this semi- automated quantification method, the free online plug in for Image J software, Neuron J, was used (Meijering et al., Cytometry Part A 2004;58A:167–176; http://www. imagescience.org/meijering/software/neuronj/). The digital images were converted to grayscale (8- bit) and sharpened twice. Afterwards all discernible vessels in the image were traced using the Neuron J tracing tool. An advantage of this method is that it allowed calculation of other parameters in addition to number of blood vessels, such as total vessel length and the total number of blood vessels.

The angiogenic responses have also been quantified in histologic sections of the CAM-biomaterial complex. Standard Haematoxylin &Eosin (H&E) sections allowed observation and counting of medium to large sized blood vessels on the CAM in cross sections (Figure 3.14). The feasibility of demonstration of blood vessels by immunohistochemical or immunofluorescence staining has also been studied. The blood vessels on the CAM could effectively be stained by fluorescent labelled α-SMA (Figure 3.15). Although effective staining could be performed on the CAM, in the presence of the biomaterial, which is PLA in this context, the autofluorescence of the material prohibited effective use of this method to quantify vessels that were in between the fibres of the material.

Figure 3.14. Quantification of angiogenic response by counting the blood vessels on Haematoxylin &Eosin (H&E) stained sections. The scaffold implanted on the surface of the CAM can be observed followşng the normal CAM tissues on the sides of the implanted scaffold. The blood vessels on the CAM are labelled with blue arrows. The scaffold on the left contains more blood vessels in the CAM tissue underneath the scaffold (therefore is more angiogenic) compared to the scaffold on the right. (Scale bars 100 μm)
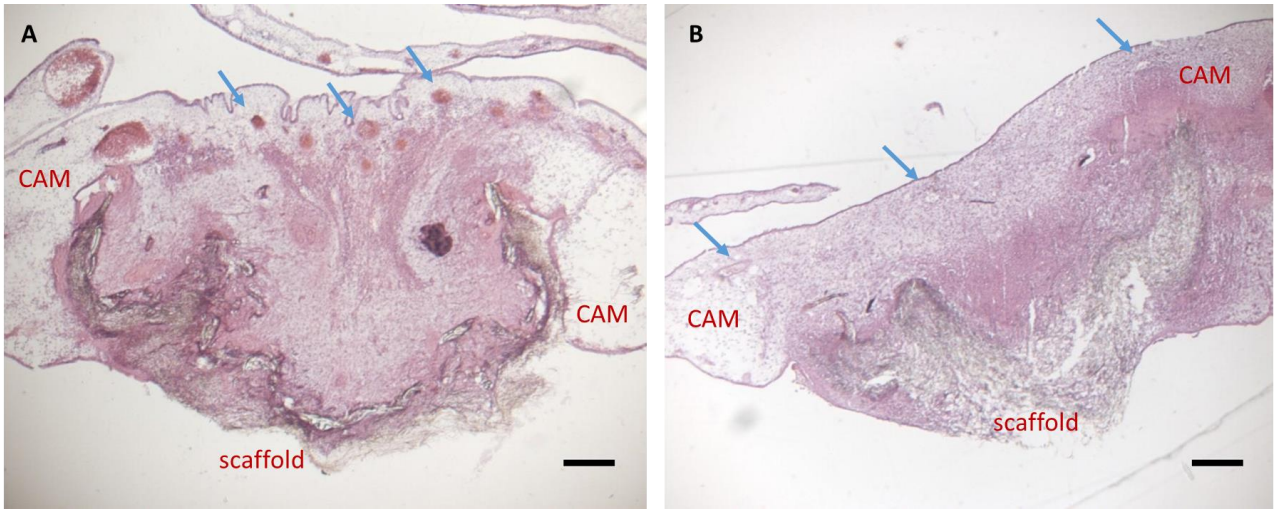
Figure 3.15. Staining properties of the CAM with antibody to alpha smooth muscle actin (α-SMA). The normal CAM has a trilayer structure with blood vessels in the mesodermal layer. Larger blood vessels (arrows) give the best results for staining with α-SMA. (scale bar 200 μm). The mounting jelly appears like an artefact in all images.
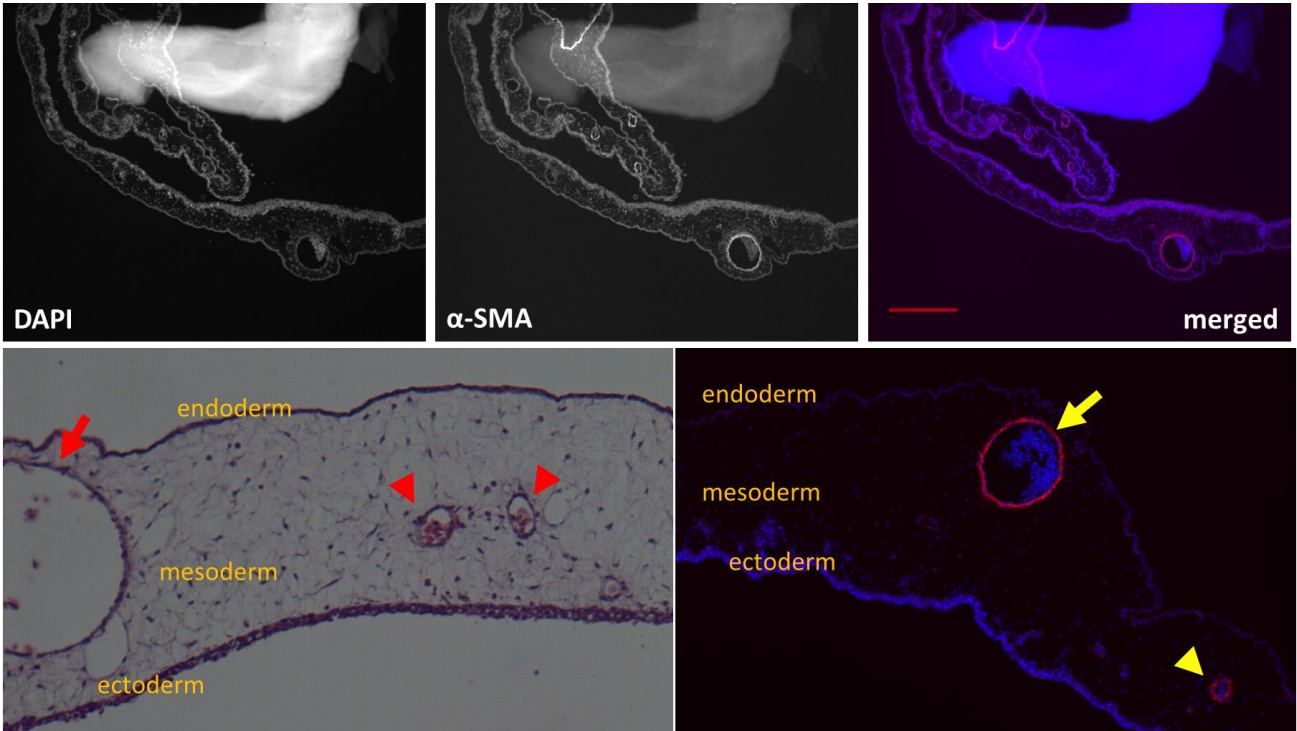
To overcome this limitation, another method was developed. A rhodamine labelled lens culinaris agglutinin [LCA], a member of the lectin family, was injected into the circulation of the CAM before sacrifice. The LCA is known to attach to the endoluminal surface of the CAM vessels by an agglutination reaction. With this method selective labelling of all blood vessels regardless of their size and shape was achieved (Figure 3.16).

Figure 3.16. Staining properties of the CAM with the lens culinaris agglutinin (LCA). Larger blood vessels (arrow head) appear more prominently stained with the LCA compared to smaller ones both in the CAM only samples and CAM+ PLA scaffold samples. In the samples with the scaffold, smaller blood vessels sectioned in different directions can be detected (arrows). (scale bars 1 mm for all images).
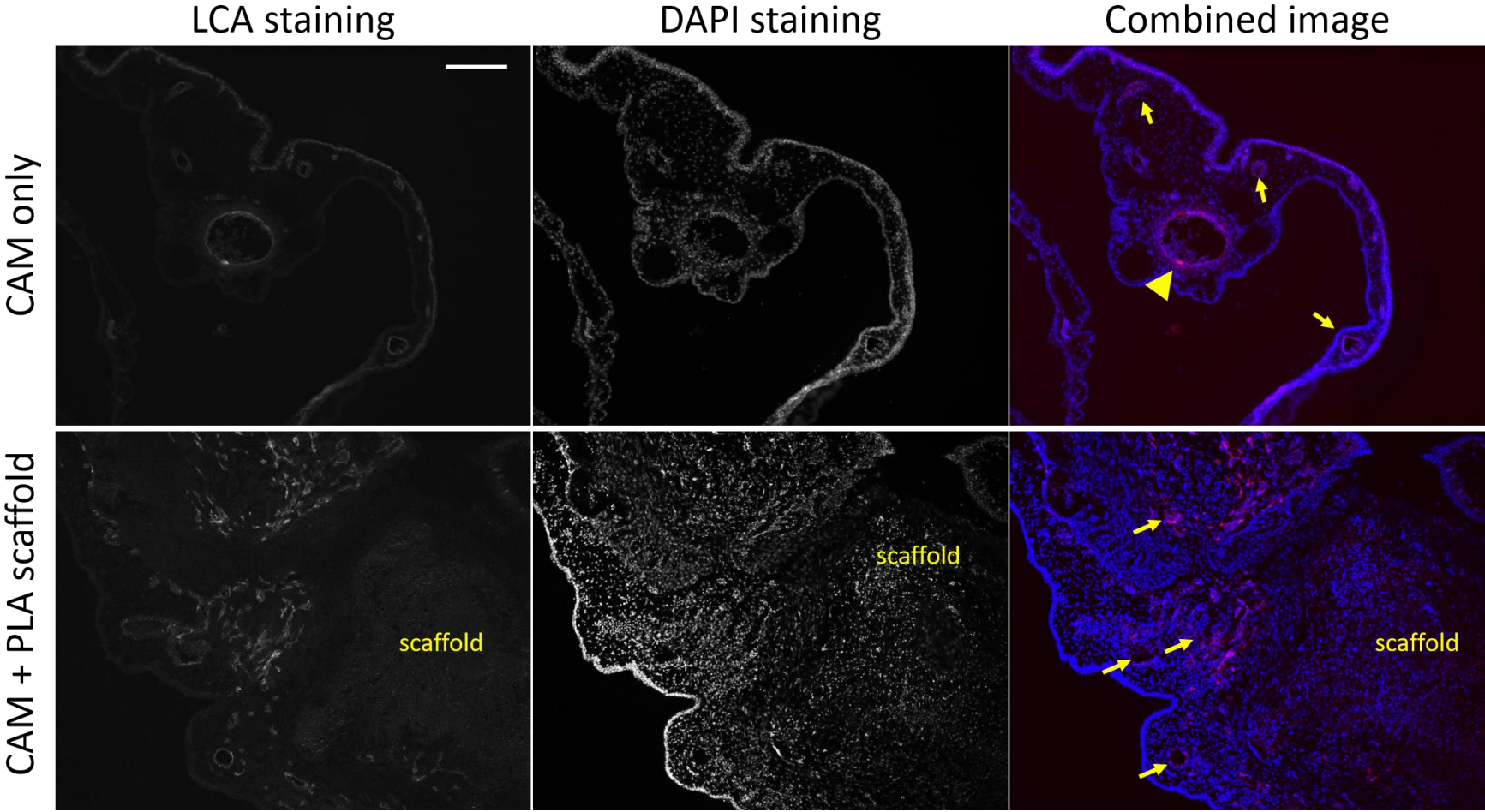
3.4.3. Evaluation of initial tissue response to biomaterials

All implanted materials placed on the CAM surface were evaluated for their biocompatability and engraftment by daily observations. Additionally the tissue sections with H&E staining were assessed for the amount of inflammatory cell infiltration in and around the material.

3.4.4. Evaluation of angiogenic potential of drugs in the CAM assay

Before the drug releasing scaffolds were placed on the CAM, each drug was tested by applying them onto the CAM surface. This was achieved by labelling the area where the drugs would be applied using a 100 µm thick plastic ring that was cut from using a6.5 mm in diameter soft needle cover using cryosectioning. Solutions of drugs (Estradiol, VEGF and Sunitinib) with various concentrations were prepared in PBS. Between EDD 7 and EDD10 drugs were applied onto the CAM delineated by the plastic ring. Two doses per day were given to each area with an application volume of 30 µl each time (Figure 3.17-1). Angiogenic responses were evaluated by observation of macrovessels and microvessels.

Macrovessels

Images of the area of drug application were taken at EDD 10 using a digital microscope. Using Image J software images were first converted to grayscale and then adaptive thresholding was performed. Finally, noise removal was performed by obtaining the binary images that went to analysis. From each image 'the percentage area covered by blood vessels' was calculated. A similar protocol was described by other authors previously [22] (Figure 3.17-2).

Microvessels

The microvasculature was imaged by confocal microscopy on fixed tissues of the CAM. The CAM vasculature was labelled using a rhodamine conjugated LCA by injecting it into chick circulation at EDD 10. On the top planar view, the microvasculature was found by focusing on the area just above the larger blood vessels of the CAM (Figure 3.17-3). The microinjection technique is demonstrated in Figure 3.18. A Zeiss LSM 510 META confocal upright microscope with Zeiss LSM Image Browser software (version 4.2.0121) was used for image acquisition. EC-plan Neofluar 5X and 10X objective lenses were used. For visualization of rhodamine LCA following parameters were used: excitation 543nm and emission 615nm; optical images were taken at every 25 μm interval, confocal settings (frame size 512 x 512, scan direction (single), scan speed (4), data depth (8 bit), pinhole (1 Airy unit), laser power and detector gain were all kept constant for all samples. These parameters were arranged initially with the help of Dr Ahtasham Raza and the same settings were used for all samples.

Figure 3.17. The process of application of drugs directly on the CAM, injection of the lens culinaris agglutinin (LCA) and imaging the vasculature on confocal microscopy.
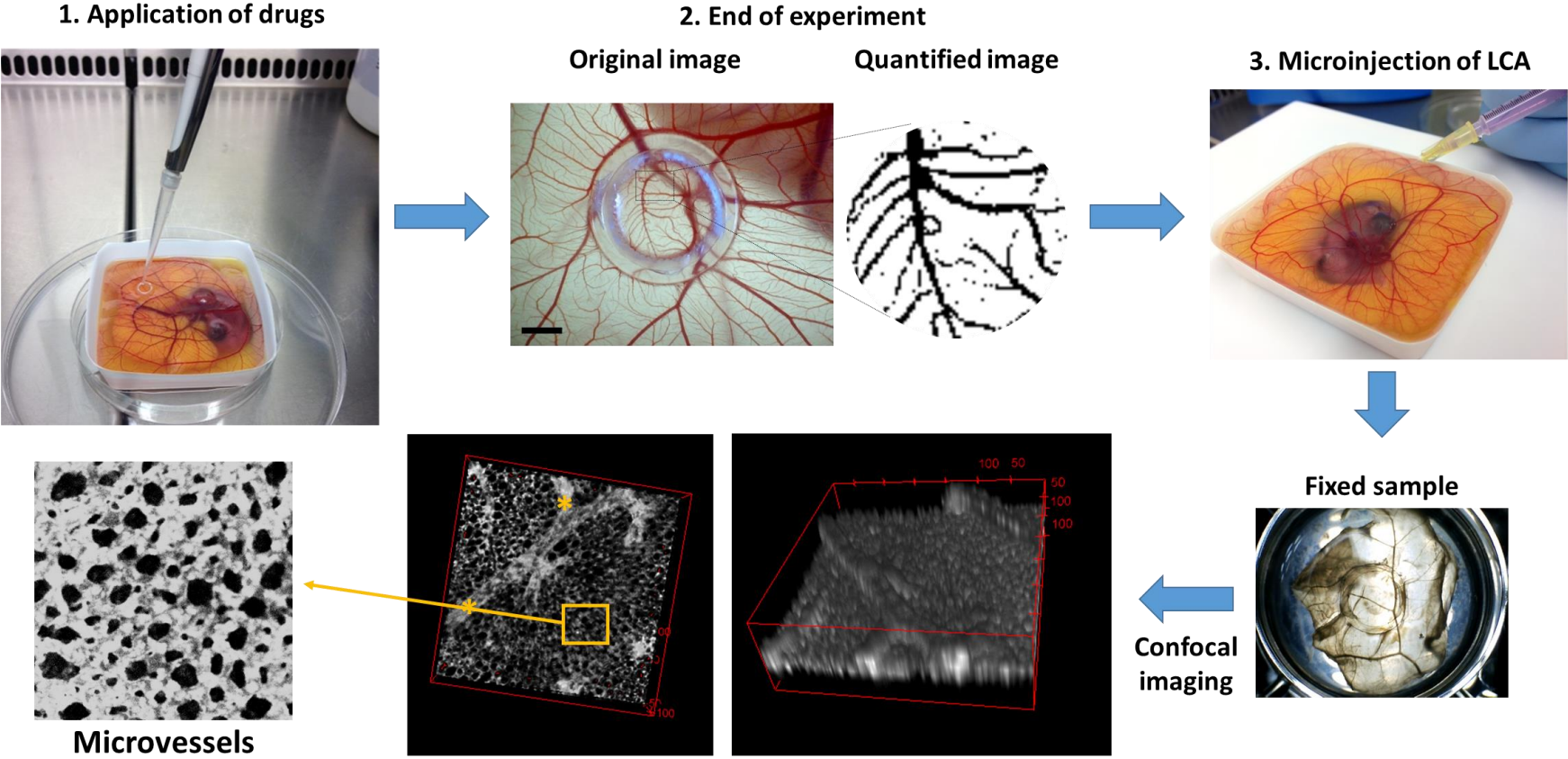
Since there is no hierarchy in the microvasculature, mainly the degree of endothelial cell hypertrophy was assessed in all samples. This was calculated on processed images constructed using Image J software. Original images were converted to grayscale, 'enhance contrast' applied, band pass filter applied and images were 'thresh holded' to be most representative of original images. The total area covered by endothelial cells in a frame was calculated. The frames were taken from randomly selected areas of the CAM within and around the plastic ring.

Figure 3.18. Demonstration of microinjection technique. A 30G hypodermic needle attached to 1 ml injector is used. A cotton swab is used to stabilize the CAM when injecting. A bifurcation in one of the vitelline veins is chosen for injection (arrow heads in 1 and 2). The needle first punctures the membrane with a 45-degree angle and then goes as horizontal as it can be to lie parallel to the membrane. Once inside the vein, a small flush demonstrates clearing of the vessel content for a few seconds (arrows in 3, 4 and 5) which confirms successful injection into the vitelline vein. After the injecting the needle is removed while pressing with the swab.
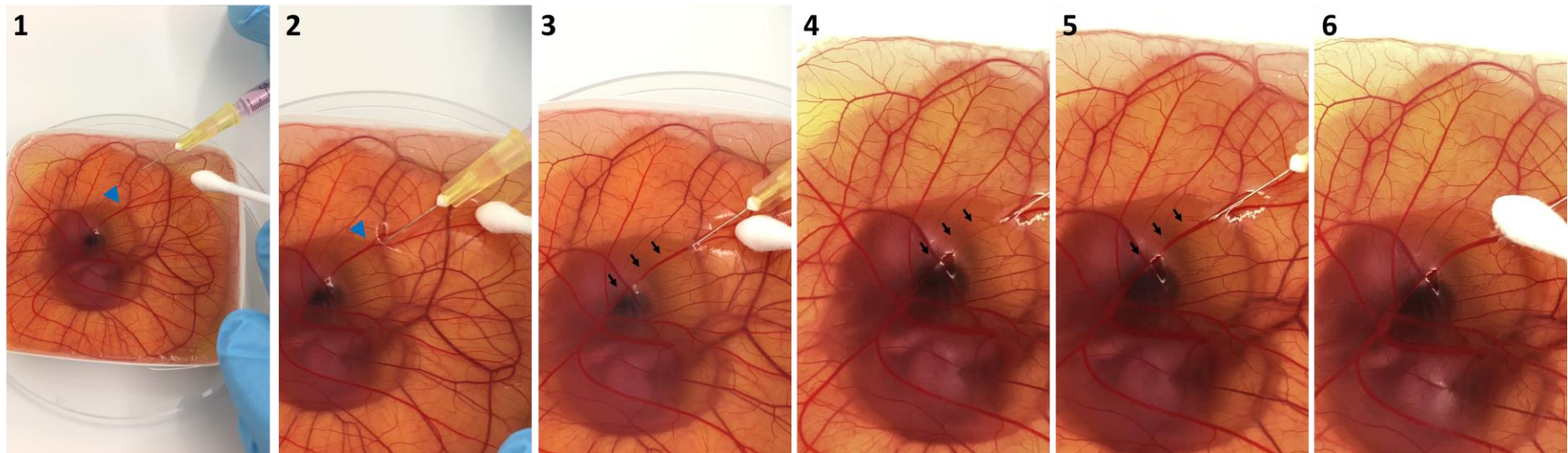
3.5. Chapter discussion

Developing the *ex ovo* technique to culture the chick embryos in our laboratory was one of the main achievements of the current doctoral studies. The current work builds on previous work of Dr Giulia Gigliobianco who first setup the necessary procedures with the *in ovo* CAM assay. Although the *ex ovo* culture method was described previously, developing the necessary equipment and the standard operating procedures in house for this assay was the main challenge addressed within these doctoral studies. As a result, this assay is now being taken up and used by a wider community of researchers within the department.

The *ex ovo* CAM assay can be used as a readily available bioassay to study the angiogenic potential of and initial tissue responses to biomaterials. The main advantages of the *ex ovo* (shell- less) modification is that a larger surface area of the CAM is available for all experimental interventions where up to 3-4 samples can effectively placed on a single embryo culture. Also the developing chick and the vascular structures are clearly visible to the researcher without effort. This could have particular importance for material testing as toxicity of some materials or their constituents can be detected.

Recently the CAM assay proved to be a useful in initial *in vivo* assessment tool to test biomaterials. Biomaterials comprise a wide range of natural and synthetic materials that are often combined with a range of bioactive molecules, proteins and/ or cells. The biocompatibility testing has to examine each of these constituents separately and in various combinations. This creates a demand for reproducible and technically simple bioassays that allow higher throughput screening of biomaterials prior to animal testing. The 3Rs principles inevitably limit the use of animals for high- throughput screening of biomaterials. Vigorous testing of biomaterials in *in vivo* assays during pre- clinical development is key to their subsequent success in clinical studies. Therefore, the CAM assay stands out as a technically simple bioassay where biomaterials can be assessed for their biocompatibility and angiogenic potential prior to animal testing.

The CAM assay is increasingly being used as a pre *in vivo* test to assess biomaterials [145]. The CAM has been effectively used as a short term host for grafted materials, organs and tissue samples where the angiogenic response and their safety and biocompatibility can be studied [142]. Also the CAM assay has recently been demonstrated to produce data that is comparable to mouse assays in testing bio-distribution and *in vivo* stability of radiopharmaceuticals [146].

Other advantages of the *ex ovo* technique is that it allows direct visualization of sprouting and intussusceptive angiogenesis *in vivo* which can be of particular importance when studying the mechanisms of angiogenesis. Other available in vivo models are expensive, do not allow high throughput screening and require expertize and sophisticated instruments (e.g. the dorsal skin fold assay). Another unique feature of the CAM assay is that it allows visualization of the capillary plexus in a top planar view under a fluorescent microscope after a fluorescently tagged lectin (lens culinaris agglutinin [LCA]) is injected into the circulation of the chick embryo. This capillary plexus is a very responsive *in vivo* system where the effect of an experimental intervention on the microcirculation can be studied.

The main disadvantage of the *ex ovo* technique has commonly been cited as decreased survival rates associated with it. However, throughout these studies survival rates of above 80% were consistently obtained. Nevertheless, there is a learning curve when conducting *ex ovo* cultures. This may explain the apparently inconsistent reports in the literature. Within the MacNeil group my research experience has accumulated and been shared with several researchers.

Within the context of this work, mainly biomaterials without cellular components have been implanted onto the CAM. However, the CAM is known to accept xenogeneic grafts that contain cells and/ or proteins in the initial stages of embryonic life. The immune system of the chick embryo starts developing later in the embryonic life after embryonic development day 11. First mononuclear phagocytes are detected in the chick embryo at EDD 9 [147] and functional macrophages which are responsible for the initiation of acute inflammatory response, were detectable in the circulation at EDD 14, the number of which suddenly increased at EDD 19 [148]. The lymphoid cells that constitute the cellular (T cells) and humoral immunity (B cells) were detected after EDD 11 and EDD 12, respectively [147]. The chick embryo is considered immunocompetent only after EDD 18.

Under our institutional regulations, the embryos can be cultured for only up to 14 days (other centres are known to have licenses for longer durations) this assay has been found useful to assess the initial *in vivo* tissue response to biomaterials. Therefore, other tissue engineered constructs, such as tissue engineered skin, can also be implanted and cultured on the CAM making use of the *in vivo* environment. However, it should be considered that this model on its own cannot be adequate in characterizing the biocompatibility and immunogenic potential of the biomaterials. Further animal studies would still be needed to achieve a complete understanding.

Other *in vivo* assays have also been used to study angiogenesis. Among these the mouse dorsal skin chamber (DSC) assay allows direct visualization of blood vessels at all times during the experiment with use of intravital microscopy [149]. This model can also accept xenogeneic grafts if nude mice are used and it can provide information on the dynamics of blood vessel development. The main limitation of mouse DSC assay is that it requires significant expertise and sophisticated equipment that may not be available in most laboratories. Furthermore, for biomaterials testing implantation of the biomaterial will be difficult as the chamber lies vertically at the back of the mouse. Therefore, the *ex ovo* CAM assay stands out as an inexpensive, reproducible and technically less challenging bioassay to allow screening of materials.

Chapter 4.
Production and assessment of Vitamin C releasing electrospun PLA scaffolds

4.1. Chapter Introduction

During and after pregnancy there is extensive connective tissue remodelling in the pelvic floor. This remodelling occurs as a result of a complex interplay between the synthesis and degradation of main components of the extracellular matrix, mainly collagen and elastin [150]. Defects in the remodelling of the ECM during and after pregnancy have been suggested as one of the mechanisms leading to development of pelvic floor disorders including SUI and POP.

The main component of ECM is collagen. Collagen accounts for 30% of all proteins in human body. Collagen fibrils allow connective tissues to withstand tensile forces. To date 27 different collagen types have been identified each of which is coded by a specific gene [151]. Most commonly encountered collagen types are collagen I and III constituting 80-90% of the collagen in human body. Collagen is synthesized as procollagen and after being secreted to the extracellular space procollagen acquires a triple helical structure and assembles into the highly ordered fibrillary collagen [152].

Collagen turnover is mediated by a balance between collagen synthesis and degradation. Collagen degradation is mainly driven by a family of matrix metalloproteinases (MMP). The action of these enzymes is regulated by interefering with their synthesis, activation and activity inhibition at the tissue (tissue MMP inhibitors) at multiple levels. On the other hand collagen synthesis is followed by a series of post- translational modification reactions which eventually lead to formation of a mature, high tensile strength double helix of collagen that can provide structural support.

4.1.1. The role of defective ECM production in POP and SUI

In women with SUI and POP, anatomical defects and/ or biochemical dysfunctions of the pelvic floor support structures have been suggested as the possible etiological factors. Changes in biochemical composition of ligaments, paravaginal tissues and vaginal wall have been reported with decreased levels of collagen I and III that can lead to reduced tensile strength of these structures [153], [154]. Also elevated levels of MMP and reduced activity of MMP inhibitors were found in paravaginal tissues [155]. Furthermore, impaired healing of tissues following pelvic floor surgery leading to recurrencd has been suggested to be due to the underlying primary defect in connective tissue metabolism. It has been reported that in women with altered collagen I and III metabolism risk of recurrence of POP after surgery was significantly higher [156]. Nevertheless it is not clear whether the observed changes in ECM composition and organization are the cause or the effect of the underlying POP [32]. Therefore defects in collagen synthesis and turnover appear to be a part of the disease process in women with SUI and/or POP but the exact pathophysiological pathways are not clear.

4.1.2. The effect of Vitamin C on collagen metabolism

Vitamin C is historically known to be the single most crucial vitamin to play a role in collagen biosynthesis. Deficiency of Vitamin C is called 'scurvy' and it has been associated with sailors who go on lengthy voyages without access to fresh fruit. Scurvy manifests itself as a severe connective tissue disorder characterized by swollen bleeding gums, non- healing wounds, edematous legs with soft tissue heamorrhage and bruising together with other constitutional symptoms.

Vitamin C exerts its effects on collagen synthesis and post-translational modification at multiple levels: (1) acting as a co- factor for the enzyme prolyl hydroxylase which is responsible for crosslinking of collagen fibrils thus forming the triple helix structure [157], (2) stimulating collagen gene expression via malondialdehyde [158] and (3) activation of collagen gene transcription and stabilization of procollagen mRNA [159], [160]. Vitamin C is absorbed in the small intestine and its blood concentrations is regulated by renal excretion. Humans rely on a continuous supply of Vitamin C in their diet.

4.1.3. Effect of Vitamin C on angiogenesis

Vitamin C can influence blood vessel formation through its effects on collagen III and IV which are the main types of collagens forming the blood vessel wall and basement membrane. Ascorbic acid is an essential co- factor in expression, maturation and deposition of collagen in ECM of cultured fibroblasts, vascular smooth muscle cells and endothelial cells [161], [162]. Some contradictory results have been reported on the effects of Vitamin C on angiogenesis. Some studies evaluating the effect of ascorbic acid on CAM demonstrated angiostatic effects for ascorbic acid [163] whereas others reported ascorbate-2- phosphate to be significantly proangiogenic [164]. This variability can be due to different experimental setups and dosages.

4.1.4.Vitamin C and POP/ SUI

Although a strong association between collagen metabolism and Vitamin C and changes in collagen structure and biochemical composition and pelvic floor disorders are known, the role of Vitamin C in pathophysiology of SUI and POP is not known. A recent study however suggested that Vitamin C supplementation during pregnancy in rats resulted in increased type I and III collagen content in cardinal and uterosacral ligaments [165]. In a cross sectional study of 96 women with and without POP, smokers with POP were found to have lower levels of Vitamin C and higher levels of MMP-9 compared to non- smokers with POP suggesting smoking can effect development of POP via depleting vitamin C levels [166]. In a population based cross sectional study between 2002 and 2005, the Boston Area Community Health survey, adult women who had high- dose Vitamin C intake were more likely to report storage type lower urinary symptoms. However normal intake of vitamin C from food and beverages decreased lower urinary tract symptoms [167]. Nevertheless the evidence is very limited to suggest Vitamin C deficiency as a cause of any pelvic floor disorder as well as a positive effect of Vitamin C supplementation in prevention of SUI and POP.

Therefore Vitamin C is a potent stimulator of collagen production and can have positive effects on new blood vessel formation. In this section Vitamin C is incorporated in scaffolds with the aim of improving tissue integration of the materials by increasing ECM production and by stimulating angiogenesis.

4.1.5. Incorporation of Vitamin C into Tissue Engineered scaffolds

Ascorbic acid (AA) is the naturally occurring and metabolically active form of Vitamin C in humans. It has been used since 1970s as a supplement in culture media to increase the collagen production of fibroblasts [168]. AA is easily oxidizable and is not stable in aerobic culture conditions [169] therefore a variety of AA derivatives such as Ascorbate-2-phosphate [A2P] and ascorbate sodium salt have been synthesized. A2P has been the most widely used synthetic form of AA with its good chemical stability (Figure 4.1) with the same activity as AA [170], [171]. Nevertheless there are a few direct comparisons of AA analogs [172], [173] in terms of their effects on collagen production by fibroblasts. A continuous supplementation of either AA or A2P in culture media so as to mimic a sustained release state from a biomaterial, has not been studied. This can be important because if a continuous supply of AA can be achieved it would abolish the need for using a more stable derivative such as A2P.

A2P was previously incorporated into PLGA scaffolds using the solvent- casting, particulate leaching technique achieving a sustained release [174]. Using the electrospinning spinning technique, substances with high hydrophilicity often fail to form stable solutions with the hydrophobic polymer solutions [169]. To overcome this the technique of 'emulsion electrospinning' was described. In this technique a surfactant is used to form a stable emulsion where hydrophilic substances are in the water phase and hydrophobic polymer solutions are in the oil phase. Upon electrospinning, the hydrophillic phase constitutes the core of the electrospun fibres whereas the hydrophobic phase forms a shell around the hydrophilic core [175], [176]. Successful encapsulation of vascular endothelial growth factor [177], Rhodamine B [178] and human nerve growth factor [179] with the emulsion electrospinning technique have been reported previously.

The aims of this section were to construct emulsion electrospun PLA scaffolds that are able to release vitamin C derivatives (AA and A2P) and assess the effects of these scaffolds on collagen production and angiogenesis.

Figure 4.1. The chemical formula of L- ascorbic acid (AA) and ascorbate-2 phosphate (A2P). AA can easily oxidize whereas A2P is more stable.
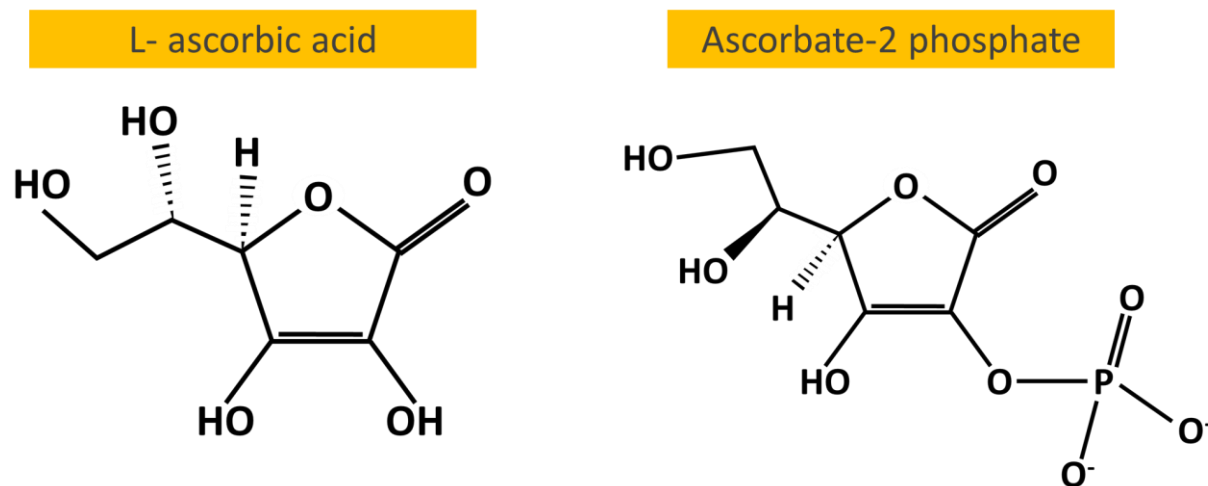
4.2. Effect of Vitamin C on collagen production of human dermal fibroblasts

The effects of Vitamin C on collagen production of human dermal fibroblasts (HDFs) were evaluated on proliferating cultures of HDFs and confluent cultures of HDFs. HDF cultures were supplemented by two forms of AA in these experiments: AA and A2P. Furthermore, to mimic a continuous release state of the drugs, as would be expected to occur with sustained release from the biomaterials, AA and A2P were supplemented in cell culture media freshly every day which was compared to routine supplementation in culture media. The flowchart of this experimental design is shown in Figure 4.2.

Figure 4.2. Flowchart of the experimental design to assess collagen production of human dermal fibroblasts on tissue culture plastic when ascorbic acid (AA) and ascorbate- 2 phosphate (A2P) are supplemented daily to mimic a continuous release state.
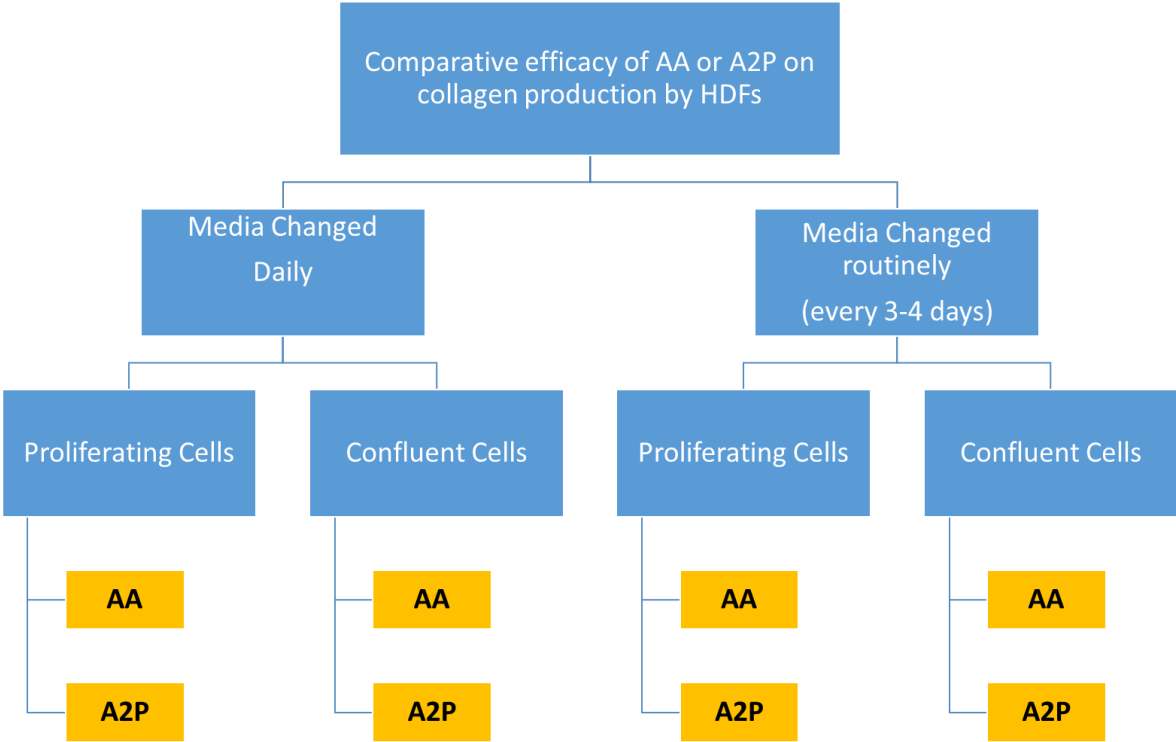
4.2.1. Effect of Vitamin C on collagen production of 'proliferating cultures of fibroblasts'

Human dermal fibroblasts (HDFs) were seeded in 12 well plates at a concentration of 50,000 cells per well. Supplementation of AA and A2P in media started next day for 'proliferating' cultures. Cell culture media consisting of DMEM supplemented with 10% FCS and 1% penicillin/streptomycin was used to prepare the following concentrations of AA and A2P in media: 0, 10, 100, 300 and 600 μM. Media was prepared freshly and changed every day for 14 days in the 'media changed daily group'. For the 'media changed every 3-4 days' group' the media was replaced every 3-4 days for 14 days. The results of collagen production in this section were presented as a percent (%) increase in collagen production compared to collagen production of fibroblasts grown in non-supplemented media.

Daily supplementation of proliferating fibroblasts with 10, 100, 300 and 600 μM concentrations of either AA or A2P resulted in a dose dependent increase in collagen production up to a maximum of 100% by 14 days of culture. Compared to supplementation every 3-4 days, which resulted in a maximum of 50% increase in total collagen production, daily supplementation of AA at a concentration of 600 μM and daily supplementation of A2P at concentrations of 100, 300 and 600 μM resulted in significantly more collagen production (Figure 4.3.).

Figure 4.3. Total collagen production of proliferating fibroblasts supplemented with either ascorbic acid (AA) or ascorbate- 2 phosphate (A2P) daily or routinely (every 3-4 days) after 14 days of culture (*p<0.05 and **p<0.005, compared to every 3-4 days' group).
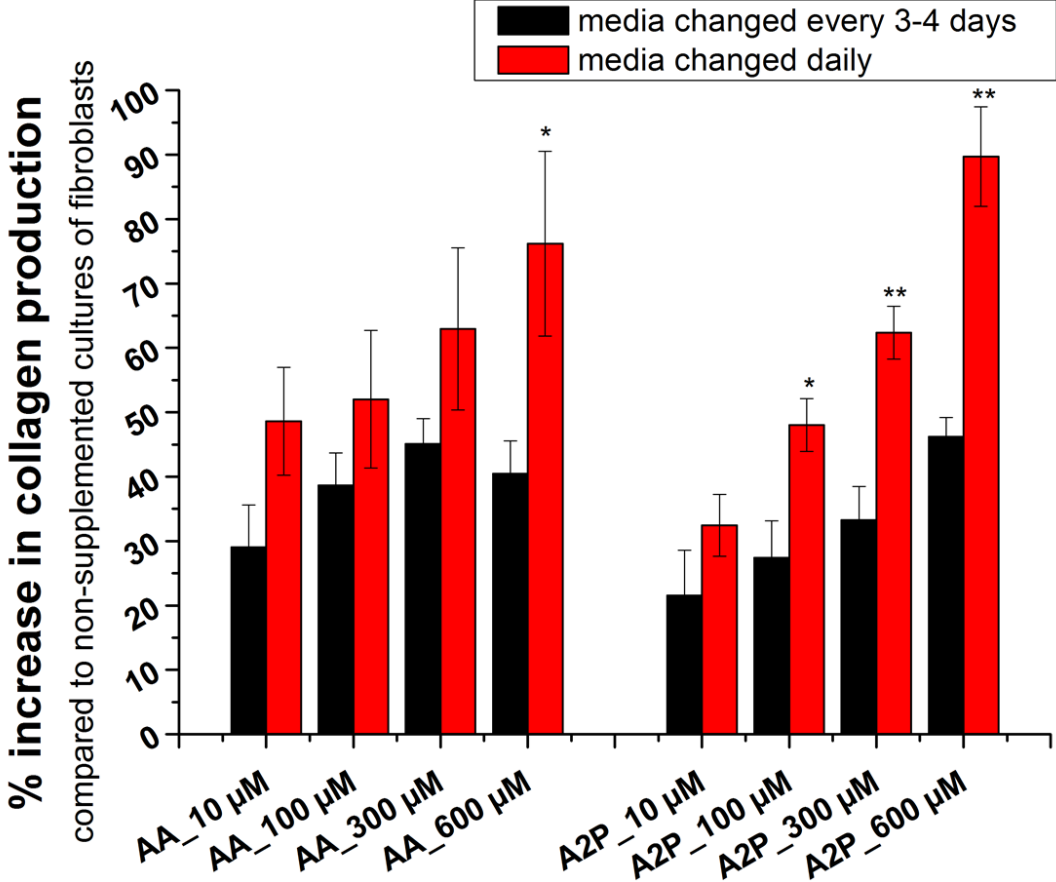
4.2.2.Effect of Vitamin C on collagen production of 'confluent cultures of fibroblasts'

Human dermal fibroblasts (HDFs) were seeded in 12 well plates at a concentration of 50 000 cells per well. Supplementation of AA and A2P in media started 3 days after seeding for 'confluent' cultures. Cell culture media consisting of DMEM supplemented with 10% FCS and 1% penicillin/streptomycin was used to prepare the following concentrations of AA and A2P in media: 0, 10, 100, 300 and 600 µM. Media was prepared freshly and changed every day for 7 days in the 'media changed daily group'. For the 'media changed every 3-4 days' group' the media was replaced every 3-4 days for 7 days. The results of collagen production were presented as a percent (%) increase in collagen production compared to collagen production of fibroblasts grown in non-supplemented media.

Daily supplementation of proliferating fibroblasts with 10, 100, 300 and 600 µM concentrations of either AA or A2P resulted in a dose dependent increase in collagen production up to a maximum of 60% at 7 days of culture was observed with significantly more collagen production at all concentrations in the daily supplemented groups (Figure 4.4.).

Figure 4.4. Total collagen production of confluent cultures of fibroblasts supplemented either with AA or A2P daily or once every 3-4 days for 7 days (*$p<0.05$ and **$p<0.005$, compared to every 3-4 days group).
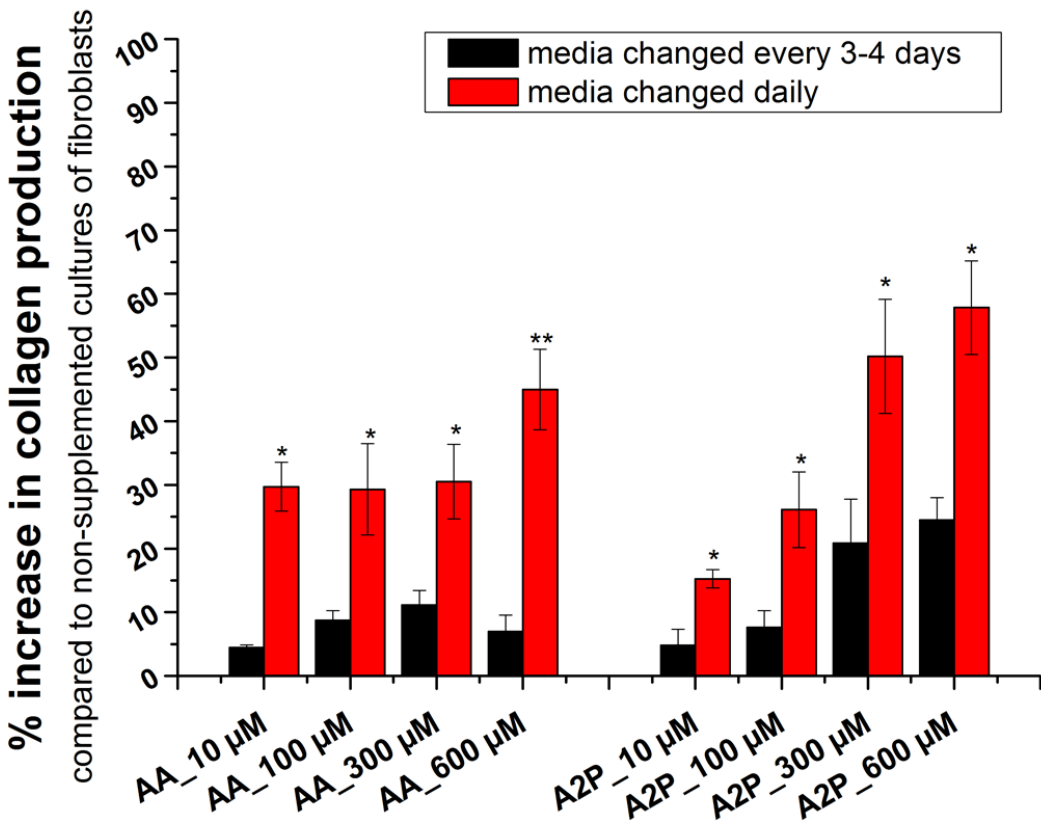
4.3. Production of Vitamin C releasing PLA scaffolds

Scaffolds containing 3 different concentrations of AA and A2P were prepared: 0.0001, 0.001 and 0.01 grams of either AA or A2P per gram of PLA (summarized in Table 4.1). AA and A2P were first dissolved in 500 µl of distilled water and with the aid of the surfactant an emulsion with the polymer solution was prepared for electrospinning. Additionally, polymer solutions containing neither AA nor A2P but only 500 µl distilled water to make the emulsion was also prepared (Vehicle scaffolds) (Figure 2.3). All emulsions were freshly prepared and electrospun immediately.

Table 4.1. Summary of all scaffolds produced in this section.

Scaffold	Acronym	Production method	Ingredients
PLA	PLA	Electrospinning	PLA
Emulsion electrospun PLA	Vehicle scaffold	Emulsion electrospinning	PLA+ surfactant+ distilled water
AA releasing emulsion electrospun PLA	AA scaffold	Emulsion electrospinning	PLA+ surfactant+ distilled water + AA
0.0001 g AA/ g of PLA	AA_0.0001		
0.001 g AA/ g of PLA	AA_0.001		
0.01 g AA/ g of PLA	AA_0.01		
A2P releasing emulsion electrospun PLA	A2P scaffold	Emulsion electrospinning	PLA+ surfactant+ distilled water + A2P
0.0001 g A2P/ g of PLA	A2P_0.0001		
0.001 g A2P/ g of PLA	A2P_0.001		
0.01 g A2P/ g of PLA	A2P_0.01		

4.3.1. Demonstration of release of Vitamin C from PLA scaffolds

All measurements of AA and A2P were performed using a UV- spectrophotometer (Thermo Scientific™ Evolution 220) at an absorbance wavelength of 252 nm. A previously constructed calibration curve (Figure 2.6) was used to determine the concentration of AA and A2P in a given solution.

Release of AA and A2P from scaffolds were studied in distilled water. Three pieces of AA and A2P scaffolds (mean weights: 0.0199± 0.002 and 0.0176± 0.002, respectively) were placed in 4 mL media and were kept in a dry incubator at 37°C. A vehicle scaffold was taken as a control. At 2, 4, 6, 8, 10 hours and 1, 2, 3, 7, 14, 21 and 28 days a sample was removed from the media, the absorbance measured and the concentration was determined with use of the calibration curve. All the media were then discarded and replaced with fresh media. Experiments were repeated three times.

Release characteristics

The sustained release of both AA and A2P over 28 days (Figure 4.5). Percentage release of the drug at each point was calculated based on the actual drug content. For AA releasing PLA scaffolds a burst release of 77% of AA in the first 2 hours was followed by the release of 90% of the actual drug content in the first 10 hours. Afterwards AA was not measurable after 72 hours. For A2P releasing PLA scaffolds a burst release of 34% was followed by the release of 60% of the actual drug content in 14 days which continued gradually until 28 days.

Therefore, AA had a significant burst release compared to the more sustained release of A2P from electrospun PLA scaffolds. The released AA from the scaffolds were depleted after 72 hours whereas A2P continued to be released over 28 days.

Figure 4.5. Cumulative release of AA and A2P over 28 days.
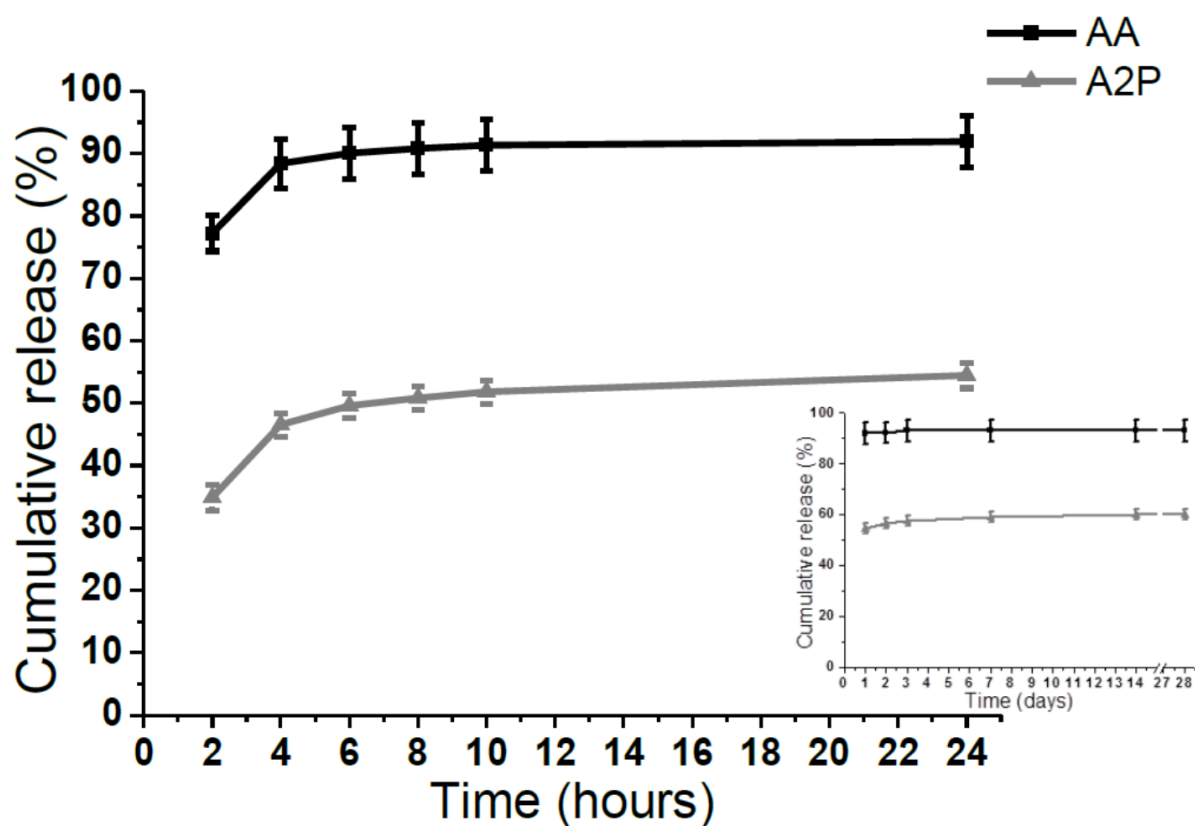
Encapsulation efficiency

The indicated concentrations of AA or A2P in scaffolds are the amount of vitamin C put into the polymer solution that went into electrospinning. This is called the 'theoretical drug content'. During the electrospinning process the amount of polymer and the vitamin that go into the electrospun fibrous mat can be disproportional. Therefore, the 'actual drug content' that is encapsulated within the micro/ nanofibers of the electrospun PLA scaffolds can be different to the 'theoretical drug content'. This can be studied by calculating the 'encapsulation efficiency'.

The electrospun scaffolds were dissolved back and vitamin content was extracted. An accurately weighed 20 mg piece of AA and A2P releasing electrospun PLA scaffold was dissolved in 10 mL of DCM. On top of the polymer- vitamin solution a 5 mL volume of distilled water was added and the suspension was vigorously vortexed intermittently for 30 min the extract all the hydrophilic vitamin C into the water phase. The suspension was then left to stand still for 60 minutes to facilitate separation of the water and oil phases. The water phase containing vitamin C was than pipetted out and absorbances were read using UV spectrophotometer. The encapsulation efficiencies for AA and A2P were calculated to be 46.8% (± 6.45) and 44.06% (± 7.14).

The encapsulation efficiency (%) was calculated using the following formula:

(Actual drug content/ Theoretical drug content) x 100.

4.4. Characterization of Vitamin C releasing PLA scaffolds

4.4.1. Ultrastructure

The effect of incorporation of AA and A2P on the ultrastructure of electrospun PLA scaffolds was studied using SEM. The SEM images of the AA and A2P releasing scaffolds are shown in Figure 4.6. The mean fibre diameter and the mean pore size for AA, A2P and Vehicle electrospun PLA scaffolds were 0.99 (±0.60); 1.04 (±0.56) and 1.11 (±0.63) and 5.66 (±3.18); 5.76 (±2.76) and 5.47 (±3.52), respectively. For PLA only scaffolds the mean fibre diameter and the mean pore size was 1.06 (±0.72) μm and 5.65 (±4.61) μm, respectively. Therefore, neither the incorporation of the surfactant (Span-80) nor the incorporation of AA or A2P in electrospun PLA scaffolds had an effect on scaffold ultrastructure.

Figure 4.6. The ultrastructure of ascorbic acid (AA) and ascorbate- 2 phosphate (A2P) releasing electrospun PLA scaffolds (scale bar represents 20 μm for all images).
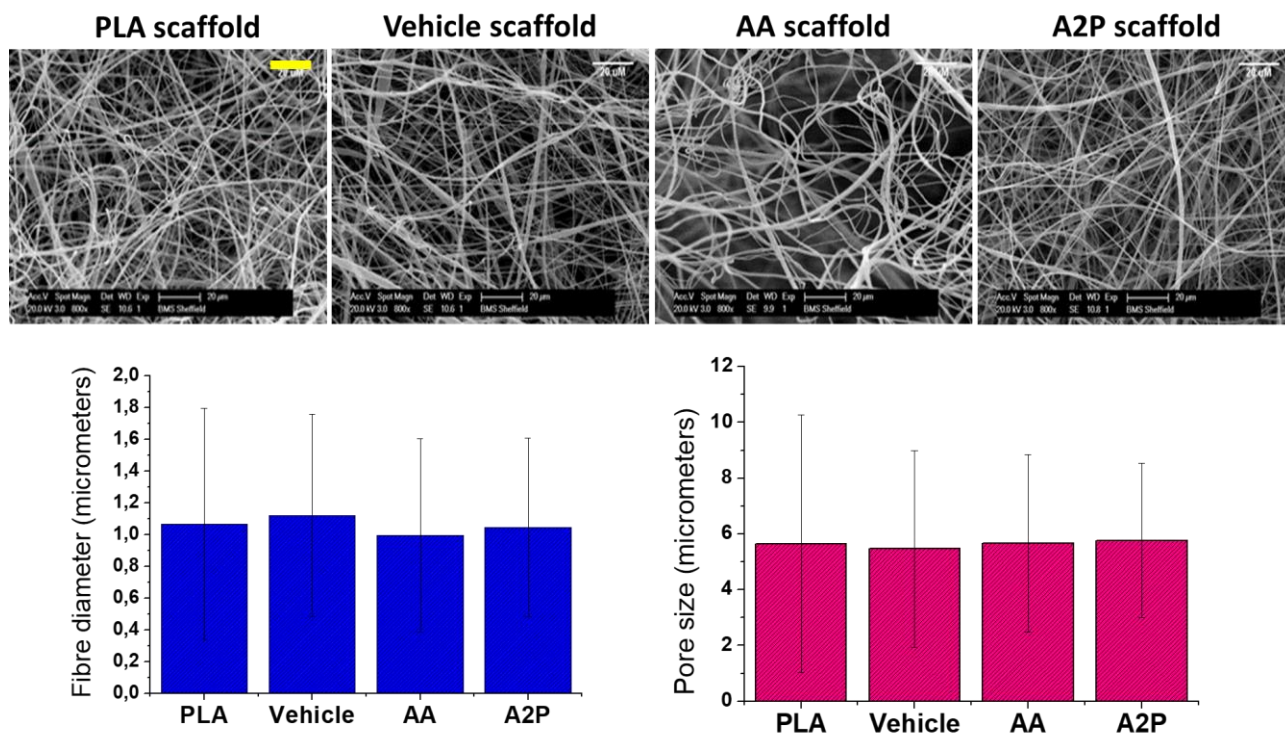
4.4.2. Wettability

The water uptake of AA, A2P and vehicle scaffolds was significantly higher than that of pure electrospun PLA scaffolds (Figure 4.7).   The water uptake (% increase in weight) of scaffolds containing AA were significantly higher in the first 7 days compared to vehicle scaffolds (355.84 [±140.36] vs 274.84 [±108.21] at day 1, p=0.005; 407.69 [±62.38] vs 299.76 [±92.2] at day 2, p=0.001; 397.74 [±53.3] vs 328.76 [±80.31] at day 3, p=0.001 and 363.64 [±45.32] vs 304.31 [±65.59] at day 7, p=0.001) whereas those of A2P containing scaffolds were significantly lower at all-time points compared to vehicle scaffolds (161, 1 [±116.36] vs 317.55 [±62.25] at day 14, p=0.001).

The wettability of AA and A2P scaffolds containing different concentrations of the drug was also evaluated. For AA scaffolds there was no difference in the wettability between AA releasing scaffolds of 0.0001 g, 0.001 g and 0.01 g of AA per gram of PLA concentrations (mean percentage increase in weight was 350.52 [±192.54], 325.41 [±191.72] and 321.06 [±186.65], respectively [p=0.49]). A2P releasing scaffolds with 0.001 g per gram of PLA were slightly more hydrophilic (mean percentage increase in weight being 72.84 [±64.24], 174.02 [±153.54] and 79.46 [±84.71] for 0.0001 g, 0.001 g and 0.01 g of A2P per gram of PLA concentrations, respectively [p=0.03]).

Figure 4.7. The wettability of emulsion electrospun PLA scaffolds. (A) Representative images of scaffolds at day 1 of water uptake experiment showing partial wetting of all AA, A2P and vehicle scaffolds when PLA only scaffolds were wetting at all (B) Percent increase in weight of the emulsion electrospun scaffolds upon incubation in PBS over 21 days (*p<0,005 compared to vehicle scaffolds) (C) Correlation of percent increase in weight (PIW) and Ultimate Tensile Strength
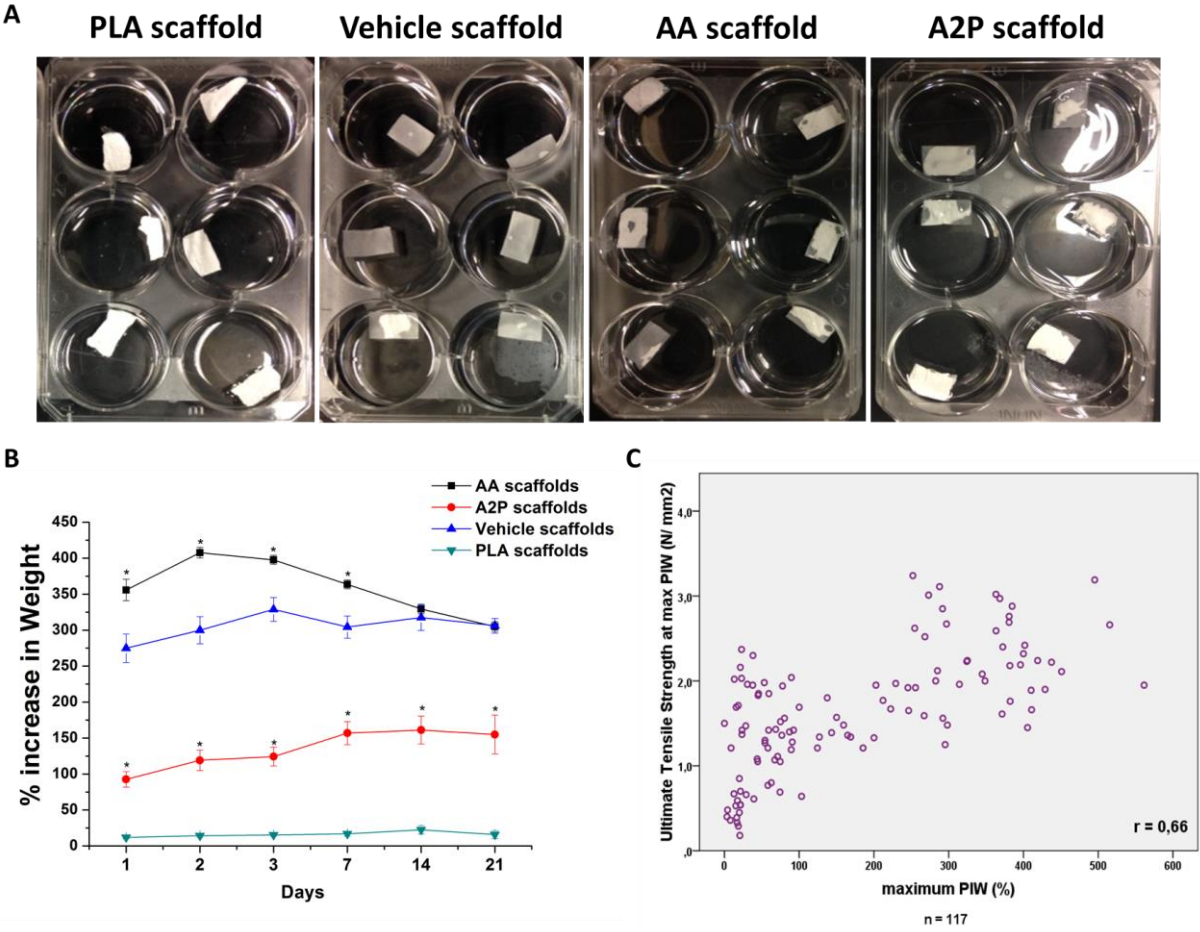
4.4.3.Mechanical properties

This was studied both in dry and wet scaffolds. Also the effect of water uptake on mechanical properties was studied. Since the water uptake of our scaffolds occurred gradually the mechanical properties in the wet state were evaluated at days 3, 7, 14 and 21 after the scaffolds were placed in PBS in incubator.

In their dry state, all emulsion electrospun scaffolds (AA, A2P and Vehicle scaffolds) had higher UTS, strain and YM values compared to pure PLA scaffolds (Figure 4.8). On the other hand, there was no difference in the mechanical properties of the emulsion electrospun PLA scaffolds.

In their wet state, the UTS and strain values of AA and Vehicle scaffolds further increased, whereas the Young' s modulus were variable. The mechanical properties of A2P scaffolds did not change significantly when wet compared to when dry. The UTS of AA scaffolds were significantly higher than Vehicle scaffolds only at day7 (Table 4.2). There was a statistically significant correlation between the percent increase in weight and the UTS of wet scaffolds at day 3, 7, 14 and 21 (Pearson r= 0, 64 [p<0,001], 0, 78 [p<0,001], 0, 67 [p<0,001] and 0, 85 [p<0,001], respectively), the strongest correlation was observed at day 21.

Figure 4.8. Mechanical properties in dry and wet states for all scaffolds. (The values in the y axis are mean of days 3, 7, 14 and 21).
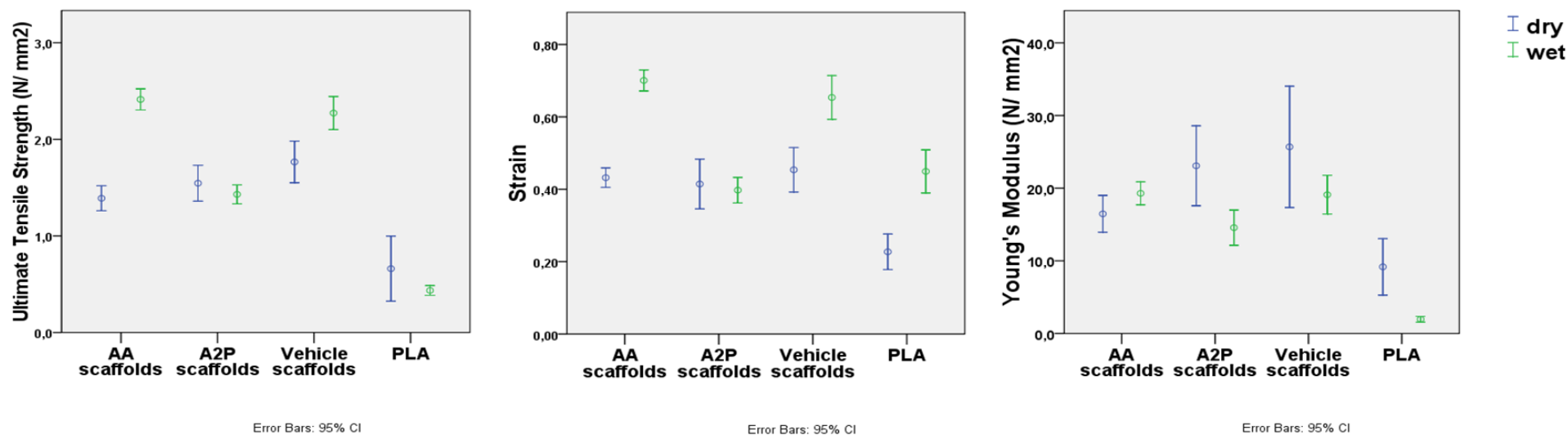
Table 4.2. Mechanical properties of AA and A2P releasing scaffolds at days 3, 7, 14 and 21 in *in vitro* culture conditions. Values are mean (standard deviation). ($^{+}p<0.05$ and $^{++}p<0.005$ compared to PLA; $^{*}p<0.05$ and $^{**}p<0.005$ compared to Vehicle scaffolds)

	Dry			Wet (day 3)			Wet (day 7)			Wet (day 14)			Wet (day 21)		
	UTS	Strain	YM	UTS	Strain	YM	UTS	Strain	YM	UTS	Strain	YM	UTS	Strain	YM
AA scaffolds	1.39$^{++,**}$	0.43^{++}	16.46$^{++,**}$	2.37^{++}	0.66^{++}	20.07^{++}	2.93$^{++,**}$	0.77^{++}	24.06^{++}	2.36^{++}	0.73^{++}	13.57^{++}	2.26^{++}	0.59^{++}	21.78$^{++,*}$
	(0.30)	(0.06)	(5.99)	(0.45)	(0.15)	(7.81)	(0.55)	(0.08)	(8.06)	(0.44)	(0.12)	(4.70)	(0.39)	(0.17)	(5.60)
A2P scaffolds	1.54^{++}	0.41^{++}	23.08^{++}	1.49$^{++,**}$	0.48	14.76^{++}	1.28$^{++,**}$	0.44**	9.62$^{+,*}$	1.52$^{++,**}$	0.37**	15.49^{++}	1.27$^{++,**}$	0.31$^{+,**}$	16.56$^{++,*}$
	(0.41)	(0.15)	(12.07)	(0.38)	(0.48)	(10.81)	(0.48)	(0.09)	(7.03)	(0.37)	(0.18)	(10.29)	(0.46)	(0.15)	(12.75)
Vehicle scaffolds	1.76^{++}	0.45^{++}	25.68^{++}	2.36^{++}	0.58^{++}	20.97^{++}	2.10^{++}	0.71^{+}	16.93^{++}	2.23^{++}	0.66^{+}	14.18^{++}	2.45^{++}	0.47^{++}	27.08^{++}
	(0.25)	(0.07)	(9.03)	(0.34)	(0.17)	(6.42)	(0.57)	(0.12)	(6.51)	(0.66)	(0.17)	(5.54)	(0.35)	(0.07)	(4.56)
PLA	0.66	0.22	9.17	0.71	0.40	3.56	0.34	0.45	1.80	0.54	0.36	2.75	0.30	0.40	1.70
	(0.36)	(0.05)	(4.20)	(0.23)	(0.11)	(2.12)	(0.10)	(0.16)	(0.73)	(0.09)	(0.15)	(1.86)	(0.04)	(0.05)	(0.79)

4.5. Effect of Vitamin C on collagen production of fibroblasts seeded on scaffolds

The SEM images showed continuous coverage of the scaffold surface by fibroblasts and extracellular matrix which was more intense in AA and A2P containing scaffolds (Figure 4.9). Although lower concentrations of AA and higher concentrations of A2P seemed to work better, no single concentration of either AA or A2P proved to be significantly different than other concentrations.

Figure 4.9. SEM images showing the ECM produced by the human dermal fibroblasts seeded on the scaffolds and corresponding DAPI staining of the cell nuclei of fibroblasts grown on scaffolds for 14 days (scale bar represents 50 µM for all images).
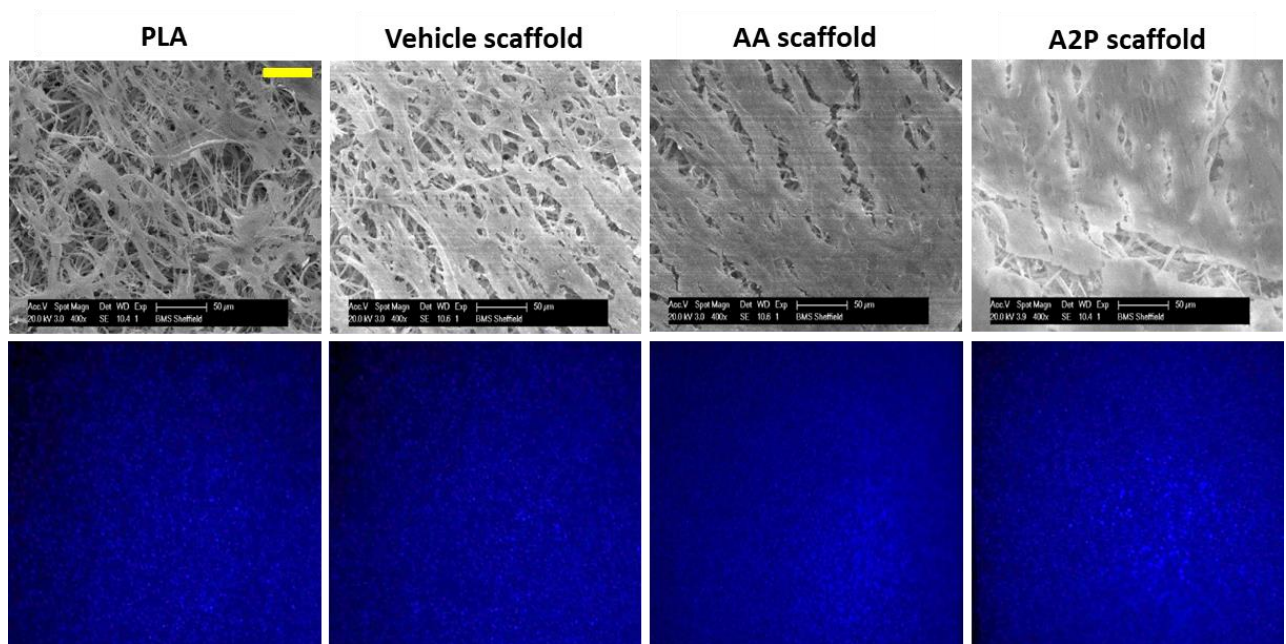
Scaffolds were cut into 8x8 mm squares using sterile forceps and scissors. A total of 500.000 HDFs were seeded and cultured on the scaffolds for 14 days. The metabolic activity of HDFs grown on scaffolds was assessed on days 3, 7 and 14 (Figure 4.10A).

Total collagen production of HDFs grown on scaffolds was assessed by Sirius red staining. HDFs produced significantly more collagen at all concentration of AA and A2P scaffolds compared to Vehicle scaffolds (Figure 4.10B). The mean corrected absorbance values (Sirius red stain/gram of PLA) were 5.44 (±0.50); 5.26 (±0.46); 4.44 (±0.49) and 4.41 (±0.41); 5.32 (±0.55); 5.50 (±0.51) for AA and A2P scaffolds with concentrations of 0.0001; 0.001; 0.01 grams of either AA or A2P per gram of PLA. respectively. Corresponding values for Vehicle and PLA scaffolds were 3.86 (±0.43) and 3.39 (±0.43), respectively.

Figure 4.10. Metabolic activity of fibroblasts grown on scaffolds over 14 days (A) and total collagen production by Sirius red staining (B).
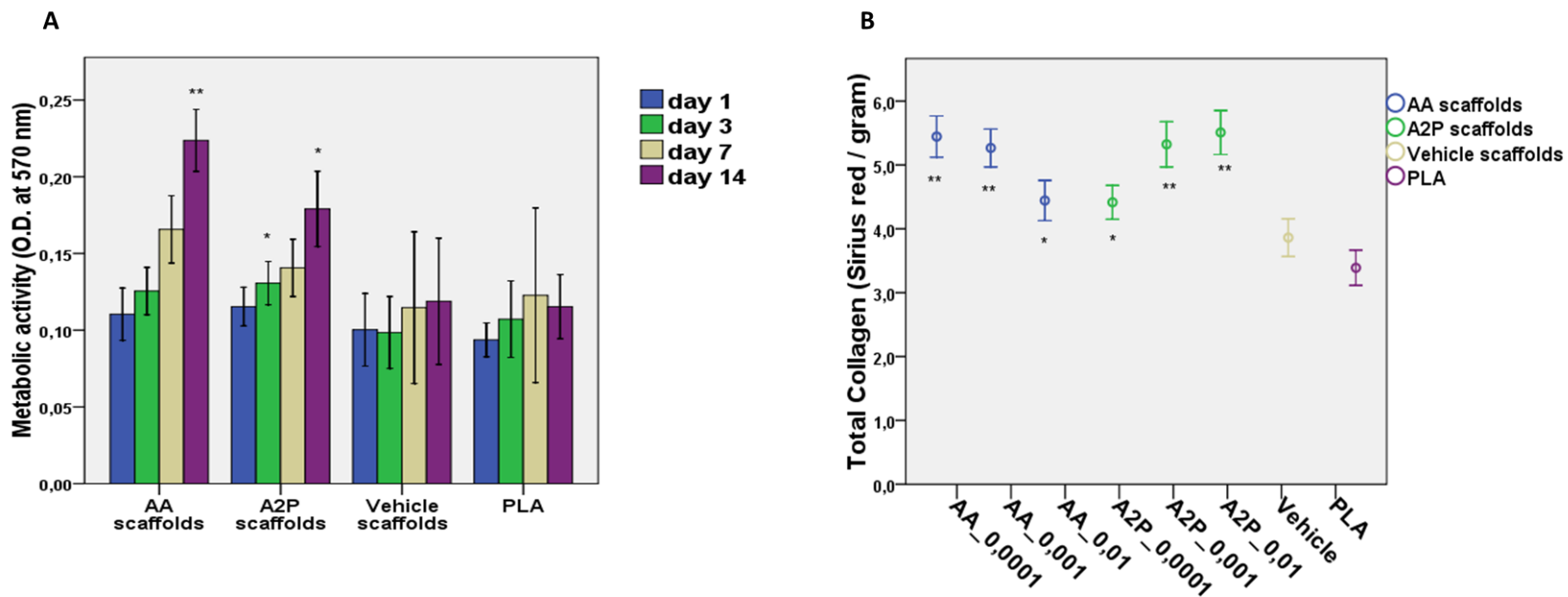
4.6. Angiogenic properties of Vitamin C releasing PLA scaffolds

4.6.1. Day of evaluation of angiogenesis

After the electrospun scaffolds are placed on the CAM at EDD 7. The angiogenic response could be evaluated between EDD 10 and 14. To determine the best time point to evaluate the angiogenic response to vitamin C releasing PLA scaffolds initial experiments were conducted by taking serial images daily starting from EDD 10 (Figure 4.11). By EDD 11 the scaffolds started to contract with the underlying CAM making it more difficult to assess a possible anti-angiogenic effect. Therefore the angiogenic responses to vitamin C releasing scaffolds were all assessed on EDD 10.

Figure 4.11. Daily follow up of the scaffolds implanted on CAM starting from EDD 10. Scaffold start contracting starting from EDD 11 obscuring a negative angiogenic response to scaffolds if evaluated after EDD 10. (scale bar represents 200 μm for all images).
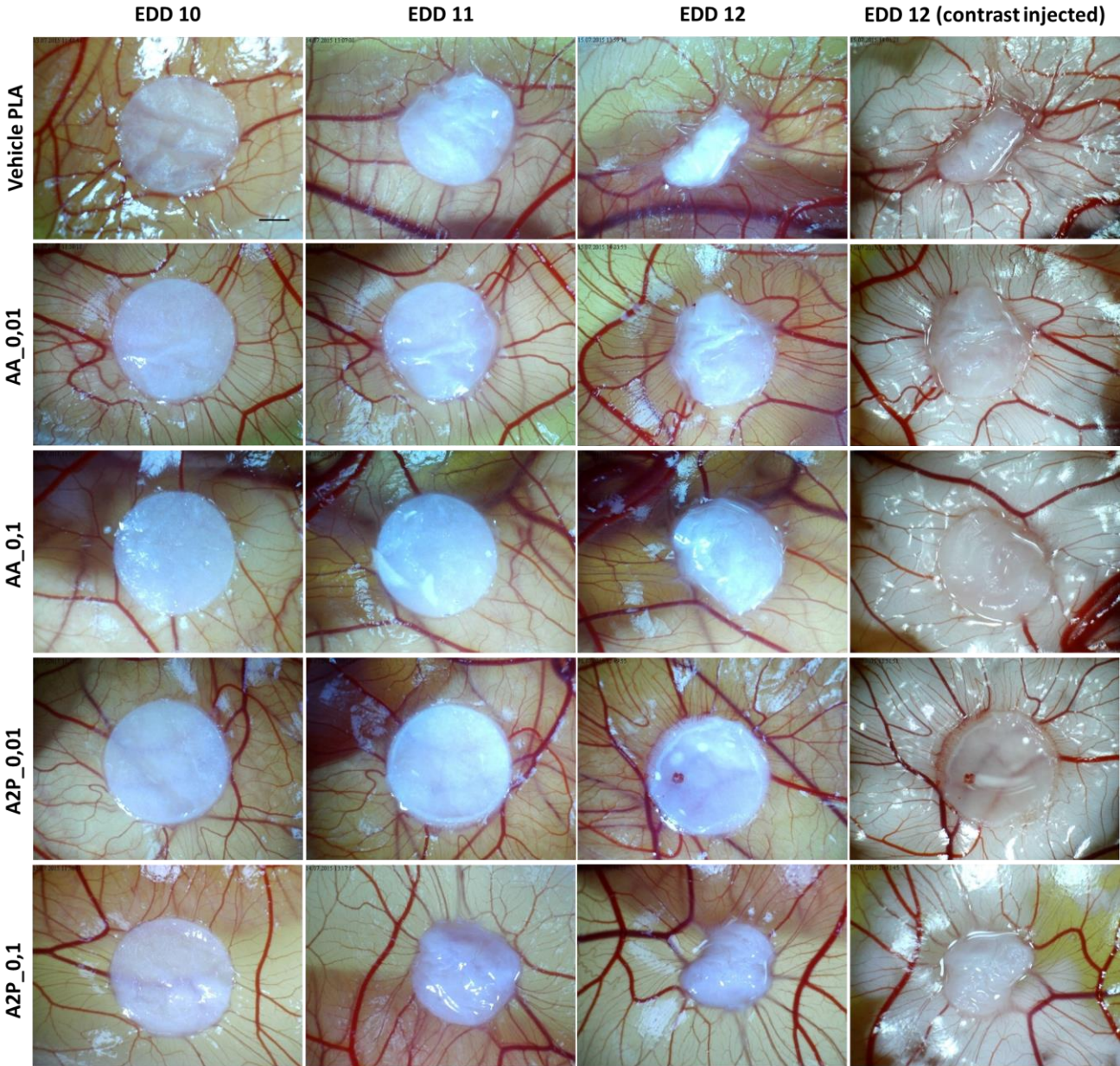
4.6.2. Angiogenic Response to vitamin C releasing PLA scaffolds

A hydrocortisone releasing electrospun PLA scaffold was used as a negative control in these experiments. For both AA and A2P scaffolds containing two different concentrations of the drug were used: 0.01 gram (low concentration) and 0.1 gram (high concentration) of AA or A2P per gram of PLA. Compared to Vehicle scaffolds. hydrocortisone releasing PLA scaffolds were angiostatic with a vasculogenic index of 11.4 (±2.6) (p=0.001) compared to 21.7 (±3.4) for the vehicle scaffolds. AA releasing scaffolds were proangiogenic at low doses (AA_0.01 g) with a vasculogenic index of 32.3 (±6.0) but angiostatic at higher doses (AA_0.1 g) with a vasculogenic index of 13.4 (±3.6) compared to Vehicle scaffolds. A2P releasing PLA scaffolds did not different from Vehicle scaffolds either at high (A2P_0.1) or low (A2P_0.01) doses of the drug (Figure 4. 12).

Figure 4. 12. Total data for the comparison of low (0.01 g per gram pf PLA) and high (0.1 g per gram of PLA) doses of AA and A2P as released from PLA scaffolds. Negative control is a hydrocortisone releasing PLA scaffold. The hydrocortisone releasing PLA scaffolds (1) decreased the number of blood vessels around the scaffold compared to controls (2). Ascorbic acid 0,01 releasing PLA scaffolds (3) stimulated angiogenesis whereas the others (4, 5 and 6) were no different to controls (scale bars represent 200 μm for all images).
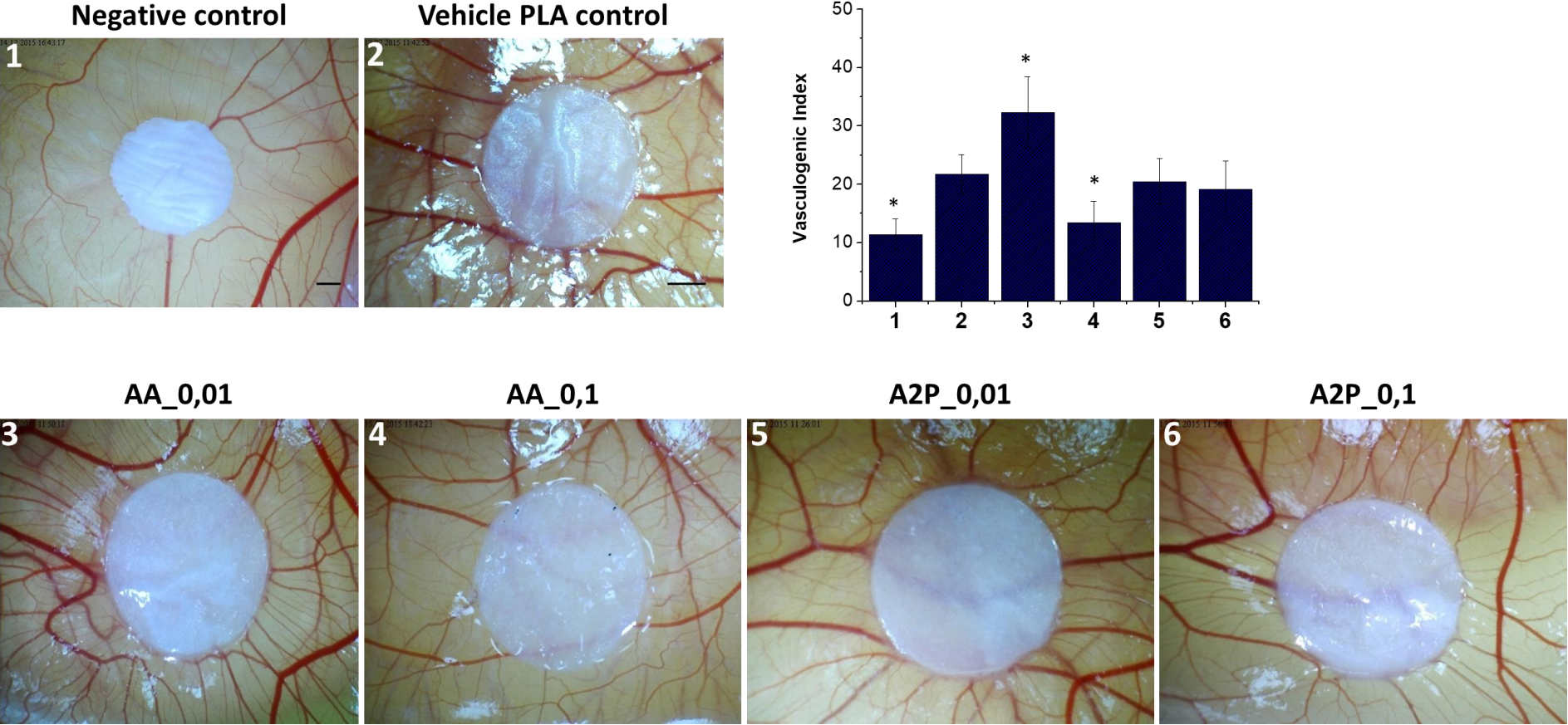
4.6.3. Initial tissue response to vitamin C releasing PLA scaffolds

The initial tissue response was only evaluated for AA releasing scaffolds as they were most proangiogenic. Both Vehicle scaffolds and AA releasing scaffolds induced a mild to moderate inflammatory response on the CAM adjacent to the scaffold with infiltration of the scaffolds by the host cells. Their appeared to be more blood vessels growing around the scaffold releasing AA in cross sections of the histologic images (Figure 4.13).

Figure 4.13. The initial tissue response to AA releasing PLA scaffolds.The interface where the PLA scaffolds integrate into CAM are shown with dotted line. Underneath the dotted line blood vessels growing underneath the scaffolds can be observed in cross section (black arrows). More blood vessels are observed in the CAM tissue adjacent to AA releasing scaffolds. Error bars represent 200 μm.
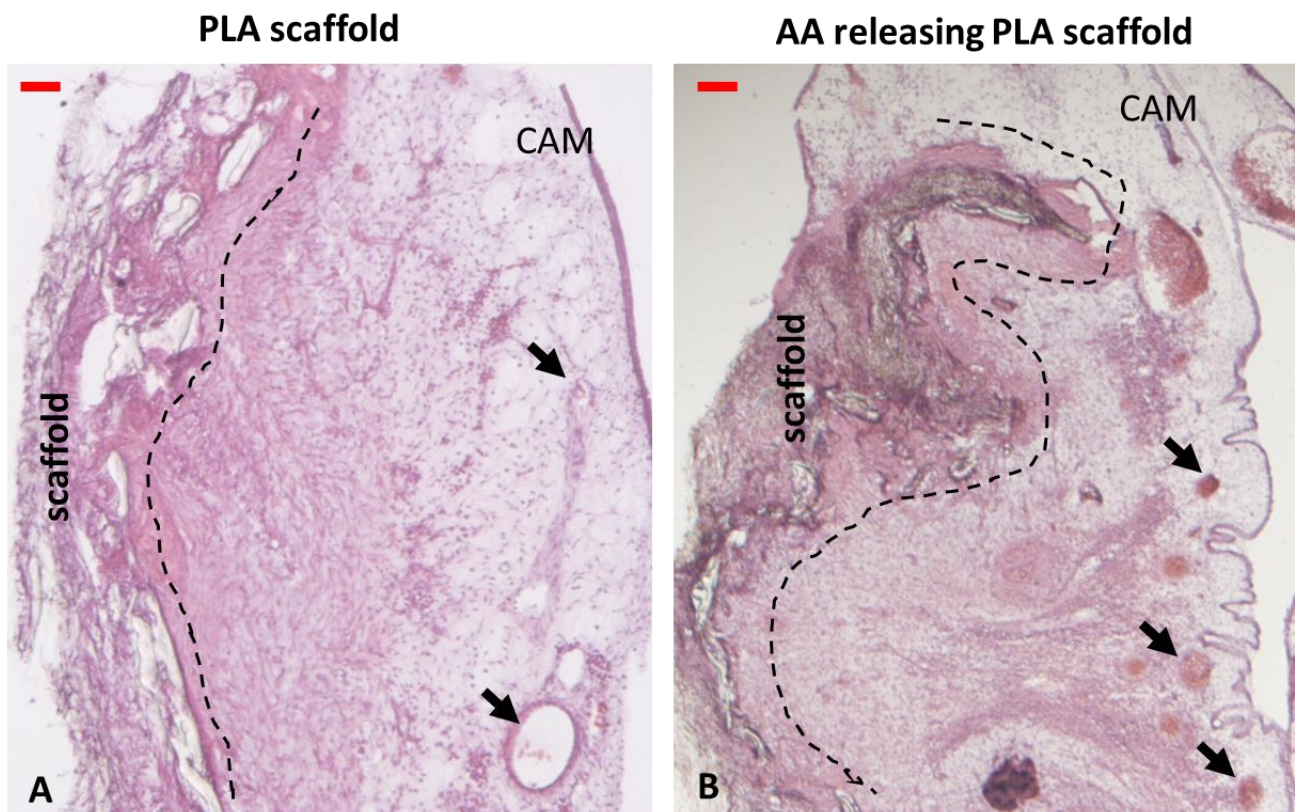
4.7. Chapter discussion

In this section PLA scaffolds with desired mechanical properties that could release AA and A2P were synthesized and assessed for for their ability to stimulate new collagen production and new blood vessel formation. The ultimate aim was to improve the tissue integration of pelvic floor repair materials once they are implanted into the host.

Firstly, these experiments showed that both derivatives of vitamin C. AA or A2P. could effectively be incorporated into biodegradable PLA scaffolds using a modification of the commonly used electrospinning setup. The first milestone in these experiments was to develop the emulsion electrospinning technique which had not been performed within the MacNeil group before. This technique allowed formation of stable emulsions of hydrophilic and hydrophobic solutions that could then be electrospun with use of a surfactant. Previous evidence demonstrated that upon electrospinning the surfactant delineates a core in the electrospun fibre that contains the hydrophilic phase whereas the hydrophobic polymer solution remains outside of the core forming an outer shell in the fibre.

The emulsion systems need to have defined concentrations and viscosity in order to be electrospun successfully [180]. The first requirement is the formation of a stable emulsion. For this purpose a surfactant (Span 80) was used and the emulsion was created by slowly pipetting droplets of water phase into the oil phase while mixing with use of rotation magnets. The resultant emulsion was stable without any phase seperation for 6 hours. During electrospinning of the emulsion. the oil phase containing the solvent rapidly evaporates leaving the high viscosity polymer to the outside of the fibre while the aqueous phase migrates to the centre of the jet. The electrostatic properties of the electrospinning solution are known to be affected by the inclusion of surfactant [181] however systematic studies do not exist on which combination of the surfactant- polymer combination will produce the desired fibre characteristics. Therefore in these experiments the non- ionic surfactant Span 80 was used at a minimum concentrations to acheive the minimum amount of an aqeuous solution containing vitamin C in the emulsion. This did not affect fibre diameter or pore sizes of the electrospun scaffolds.

Another technique of electrospinning, co- axial electrospinning, could have been used to contain bioactive substances in a core- shell morphology within the electrospun fibres [182]. The co- axial electrospinning has the advantage of not requiring a surfactant to separate water and oil phases. Instead phases are carried to the tip of the needle in separate channels which only mix together in the Taylor' s cone. However it requires a special setup using a specifically designed co- axial electrospinning needle. This technique was not used as we lacked this equipment.

The core- shell fibre structure formed by the emulsion electrospinning has also been suggested as a means to achieve a sustained release of bioactive factors encapsulated in the core of the fibres. For AA and A2P releasing PLA fibres, a successful encapsulation of the drugs was demonstrated that is consistent with the previous literature reporting encapsulation efficiencies of between 17- 90% [183]–[186]. The difference in the encapsulation and release pattern of AA and A2P can be explained by the difference in their chemical structure.

With regards to release of AA and A2P from electrospun PLA fibres. a burst release of 30- 70% of both drugs occurred within the first 10 hours. Previously. the same core- shell morphologies of hydrophilic drugs have been reported to produce burst release rates between 20- 73% with different drug- polymer combinations [179], [185], [187]. A limitation of the current release studies relates to use of distilled water as a medium in which to study drug release. Distilled water is not an ideal medium when conducting an *in vitro* release experiment as it is not similar to physiologic fluids. However, distilled water was the only option when studying AA release as PBS rapidly oxidized AA with the metal ions it contained within it making it impossible to detect the released amount of AA. AA could also be oxidized by the oxygen in air even when distilled water is used however this did not happen immediately (after 6 hours in our experiments) allowing us to carry out the experiment at 2 hourly intervals. Nevertheless, ideal release experiment would be expected to be conducted in an environment devoid of oxygen which was not possible in the given circumstances.

AA is well documented for its effect in stimulating collagen production in in vitro cultures of fibroblasts. Among the various derivatives of it. A2P appeared to be the most commonly used derivative due to its increased stability in culture conditions. However, achieving a sustained release of AA could abolish the need for A2P. Therefore, the comparative effectiveness of AA and A2P on collagen production of cultured fibroblasts in 2D was first evaluated in these experiments. No such comparative data was available in the literature. The results demonstrated that when a continuous release state was mimicked in culture conditions both AA and A2P increased collagen production of fibroblasts to a similar extent in a dose dependent manner. The toxic concentration of AA was 600 µM whereas there was no toxicity for A2P up to the highest concentration studied in these experiments.

The next step was to test the effect of the AA and A2P releasing PLA scaffolds on cell viability and collagen production of fibroblasts seeded on them. This was done using scaffolds containing three different concentrations of each drug. Overall, a significant increase in collagen production of fibroblasts up to about 60% was observed with both AA and A2P scaffolds compared to controls. It was important to note that the scaffolds containing the highest concentration of AA was least effective, although better than the control scaffolds. This could be due to higher local concentration of the drug that may have occured in micropores of the scaffold resulting in a similar toxicity to that observed in 2D experiments.

With regards to scaffold ultrastructure. incorporation of neither the surfactant nor either of the bioactive factors, AA and A2P, changed the fibre diamater and pore size of the electrospun fibres. However, all emulsion electrospun PLA scaffolds became more hydrophilic compared to control PLA electrospun scaffolds. Among the emulsion electrospun scaffolds AA releasing PLA scaffolds were the most hydrophilic followed by Vehicle scaffolds and A2P releasing scaffolds. Furthermore, AA and Vehicle scaffolds became stronger with higher UTS values and more elastic as they became wet whereas there was no difference between dry and wet states for the A2P scaffolds. Also there was a positive correlation between water uptake and the ultimate tensile strength when all emulsion electrospun were taken into account. Therefore both the addition of surfactant and a combination of AA and surfactant appear to have a plasticizing role [35]. Other surfactants such as polyethylene glycol and glucose monoesters. are reported to have acted as plasticisers [36].

The mechanical properties of the candidate materials are of particular importance when producing materials for use in female pelvic floor. Although the design requirements in terms of mechanical properties are not clearly defined for the pelvic floor. the range of normal female pelvic floor tissues is reported as a mean maximum tensile strength of 0.79 ± 0.05 Mpa and Young' s modulus of 6.65 ± 1.48 Mpa for pre-menopausal tissues [28]. Therefore, the AA and A2P releasing scaffolds are slightly above this target.

The introduction of AA into electrospun scaffolds not only stimulated more collagen production but also exerted a proangiogenic effect. Particularly AA scaffolds secreting lower concentrations of AA appeared to be signigicantly better than control scaffolds at stimulating new blood vessel formation. Surprisingly a higher concentration of AA was angiostatic porbably due to local acidic effects of AA. On the other hand scaffolds releasing A2P did not cause any change in blood vessel formation at any concentration. This raises the question of the chick embryos ability to convert A2P to AA which is performed in humans by the enzyme acid phosphatase on the cell membrane.

Taken altogether, among the scaffolds constructed in this section electrospun PLA scaffolds releasing lower concentrations of AA appear to be the best candidate to take into further analysis with their ability to stimulate new collagen formation and angiogenesis. Initial tissue responses studied on the CAM for 5 days of impantation shows a moderate cell infiltration of the scaffolds which is promising however these scaffolds needs to be further evaluated in relevant animal models with regards to their efficacy and safety.

Chapter 5.
Production and assessment of Estradiol releasing electrospun PLA scaffolds

Mangır N, Hillary CJ, Chapple CR, MacNeil S. Oestradiol-releasing biodegradable mesh stimulates collagen production and angiogenesis: An approach to improving biomaterial integration in pelvic floor repair. European urology focus. 2017 Jun 3.

Mangir, N; Eke, G; Hasirci N; Chapple C; Hasirci, V; MacNeil, S, "An Estradiol releasing hydrogel to be used as a proangiogenic biomaterial for use as a tissue interposition graft in urogenital reconstruction," accepted for publication Neurourol. Urodyn., 2019.

5.1. Chapter Introduction

Another potential drug that could be incorporated into the electrospun PLA scaffolds to improve the tissue integration is Estradiol. Estradiol is the major estrogen secreted by the premenopausal ovary to act not only on the female reproductive organs but also on many other non- reproductive organs such as the skeletal, cardiovascular, nervous and immune systems.

The three most abundant forms of estrogens in females are estrone (E1), estradiol (E2) and estriol (E3). Estrogens are steroid hormones synthesized from cholesterol most of which comes from the plasma low density lipoprotein derived from dietary cholesterol. Human adrenal gland can also synthesize cholesterol from acetate. Steroid biosynthesis is mainly derived by two enzymes: cytochrome P450s or hydroxysteroid dehydrogenases [188]. These enzymes are expressed highly in ovaries of premenopausal women, placenta in pregnant women and adipose tissue in both postmenopausal women and men. Estradiol is synthesized by the aromatization of testosterone. It can be converted to estrone with the enzyme 17β hydroxysteroid dehydrogenase while estrone can also be synthesized from androstenedione (Figure 5.1). In premenopausal women, estradiol is mainly synthesized in the ovaries to act on target tissues all over the body. After the menopause small amounts of estradiol are produced mainly at extragonadal sites including adipose tissue, bone, vascular endothelial and smooth muscle cells to act locally [189].

Estrogens exert their effects via several well defined pathways. One of the ways estrogens function is via binding of the hormone to the intracellular estrogen receptors (ER- α and β) which then modulate transcription of target genes. ER-α is mainly expressed in the uterus, mammary gland, ovary (thecal cells), bone and adipose tissue whereas ER- β is present in ovary (granulosa cells), immune system, colon and bladder. Both receptor subtypes can be found in the cardiovascular and central nervous system [190]. Therefore, the physiological functions of estrogens can also be controlled by modifying the receptor expression. Sex steroid receptors have been investigated for their role in the development of POP (reviewed in [191]) however there is limited data to reach to a conclusion.

Figure 5.1. The chemical formula and synthesis of Estradiol and its two main derivatives.
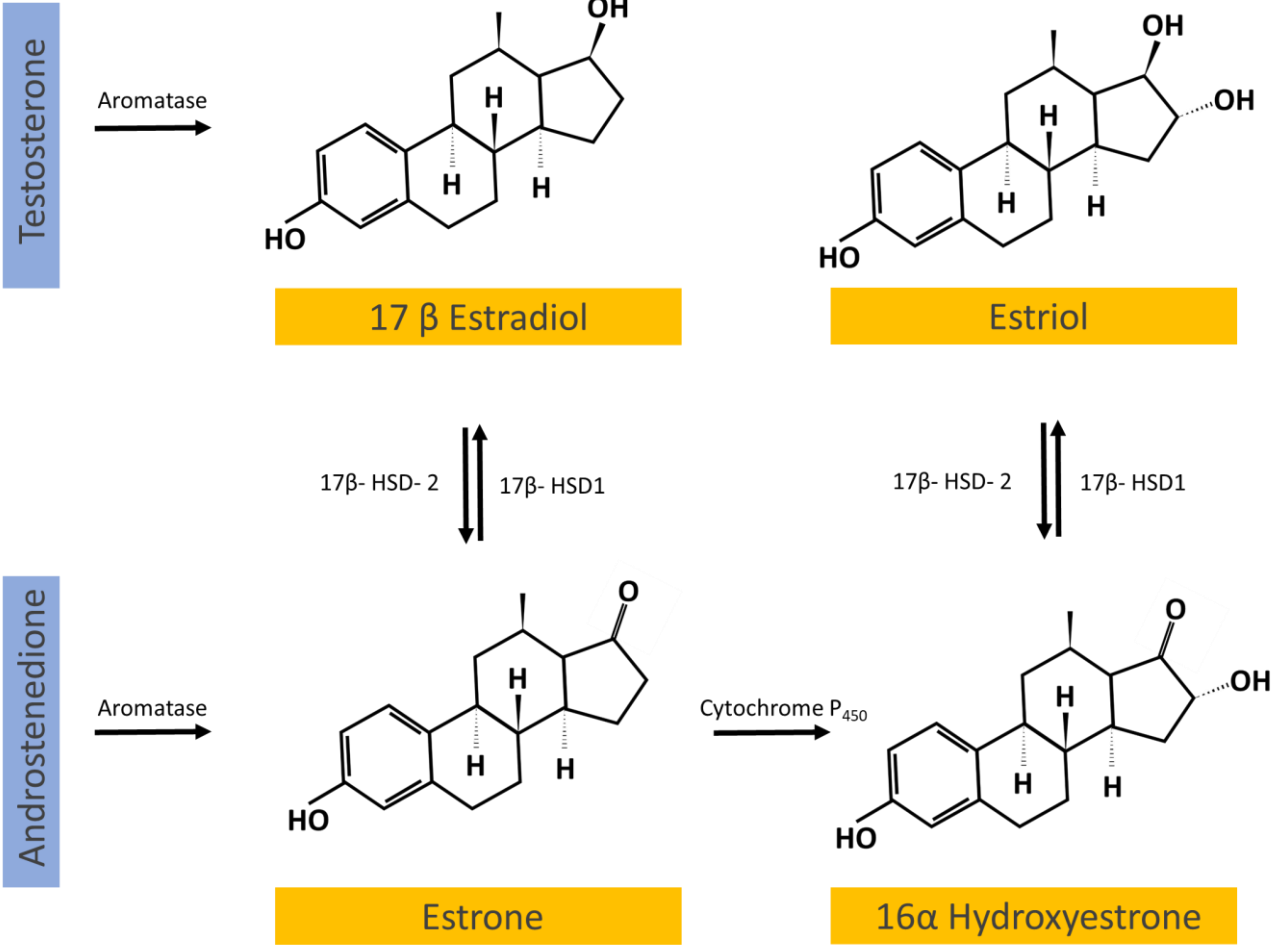
5.1.1. The role of Estradiol in the pathophysiology of pelvic floor disorders

Estrogens play vital roles in normal structure and functions of female genital and lower urinary tract organs [192], [193]. Estrogen receptors are present in the tissues of female urethra, bladder neck, vagina and all connective tissues of the pelvic floor including smooth muscles and ligaments. Although estrogen deficiency is recognized as one of the main factors leading to the occurrence of SUI and POP the exact mechanisms are not completely known. One possible mechanism of estrogens influencing the female urogenital tract is through modifying collagen metabolism. The total collagen content of the vaginal mucosa was significantly reduced in premenopausal women with POP compared to controls. Furthermore, their MMP activity was significantly higher [193]. Estrogen levels can also affect the pathophysiology of POP by differential expression of estrogen- related genes. Recent microarray studies identified expression changes of transcriptional response and signal transduction genes associated with estrogens in the uterosacral ligaments of women with POP [194].

Another mechanism by which estrogens relate to development of SUI and POP could be via changing the blood flow to pelvic organs. Estrogens are known to be involved in many other physiologic and pathologic processes characterized by neovascularization such as lupus, Takayasu's arteritis and menstrual bleeding [195]. The relationship between angiogenesis and development of pelvic floor disorders is much less studied. However a measurable decrease in vaginal blood flow has been demonstrated in postmenopausal women which improved significantly with exogenous estrogen replacement [124]. Additionally, recent work has suggested that Estradiol can be involved in pathophysiologic processes leading to development of many pelvic floor disorders via its effects on vaginal microcirculation [196], [197].

Estrogen replacement was shown to increase the collagen content of skin by 48% in postmenopausal women compared to controls [198]. The role of estrogen replacement therapy in the regulation of collagen metabolism in female pelvic tissues is less clear. It is well known that topical estrogen treatment increases the vaginal epithelial thickness and promotes revascularization [199]. The change in collagen content in the subepithelial tissues in response to estrogen supplementation has been studied in animal models. In ovariectomized rhesus macaque vaginal estrogen treatment increased collagen gene transcription in the vaginal connective tissues indicating an increase in total collagen production [200]. In ovariectomized rats low doses of vaginal estrogen replacement resulted in increased vaginal weight, increased collagen I/ collagen III ratio and increased distensibility of the vaginal wall. Low dose vaginal treatment was superior to high dose vaginal treatment regimen and systemic supplementation [201].

Currently there is evidence to support the effectiveness of vaginal estrogens in the treatment of vaginal atrophy [202] however there is no clinical evidence to support the use of vaginal estrogens for prevention or management of POP [203]. With regards to SUI, exogenous replacement of estrogen does not necessarily lead to an improvement of SUI symptoms. It was shown that estrogen replacement reduced total collagen concentration, decreased collagen cross- linking and increased collagen turnover. Also estrogen supplementation increased collagen to smooth muscle ratio in the lower urinary tract that may lead to reduced bladder compliance and storage symptoms. Therefore, systemic estrogen treatment although it has historically been used, can have negative impact when treating SUI. Nevertheless there is some evidence to support the use of vaginal estrogens for treatment of SUI [204]. Clinical guidelines recommend use of vaginal estrogens to treat SUI only when it is associated with vaginal atrophy [38].

5.1.2. The effect of Estradiol on angiogenesis

In adult organisms angiogenesis is normally absent unless there is tissue injury and repair or tumours. An exception to this is in the female reproductive tract where physiologic neoangiogenesis takes place monthly in menstruating women. This suggests that sex steroids influence neovascularization [195]. Additionally estradiol prevents endothelial dysfunction and promotes vascular endothelial repair and angiogenesis [205], [206]. Both estrogen receptors alpha and beta are expressed in vascular endothelium. Estradiol has direct actions on endothelial cells including accelerating endothelial cell migration, proliferation and organization of endothelial cells *in vitro* [205], [207]. Estradiol can directly stimulate vascular endothelial cells through the estrogen receptors [208]. Vascular endothelial growth factor (VEGF) is a potent stimulator of angiogenesis. Estrogen receptor elements are thought to be responsible for direct activation of VEGF gene transcription [209]. Also *in vivo* experiments showed bovine corpus luteum to increase neovascularization in the CAM assay [210].

In this section, it was hypothesized that estradiol could effectively be introduced to electrospun PLA scaffolds and that it could stimulate neovascularisation as released from the scaffolds. Incorporating drugs into tissue engineered constructs is a well- established strategy to improve the intrinsic angiogenic potential of a tissue engineered materials [126]. Estradiol has been shown to be a potent stimulator of angiogenesis as released from electrospun materials [72], [138]. Clinically its pro- angiogenic properties are used in disease states such as cardiac ischaemia [211] and wound healing to improve tissue vascularization. Additionally topical Estrogen treatment is also believed to improve post- operative wound healing and it is a common practice among surgeons to use topical vaginal estrogens before and after vaginal surgery especially in the presence of vaginal atrophy [212].

5.2. The effective concentrations of Estradiol to stimulate collagen production

This was studied on monolayer cultures of human dermal fibroblasts (HDFs). HDFs were isolated from consented donors as described in Chapter 2. A total of 100. 000 cells were seeded on each well of a 12 well plate. After overnight incubation the culture media was replaced with same media supplemented with different concentrations of Estradiol. First a dose finding experiment was conducted using the following concentrations: 10 nM, 100 nM, 1 µM, 10 µM and 50 µM.   Collagen production was assessed with Sirius red staining and expressed as percentage increase in collagen production compared to non-supplemented controls.   Concentrations of Estradiol above 100 nM decreased collagen production and concentrations of 50 µM reduced collagen production. Additionally as the concentration increased there appeared to be a reduction in cell metabolic activity (Figure 5.2).

Figure 5.2. Dose response study for the effects of Estradiol on cell metabolic activity (A) and collagen production (B) of human dermal fibroblasts.
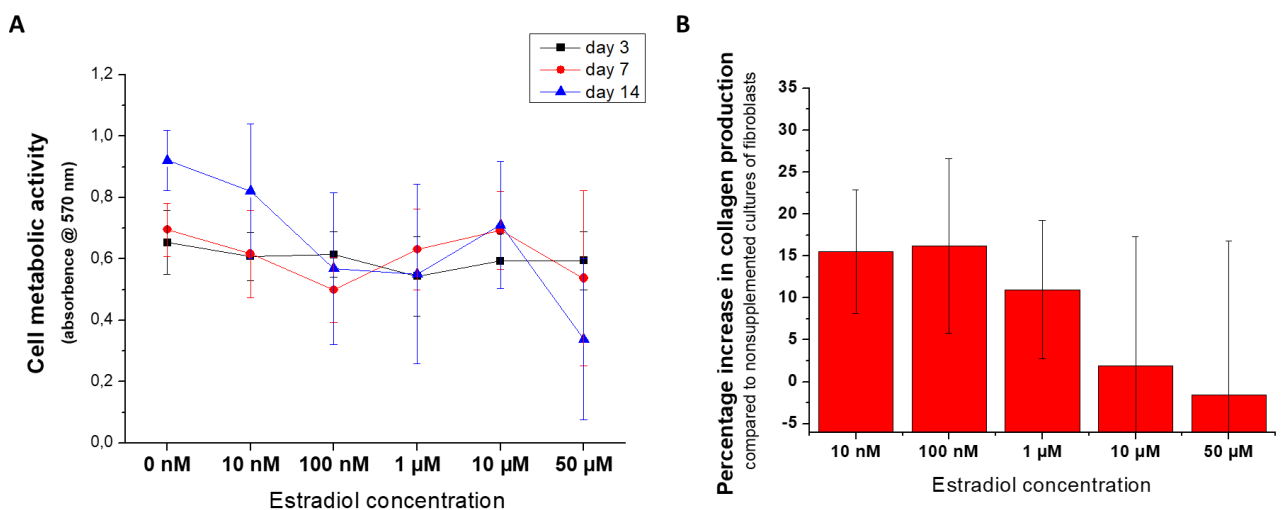
Therefore, a second set of experiments were conducted using the following concentrations: 2 nM, 5 nM, 10 nM, 25 nM and 50 nM. Within this concentration range cell metabolic activity increased for all concentrations from day 7 to day 14. The most effective concentration for Estradiol to stimulate collagen production appeared to be 2 nM and 5 nM (Figure 5.3).

Figure 5.3. The effect of different concentrations of Estradiol on cell metabolic activity (A) and collagen production (B) of human dermal fibroblasts.
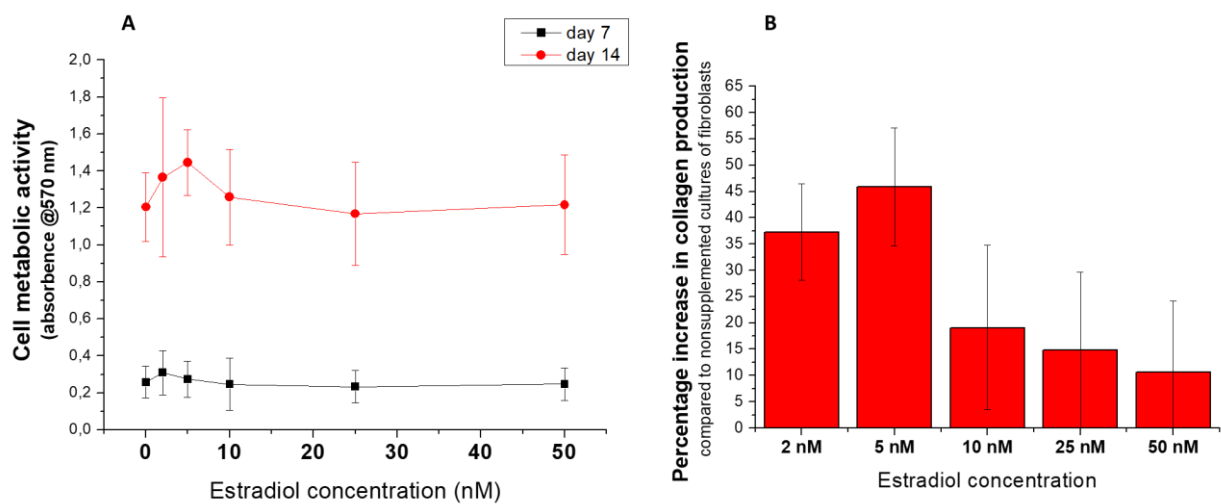
5.3. The effective concentrations of Estradiol to stimulate endothelial cell proliferation and sprouting

The effect of different concentrations of Estradiol on endothelial cell proliferation and sprouting was assessed using the chick aortic arch assay. Chicken embryos were sacrificed between EDD 14, aortic arches removed from aortic branches were cut into 1 mm rings under a stereomicroscope. Aortic rings were embedded in 50 µL of Matrigel® (Basement Membrane Matrix, Corning®) in a 24 well plate. Cell culture media, DMEM (supplemented with 2.5% FCS, containing 0, 1, 10, 30, 50 and 100 nM of 17-β Estradiol were added into wells. Vascular endothelial growth factor (VEGF) at a concentration of 100 nM was used a positive control in this assay. The endothelial sprouts were observed under an inverted microscope on the 5th day of culture. The longest sprout was measured on the digital images using Image J software (U. S. National Institutes of Health, Bethesda, Maryland, USA). The mean sprout length was calculated for each sample (Figure 5.4).

The aortic arch assay was used to effectively demonstrate a significant difference in the mean sprout length between the control and VEGF supplemented groups, mean sprout length 211 (±24) µM and 315 (±21) µM, respectively (p=0,003). Estradiol stimulated endothelial cell sprouting at concentrations of 1, 10 and 30 nM, mean sprout length 358 (±34), 362 (±42) and 357 (±26) µM, respectively (all p values >0,05 compared to control). Estradiol concentrations of 50 and 100 nM did not increase endothelial cell sprouting with mean sprout lengths of 215 (±34) and 131 (±19) µM, respectively. The number of samples included in this analysis for each group were as follows: control (n=19), Estradiol 1 nM (n=8), Estradiol 10 nM (16), Estradiol 30 nM (n=11), Estradiol 50 nM (n=14), Estradiol 100 nM (n=9) and VEGF 100 nM (n=20).

Figure 5.4. The effect of different concentrations of Estradiol on endothelial cell sprouting. Concentrations of Estradiol between 1- 30 nM appear to stimulate longer endothelial cell sprouting compared to controls whereas a concentration of 50 nM seems to result in shorter endothelial cell sprouts. The VEGF is used as a positive control (scale bars 200 µM).
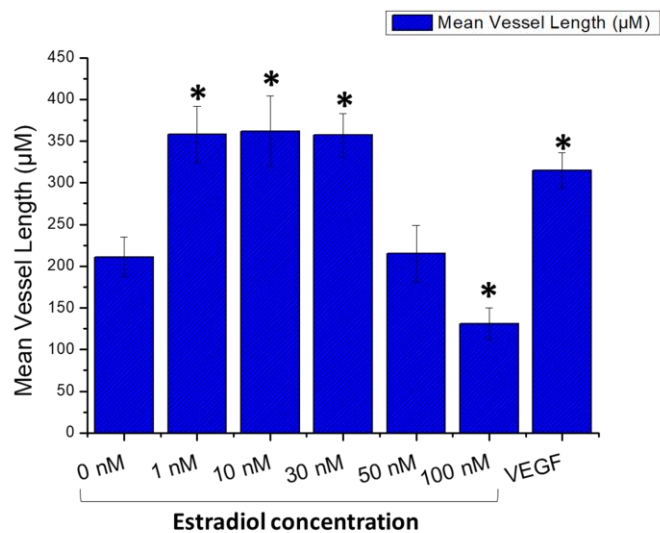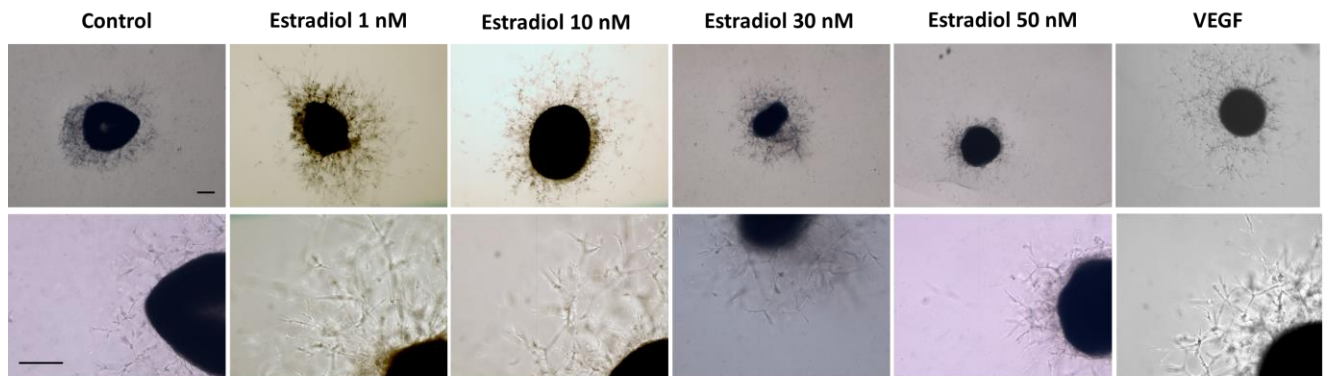
5.4. The effect of Estradiol on angiogenesis in the CAM assay

Macrovessels

Another way of evaluating the effect of Estradiol on new blood vessel formation was applying the drug solution to the CAM. For this purpose, a 2 mm thick plastic ring was cut from a soft 30G needle cover was placed on the CAM. A 50 nM solution of Estradiol in PBS was prepared together with positive and negative controls of VEGF (100 nM) and Sunitinib (50 μg/ ml). The solutions were prepared freshly for each experiment and an injection volume of 30 μl was pipetted slowly onto the CAM marked by the plastic ring. The drugs were given twice every day between EDD 8 to 11. Each group contained 6 eggs for each experiment. EDD 11 the CAM area around the plastic ring was imaged.

The macrovascular response to VEGF and Sunitinib could effectively be observed on the CAM images (Figure 5.5). Especially with Sunitinib the decrease in the number and intensity of the blood vessels is very dramatic. However, the response to Estradiol never appeared as dramatic as it was in the *in vitro* assays. This could be due to the difficulty in achieving a positive effect with twice daily applications of the drug.

Figure 5.5. The comparative effectiveness of Estradiol on macrovessels in the CAM assay (Scale bar represents 500 µM for all images).
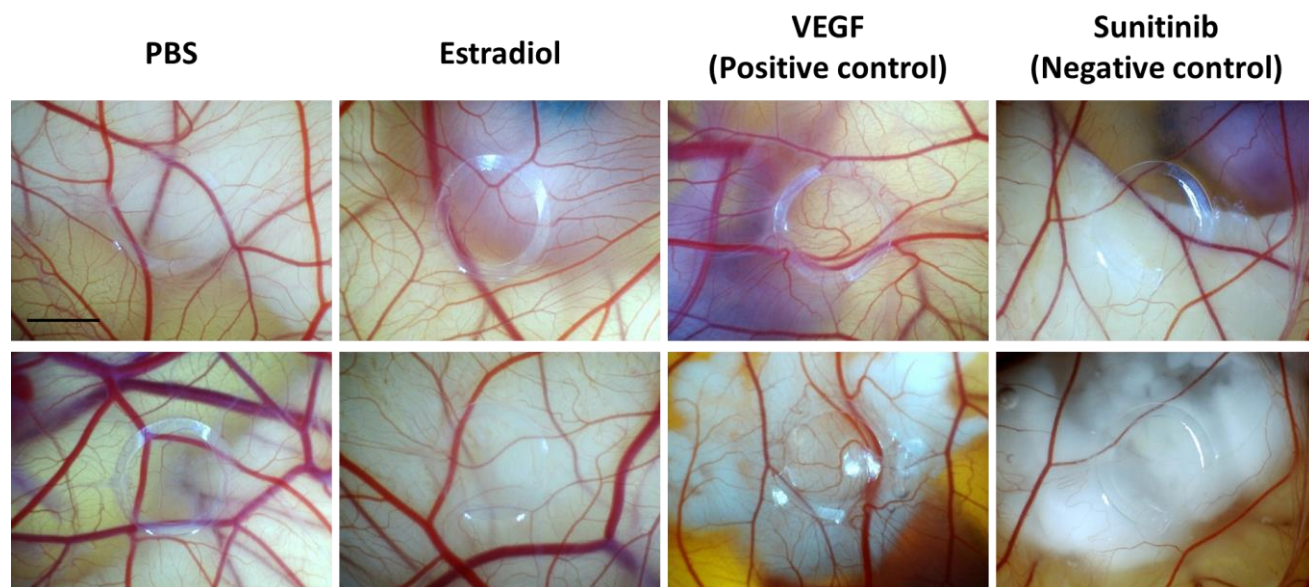
Microvessels

After imaging the macrovessels, a rhodamine labelled lens culinaris agglutinin (LCA) (Vector laboratories) (50 µL of a 5µg/ mL of) was injected into one of the major vitelline veins of the chick embryo using a 30G hypodermic needle attached to a 1 mL syringe. A maximum of 100 µl of LCA solution was injected into each embryo. Embryos were then sacrificed and the area of the CAM involving the plastic rings were cut by wedge resection and fixed immediately in 3.7% paraformaldehyde (Sigma Aldrich, USA) in PBS. These samples were used for confocal imaging to visualize the microvasculature. When imaging the microvasculature Estradiol effects appeared more quantifiable. Estradiol resulted in a response similar to that of VEGF with endothelial cell hypertrophy with smaller lacunar spaces (Figure 5.6). The percentage areas covered by endothelial cells were 52.6±14.3, 87.0±3.7, 87.1±3.5 and 11.7±5.7% respectively in control, Estradiol, VEGF and Sunitinib groups (all p values < 0.005 compared to controls for all three).

Figure 5.6. The comparative effectiveness of Estradiol on the microvasculature on the CAM. The normal honey- comb like appearance of the CAM microvasculature can be observed in PBS treated samples. With application of Estradiol and VEGF, endothelial cell hypertrophy with smaller lacunar spaces are observed. Sunitinib resulted in loss of endothelial cell coverage with larger lacunar spaces. Error bars represent 50 μm.
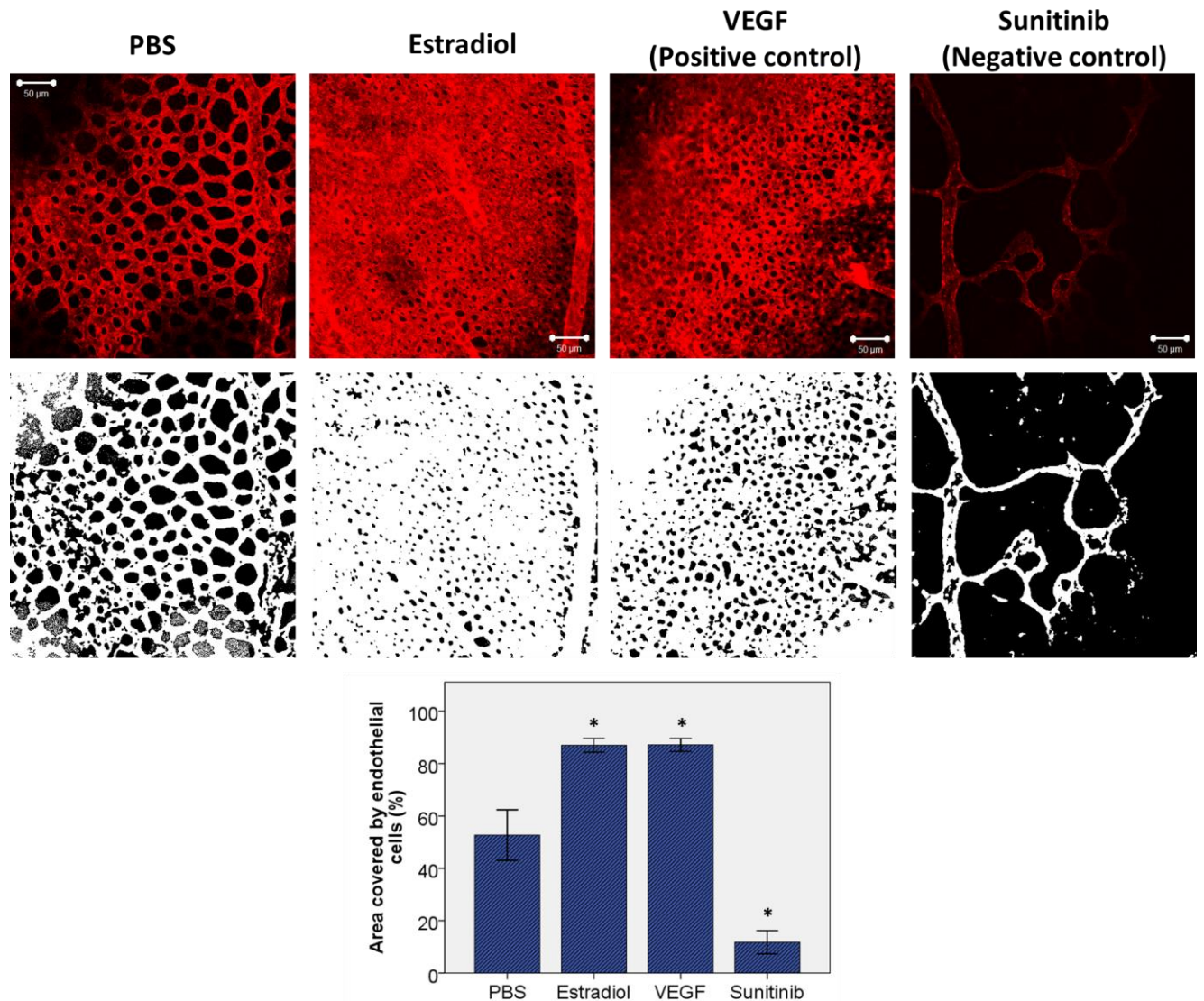
In summary, Estradiol at concentrations between 1- 50 nM stimulated endothelial cell proliferation and sprouting *in vitro*. In the CAM assay, although the microvasculature could easily quantify the Estradiol effects, the effect of Estradiol on macrovasculature was not clearly observable. Therefore, a continuous release system for Estradiol was investigated next.

5.5. Achieving a sustained release of Estradiol from a hydrogel

To achieve a sustained release of Estradiol a hydrogel was used as a carrier. This hydrogel was constructed as described previously by a visiting researcher (Dr. Gözde Eke) and supplied in a ready to use powder form. Briefly, methacrylated gelatin (GelMA) and methacrylated hyaluronic acid (HAMA) were synthesized as described previously [140]. GelMA (15%, w/v) and HAMA (1%, w/v) were mixed with cell culture media containing photoinitiator (Irgacure 2959, 0.3% w/v). Estradiol was added into this solution at a concentration of (10 µg/1 mL). After complete dissolution at 37°C, 100 µL of hydrogel solution was placed on to a petri dish and immediately photo- crosslinked by exposing to UV light at a wavelength of 365 nm for 40 sec (Omnicure s1000) (Figure 5.7). The release of Estradiol from the hydrogels were confirmed for three days.

Figure 5.7. Graphical demonstration of construction of a UV- crosslinkable, transparent hydrogel system to achieve a sustained release of Estradiol. (A) The hydrogel is constructed from methacrylated gelatin and methacrylated hyaluronic acid which are first dissolved in media, then the photoinitiator and Estradiol are added. The final solution was crosslinked by exposing to UV light for 40 seconds. (B) The final hydrogel can easily be handled by a fine forceps. (C) A summary of the physical properties of the hydrogel has been described previously.
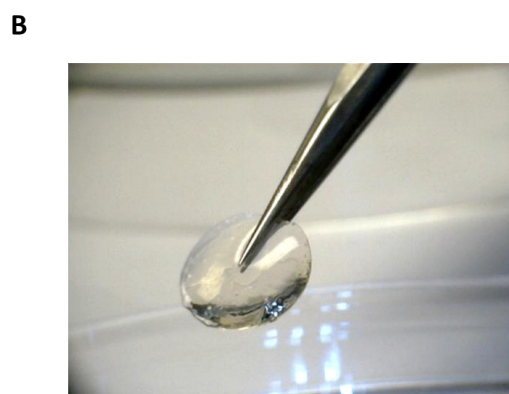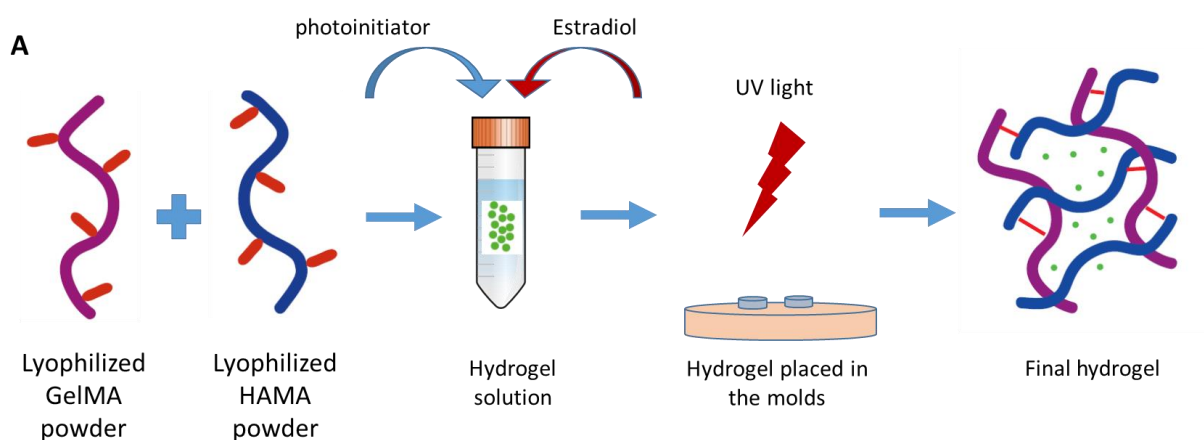
Pore size	120±76 µm
Porosity	79%
Maximum Compression Strength	12.86± 1.23 kPa
Compression Modulus	6.17± 2.05 kPa
Hydrophilicity (degree of swelling at equilibrium in water)	227%
Precent degradation in vitro	50% in 21 days

The Estradiol releasing and control hydrogels were placed on CAM on EDD 7 and incubated for 8 days. On EDD 14, the hydrogels and surrounding CAM area were imaged by digital microscope. Digital images were analysed and the vasculogenic index calculated. Estradiol releasing hydrogels resulted in a significant increase in the number of newly formed blood vessels growing towards the hydrogel in a spoke wheel pattern compared to control hydrogels. The vasculogenic index was 35.0±4.6 and 21.3±3.5, respectively for control and Estradiol releasing hydrogels (p: 0.005) (Figure 5.8).

Figure 5.8. Angiogenic response to the Estradiol releasing hydrogel in the chick chorioallantoic membrane (CAM) assay. Micrographs of the control and Estradiol releasing hydrogels taken on day 14 of embryonic development demonstrate a significant increase in the mean vessels count with Estradiol releasing hydrogels compared to controls (n= 6 for each group) (Scale bar 500 µm).
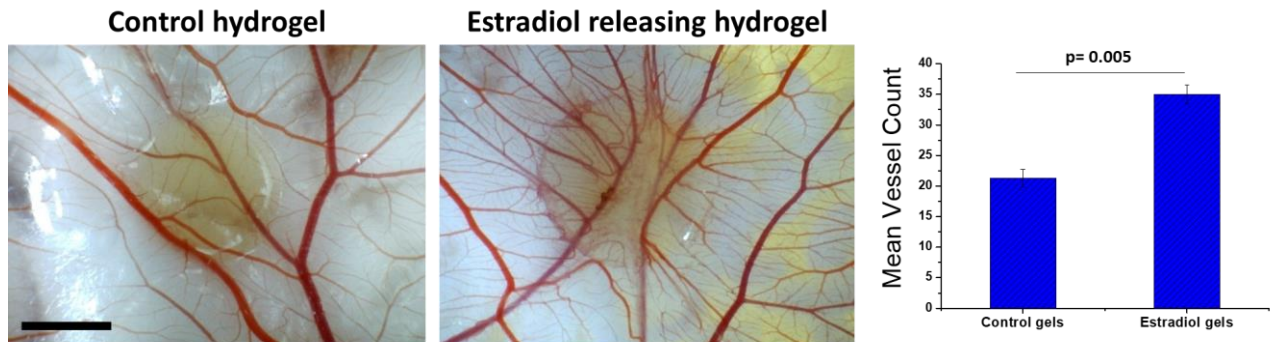
Therefore, a sustained release of Estradiol from a hydrogel resulted in an increase in the number of blood vessels growing around the hydrogel. This hydrogel had two main advantages in this experimental set up. Firstly, it did not trigger an inflammatory response that could have interfered with the angiogenetic process. Secondly, because it was transparent all the blood vessels underneath the hydrogel were clearly visible during the experiment.

5.6. Construction and characterization of Estradiol releasing PLA scaffolds

A total of 50 mg of Estradiol was dissolved in 10 mL of DCM into which 1 gram of PLA added to produce a homogenous solution of PLA and Estradiol. This solution was then electrospun. Micro/ nanoporous scaffolds of Estradiol incorporated PLA with a mean fibre diameter of 0.71±0.28 µm and a pore size of 4.25±2.04 µm were produced. Control PLA scaffolds without any Estradiol had a fibre diameter and pore size of 0.65±0.30 µm and 4.26±2.29 µm, respectively (Figure 5.9).

Figure 5.9. The ultrastructure of Estradiol releasing PLA scaffolds as shown by scanning electron microscopy. There was no difference in the fibre diameter and pore sizes of both scaffolds. Scale bar represent 10 µm.
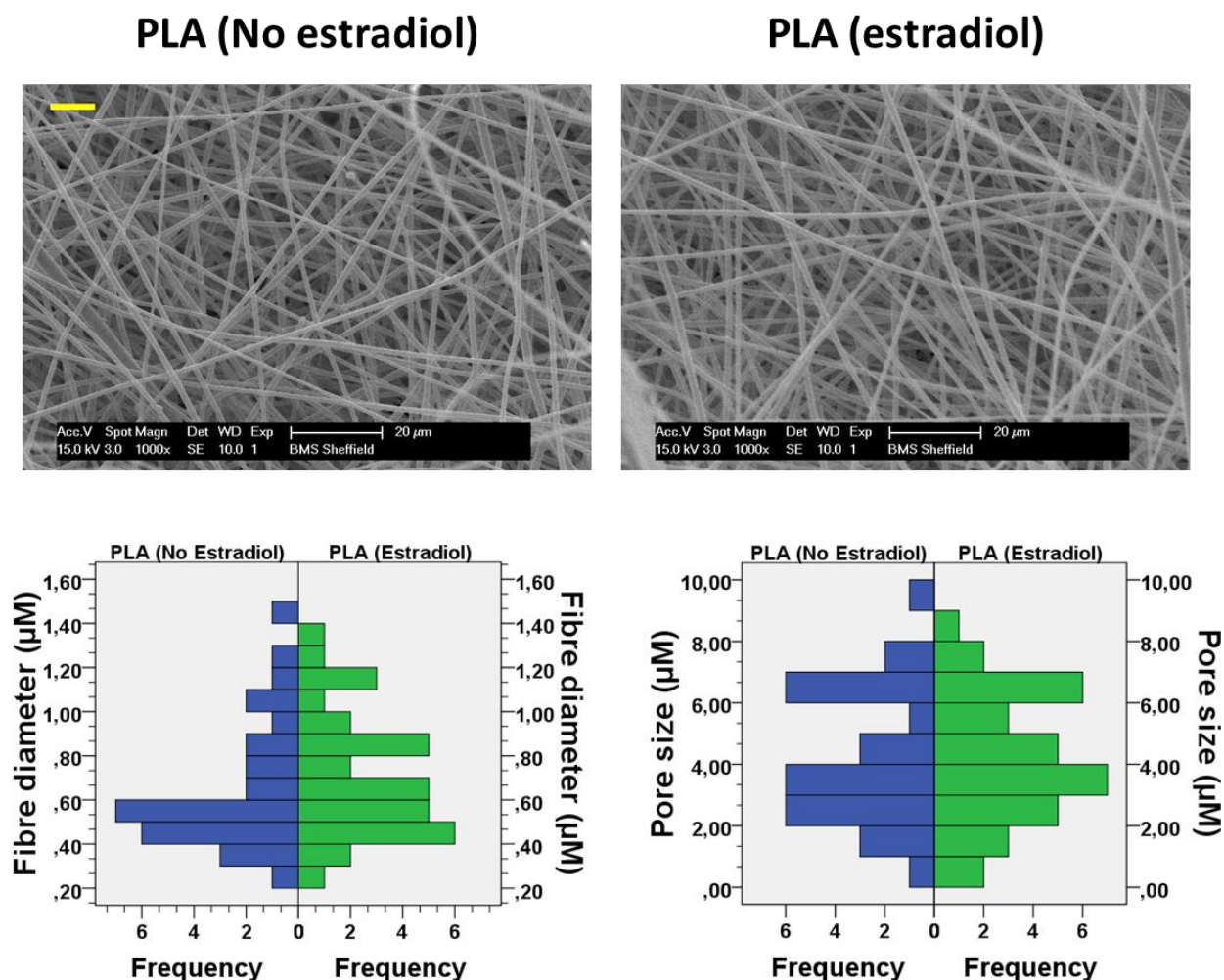
Mechanical testing of scaffolds was previously performed by Dr. Chris Hillary demonstrating no significant change in mechanical properties of PLA scaffolds with incorporation of Estradiol, apart from a slight increase in UTS and Young's modulus. Therefore, the mechanical testing was not repeated here.

Release of estradiol from scaffolds over 5 months

Scaffolds were cut and standardised by mass to equate to 1% of the entire electrospun mat. All scaffolds were washed and incubated in 1ml/well of Phosphate buffered saline (PBS) in a 12-well tissue culture plate. The relative fluorescence of PBS was measured intermittently (Kontron SFM 25 spectrofluorimeter) at λ_{ex}277nm/λ_{em}310nm, with fresh PBS replaced following each sampling over a 5- month period. New standard curves were prepared at each sampling time-point.

Figure 5.10. The release of Estradiol from PLA scaffolds over 133 days in a concentration dependent manner. (This experiment was conducted by Dr. Chris Hillary)
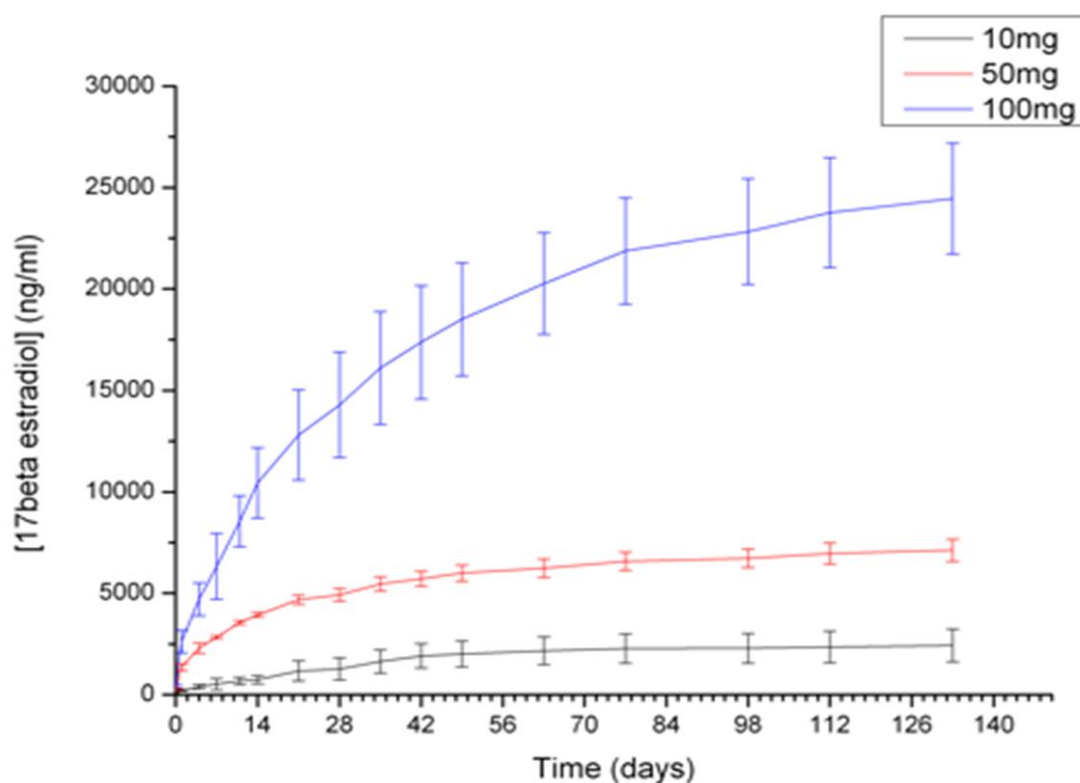
The concentration of estradiol released from each of the 3 scaffold groups (10mg (1% wt/vol), 50mg (5% wt/vol) and 100mg (10% wt/vol)) was measured fluorimetrically against solutions of known concentration (n=6 per group). The cumulative release of estradiol increased for each time-point, until no further estradiol was released (at 133 days) as demonstrated in Figure 5.10. The total released estradiol from the scaffolds was equivalent to 2.5%, 1.4% and 2.45% of the estradiol present in the polymer solution for the 10mg, 50mg and 100mg estradiol scaffolds respectively prior to the electrospinning process, while 40%, 50% and 40% of estradiol was released over the initial 14 days for each of the 3 scaffold groups respectively; the rate of release was proportional to the amount of estradiol present in the scaffold and reduced over time.

5.7. Assessment of angiogenic potential of Estradiol releasing electrospun PLA scaffolds

This was assessed by both co- culturing the scaffolds with chick aortic rings and by implanting the scaffolds on the CAM.

Co- culture of scaffolds with chick aortic rings

Three 1x1 cm piece of control and Estradiol releasing PLA scaffolds were cut and placed in transparent tissue culture inserts (Greiner Bio-One GmbH). Chick aortic rings were embedded in Matrigel in 48 well plates and co- cultured with scaffolds for 5 days. Estradiol releasing scaffolds stimulated more endothelial cell sprouting compared to controls, with a sprout length/radius of 1.6 (±0.51) and 1.0 (±0.44), respectively (P=0.01) (Figure 5.11).

Figure 5.11. The effect of estradiol on endothelial cell proliferation and sprouting as released from PLA scaffolds. Representative images are shown in (A) showing increased endothelial cell sprouting at 5 days of culture compared to controls. (B) Fluorescent microscopy images of immunological staining. Lectin IB4 - endothelial cells stained green, nuclear components stained blue (DAPI). C) Sprout length/radius results taken from 11A, * P=0.01. (Scale bars represent 50 μm).
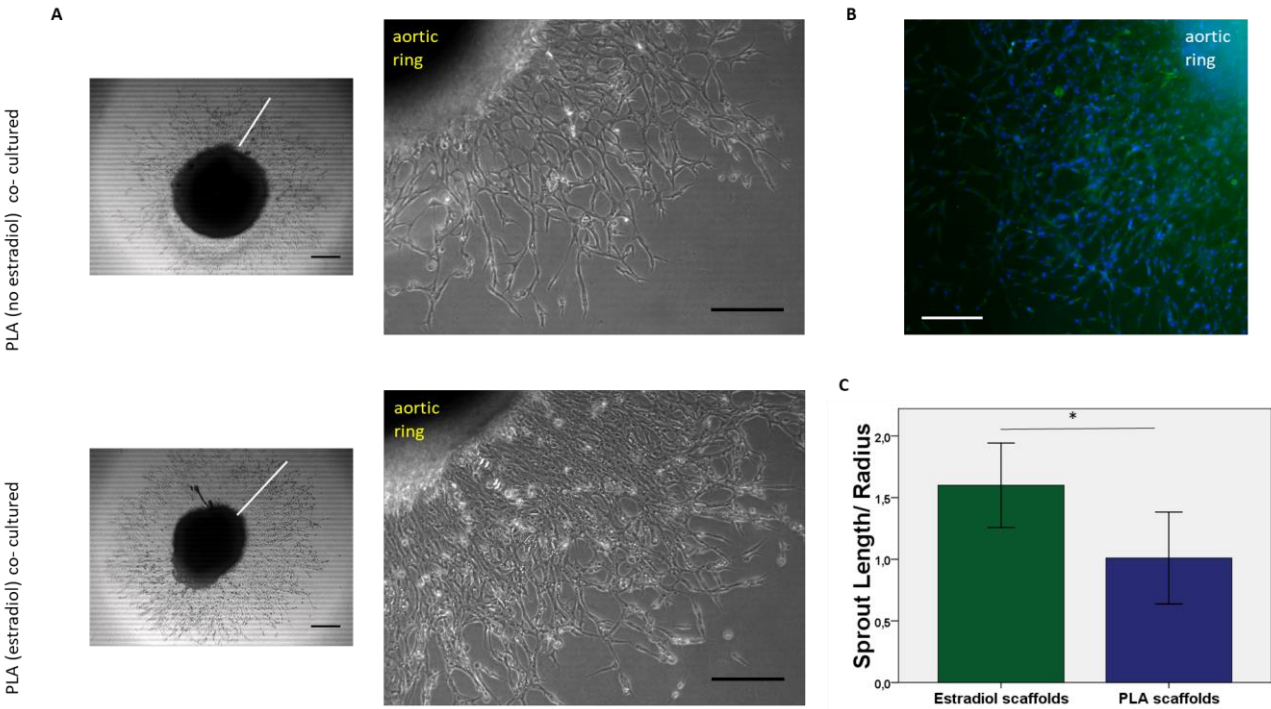
Implantation of scaffolds on the CAM

PLA scaffolds with or without Estradiol were cut into 0.65 cm circles with use of an Epilog Laser Cutter (Clevedon, UK), placed in 1 mL PBS for pre-wetting and kept under UV light for 30 min for sterilization. At EDD 7 pieces of circular scaffolds were placed on the CAM and incubated for 8 days. At EDD 14 pictures of scaffolds and surrounding CAM were taken with a digital camera. A 20% emulsion was injected just underneath the CAM when necessary. For better visualization of blood vessels on histologic sectioning, the LCA was injected into one of the vitelline veins before sacrificing the embryo cultures. The embryos were sacrificed by cutting their vitelline arteries, scaffolds were resected from the CAM surface together with a rim of membrane and samples were fixed.

On the digital images 'vasculogenic index' was calculated. Estradiol releasing scaffolds (50 mg/ gram of PLA) resulted in a significant increase in the number of blood vessels growing towards them in a spoke- wheel pattern compared to control PLA scaffolds. The mean vessel counts were 25.0 ($\pm$5.29) and 10.67 ($\pm$2.64), respectively ($P<0.001$) (Figure 5.12).

Initial tissue response to Estradiol releasing PLA scaffolds

Retrieved scaffold- CAM complexes were fixed in paraformaldehyde and were placed into moulds for cryo-sectioning filled with OCT solution (Leica, Germany). They were left to freeze at 80°C and 10 µm sections were cut with the cryostat Leica CM1860UV (Leica Germany). Slides were then stained with haematoxylin & eosin solutions (H&E), according to the standard protocol for frozen slides. Slides were then covered with DPX (Sigma-Aldrich, USA) and a glass coverslip to be imaged with a light microscope (Motic, China) (Figure 5.13).

Both estradiol releasing PLA and control PLA scaffolds became infiltrated with host tissues (CAM interstitial cells) together with a moderate inflammatory reaction. The CAM tissue adjacent to the estradiol scaffolds demonstrated more blood vessels compared with PLA only scaffolds. Moreover, a greater proportion of blood vessels were observed in between the fibres of the estradiol releasing PLA scaffolds as compared to controls (Figure 5.13).

Figure 5.12. Angiogenic potential of estradiol releasing PLA scaffolds compared to control PLA scaffolds. A normal distribution of blood vessels was observed with the control PLA scaffolds whereas with the estradiol releasing scaffolds resulted in a significant increase in the number of blood vessels growing towards the scaffold (A). The mean vessel count of estradiol releasing meshes was double that of the PLA meshes (B) and the embryo survival rate was the same between the two groups (C). (Scale bars represent 3mm).
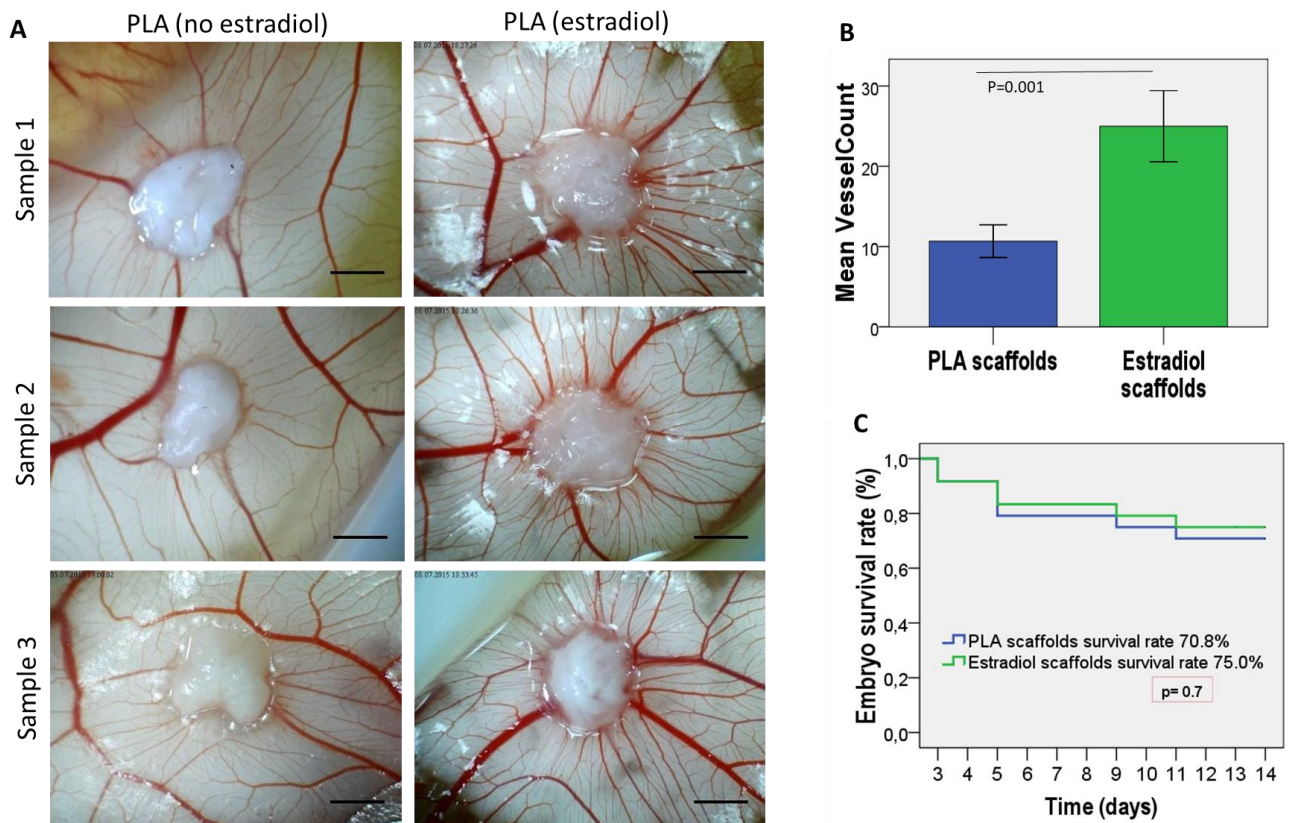
Figure 5.13. Histologic evaluation of tissue- mesh interface. A mild inflammatory reaction together with a normal distribution of blood vessels on the CAM adjacent to the PLA mesh (upper raw) can be observed compared to a significantly increased number of large blood vessels in response to Estradiol releasing PLA mesh (lower raw) at day 14, Haematoxylen &Eosin (H&E) staining (left side). Also on higher magnification several small blood vessels could be observed in between the PLA fibers which were more abundant in the presence of Estradiol (middle). On the right endothelial cells lining all sizes of blood vessels appear stained Rhodamine- conjugated Lens culinaris agglutinin and cell nuclei are stained with DAPI. Scale bars represent 100 μm.
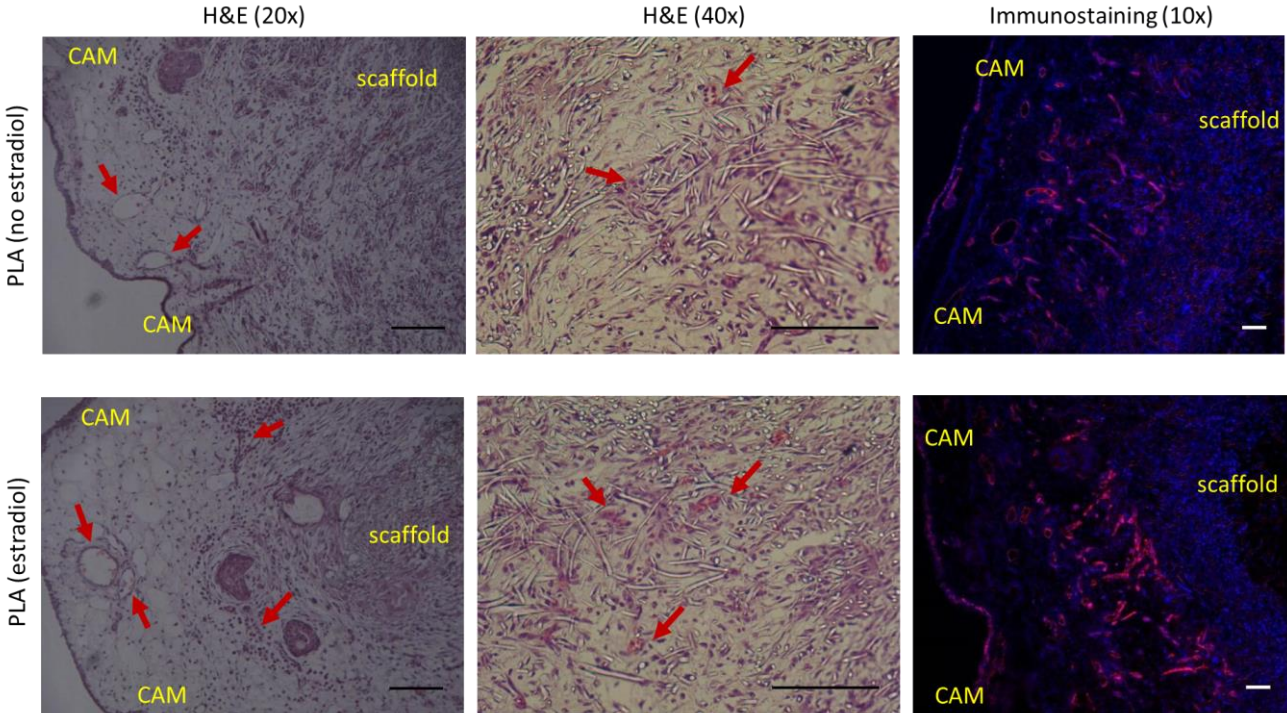
5.8. Chapter discussion

In this set of experiments, estradiol was first confirmed as a potent stimulator of collagen production and endothelial cell proliferation and sprouting. Next, an estradiol releasing electrospun PLA scaffold with desired ultrastructural and mechanical properties was constructed. The most striking finding of this section was the ability of estradiol releasing scaffolds to stimulate new blood vessel formation around itself in the CAM assay. Finally, the initial *in vivo* tissue response was assessed in the CAM assay.

Despite the association of pelvic floor disorders with estrogen deficiency and increasing age, the exact role of estradiol in the pathophysiology of pelvic floor disorders is not clear. Here, estradiol was not used for the purposes of estrogen replacement but to improve the tissue integration of the biomaterial by stimulating new ECM production and new blood vessels formation. Estradiol is a known stimulator of collagen production. Previously, effective concentrations of estradiol to stimulate collagen synthesis were reported to range between 1 nM- 10 µM [213], [214]. Additionally, inhibitory concentration of estradiol to suppress collagen production were found to be above 10 µM [214]. These are all in line with our findings demonstrating a significant decrease in collagen production by human dermal fibroblasts with supplementation of more than 10 µM of estradiol.

For evaluation of collagen production by HDFs, donated skin from anonymous donors were used. The source of the donated skin to the laboratory was mostly the Plastic surgery unit and the vast majority of the donated skin and fat were obtained from breast reduction and abdominoplasty surgeries. Therefore, most patients would be expected to be females. Yet the gender of the patient is not known to the researchers in this set up. This could potentially be important when assessing the effect of estrogens on cellular functions. Males are known to express estrogen receptors in their reproductive as well as non- reproductive organs such as liver, muscle, kidney [215]. However, the affinity of these receptors could differ in male and females which could have increased the variability in the presented results.

Estradiol is also known to be an effective stimulator of endothelial cell proliferation and tube formation *in vitro* and *in vivo* [216], [217]. The effective concentrations of estradiol in endothelial cultures were between 1- 10 nM [216], [218]. Angiogenesis is a process where a complex interaction between endothelial and non- endothelial cells as well as many enzymes, growth factors and adhesion molecules are crucial and for this reason the widely used, traditional monolayer cultures of endothelial cells are limited. In this section, the angiogenic properties of estradiol were studied in an organ culture assay, the chick aortic ring assay, and an *in vivo* CAM assay both of which allowed the study of the process of angiogenesis with all the elements playing a role in it. In this section it has been demonstrated that the effective concentration for estradiol to stimulate endothelial cell proliferation, sprouting and tube formation was 1- 30 nM. Interestingly, estradiol had obvious negative effects on endothelial proliferation and sprouting at concentrations of 100 nM. The chick aortic arch assay was found to be a very responsive assay and could effectively be used to screen various concentrations of drugs. A limitation of this assay is that the cultured organ is an embryonic tissue with a high proliferative capacity. Even in the absence of a pro- angiogenic factor endothelial cell sprouting can be observed. Additionally, a common limitation to all of the *in vitro* experiments with estradiol might be the interference with the estrogens that are naturally present in the fetal calf serum (FCS). There is approximately 0.05 pM of estradiol in the FCS [219]. This value may vary between batches and that could potentially interfere with the results.

In addition to confirming the findings reported in the literature previously, a direct comparison of Estradiol with the well- known pro and anti- angiogenic drugs was also included in the current studies. Using the CAM assay, the pro- angiogenic (VEGF) and anti- angiogenic (Sunitinib) were compared with estradiol. In this experimental set up, a biomaterial was not used to allow observation of the drug effect only. Although the positive and negative controls worked stunningly well, particularly the negative control, estradiol did not work as was expected. This could have been due to its administration via a the twice- daily dosage. Therefore, we postulated that a sustained release system for estradiol might prove more effective.

Among the available drug carriers, a photocrosslinkable transparent hydrogel appeared to be a reasonable carrier for this experiment. The estradiol releasing hydrogel was therefore used to achieve a continuous release of estradiol. This proved that a sustained release state of the drug appeared to produce more obvious results.

Another dramatic effect of estradiol was on microvasculature. The absence of a hierarchical organisation of the vasculature allowed more accurate assessments and easier quantification of angiogenesis on the microvasculature. The CAM assay offers an experimental system where the microvasculature can be studied. Although the CAM microvasculature would be expected to have differences to the microcirculation of mammals, it could be used in initial screening. Methods to assess vaginal microcirculation have recently been developed with unknown efficacy and uptake by the scientific and clinical community [220]. The role of vaginal microvasculature in the pathophysiology of pelvic floor disorders such chronic pelvic pain and pelvic organ prolapse is increasingly being studied [196], [221]. Poor vaginal microcirculation can be the final common pathway where all factors that are related to development of pelvic floor disorders such as aging, birth trauma, smoking, poor estrogenization and previous surgeries meet to result in the clinical presentation of these conditions. The current findings cannot suggest a relationship between estradiol and vaginal microcirculation but only shows a potential effect of the drug on microcirculation.

After determination of the effective concentrations of estradiol to stimulate collagen production and angiogenesis the blend electrospinning technique was used to construct estradiol releasing electrospun PLA scaffolds. Estradiol is highly lipid soluable and could effectively be dissolved in polymer solution before electrospinning. The drug would be blended in the polymer fibres and be expected to be released as the polymer degrades. The release of estradiol from electrospun PLA scaffolds continued for nearly 5 months. Estradiol releasing biomaterials have previously been described for a variety of clinical applications. An estradiol releasing polyurethane- dextran nanofibrous mat was introduced as a wound dressing for post- menopausal women. In this study a higher concentration of estradiol (2 wt%) was incorporated into the scaffolds and in an in vivo wound model estradiol releasing mats were shown to accelerate cutaneous wound healing [222]. However, in this study the angiogenic effects of the scaffolds were not studied. In another study, estradiol was demonstrated to stimulate endothelial cells to produce VEGF when cultured on collagen based scaffolds in the presence of estradiol [25]. Here we demonstrate for the first time that

estradiol as released from an electrospun scaffold could dramatically stimulate new blood vessel formation in and around the material. Although we have designed this material for use in pelvic floor repair, we believe it can have wider applications in all areas of tissue engineering as a pro-angiogenic scaffold.

The most striking property of this Estradiol releasing hydrogel is its ability to stimulate and attract new blood vessel formation. Adequate blood supply to the wound is critical to ensure good wound healing. This could be even more important in women when the blood supply to the vaginal tissues are already compromised after menopause or as a result of other medical conditions such as diabetes, previous pelvic surgeries and radiotherapy. A severe mesh related complication is mesh erosion (extrusion) which is described as 'vaginal mesh being visualized through the separated vaginal epithelium'. This most commonly occurs in the midline where the surgical incision is made as if there was a wound dehiscence [1] implying a poor wound healing process. With use of the current mesh material, previous studies have demonstrated the presence of a maladaptive remodelling response [223] and triggered an unfavourable macrophage response [106] however the effect of surgical mesh on vaginal wound healing has not been investigated before. Nevertheless, when mesh erosion occurs clinically, a common practice among surgeons is to apply topical estrogen creams for the initial treatment of smaller mesh erosions. Taken all together, the estradiol releasing PLA scaffolds appear to be good candidates to stimulate angiogenesis and wound healing at the site of implantation. This needs to be studied further in relevant animal models.

The current results will need to be taken into account considering that so far only the chorioallantoic membrane of chick embryos were used to study angiogenesis. The CAM assay is a well- established method to evaluate angiogenesis *in vivo* and it allows direct visualization of the newly forming vessels in a cheap, quick way that can be readily available to most laboratories. Furthermore, this method can be used as a rapid, simple and low cost screening tool to test the initial tissue response to biomaterials, as a pre *in vivo* method. The presented results show that CAM tissues can penetrate the scaffold and blood vessels can grow in between the fibres of the electrospun PLA scaffolds which was observed to be more prominent in case of estradiol releasing PLA. One limitation of relying on this model to characterize the immune response to the implanted material is related to the fact that the immune system of the chick embryo develops after day 11 of embryonic life, thus these results need to be confirmed on animal models. Therefore, these promising results now need to be confirmed in relevant animal models.

Chapter 6.
Evaluation of the effects of mesenchymal stem cells on tissue integration and angiogenic potential of electrospun scaffolds

G. Eke*, N. **Mangir***, N. Hasirci, S. MacNeil, and V. Hasirci, "Development of a UV crosslinked biodegradable hydrogel containing adipose derived stem cells to promote vascularization for skin wounds and tissue engineering," Biomaterials, vol. 129, 2017. (*shared first co- authors)

S. Shafaat, **N. Mangir**, S. R. Regureos, C. R. Chapple, and S. MacNeil, "Demonstration of improved tissue integration and angiogenesis with an elastic, estradiol releasing polyurethane material designed for use in pelvic floor repair," *Neurourol. Urodyn.*, vol. 37, no. 2, 2018.

S. Roman, **N. Mangir**, L. Hympanova, C. R. Chapple, J. Deprest, and S. MacNeil, "Use of a simple in vitro fatigue test to assess materials used in the surgical treatment of stress urinary incontinence and pelvic organ prolapse," *Neurourol. Urodyn.*, Sep. 2018.

6.1. Chapter Introduction

Another way of improving the tissue integration of biomaterials designed for use in pelvic floor could be to incorporate cell sources that can stimulate tissue regeneration and angiogenesis into the biomaterials. Mesenchymal stem cells (MSCs) have long been recognised to play a vital role in normal tissue regeneration/repair.

MSCs, were first isolated from bone marrow. This was followed by isolation of MSCs from almost all adult tissues including adipose tissue, skeletal muscle and central nervous system. MSCs are characterized by their ability to self- renew and to differentiate into other phenotypes (multipotency) [224]. Although a standard definition for an MSC has been established and widely used by the scientific community, there is a lot of discussion around the limitations of such a definition. The main limitation about the current definition of an MSC is about the multi differentiation capacity of MSCs which currently is only proven for bone marrow derived MSCs *in vivo* [225]. In other words, although MSCs has been shown to differentiate into other lineages *in vitro*, the expectation of replacement of damaged tissues by these cells *in vivo* has not yet been met. Nevertheless, a therapeutic effect of MSCs has consistently been demonstrated in in vivo studies that may not necessarily relate to their ability to differentiate into other lineages to replace damaged tissue.

MSCs achieve their therapeutic effects by producing a wide range of bioactive molecules. This is known as paracrine action of MSCs and up to now paracrine actions of MSCs involve stimulation of angiogenesis, modulation of immune and inflammatory responses, inhibition of apoptosis and trophic effects such as stimulation of mitosis, proliferation and differentiation of intrinsic stem/ progenitor cells [226]. Most paracrine actions of MSCs are exerted as part of a 'homing' process. These cells are known to follow the biochemical cues to migrate to sites of tissue damage caused by ischemia, inflammation, trauma or tumour invasion when delivered systemically. Just like the well- defined leukocyte adhesion cascade, MSC trafficking involves migration within the blood stream (chemotaxis), cell attachment and rolling in vessel lumen and finally transmigration of MSCs across the endothelium and invasion into the tissue stroma [227].

Chemotaxis is migration of MSCs to the sites of tissue injury following the chemical signals pooled at the sites of injury. This process is facilitated by the chemokine receptors classified as G- protein coupled receptors for CXC, CC, C and CX3C chemokines [228]. MSCs are demonstrated to express CCR1- 10, CXCR1- 2, CXCR4- 6 and CX3CR1 receptors with a high variability depending on the tissue of isolation, passage number of cells analysed and different isolation/ cultivation protocols [229]. A well- studied chemokine- receptor interaction both *in vivo* and *in vitro* is CXCL12 (or stromal cell derived factor [SDF]-1)-CXCR4 [230], [231]. It was shown *in vitro* that MSCs express increase their expression of CXCR4 upon stimulation by cocktails containing IGF- 1 [232] and TNF- α [233], [234]. After attachment of MSCs to the vascular endothelium migration occurs following several coordinated steps involving rolling along the endothelium by selectins and their ligands, firm adhesion after activation of integrins by chemokines, diapedesis across the endothelial tight junctions and basement membrane and finally invasion through extracellular matrix.

6.1.1. Paracrine effects of mesenchymal stem cells

Most effects of MSCs are attributed their rich secretome, known as paracrine action, and involves modulation of immune and inflammatory responses, inhibition of apoptosis and trophic effects such as stimulation of mitosis, proliferation and differentiation of intrinsic stem/ progenitor cells and stimulation of angiogenesis [226].

Immunomodulation

MSCs can adopt pro-inflammatory or anti- inflammatory phenotypes within their microenvironments. MSCs acquire an immune-suppressive phenotype in the presence of high levels of TNF- alpha and IFN- gamma levels in the microenvironment. On the other hand, low levels of these cytokines induce a pro-inflammatory phenotype [235]. The cell surface receptors on MSCs, the Toll like receptors (TLR), are thought to contribute to differentiation into either of these phenotypes via stimulation of either TLR- 3 and TLR- 4 receptors to derive an anti- inflammatory (MSC 2) or pro- inflammatory (MSC 1) phenotype, respectively [236]. In analogy to macrophage polarization, this process of MSCs is called the MSC polarization to which interactions with other cells of the innate immune system such as monocytes are also reported to contribute. Conclusively, MSCs play a regulatory role in several phases of immune response through diverse mechanisms of actions and on various cell types.

Angiogenesis

Angiogenesis involves a complex interaction between endothelial and non- endothelial cells as well as many enzymes, chemokines, growth factors, matrix metalloproteinase and adhesion molecules. A defective angiogenesis is implicated in many disease states such as ischemic heart disease, peripheral vascular disease and all defective wound healing processes. MSCs have demonstrated to secrete a wide variety of pro- angiogenic factors such as vascular endothelial growth factor, fibroblast growth factor 2, interleukin- 6 that are shown to act in each step of the angiogenesis (endothelial cell proliferation, migration and tube formation [237]. The secretion of pro- angiogenic factors by MSCs has been shown to be increased significantly by exposing the cultured MSCs to hypoxia (hypoxic pre conditioning) [238] resulting in better regenerative capability *in vivo* [239].

Tissue growth and regeneration

Another important property of MSCs is to secrete growth factors and other chemokines to induce cell proliferation and tissue regeneration in many organ systems including peripheral nerves. Some of the important growth factors that have been shown to be included in the secretome of the MSCs are NGF (nerve growth factor), BDNF (brain-derived neurotrophic factor) and GDNF (glial cell line-derived neurotrophic factor) [240], [241].   MSCs also modify the microenvironment in a pro- proliferative way, by secreting anti- apoptotic proteins and by direct cell- to- cell communications. On MSC co- culture experiments, MSCs improved survival of ischaemic cardiac cells via direct cell- cell connections and intercellular nanotube formation [242]. The secretome of MSCs also contain anti- apoptotic factors [243], [244] as MSC- conditioned medium without any cells have shown to decrease Caspase-3 activity in the myocardium and improved functional outcomes in pig models [245].

Therefore, MSCs can provide beneficial effects on tissue regeneration and integration of the tissue engineered products by secreting factors that promote tissue regeneration and new blood vessel formation.   In this section, the effect of stem cells on new blood vessel formation was first investigated. Than the added effect of combining a drug releasing scaffold with stem cell implantation is investigated.

6.2. Effect of adipose derived stem cells on angiogenesis

In these experiment a hydrogel was used as a stem cell carrier to be able demonstrate a measurable paracrine effect of MSCs both in aortic ring assay and the CAM assay a high number of cells would need to be concentrated in a small surface area which required a three dimentional structure. For example, when testing the effects of stem cells on endothelial cell sprouting in the chick aortic ring assay a 24 well plate was used which was necessary to ensure minimal dilution of the growth factors that naturally existed in the piece of the cultured organ. The culture insert that could go with a 24 well plate to achieve a co- culture system could only accommodate   100.000 cells at confluency which did not allow demonstration of a measurable difference in endothelial cell sprouting using this set up.

The feasibility of implantation of cells directly on the CAM was also investigated in the preliminary experiments. Similar to the experimental set up used to test the effect of estradiol on CAM a plastic ring was placed on the CAM at EDD 7 into which a suspension of 100k cells were seeded. Human dermal fibroblasts were first used as cellular controls and melanoma (C8161) cells were planned to constitute positive controls for ADSCs. When the cells were directly seeded on a circumscribed area on the CAM, the maximum measurable angiogenic response was not considered to be ideal. This could have been due to invasion of the CAM stroma by the tumour cells and failure of these cells to get concentrated on a single spot or the number of cells would not have been enough to allow a visible change in angiogenesis. Therefore, a hydrogel system was used as a carrier of more cells. The preliminary experiments demonstrated that up to 1000k cells could be encapsulated into the hydrogels resulting in more dramatic increase in angiogenesis (Figure 6.1). However, the blood vessels in tumour induced angiogenesis appeared tortuous and disordered. Therefore, although the the hydrogel system worked well to concentrate enough number of cells on a singke area on CAM, the tumour cells were abandoned as a positive control as they induced a pathological neovascularization.

Figure 6.1. Preliminary experiments to establish control groups for testing angiogenic potential of adipose derived stem cells (ADSCs). Here human dermal fibroblasts (HDFs) were used as cellular controls whereas melanoma (C8161) cell line was included as a possible positive control. Both cell types were first implanted directly on CAM (upper raw) which did not result in an obvious change in vascularization at the site of implantation. After HDfs and C8161 cells were encapsulated in a hydrogel (lower raw) tumour cells resulted in an increase in vascularization however this time the blood vessels were tortuous as would be expected with tumour cells.
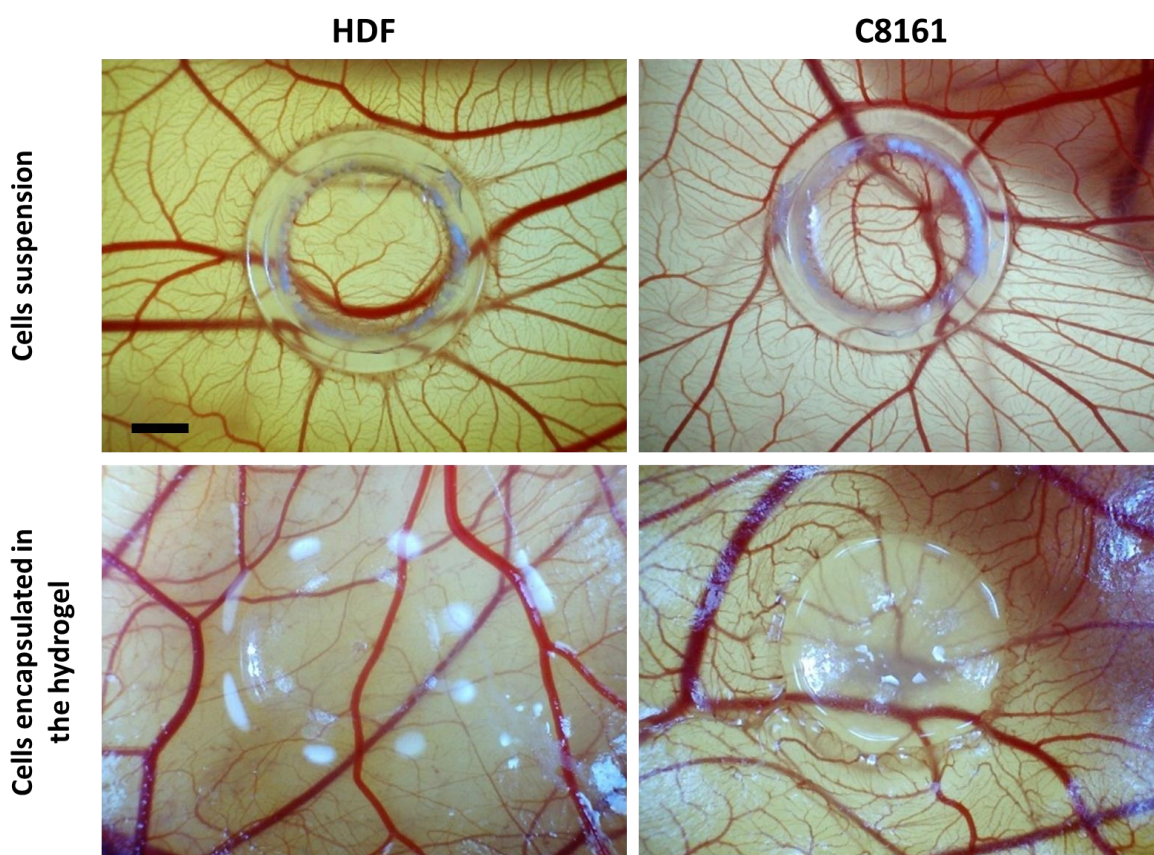
Construction of the hydrogel cell carrier

A bicomponent hydrogel was constructed using methacrylated gelatin and methacrylated hyaluronic acid by UV- crosslinking. This hydrogel was designed and synthesized in BIOMATEN Center of Excellence in Biomaterials and Tissue Engineering, Middle East Technical University, Ankara, Turkey by Dr. Gozde Eke and Prof Vasif Hasirci. Previously synthesized and characterized powders of lyophilized gelatin and hyaluronic acid were received in Kroto Research Institute which were than weighed, dissolved and crosslinked in house. The main characteristics of the hydrogel has been published previously [140] and summarized in Figure 6.2.

Figure 6.2. Graphical demonstration of synthesis, assembly and basic in vivo evaluation of the hydrogel used to encapsulate adipose derived stem cells (ADSC) in these experiments. Synthesis of components of the hydrogel by methacrylate groups (upper raw). Assembly of hydrogel can be easily performed by crosslinking a solution of methacrylated gelatin (GelMA) and methacrylated hyaluronic acid (HA-MA) using UV irradiation (middle raw). In vivo testing of biocompatability of the hydrogel by demonstrating growth and DNA synthesis over 21 days in the hydrogel (lower raw). More detailed information in reference [140].
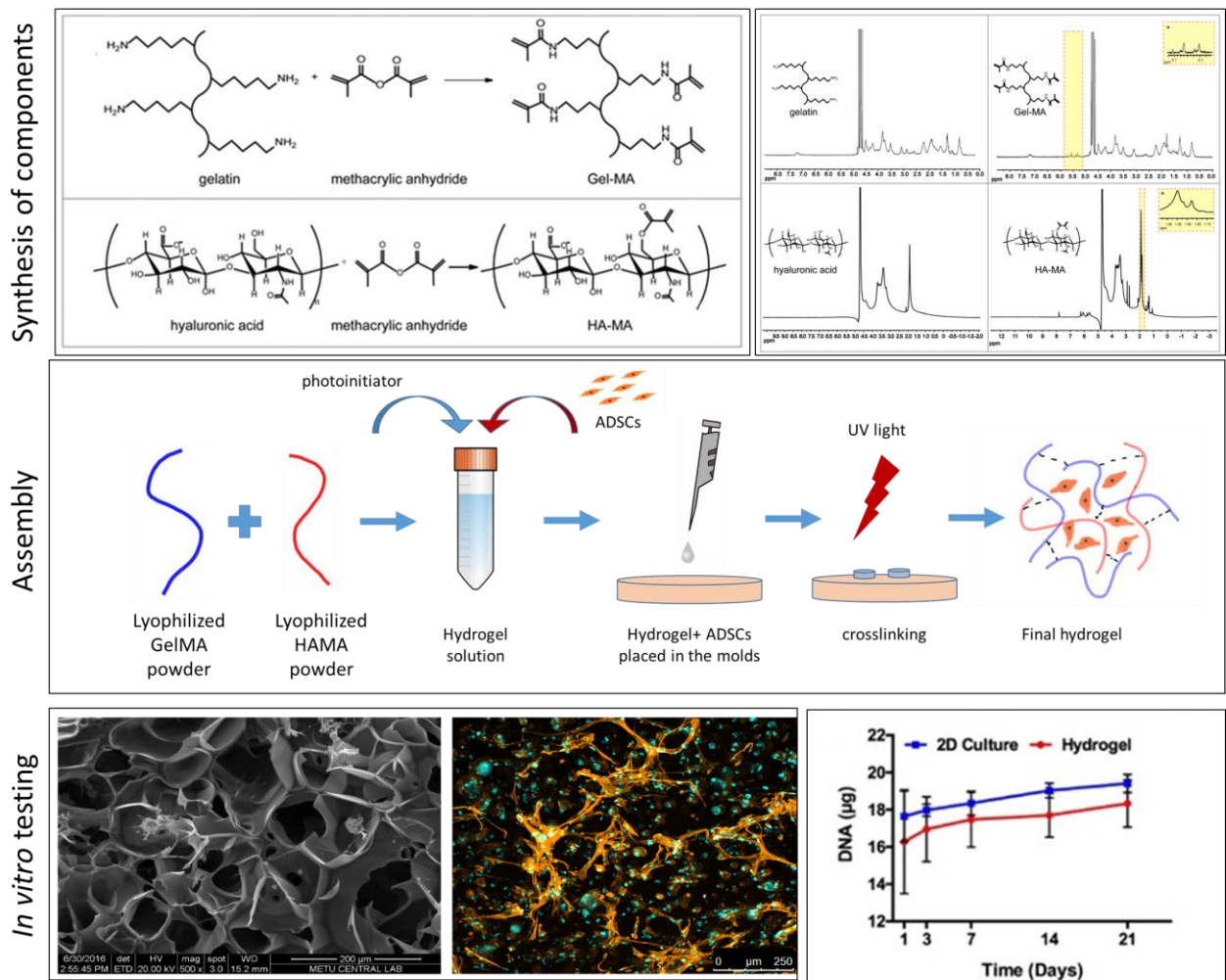
Briefly, gelatin and hyaluronic acid were methacrylated by dropwise addition of methacrylic anhydride with degree of methacrylations of 63% and 25%, respectively, as detected with NMR analysis. Methacrylated polymers were dialyzed against distilled water and than lyophilized. The lyophilized polymers were weighed and dissolved in media at a ratio of 15:1 (w:w) together with a Photoinitiator (Irgacure 2959, 0.3% w/v). The solution was than placed into molds and exposed to 365 nm UV (Omnicure s1000) for 40 seconds resulting in a solid mass. The final hydrogel had a highly porous structure with an average pore size of 120±76 µm and 79% porosity. Once in media, the hydrogels further absorbed water to reach to 200% of their original weight equilibrating at 48 hours. The proliferation of adipose derived stem cells in the hydrogels were assessed by quantification of DNA with Picogreen staining. ADSCs in the hydrogels proliferated at a rate similar to that in their growth on tissue culture plastic increasing throughout the 21 days of incubation as quantified by the measurement of increase in the amount of DNA. ADSCs appeared mostly encapsulated in the hydrogel in the first 3 days. On Day 14 of *in vitro* culture, ADSCs appeared more elongated and spreading.

In summary, this hydrogel was used as a cell carrier to test the effects of ADSCs on angiogenesis and was not considered as a candidate material for use in pelvic floor repair.

Chick aortic ring assay

The effect of three different concentrations of ADSCs encapsulated in the hydrogel (250k, 500k and 1000k) was assessed in the chick aortic ring assay by co- culturing the hydrogels together with the aortic rings via a transparent tissue culture insert. The results were evaluated at day 5 of culture and results were expressed as mean sprout length for each group. The endothelial cell sprouts were significantly longer with increasing concentrations of ADSCs. The mean sprout length for control, 250k, 500k and 1000k ADSC encapsulated groups were 84 (±6.1), 11.2 (±19.3), 203 (±25.3) and 397 (±96.2), respectively (Figure 6.3). Additionally the endothelial cell sprouts were characterized by staining positively with the endothelial cell marker Isolectin B4.

Figure 6.3. Assessment of endothelial cell proliferation and sprouting in response to different number of ADSCs loaded hydrogels. Hydrogels were co-cultured with chick aortic rings for 5 days. Characterization of endothelial cell sprouts (arrows) by lectin IB4 (green) and cell nuclei with with DAPI (blue) (A). The change in the length of endothelial sprouts with the seeding density of ADSCs (B) and representative images (C). (scale bars 250 μm).
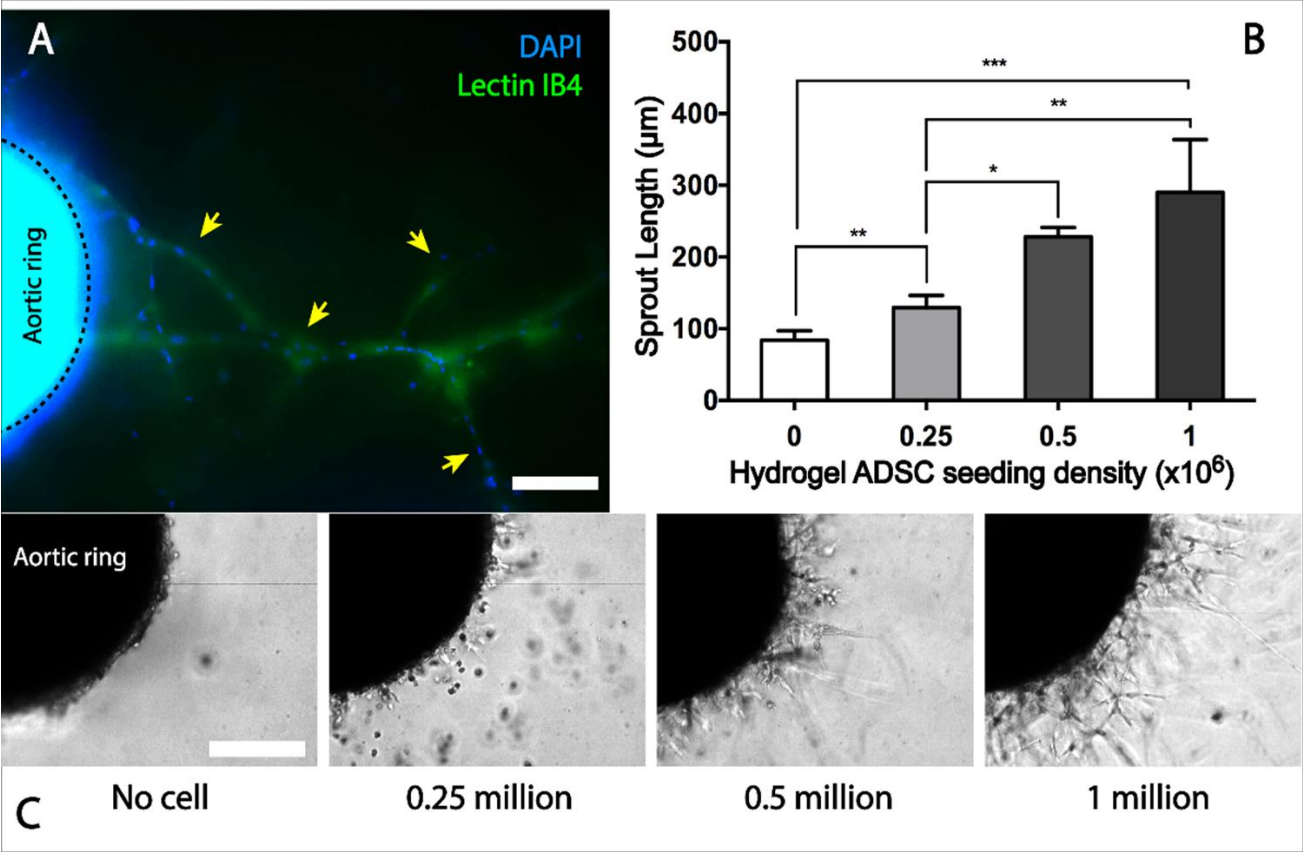
One million ADSCs were put into the hydrogel solution containing methacrylated gelatin and hyaluronic acid and photoinitiator that was warmed up to 37°C beforehand. After gentle pipetting, 100 µl of this solution was pipetted on to Petri dishes and immediately exposed to UV light for 40 seconds. The ADSC containing hydrogels were implanted on to the CAM at EDD 7. Hyrogels without any cells and hydrogel containing 100 ng of VEGF was used as controls (Figure 6.4). Three parametres were calculated on digital images using the Image J software and the Neuron J plugin: the total vessel count, the total vessel length and the vasculogenic index (Table 6.1).

Figure 6.4. Evaluation of the angiogenic properties of ADSCs encapsulated into the hydrogel in the chick chorioallantoic membrane (CAM) assay. Micrographs (upper row) and semi-automatic processed images (lower row) of the hydrogel, hydrogel containing ADSCs and hydrogel containing VEGF (positive control), taken on day 14 of embryonic development.
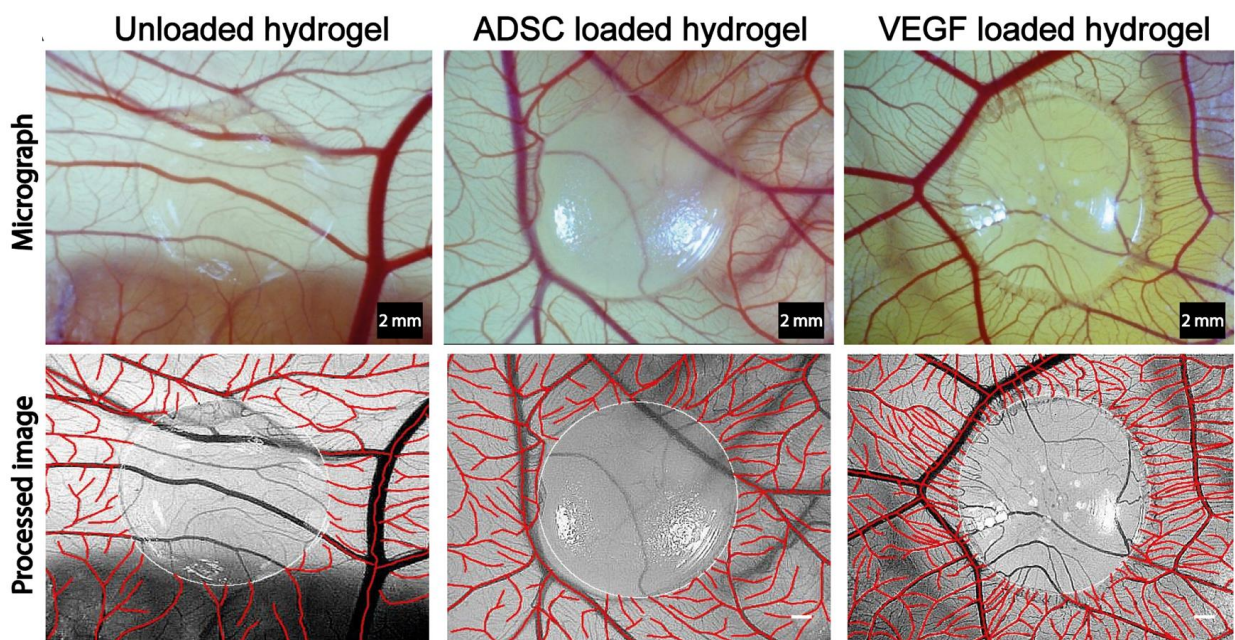
Table 6. 3. The summary of CAM assay findings comparing hydrogels with and without adipose derived stem cells (ADSCs). (*p<0.05 compared to control hydrogels; +p<0.05 compared to VEGF hydrogels)

	Control hydrogels	ADSC hydrogels	VEGF hydrogels
Total vessel count (mean± SD)	59.2 (±15.1)	93.2 (±12.7)*	117.6 (±14.3)*
Total vessel length (mean±SD)	97.6 (±16.3)	136.0 (±16.7)*, +	168.6 (±11.5)*
Vasculogenic index	14.6 (±1.8)	21.0 (±2.7)*,+	27.0 (±3.8)*

On EDD 14 the hydrogel- CAM complex were gently resected and fixed in formaldehyde. The first observation was that unlike fibrous scaffolds the hydrogels could easily be detached from the CAM. The H&E staining confirmed this showing almost no tissue integration into the hydrogels. Additionally the hydrogels did not induce any inflammatory reaction on the underlying CAM tissue (Figure 6.5.). This made it easier to count the blood vessels on the adjacent CAM.   The angiogenic response to the hydrogels were quantified by measuring the area stained positive for α-SMA on fluorescent images. Therefore, histologic examination of CAM-hydrogel complex have confirmed a significantly increased area of α-SMA positive blood vessels in CAM tissue under and adjacent to the VEGF loaded hydrogel compared to the hydrogel alone whereas ADSC loaded hydrogel was associated with a moderate increase in the number of blood vessels. Also there was almost no cellular/ inflammatory cell infiltration in the CAM underneath the hydrogel.

In conclusion ADSCs on their own appeared to stimulate angiogenesis through their paracrine effects. Compared to VEGF, ADSCs have mild to moderate pro- angiogenic properties.

Figure 6.5. Histological evaluation of angiogenic properties of ADSCs encapsulated in hydrogels. A) Normal appearance of CAM structure on Haematoxylin &Eosin (H&E) staining and fluorescence staining of CAM vessels with alpha-smooth muscle actin (α-SMA) and 4′,6-diamidino-2-phenylindole dihydrochloride (DAPI). B) Area coverred by blood vessels (stained positive for α-SMA) (**: p<0.01; ***: p<0.005). C) Representative images from each group demonstrating more blood vessels in the area adjacent to the hydrogels. Additionally hydrogels caused a mild inflammatory response on the CAM. (Scale bars: 100 µm).
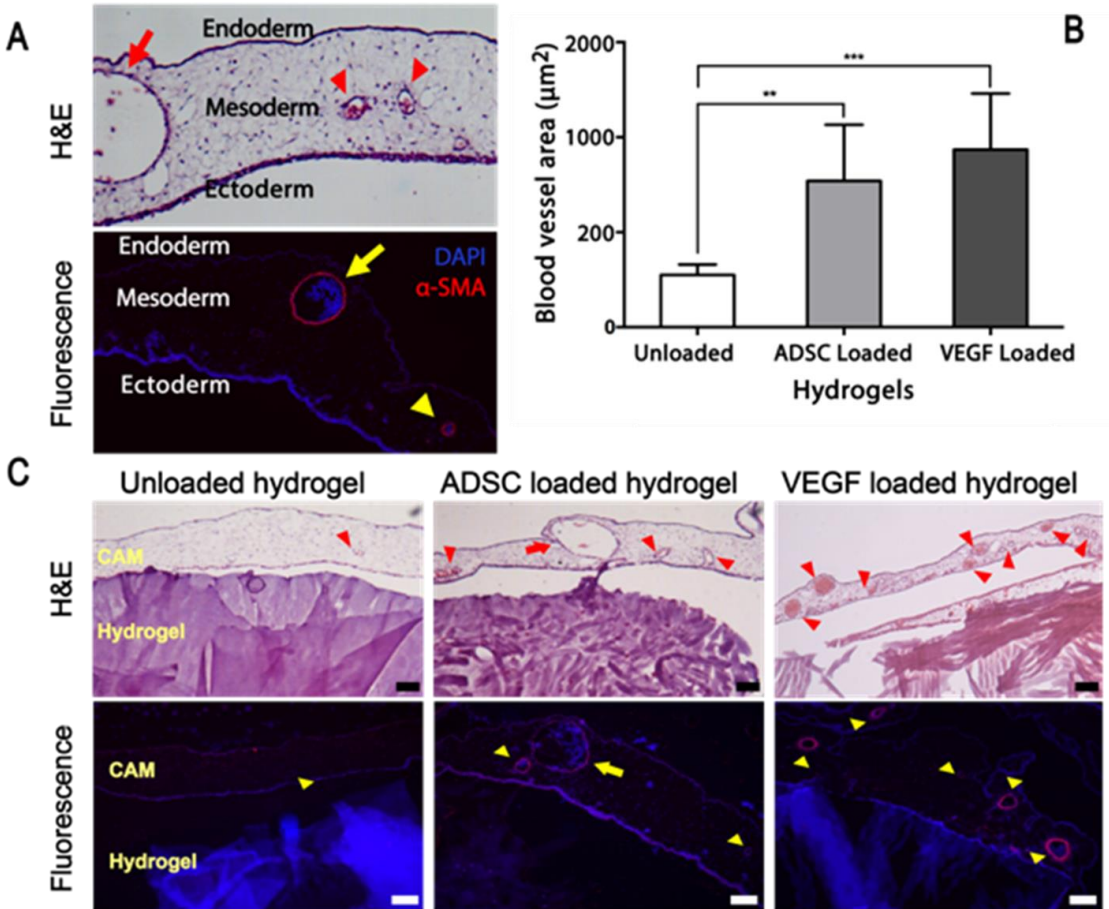
6.3. Combining electrospun scaffolds with ADSCs to improve tissue integration

In this section a polyurethane scaffolds used to follow on the work within the group suggesting PU material could have beneficial mechanical properties with improved elasticity. All the work presented in this section was a part of the masters thesis of Miss Sarah Shafaat which has been published [72]. The PhD scholar has direct contribution to all satges of the experiments at all levels including planning, conducting and results evaluation.

Briefly, polyurethane (PU) Z3 (Biomer technologies, Cheshire, UK) was dissolved (8% w/v) in a mixture of 70% v/v N,N-Dimethylformamaide and 30% v/v tetrahydrofuran. Into the polymer solution 50 mg of Estradiol was added and electrospun. Eight milliliters of 10% PLA was first electrospun as a sacrificial layer. Electrosinning parameters were rotation at a rate for collector of 265 rpm, 20 cm of distance from the tip of the needle to the collector, feed rate of 40 µl/min and an accelerating voltage of 17.4 kV. Estradiol was released from these scaffolds gradually after an initial burst release of 30-40% in the first 10 days as measured by UV-spectrophotometer at a wavelength of 272nm. Incorporation of estradiol into the PU scaffolds did not effect scaffold ultrastructure but increased total collagen production by ADSCs compared to PU only scaffolds.

Evaluation of mechanical properties of PU scaffolds

The main advantage of PU materials is related to their inherent elasticity. The mechanical properties of electrospun PU scaffolds were evalauted by both uniaxial and cyclic mechanical testing. The cyclic mechanical testing is performed to demonsrate a deformation of the material by repeated loading and unloading (Figure 6.6).

Figure 6.6. Graphical explanation of using a cyclic mechanical testing to demonstrate material deformation. (A) The BOSE tensiometer for uniaxial testing. (B) The stress- strain curve produced by uniaxial tensile testing. The change in the appearance of the sample during the test is shown in the inset. (C) Demonstration of deformation of the material in cyclic mechanical testing applying a 25% displacement (strain) to the material. The deformation of the material can be measured by the lack of stress starting from the second cycle.
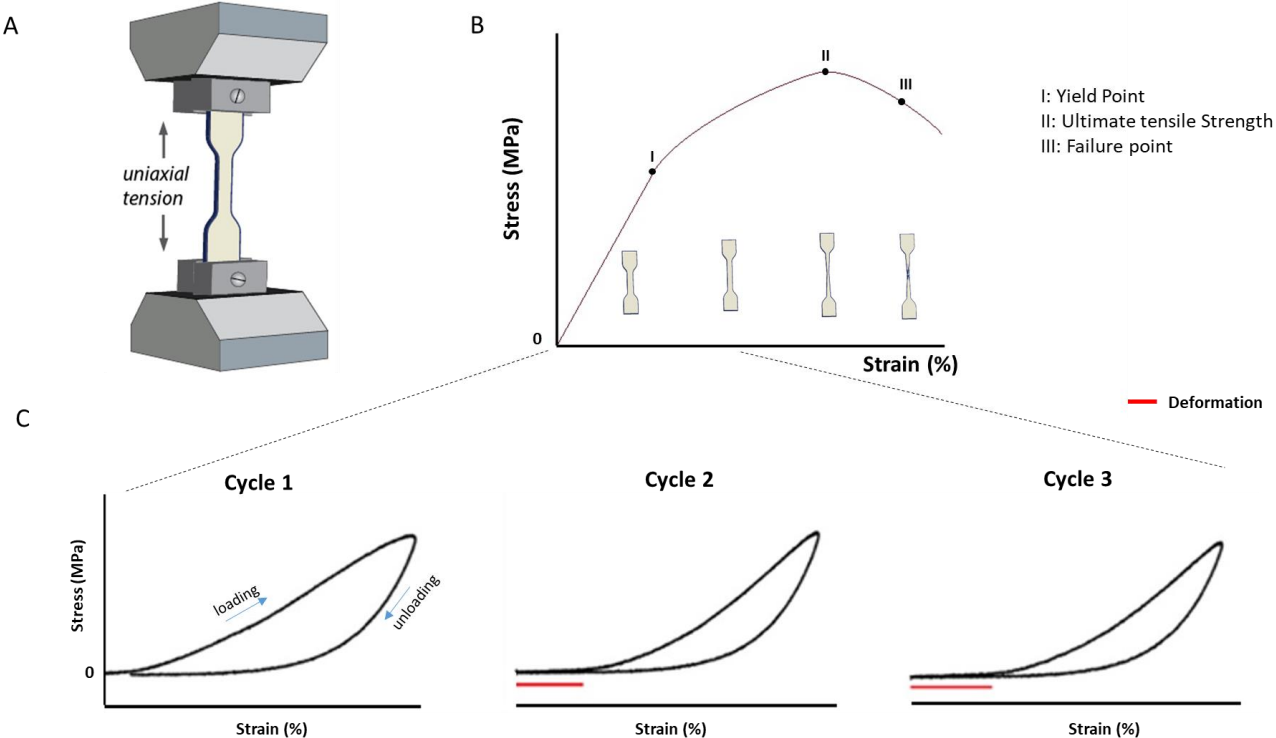
In uniaxial testing, incorporation of estradiol significantly increased the ultimate tensile strength (UTS) (N/mm2) and Young' s modulus (YM) (N/mm2) of PU scaffolds compared to controls, UTS and YM were 5.79± 0.336 and 3.26±0.46 (p<0.005) and 11.5±1.6 and 9.8±0.7 (p<0.005), respectively (Figure 6.7). These values were 30-40% higher than the reference range for the healthy native fascia (YM 6.4-10.1 N/mm2). In the cyclic mechanical testing, all PU scaffolds underwent deformation from cycle 1 to cycle 2, with reduced YM values for estradiol releasing PU scaffolds from 20.2±2.4 in the first cycle to 14.7±1.4 in the second cycle (Figure 6.8).

Figure 6.7. Mechanical testing of PU only and Estradiol releasing PU scaffolds on uniaxial mechanical testing.
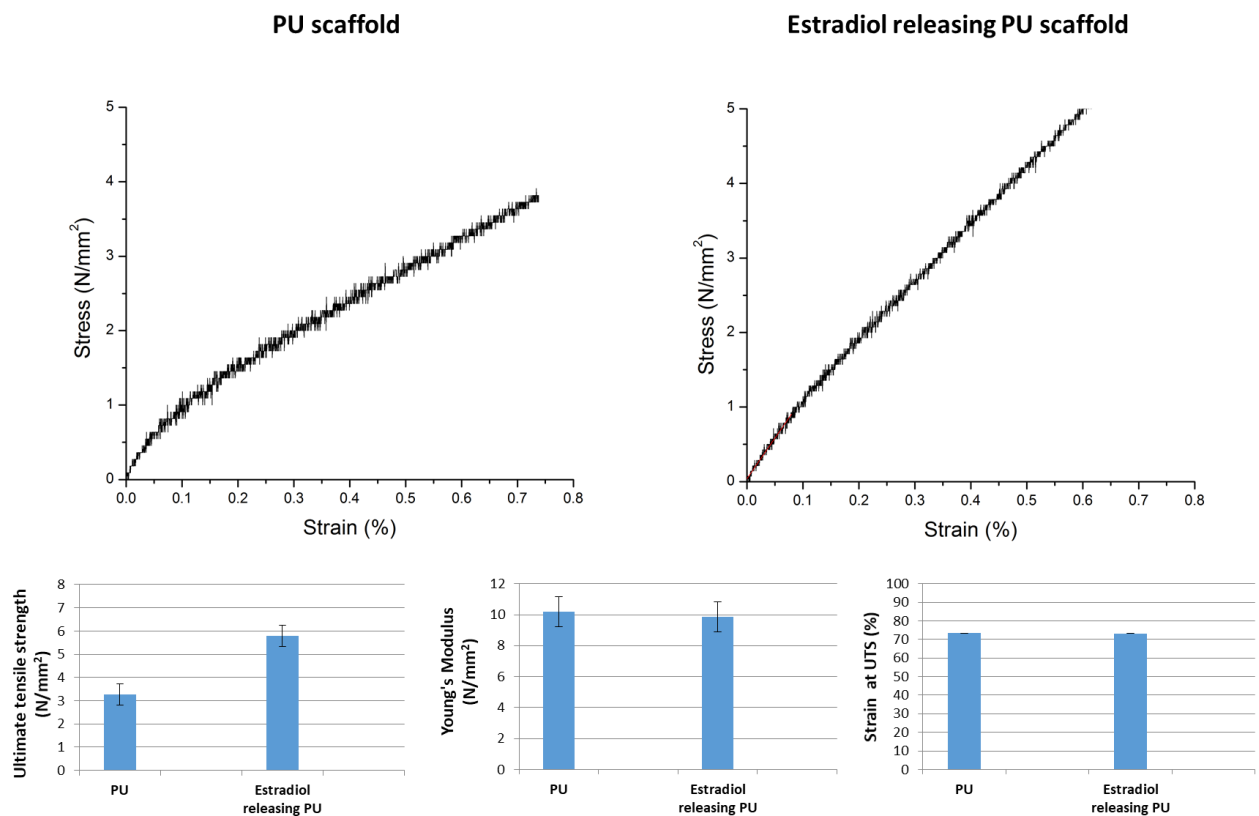
Figure 6.8. Cyclic mechanical testing on PU only and estradiol releasing PU scaffolds to demonstrate material deformation (*: p<0.05).
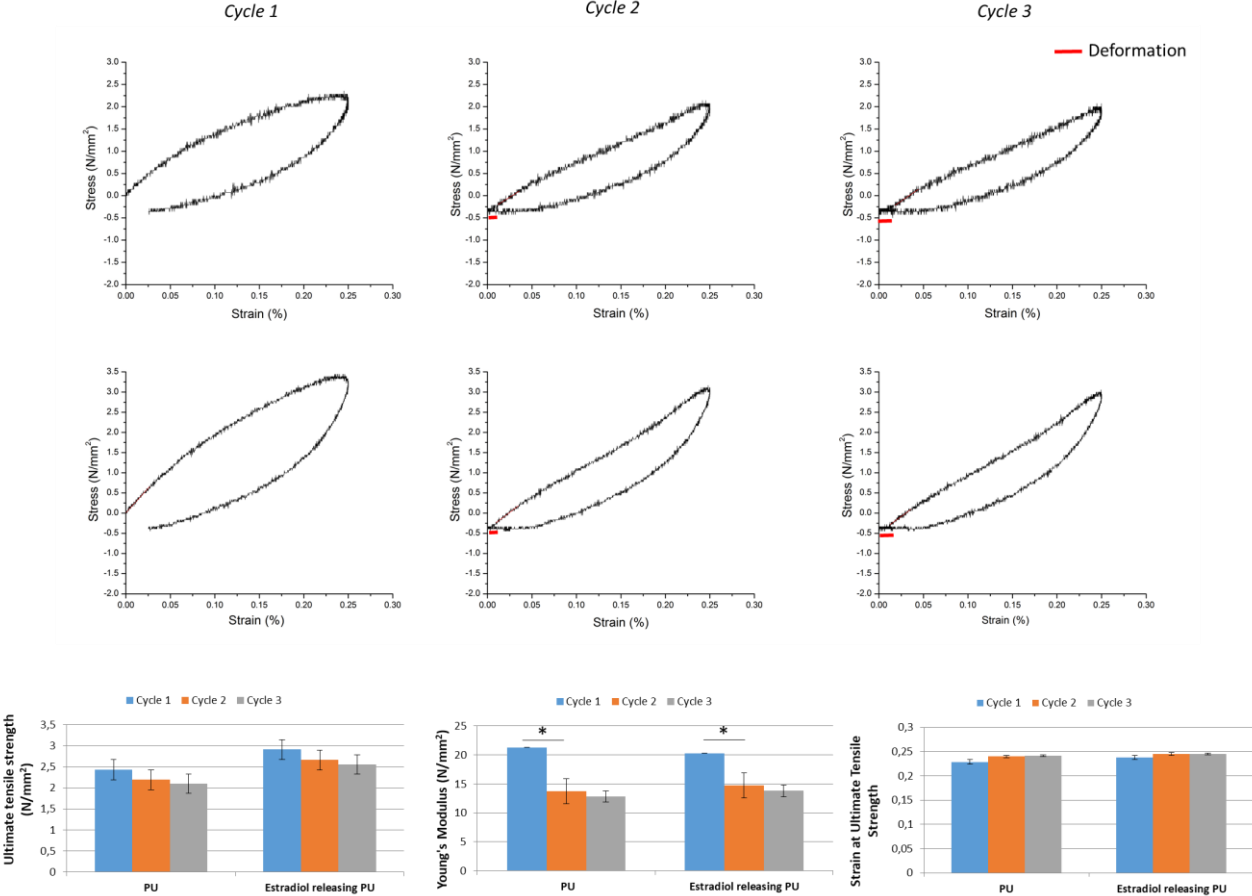
In another study conducted within the group in collaboration with Dr. Sabiniano Roman, the deformation of various mesh materials under cyclic mechanical testing was compared to two other electrospun materials. This has shown that all materials underwent plastic deformation after cyclic loading mainly between cycle 1 and cycle 2. However it appeared that the commercial meshes demonstrated significantly higher deformation compared to electrospun meshes after 10 cycles. The percentage deformation for commercial meshes were 6.69% (±0.75), 8.51% (±0.47), 4.77% (±1.08) and 3.60% (±0.52), respectively for Gynemesh®, Restorelle®, DynaMesh-ENDOLAP® and DynaMesh-PR4®. In contrast the percentage deformation for electropun meshes (UPy-PC and PU) were 1.92% (±1.19) and 0.58% (±0.32) (Figure 6.9).

Figure 6.9. Comparison of electrospun polyurethane (PU) scaffold with available meshes currently used in the treatment of SUI and POP. (This experiment performed by Dr. Sabiniano Roman)
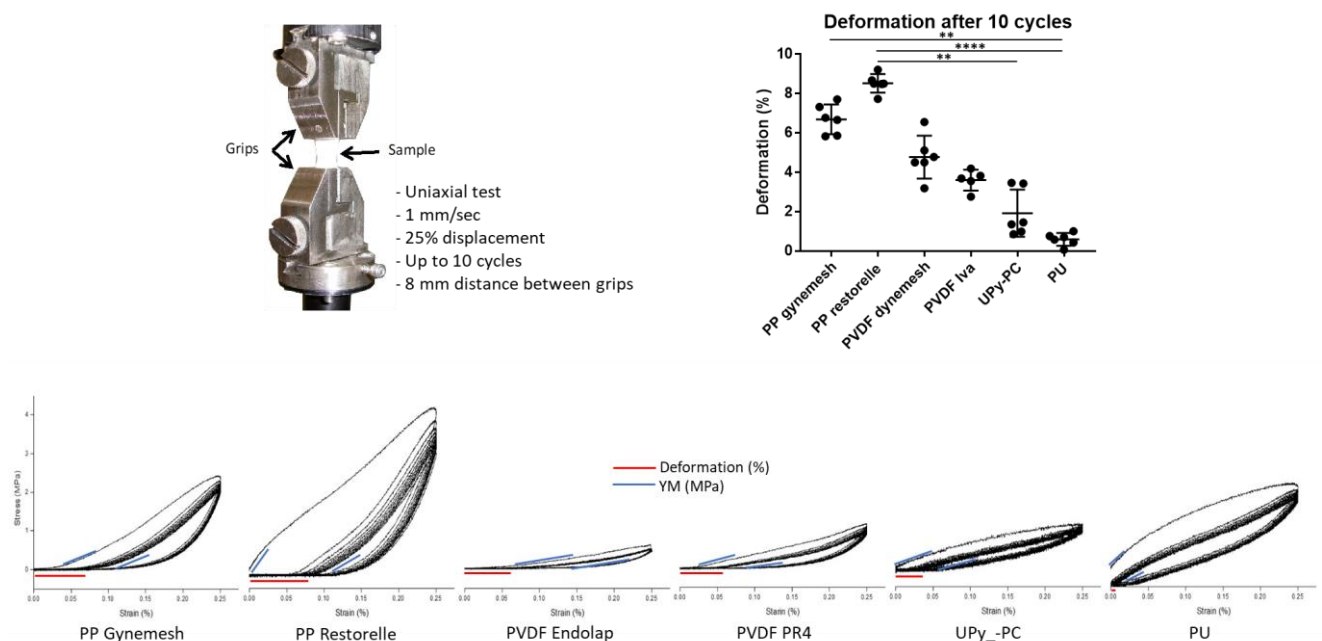
Evaluation of scaffold and stem cell constructs for their effects on angiogenesis

PU scaffolds with and/ or without estradiol were cut into 1x1 cm squares and were UV sterilized. ADSCs between passages 3 and 8 were seeded on the estradiol releasing PU and control scaffolds at a density of 250k and incubated at 37 °C and 5% CO_2 until they were implanted onto the CAM next day. HDFs were used as a cellular control in these experiments. The scaffolds were then implanted on the surface of CAM by placing the cell seeded surface in direct contact with CAM tissue.

Estradiol releasing PU scaffolds were significantly more angiogenic compared to controls, vasculogenic index 33.5 ($\pm$7.2) and 15.8 ($\pm$3.5), respectively ($p < 0.05$). When ADSCs were seeded on the estradiol releasing and control scaffolds the vasculogenic index went up to 55.2 ($\pm$7.2) and 43 ($\pm$3.6), respectively. Therefore ADSCs increased the vasculogenic potential of PU scaffolds compared to PU only scaffolds (Figure 6.10).

Figure 6.10. The effect of incorporating ADSCs into the tissue engineered constructs on the angiogenic potential of estradiol releasing PU and control scaffolds. (scale bars represent 200 μm; *p<0.05 compared to PU only scaffolds). (This experiment was performed by Miss Sarah Shafaat)
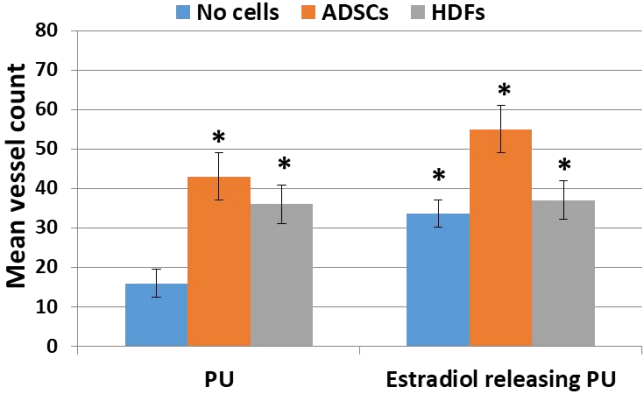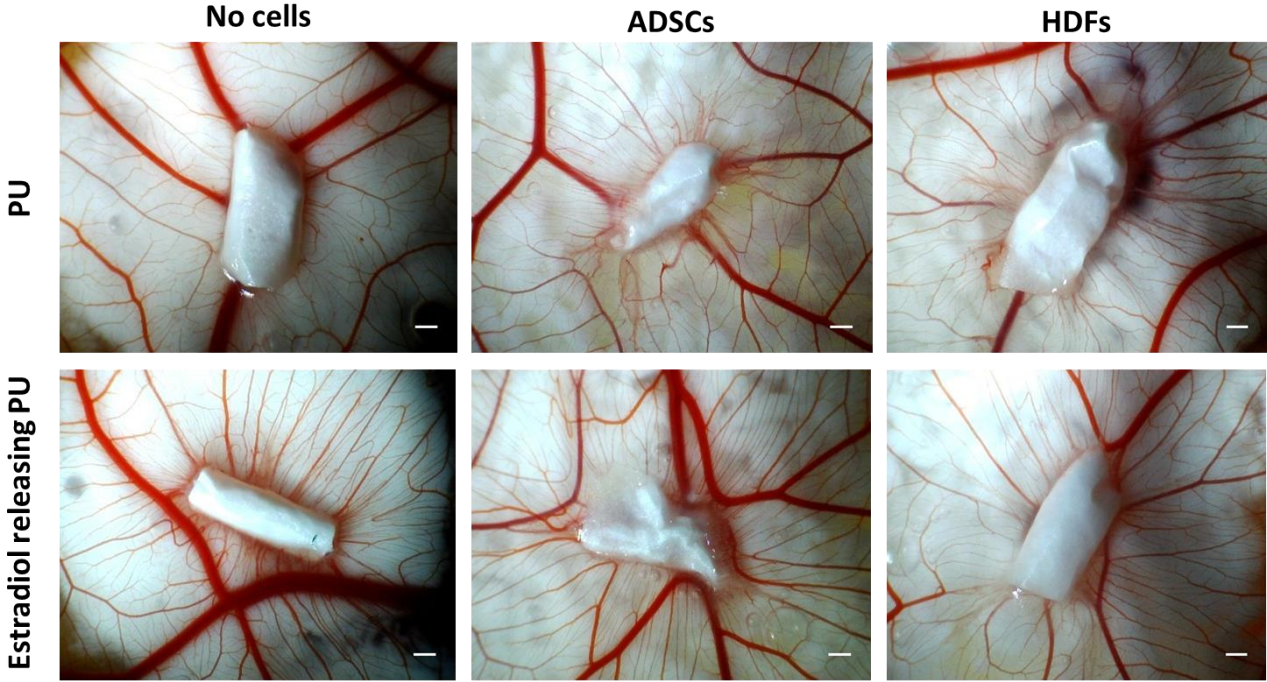
Evaluation of tissue integration of scaffold- ADSC constructs

Histologic examination of the ADSC seeded PU scaffolds resulted in good tissue integration into the CAM tissues after 8 days of implantation. There was no significant difference between estradiol releasing and PU only scaffolds (Figure 6.11). A mild inflammatory response in the CAM tissue adjacent to tissue engineered constructs could be seen in all samples.

Figure 6.11. The effect of incorporating ADSCs on tissue integration of estradiol releasing and control scaffolds. Haematoxylin and Eosin (H&E) staining of CAM- scaffold complexes after 8 days of incubation. Scale bar represents 100µm and applies to all images (PU=Polyurethane) (*CAM tissue, ** implant/scaffold). (This experiment was performed by Miss Sarah Shafaat)
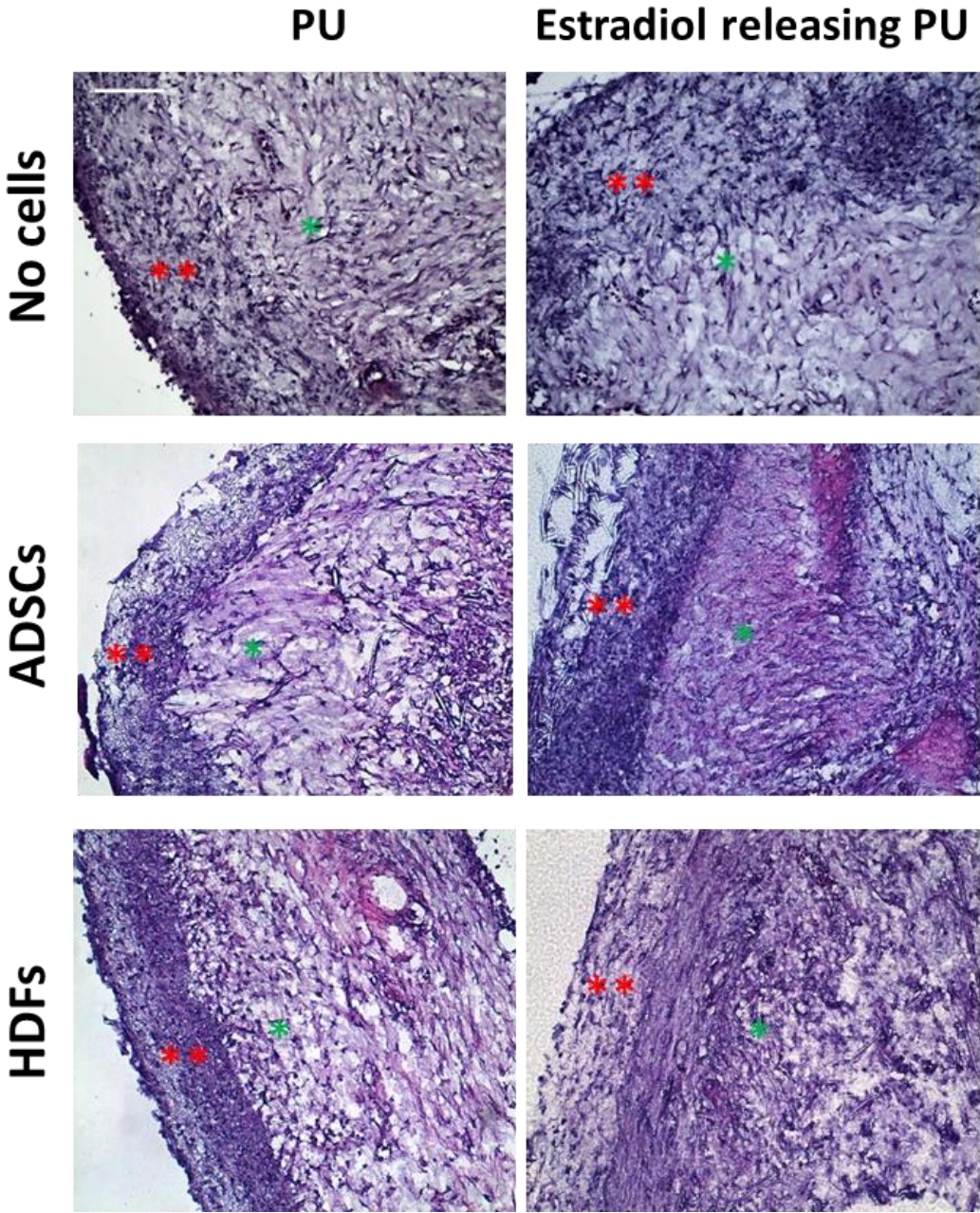
6.4. Chapter discussion

Mesenchymal stem cell (MSC) therapy has emerged in the last 10 years as an important cellular source to stimulate tissue regenration and promote angiogenesis with several cell based therapeutic applications being tested in clinical trials [246]. In this section, the added effects of incorporating stem cells inthe tissue engineered constructs designed for pelvic flor repair is evaluated. The data presented shows that stem cells alone have a mild to moderate effects on stimulating new blood vessel formation in the CAM assay and combination of electrospun matrices with stem cells can have an added effect when stimulating angiogenesis. Nevertheless the involvement of cellular components in the tissue engineered constructs would mean more complicated routes when translating into clinic compared to biomaterials without cells.

From a regulatory perspective, regenerative medicine refers to methods to replace or regenarate human cells, tissues or organs to restore or establish normal function. This includes cell therapies, tissue engineering, gene therapy and biomedical engineering techniques as well as more traditional treatments involving pharmaceuticals, biologics and devices. On the other an advances medicinal therapy product (ATMP) is a medicinal product which is either a gene therapy medicinal product, a somatic cell therapy medicinal product or a tissue engineered product [247]. Among these gene therapy medicinal products and somatic cell therapy medicinal products have legal definitions, a tissue engineered product rather more difficult to define due to the extent and complexity it encompassess. For medicinal products that do not contain viable cells the mode of action is primarily by physical means. However if they contain viable cells or tissues, regardless of the role that the material component play, the primary mode of action of the combined product should be considered to be a function of the pharmacological, immunological or metabolic effects of the cells. Hence the regulatory evaluation of ATMPs often require very specific expertise covering the areas of biotechnology and medical devices.

Under the new EU directive, a tissue engineered product is defined as "a product that contains or consists of engineered cells or tissues and is presented as having properties for, or is used in or adminised to human beings with a view to regenerating, repairing or replacing a human tissue" [247]. An 'engineered cell' is defined as "a cell that fulfil at least one of hte following: i) the cells or tissues have been subject to substantial manipulation so that biological characteristics, physiological functions or structural properties relevant for the intended regeneration, repair or replacement are achieved" [247]. Article 2(1)(c) of the directive defines specific procedures that are not considered as substantial manipulations. These are: cutting, grinding, shaping, centrifugation, soaking in antibiotic or antimicrobial solutions, sterilization, irradiation, cell separtion, concentration or purification, filtering, lyophilization, freezing, cryopreservation, vitrification ; ii) the cells or tissues are not intended to be used for the same essential function or functions in the recipient as in the donor. Therefore adipose tissue derived cells, even if not substantially manipulated, will be considered an ATMP when used to serve functions other than being adipose tissue. This means that the necessary regulatory approval before translation of these products would be difficult.

The main challanges that lie ahead of the clinical translation of MSCs for many applications are related to lack of a more specific definition of an MSC, the uncertainties about the mechanisms of actions, reproducable manufacturing of adequate amounts of MSCs, distribution and costs. The widely accepted minimal criteria to define a mesenchymal stem cell [224], although useful to have one, covers a hugely diverse cell population that could result in high variability among result findings. Also, the *in vivo* fade of MSCs at the site of tissue injury is not clear. It has been shown that after intravenous injection most of the MSCs are trapped in the lungs initially, however they eventually home to sites of tissue injury and finally 0.1% to 2.7% of MSCs can be found engrafted to the sites of injury after 2 weeks [248]. Furthermore, in most pre- clinical research the MSCs are used without pre- labelling and the fate was not tracked. Instead it has been a common practice to report efficacy of stem cells based on functional outcomes. This has also been referred to as 'the beneficial effects given as a reason to move fast from insufficient science to translation or therapy are not clearly defined' [225].

In addition, the efficacy and bioavailability of stem cells as a function of the method of delivery is highly variable and not comparatively studied. For example, most pre- clinical and clinical research on using MSCs for treatment of erectile dysfunction applied stem cells by intracavernousal injections where the main tissue damage was actually in the cavernous nerve in the pelvis [246], [249]. This assumes an effective homing of MSCs to the sites of tissue injury however this has not been assessed in many studies. The bioavailability and efficacy of any therapeutic agent is affected by its method of delivery. A direct comparison of intravenous, intracoronary and endocardial injections of MSCs in a swine model of acute MI demonstrated a better engraftment of MSCs in intracoronary and endocardial injections compared to IV delivery [250]. In the context of pelvic floor repair materials, the MSCs is envisaged to be seeded on scaffolds before implantation. Hence they will be implanted at the site of the intended tissue repair however the fate of the MSCs in this scenario still needs to be studied.

Some of the above challanges can be overcome by innovative methods of cell labelling and together with use of non- invasive imaging technologies. The detection of MSCs in fixed tissue samples requires scarification of groups of animals at several time points and harvesting organs for histologic sectioning. These disadvantages led to development of dynamic imaging modalities. The non- invasive dynamic imaging studies include MR imaging of magnetic particle labelled cells [251]–[253], single photon emission computed tomography (SPECT) imaging of radioisotope (^{111}In oxine, ^{99m}Tc) MSCs [254] and quantum dot labelling [255]. Each of these non- invasive imaging modalities have their own advantages and limitations however they are very likely to become an integral part of stem cell based therapies and further improvements in this area needed.

Another issue that is addressed within this section is related to the cyclic mechanical properties of the biomaterials designed for pelvic floor reconstruction. Looking back critically on the currently used mesh materials, mainly PPL, it appears that many authors agree on the biological and mechanical incompatability of the PPL mesh to the pelvic floor. Briefly, it is known that the host response to PPL mesh is more representative of a chronic inflammation resulting in poor tissue integration and significant fibrosis around the implant [256]–[258], especially in cases of vaginal implantation rather than abdominal [101]. This unfavourable biological response to PPL mesh, is much less studied compared to its mechanical failure. It has been commonly suggested that the mesh is too strong and too stiff for applications in the female pelvic floor. Theoretically, this can lead to a phenomenon called 'stress shielding' which is more commonly used for orthopaedic implants. Stress shielding is when a strong material carries all the load and depriving the adjacent issues of mechanical stimuli that eventually results in defective extracellular matrix production in the tissues adjacent to the implant. The same phenomenon can explain the poor tissue healing and erosion associated with vaginal mesh implant surgeries.

Furthermore, PPL mesh is probably not only too strong but also it can mechanically fail when exposed to cyclic distension at the site of implantation. The cyclic loading experienced by the materials are known to lead to plastic deformation of the material a little at a time when they are exposed to loads above their yield point. This can contribute to material failure and/ or change in its mechanical properties overtime [74]. The available evidence on the effects of cyclic loading on mechanical properties of the PPL mesh is not well studied. Cyclic uniaxial loading studies are conducted to study the deformation of the material under repetitive sub-failure loads [259]. Previous studies have shown the results when such tests were run for up to 10 cycles [259], [260] and despite showing 'deformation', they were not planned to demonstrate 'failure'. Fatigue testing of materials for longer durations of cyclic mechanical loading under simulated physiological conditions can show material failure. These tests have been commonly performed for biomedical implants such as heart valves and stents however they were never considered for evaluation vaginal meshes.

Mechanical testing studies within the pelvic floor research group in the Kroto Research Institute, have led to describing a simple protocol that could be used as a fatigue testing to demonstrate the mechanical failure of the materials starting from early stages of development [261]. This is important because although previous studies have used 'dynamic mechanical assessment' techniques to test surgical meshes [262], such tests require sophisticated equipment and expertise making it difficult to adopt for many research groups. Nevertheless, the failure of Ultrapro mesh after 16,000 cycles has been reported together with permanent change in yarn structure [263]. In conclusion, using the simple fatigue testing under physiologic conditions electrospun polyurethane (PU) is shown to survive 80% strain equally well before and after the fatigue testing, while the commercial meshes failed the uniaxial tensile test after fatigue testing.

A limitation of using such a fatigue testing protocol to detect material failure early during development is related to the current inability to estimate the cyclic loading conditions that the material will undergo at the site of implantation. This is mainly due to lack of understanding of the biomechanics of the female pelvic floor. Not only the anatomy is complex and the biomechanics are poorly understood, but also the consequences of other risk factors such as carrying full term pregnancies, vaginal deliveries and the loss of oestrogens at the menopause are not known.

A comparison of fatigue behaviour of available candidate materials within the group demonstrated that electrospun PLA scaffolds underwent significant deformation after 7 days of dynamic distention in 7 days while electrospun PU Z1 and Z3 scaffolds remained elastic [113]. Hence the PU scaffolds has been studied as another good candidate to functionalized by incorporation of Estradiol and MSCs in the current section. The results demonstrated that Estradiol could effectively be blended into PU scaffolds and achieve a sustained release without having a negative effect on scaffold ultrastructure and mechanical properties. PU scaffolds survived the fatigue test better compared to commercial meshes and they stimulated new blood vessel formation with good tissue integration. Therefore, Estradiol releasing PU scaffolds could be used effectively to stimulate new blood vessel formation and improve tissue integration for applications where non- degradable materials are desired.

Chapter 7.
Summary and Future Work

7.1. Summary

In summary this thesis explored the feasibility of functionalization of biomaterials by addition of drugs and cells with the ultimate aim of improving the biocompatability of the biomaterials by acheiving increased angiogenesis and tissue integration.

Firstly, an *in vivo* methodology to study the angiogenic potential of and the initial tissue response to constructed biomaterials was developed. The *ex ovo* CAM assay proved to be a feasible and effective bioassay to assess the angiogenic potential of biomaterials with a unique advantage of allowing visualization of the developing blood vessels at all times during the experiment. The main limitations of this method was the inability to run the experiments beyond 14 days under in- house Home Office regulations and the lack of a developed immune system in the chick embryo in the early stages of embryonic development. The latter mainly limited the assessment of the initial tissue response to the constructed materials. This methodology was used as the main assay for assessing angiogenesis and early stage biocompatibility throughout the thesis.

Electrospinning was selected for the material production method and polylactic acid (PLA) was the main polymer used with its excellent biocompatiblity, drug releasing properties and degradability. The accumulated knowledge within the group was helpful in assessing two candidate drugs to be incorporated into the constructed scaffolds to stimulate new blood vessel formation and tissue integration: Vitamin C and Estradiol. Both Vitamin C and Estradiol could effectively be incorporated into the electrospun PLA scaffolds without causing significant disruptions to the ultrastructural and mechanical properties of the scaffolds. Vitamin C was released from the scaffolds over several weeks whereas Estradiol was released over months.

Both drugs increased extracellular matrix production of cells cultured on the scaffolds. Although both Vitamin C and Estradiol increased the angiogenic potential of the PLA scaffolds, Estradiol resulted in a more dramatic increase in new blood vessel formation.

Stimulation of both ECM production and new blood vessel formation by drug releasing PLA scaffolds could prositively affect tissue integration of these materials. This was assessed by implantation on the CAM for seven days which demonstrated a good tissue integration for all electrospun PLA scaffolds with no significant differences between drug releasing and plain scaffolds. The contribution of Vitamin C or Estradiol released from electrospun PLA scaffolds now needs be assessed in longer term *in vivo* assays.

The last stage of functionalization of the scaffolds that was assessed in the current studies whether the ability of the drug releasing scaffolds to stimulate angiogenesis and better tissue integration would be improved with addition of mesenchymal stem cells (MSCs). Firstly, MSCs alone were demonstrated to have a mild pro- angiogenic effect on the CAM assay. MSCs in this case were initially implanted on the CAM using a hydrogel as a cell carrier system. Secondly, Estradiol releasing electrospun scaffolds pre-seeded with MSCs were shown to have an added effect on new blood vessel formation compared to plain Estradiol releasing electrospun scaffolds. However, the size of this additional effect was small. Additionally, pre- seeded scaffolds appeared to have a similar ability to integrate into tissues in short term implantation over seven days. Therefore, from a clinical translational point of view the use of pre- seeded biomaterials would need to be balanced with the complexities and expense of manufacturing an advanced therapy medicinal product. At the time of writing the additional angiogenic benefit of adding cells to the drug releasing scaffolds does not seem justified.

7.2. Future Work

The first line of future work would involve confirmation of the pro- angiogenic and tissue integration properties of Estradiol releasing electrospun PLA scaffolds in small animal models. After the confirmatory study, the materials will need to be implanted in large animals for efficacy testing. Two large animal species have been used in the literature. The most widely used animal for vaginal implantation of a candidate mesh material is the sheep. The sheep stands out as it has a vagina that is very similar in size to the human female vagina. Other animals such as rabbit have also been used a recipients of vaginal soft tissue implants before [264] however due to the smaller size of the vagina these could only accept implantation of a small piece of mesh material. This did not demonstrate vaginal mesh erosion in most studies [265] although some authors reported observation of mesh erosion with rabbit vaginal implants in the longer term [266]. It is important to use a model that can re- create mesh erosion as it is a significant mesh- related adverse effect. Vaginal implantation of mesh material into sheep vagina was demonstrated to lead to development of mesh erosion in 30% of sheep which received a vaginal mesh implant [101]. Additionally sheep are known to develop pelvic organ prolapse spontaneously after repeated pregnancies/ births like humans.

Another animal that has been used in vaginal implant testing is the rhesus macaque. These studies are mostly performed in the United States. The obvious advantage of the rhesus macaque is that they are standing upright similar to humans. Also rhesus macaque develop spontaneous pelvic organ prolapse, they have pelvic floor anatomy similar to women with hormone sensitive ligaments in paravaginal attachments. Additionally the fibroblast activities in the connective tissues of the pelvic floor of these animals was responsive to hormonal treatment in a way similar to that of humans [267]. However the implantation of three commercial meshes in rhesus macaque resulted in erosion in only in 1 out of 32 animals [256], regardless of the mesh weight and textile structure. However in this study the meshes were implantated abdominally after hysterectomy and this does not represent vaginal implantation. Another study reported vaginal implantation without using a vaginal mucosal incision [257] precluding the applicability of this data to represent vaginal mesh implantation surgeries. Hence, the available evidence supports the use of sheep for testing of candidate vaginal implant materials. After safety and efficacy testing in relevant animals the candidate material can go on to first pilot clinical trial.

Another important point to consider during translation of these products into the clinic is about the changing regulatory approval processes for biomedical devices. It is increasingly being acknowledged that the available medical device regulations allowed the 'faulty' medical devices onto the market failing to ensure public and patient safety [257]. The scientific and surgical communities have also raised concerns on the 'commercially privileged relationship' between manufacturers and regulatory authorities [268]. A part of the problem is probably related to the inability of the old regulations to keep up with the pace of rapid technological and scientific developments in biomedical sciences and technologies in the last few decades. Although this new field of biomedical engineering offers new opportunities for treatment of disease and replacement of organs/ tissues in human body, the necessary novel legal definitions, new rules on governing their production and distribution and new processes for regulatory approval to safeguard public health appear to be missing.

Recently, two new EU regulations on medical devices entered into force [269] with the aim of establishing a robust, transparent, predictable and sustainable regulatory framework for medical devices which ensures public safety while supporting innovation. For this purpose the new EU regulations introduced new definitions such as 'active device', 'implantable device' and 'single use device' in addition to the medical device definition. Separate regulations for placing products on the market, traceability of supply chains and registration of devices and post- market surveillance are implicated. Therefore, future work needs to consider these regulations.

Another useful tool to guide safe and effective introduction of new surgical innovations is the IDEAL (Idea, Development, Exploration, Assessment and Long Term follow-up) guidelines, that define clear guidance on the types of studies and specific data requirements for each stage of approval and surveillance [270]. This involves stages of 0 to 4, where stage 0 involves pre- clinical development with materials and components testing following real-world situations. Stage 1 is the first in human trial with a few studies followed by safety and efficacy studies (Stage 2) and then randomized controlled trials to study comparative effectiveness involving hundreds of patients (Stage 3). The final stage involves long term studies for quality assurance making use of device registries. No matter what scheme is followed, it is important to ensure a system whereby the issues with implantable medical devices can be identified.

References

[1]   B. T. Haylen *et al.*, "An International Urogynecological Association (IUGA)/International Continence Society (ICS) joint report on the terminology for female pelvic floor dysfunction," *Int. Urogynecol. J.*, vol. 21, no. 1, pp. 5–26, Jan. 2010.

[2]   D. E. Irwin *et al.*, "Population-Based Survey of Urinary Incontinence, Overactive Bladder, and Other Lower Urinary Tract Symptoms in Five Countries: Results of the EPIC Study," *Eur. Urol.*, vol. 50, no. 6, pp. 1306–1315, Dec. 2006.

[3]   K. S. Coyne *et al.*, "The prevalence of lower urinary tract symptoms (LUTS) in the USA, the UK and Sweden: results from the Epidemiology of LUTS (EpiLUTS) study," *BJU Int.*, vol. 104, no. 3, pp. 352–360, Aug. 2009.

[4]   L. Zhang *et al.*, "A Population-based Survey of the Prevalence, Potential Risk Factors, and Symptom-specific Bother of Lower Urinary Tract Symptoms in Adult Chinese Women," *Eur. Urol.*, vol. 68, no. 1, pp. 97–112, Jul. 2015.

[5]   D. E. Irwin, Z. S. Kopp, B. Agatep, I. Milsom, and P. Abrams, "Worldwide prevalence estimates of lower urinary tract symptoms, overactive bladder, urinary incontinence and bladder outlet obstruction," *BJU Int.*, vol. 108, no. 7, pp. 1132–1138, Oct. 2011.

[6]   J. Cooper, M. Annappa, D. Dracocardos, W. Cooper, S. Muller, and C. Mallen, "Prevalence of genital prolapse symptoms in primary care: a cross-sectional survey," *Int. Urogynecol. J.*, vol. 26, no. 4, pp. 505–510, Apr. 2015.

[7]   S. L. Hendrix, A. Clark, I. Nygaard, A. Aragaki, V. Barnabei, and A. McTiernan, "Pelvic organ prolapse in the women's health initiative: Gravity and gravidity," *Am. J. Obstet. Gynecol.*, vol. 186, no. 6, pp. 1160–1166, Jun. 2002.

[8]   L. Wilson, J. S. Brown, G. P. Shin, K. O. Luc, and L. L. Subak, "Annual direct cost of urinary incontinence.," *Obstet. Gynecol.*, vol. 98, no. 3, pp. 398–406, Sep. 2001.

[9]   M. Imamura *et al.*, "Systematic review and economic modelling of the effectiveness and cost-effectiveness of non-surgical treatments for women with stress urinary incontinence," *Health Technol. Assess. (Rockv).*, vol. 14, no. 40, pp. 1–188, iii–iv, Aug. 2010.

[10]   S. Bartoli, G. Aguzzi, and R. Tarricone, "Impact on Quality of Life of Urinary Incontinence and Overactive Bladder: A Systematic Literature Review," *Urology*, vol. 75, no. 3, pp. 491–500, Mar. 2010.

[11]   K. S. Coyne, Z. Zhou, C. Thompson, and E. Versi, "The impact on health-related quality of life of stress, urge and mixed urinary incontinence," *BJU Int.*, vol. 92, no. 7, pp. 731–735, Oct. 2003.

[12]   N. Y. Siddiqui *et al.*, "Mental Health, Sleep and Physical Function in Treatment Seeking Women with Urinary Incontinence," *J. Urol.*, vol. 200, no. 4, pp. 848–855, Oct. 2018.

[13]   V. A. Minassian, X. Yan, M. J. Lichtenfeld, H. Sun, and W. F. Stewart, "The iceberg of health care utilization in women with urinary incontinence," *Int. Urogynecol. J.*, vol. 23, no. 8, pp. 1087–1093, Aug. 2012.

[14]   X. Fritel, N. Varnoux, M. Zins, G. Breart, and V. Ringa, "Symptomatic pelvic organ prolapse at midlife, quality of life, and risk factors.," *Obstet. Gynecol.*, vol. 113, no. 3, pp. 609–16, Mar. 2009.

[15]   J. L. Lowder, C. Ghetti, C. Nikolajski, S. S. Oliphant, and H. M. Zyczynski, "Body image perceptions in women with pelvic organ prolapse: a qualitative study," *Am. J. Obstet.*

Gynecol., vol. 204, no. 5, p. 441.e1-441.e5, May 2011.

[16]   J. E. Jelovsek and M. D. Barber, "Women seeking treatment for advanced pelvic organ prolapse have decreased body image and quality of life," *Am. J. Obstet. Gynecol.*, vol. 194, no. 5, pp. 1455–1461, May 2006.

[17]   J. O. L. DeLancey, R. Kearney, Q. Chou, S. Speights, and S. Binno, "The appearance of levator ani muscle abnormalities in magnetic resonance images after vaginal delivery.," *Obstet. Gynecol.*, vol. 101, no. 1, pp. 46–53, Jan. 2003.

[18]   K. Shek and H. Dietz, "Intrapartum risk factors for levator trauma," *BJOG An Int. J. Obstet. Gynaecol.*, vol. 117, no. 12, pp. 1485–1492, Nov. 2010.

[19]   S. J. Snooks, M. Setchell, M. Swash, and M. M. Henry, "Injury to innervation of pelvic floor sphincter musculature in childbirth.," *Lancet (London, England)*, vol. 2, no. 8402, pp. 546–50, Sep. 1984.

[20]   A. R. Smith, G. L. Hosker, and D. W. Warrell, "The role of partial denervation of the pelvic floor in the aetiology of genitourinary prolapse and stress incontinence of urine. A neurophysiological study.," *Br. J. Obstet. Gynaecol.*, vol. 96, no. 1, pp. 24–8, Jan. 1989.

[21]   B. Chen and J. Yeh, "Alterations in Connective Tissue Metabolism in Stress Incontinence and Prolapse," *J. Urol.*, vol. 186, no. 5, pp. 1768–1772, Nov. 2011.

[22]   J. O. L. DeLancey, "Anatomie aspects of vaginal eversion after hysterectomy," *Am. J. Obstet. Gynecol.*, vol. 166, no. 6, pp. 1717–1728, Jun. 1992.

[23]   D. Knudson, "Introduction to Biomechanics of Human Movement," in *Fundamentals of Biomechanics*, Boston, MA: Springer US, pp. 3–22.

[24]   P. Martins *et al.*, "Biomechanical properties of vaginal tissue in women with pelvic organ prolapse.," *Gynecol. Obstet. Invest.*, vol. 75, no. 2, pp. 85–92, 2013.

[25]   P. A. Moalli *et al.*, "A rat model to study the structural properties of the vagina and its supportive tissues.," *Am. J. Obstet. Gynecol.*, vol. 192, no. 1, pp. 80–8, Jan. 2005.

[26]   J. M. Choe, R. Kothandapani, L. James, and D. Bowling, "Autologous, cadaveric, and synthetic materials used in sling surgery: comparative biomechanical analysis.," *Urology*, vol. 58, no. 3, pp. 482–6, Sep. 2001.

[27]   S. Abramowitch and D. Easley, "Introduction to Classical Mechanics," *Biomech. Female Pelvic Floor*, pp. 89–107, Jan. 2016.

[28]   L. Lei, Y. Song, and R. Chen, "Biomechanical properties of prolapsed vaginal tissue in pre- and postmenopausal women," *Int. Urogynecol. J.*, vol. 18, no. 6, pp. 603–607, Apr. 2007.

[29]   J. A. Kruger, X. Yan, X. Li, P. M. F. Nielsen, and M. P. Nash, "Applications of Pelvic Floor Modeling and Simulation," in *Biomechanics of the Female Pelvic Floor*, Elsevier, 2016, pp. 367–382.

[30]   S. Roman, N. Mangir, J. Bissoli, C. R. Chapple, and S. MacNeil, "Biodegradable scaffolds designed to mimic fascia-like properties for the treatment of pelvic organ prolapse and stress urinary incontinence," *J. Biomater. Appl.*, vol. 30, no. 10, pp. 1578–1588, May 2016.

[31]   S. W. Bai, B. H. Choe, J. Y. Kim, and K. H. Park, "Pelvic organ prolapse and connective tissue abnormalities in Korean women.," *J. Reprod. Med.*, vol. 47, no. 3, pp. 231–4, Mar. 2002.

[32]   M. H. Kerkhof *et al.*, "Changes in tissue composition of the vaginal wall of premenopausal

women with prolapse," *Am. J. Obstet. Gynecol.*, vol. 210, no. 2, p. 168.e1-168.e9, Feb. 2014.

[33]   P. Rocha, M. Parente, T. Mascarenhas, A. Fernandes, and R. N. Jorge, "Effect of surgical mesh implant in the uterine prolapse correction," in *2015 IEEE 4th Portuguese Meeting on Bioengineering (ENBENG)*, 2015, pp. 1–4.

[34]   P. E. Petros and U. I. Ulmsten, "An integral theory of female urinary incontinence. Experimental and clinical considerations.," *Acta Obstet. Gynecol. Scand. Suppl.*, vol. 153, pp. 7–31, 1990.

[35]   P. Petros, "Creating a gold standard surgical device: scientific discoveries leading to TVT and beyond: Ulf Ulmsten Memorial Lecture 2014.," *Int. Urogynecol. J.*, vol. 26, no. 4, pp. 471–6, Apr. 2015.

[36]   J. O. DeLancey, "Structural support of the urethra as it relates to stress urinary incontinence: the hammock hypothesis.," *Am. J. Obstet. Gynecol.*, vol. 170, no. 6, pp. 1713-20; discussion 1720–3, Jun. 1994.

[37]   A. H. Kegel, "PHYSIOLOGIC THERAPY FOR URINARY STRESS INCONTINENCE," *J. Am. Med. Assoc.*, vol. 146, no. 10, p. 915, Jul. 1951.

[38]   F. Burkhard *et al.*, "Urinary Incontinence in Adults EAU Guidelines on."

[39]   K. Bø, B. Kvarstein, and I. Nygaard, "Lower Urinary Tract Symptoms and Pelvic Floor Muscle Exercise Adherence After 15 Years," *Obstet. Gynecol.*, vol. 105, no. 5, Part 1, pp. 999–1005, May 2005.

[40]   J. M. Wu, C. A. Matthews, M. M. Conover, V. Pate, and M. Jonsson Funk, "Lifetime risk of stress urinary incontinence or pelvic organ prolapse surgery.," *Obstet. Gynecol.*, vol. 123, no. 6, pp. 1201–6, Jun. 2014.

[41]   N. A. Black, A. Bowling, J. M. Griffiths, C. Pope, and P. D. Abel, "Impact of surgery for stress incontinence on the social lives of women," *BJOG An Int. J. Obstet. Gynaecol.*, vol. 105, no. 6, pp. 605–612, Jun. 1998.

[42]   M. P. Rutman and J. G. Blaivas, "Surgery for Stress Urinary Incontinence: Historical Review," in *Continence*, London: Springer London, 2009, pp. 117–132.

[43]   H. A. Kelly and W. M. Dumm, "Urinary incontinence in women, without manifest injury to the bladder. 1914.," *Int. Urogynecol. J. Pelvic Floor Dysfunct.*, vol. 9, no. 3, pp. 158–64, 1998.

[44]   E. J. Mcguire and B. Lytton, "Pubovaginal sling procedure for stress incontinence.," *J. Urol.*, vol. 119, no. 1, pp. 82–4, Jan. 1978.

[45]   Y. Barbalat and H. S. G. R. Tunuguntla, "Surgery for Pelvic Organ Prolapse: A Historical Perspective," *Curr. Urol. Rep.*, vol. 13, no. 3, pp. 256–261, Jun. 2012.

[46]   J. MOORE, J. T. ARMSTRONG, and S. H. WILLIS, "The use of tantalum mesh in cystocele with critical report of ten cases.," *Am. J. Obstet. Gynecol.*, vol. 69, no. 5, pp. 1127–35, May 1955.

[47]   S. Ozbek, P. G. Balasubramanian, R. Chiquet-Ehrismann, R. P. Tucker, and J. C. Adams, "The evolution of extracellular matrix.," *Mol. Biol. Cell*, vol. 21, no. 24, pp. 4300–5, Dec. 2010.

[48]   H. Rehman, C. A. Bezerra, H. Bruschini, J. D. Cody, and P. Aluko, "Traditional suburethral sling operations for urinary incontinence in women," *Cochrane Database Syst. Rev.*, vol. 7, p. CD001754, Jul. 2017.

[49]   C. Maher, B. Feiner, K. Baessler, C. Christmann-Schmid, N. Haya, and J. Marjoribanks,

"Transvaginal mesh or grafts compared with native tissue repair for vaginal prolapse," *Cochrane Database Syst. Rev.*, vol. 2, p. CD012079, Feb. 2016.

[50] C. M. Glazener *et al.*, "Mesh, graft, or standard repair for women having primary transvaginal anterior or posterior compartment prolapse surgery: two parallel-group, multicentre, randomised, controlled trials (PROSPECT).," *Lancet (London, England)*, vol. 389, no. 10067, pp. 381–392, Jan. 2017.

[51] M. A. GOLDBERGER and A. M. DAVIDS, "The treatment of urinary stress incontinence by the implantation of a tantalum plate.," *Am. J. Obstet. Gynecol.*, vol. 54, no. 5, pp. 829–37, Nov. 1947.

[52] J. C. Moir, "The gauze-hammock operation. (A modified Aldridge sling procedure).," *J. Obstet. Gynaecol. Br. Commonw.*, vol. 75, no. 1, pp. 1–9, Jan. 1968.

[53] J. E. Morgan, "A sling operation, using Marlex polypropylene mesh, for treatment of recurrent stress incontinence.," *Am. J. Obstet. Gynecol.*, vol. 106, no. 3, pp. 369–77, Feb. 1970.

[54] J. E. Morgan, G. A. Farrow, and F. E. Stewart, "The Marlex sling operation for the treatment of recurrent stress urinary incontinence: a 16-year review.," *Am. J. Obstet. Gynecol.*, vol. 151, no. 2, pp. 224–6, Jan. 1985.

[55] A. A. Ford, L. Rogerson, J. D. Cody, and J. Ogah, "Mid-urethral sling operations for stress urinary incontinence in women.," *Cochrane database Syst. Rev.*, no. 7, p. CD006375, Jul. 2015.

[56] K. L. Ward, P. Hilton, and UK and Ireland TVT Trial Group, "Tension-free vaginal tape versus colposuspension for primary urodynamic stress incontinence: 5-year follow up.," *BJOG*, vol. 115, no. 2, pp. 226–33, Jan. 2008.

[57] A. L. Milani, A. Damoiseaux, J. IntHout, K. B. Kluivers, and M. I. J. Withagen, "Long-term outcome of vaginal mesh or native tissue in recurrent prolapse: a randomized controlled trial.," *Int. Urogynecol. J.*, Nov. 2017.

[58] C. Wang, A. L. Christie, and P. E. Zimmern, "Long-term occurrence of secondary compartment pelvic organ prolapse after open mesh sacrocolpopexy for symptomatic prolapse.," *Neurourol. Urodyn.*, Oct. 2017.

[59] C. Maher, B. Feiner, K. Baessler, E. J. Adams, S. Hagen, and C. M. Glazener, "Surgical management of pelvic organ prolapse in women.," *Cochrane database Syst. Rev.*, no. 4, p. CD004014, Apr. 2010.

[60] G. W. Cundiff *et al.*, "Risk factors for mesh/suture erosion following sacral colpopexy.," *Am. J. Obstet. Gynecol.*, vol. 199, no. 6, p. 688.e1-5, Dec. 2008.

[61] I. Nygaard *et al.*, "Long-term outcomes following abdominal sacrocolpopexy for pelvic organ prolapse.," *JAMA*, vol. 309, no. 19, pp. 2016–24, May 2013.

[62] V. R. Sastri, "Polymer Additives Used to Enhance Material Properties for Medical Device Applications," in *Plastics in Medical Devices : Properties, Requirements, and Applications*, Elsevier, 2013, pp. 55–72.

[63] S. Modjarrad, Kayvon; Ebnesajjad, "Plastics Used in Medical Devices," in *Handbook of Polymer Applications in Medicine and Medical Devices*, Elsevier, 2014, pp. 25–36.

[64] V. R. Sastri, "Regulations for Medical Devices and Application to Plastics Suppliers," in *Handbook of Polymer Applications in Medicine and Medical Devices*, Elsevier, 2010, pp. 337–346.

[65]   V. V. Iakovlev, S. A. Guelcher, and R. Bendavid, "Degradation of polypropylene *in vivo* : A microscopic analysis of meshes explanted from patients," *J. Biomed. Mater. Res. Part B Appl. Biomater.*, vol. 105, no. 2, pp. 237–248, Feb. 2017.

[66]   A. D. Talley, B. R. Rogers, V. Iakovlev, R. F. Dunn, and S. A. Guelcher, "Oxidation and degradation of polypropylene transvaginal mesh," *J. Biomater. Sci. Polym. Ed.*, vol. 28, no. 5, pp. 444–458, Mar. 2017.

[67]   J. R. Fried, *Polymer science and technology*. Prentice Hall, 2014.

[68]   M. Vert, S. M. Li, G. Spenlehauer, and P. Guerin, "Bioresorbability and biocompatibility of aliphatic polyesters," *J. Mater. Sci. Mater. Med.*, vol. 3, no. 6, pp. 432–446, Nov. 1992.

[69]   A. Holmes-Walker, "Materials in a Hostile Environment," in *Life-Enhancing Plastics*, vol. 2, IMPERIAL COLLEGE PRESS, 2004, pp. 61–70.

[70]   T. C. Liebert, R. P. Chartoff, S. L. Cosgrove, and R. S. McCuskey, "Subcutaneous implants of polypropylene filaments.," *J. Biomed. Mater. Res.*, vol. 10, no. 6, pp. 939–51, Nov. 1976.

[71]   A. Imel, T. Malmgren, M. Dadmun, S. Gido, and J. Mays, "In vivo oxidative degradation of polypropylene pelvic mesh," *Biomaterials*, vol. 73, pp. 131–141, Dec. 2015.

[72]   S. Shafaat, N. Mangir, S. R. Regureos, C. R. Chapple, and S. MacNeil, "Demonstration of improved tissue integration and angiogenesis with an elastic, estradiol releasing polyurethane material designed for use in pelvic floor repair," *Neurourol. Urodyn.*, vol. 37, no. 2, 2018.

[73]   B. Röhrnbauer, Y. Ozog, J. Egger, E. Werbrouck, J. Deprest, and E. Mazza, "Combined biaxial and uniaxial mechanical characterization of prosthetic meshes in a rabbit model," *J. Biomech.*, vol. 46, no. 10, pp. 1626–1632, Jun. 2013.

[74]   A. S. Pandit and J. A. Henry, "Design of surgical meshes - an engineering perspective.," *Technol. Health Care*, vol. 12, no. 1, pp. 51–65, 2004.

[75]   V. Czerny, "Beiträge zur operativen Chirurgie," 1878.

[76]   J. T. WOLSTENHOLME, "Use of Commerical Dacron Fabric in the Repair of Inguinal Hernias and Abdominal Wall Defects," *Arch. Surg.*, vol. 73, no. 6, p. 1004, Dec. 1956.

[77]   F. C. USHER, "A new plastic prosthesis for repairing tissue defects of the chest and abdominal wall.," *Am. J. Surg.*, vol. 97, no. 5, pp. 629–33, May 1959.

[78]   F. C. USHER and S. A. WALLACE, "Tissue reaction to plastics; a comparison of nylon, orlon, dacron, teflon, and marlex.," *AMA. Arch. Surg.*, vol. 76, no. 6, pp. 997–9, Jun. 1958.

[79]   F. C. USHER, J. E. ALLEN, R. W. CROSTHWAIT, and J. E. COGAN, "Polypropylene monofilament. A new, biologically inert suture for closing contaminated wounds.," *JAMA*, vol. 179, pp. 780–2, Mar. 1962.

[80]   A. I. Gilbert, M. F. Graham, and J. Young, "Polypropylene:the Standard of Mesh Materials," in *Meshes: Benefits and Risks*, Berlin, Heidelberg: Springer Berlin Heidelberg, 2004, pp. 101–104.

[81]   W. Meyer, "IX. The Implantation of Silver Filigree for the Closure of Large Hernia Apertures.," *Ann. Surg.*, vol. 36, no. 5, pp. 767–78, Nov. 1902.

[82]   P. B. PRICE, "PLASTIC OPERATIONS FOR INCONTINENCE OF URINE AND OF FECES," *Arch. Surg.*, vol. 26, no. 6, p. 1043, Jun. 1933.

[83]   D. . Bloom, G. Uznis, D. Kraklau, and E. . McGuire, "Frederick C. McLellan and Clinical

Cystometrics," *Urology*, vol. 51, no. 1, pp. 168–172, Jan. 1998.

[84]   G. L. Burke, "THE CORROSION OF METALS IN TISSUES; AND AN INTRODUCTION TO TANTALUM.," *Can. Med. Assoc. J.*, vol. 43, no. 2, pp. 125–8, Aug. 1940.

[85]   W. J. Flynn, A. E. Brant, and G. G. Nelson, "A Four and One-Half Year Analysis of Tantalum Gauze Used in the Repair of Ventral Hernia.," *Ann. Surg.*, vol. 134, no. 6, pp. 1027–34, Dec. 1951.

[86]   A. H. Aldridge, "Transplantation of fascia for relief of urinary stress incontinence," *Am. J. Obstet. Gynecol.*, vol. 44, no. 3, pp. 398–411, Sep. 1942.

[87]   F. C. USHER and J. P. GANNON, "Marlex mesh, a new plastic mesh for replacing tissue defects. I. Experimental studies.," *AMA. Arch. Surg.*, vol. 78, no. 1, pp. 131–7, Jan. 1959.

[88]   F. E. LANE, "Repair of posthysterectomy vaginal-vault prolapse.," *Obstet. Gynecol.*, vol. 20, pp. 72–7, Jul. 1962.

[89]   J. P. Chevrel, "[The treatment of large midline incisional hernias by "overcoat" plasty and prothesis (author's transl)].," *Nouv. Presse Med.*, vol. 8, no. 9, pp. 695–6, Feb. 1979.

[90]   R. E. Stoppa, "The treatment of complicated groin and incisional hernias," *World J. Surg.*, vol. 13, no. 5, pp. 545–554, Sep. 1989.

[91]   U. Ulmsten and P. Petros, "Intravaginal slingplasty (IVS): an ambulatory surgical procedure for treatment of female urinary incontinence.," *Scand. J. Urol. Nephrol.*, vol. 29, no. 1, pp. 75–82, Mar. 1995.

[92]   P. K. Amid, "Classification of biomaterials and their related complications in abdominal wall hernia surgery," *Hernia*, vol. 1, no. 1, pp. 15–21, May 1997.

[93]   P. Dällenbach, "To mesh or not to mesh: a review of pelvic organ reconstructive surgery.," *Int. J. Womens. Health*, vol. 7, pp. 331–43, 2015.

[94]   B. Klosterhalfen, U. Klinge, and V. Schumpelick, "Functional and morphological evaluation of different polypropylene-mesh modifications for abdominal wall repair.," *Biomaterials*, vol. 19, no. 24, pp. 2235–46, Dec. 1998.

[95]   S. B. Orenstein, E. R. Saberski, D. L. Kreutzer, and Y. W. Novitsky, "Comparative Analysis of Histopathologic Effects of Synthetic Meshes Based on Material, Weight, and Pore Size in Mice," *J. Surg. Res.*, vol. 176, no. 2, pp. 423–429, Aug. 2012.

[96]   S. Schmidbauer, R. Ladurner, K. K. Hallfeldt, and T. Mussack, "Heavy-weight versus low-weight polypropylene meshes for open sublay mesh repair of incisional hernia.," *Eur. J. Med. Res.*, vol. 10, no. 6, pp. 247–53, Jun. 2005.

[97]   M. Binnebösel *et al.*, "Impact of mesh positioning on foreign body reaction and collagenous ingrowth in a rabbit model of open incisional hernia repair," *Hernia*, vol. 14, no. 1, pp. 71–77, Feb. 2010.

[98]   J. L. Holihan, D. H. Nguyen, M. T. Nguyen, J. Mo, L. S. Kao, and M. K. Liang, "Mesh Location in Open Ventral Hernia Repair: A Systematic Review and Network Meta-analysis," *World J. Surg.*, vol. 40, no. 1, pp. 89–99, Jan. 2016.

[99]   S. Bachman and B. Ramshaw, "Prosthetic material in ventral hernia repair: how do I choose?," *Surg. Clin. North Am.*, vol. 88, no. 1, p. 101–12, ix, Feb. 2008.

[100]   R. de Tayrac, A. Alves, and M. Thérin, "Collagen-coated vs noncoated low-weight

polypropylene meshes in a sheep model for vaginal surgery. A pilot study.," *Int. Urogynecol. J. Pelvic Floor Dysfunct.*, vol. 18, no. 5, pp. 513–20, May 2007.

[101] S. Manodoro *et al.*, "Graft-related complications and biaxial tensiometry following experimental vaginal implantation of flat mesh of variable dimensions," *BJOG An Int. J. Obstet. Gynaecol.*, vol. 120, no. 2, pp. 244–250, Jan. 2013.

[102] D. R. Ostergard, "Polypropylene vaginal mesh grafts in gynecology.," *Obstet. Gynecol.*, vol. 116, no. 4, pp. 962–6, Oct. 2010.

[103] S. Todros, P. G. Pavan, and A. N. Natali, "Biomechanical properties of synthetic surgical meshes for pelvic prolapse repair," *J. Mech. Behav. Biomed. Mater.*, vol. 55, pp. 271–285, Mar. 2016.

[104] A. Feola *et al.*, "Deterioration in biomechanical properties of the vagina following implantation of a high-stiffness prolapse mesh.," *BJOG*, vol. 120, no. 2, pp. 224–232, Jan. 2013.

[105] A. Feola, S. Pal, P. Moalli, S. Maiti, and S. Abramowitch, "Varying degrees of nonlinear mechanical behavior arising from geometric differences of urogynecological meshes.," *J. Biomech.*, vol. 47, no. 11, pp. 2584–9, Aug. 2014.

[106] D. M. Faulk *et al.*, "ECM hydrogel coating mitigates the chronic inflammatory response to polypropylene mesh.," *Biomaterials*, vol. 35, no. 30, pp. 8585–95, Oct. 2014.

[107] A. L. Milani, W. M. Heidema, W. S. van der Vloedt, K. B. Kluivers, M. I. J. Withagen, and M. E. Vierhout, "Vaginal prolapse repair surgery augmented by ultra lightweight titanium coated polypropylene mesh.," *Eur. J. Obstet. Gynecol. Reprod. Biol.*, vol. 138, no. 2, pp. 232–8, Jun. 2008.

[108] D. Wood and J. Southgate, "Current status of tissue engineering in urology," *Curr. Opin. Urol.*, vol. 18, no. 6, pp. 564–569, Nov. 2008.

[109] M.-J. Hung, M.-C. Wen, Y.-T. Huang, G.-D. Chen, M.-M. Chou, and V. C. Yang, "Fascia tissue engineering with human adipose-derived stem cells in a murine model: Implications for pelvic floor reconstruction," *J. Formos. Med. Assoc.*, vol. 113, no. 10, pp. 704–715, Oct. 2014.

[110] Q. Li, J. Wang, H. Liu, B. Xie, and L. Wei, "Tissue-engineered mesh for pelvic floor reconstruction fabricated from silk fibroin scaffold with adipose-derived mesenchymal stem cells," *Cell Tissue Res.*, vol. 354, no. 2, pp. 471–480, Nov. 2013.

[111] D. Ulrich *et al.*, "Human endometrial mesenchymal stem cells modulate the tissue response and mechanical behavior of polyamide mesh implants for pelvic organ prolapse repair.," *Tissue Eng. Part A*, vol. 20, no. 3–4, pp. 785–98, Feb. 2014.

[112] S. Fredenberg, M. Wahlgren, M. Reslow, and A. Axelsson, "The mechanisms of drug release in poly(lactic-co-glycolic acid)-based drug delivery systems—A review," *Int. J. Pharm.*, vol. 415, no. 1–2, pp. 34–52, Aug. 2011.

[113] C. J. Hillary, S. Roman, A. J. Bullock, N. H. Green, C. R. Chapple, and S. MacNeil, "Developing Repair Materials for Stress Urinary Incontinence to Withstand Dynamic Distension," *PLoS One*, vol. 11, no. 3, p. e0149971, Mar. 2016.

[114] L. Hympánová *et al.*, "Assessment of Electrospun and Ultra-lightweight Polypropylene Meshes in the Sheep Model for Vaginal Surgery," *Eur. Urol. Focus*, Jul. 2018.

[115] F. J. Bye *et al.*, "Development of bilayer and trilayer nanofibrous/microfibrous scaffolds for

regenerative medicine," *Biomater. Sci.*, vol. 1, no. 9, p. 942, Jul. 2013.

[116]   S. Roman, A. Mangera, N. I. Osman, A. J. Bullock, C. R. Chapple, and S. MacNeil, "Developing a tissue engineered repair material for treatment of stress urinary incontinence and pelvic organ prolapse-which cell source?," *Neurourol. Urodyn.*, vol. 33, no. 5, pp. 531–537, Jun. 2014.

[117]   S. Roman Regueros *et al.*, "Acute *In Vivo* Response to an Alternative Implant for Urogynecology," *Biomed Res. Int.*, vol. 2014, pp. 1–10, 2014.

[118]   B. D. Ulery, L. S. Nair, and C. T. Laurencin, "Biomedical applications of biodegradable polymers," *J. Polym. Sci. Part B Polym. Phys.*, vol. 49, no. 12, pp. 832–864, Jun. 2011.

[119]   D. F. (David F. Williams, *The Williams dictionary of biomaterials*. Liverpool University Press, 1999.

[120]   B. D. Ratner, "Healing with medical implants: The body battles back," *Sci. Transl. Med.*, vol. 7, no. 272, p. 272fs4-272fs4, Jan. 2015.

[121]   B. D. Ratner, "The Biocompatibility Manifesto: Biocompatibility for the Twenty-first Century," *J. Cardiovasc. Transl. Res.*, vol. 4, no. 5, pp. 523–527, Oct. 2011.

[122]   B. D. Ratner, "A pore way to heal and regenerate: 21st century thinking on biocompatibility.," *Regen. Biomater.*, vol. 3, no. 2, pp. 107–10, Jun. 2016.

[123]   J. Rouwkema, N. C. Rivron, and C. A. van Blitterswijk, "Vascularization in tissue engineering," *Trends Biotechnol.*, vol. 26, no. 8, pp. 434–441, Aug. 2008.

[124]   J. P. Semmens and G. Wagner, "Estrogen deprivation and vaginal function in postmenopausal women.," *JAMA*, vol. 248, no. 4, pp. 445–8, Jul. 1982.

[125]   C. R. Chapple *et al.*, "Consensus Statement of the European Urology Association and the European Urogynaecological Association on the Use of Implanted Materials for Treating Pelvic Organ Prolapse and Stress Urinary Incontinence," *Eur. Urol.*, vol. 72, no. 3, pp. 424–431, Sep. 2017.

[126]   H. Naderi, M. M. Matin, and A. R. Bahrami, "Review paper: Critical Issues in Tissue Engineering: Biomaterials, Cell Sources, Angiogenesis, and Drug Delivery Systems," *J. Biomater. Appl.*, vol. 26, no. 4, pp. 383–417, Nov. 2011.

[127]   N. Mangır, A. J. Bullock, S. Roman, N. Osman, C. Chapple, and S. MacNeil, "Production of ascorbic acid releasing biomaterials for pelvic floor repair," *Acta Biomater.*, vol. 29, pp. 188–197, Jan. 2016.

[128]   T. Z. Liu, N. Chin, M. D. Kiser, and W. N. Bigler, "Specific spectrophotometry of ascorbic acid in serum or plasma by use of ascorbate oxidase.," *Clin. Chem.*, vol. 28, no. 11, pp. 2225–8, Nov. 1982.

[129]   I. F. Benzie, "An automated, specific, spectrophotometric method for measuring ascorbic acid in plasma (EFTSA).," *Clin. Biochem.*, vol. 29, no. 2, pp. 111–6, Apr. 1996.

[130]   T. A. Bensinger *et al.*, "An Enzymatic Method for Measurement of Ascorbate-2-Phosphate."

[131]   R. F. Nicosia and A. Ottinetti, "Modulation of microvascular growth and morphogenesis by reconstituted basement membrane gel in three-dimensional cultures of rat aorta: a comparative study of angiogenesis in matrigel, collagen, fibrin, and plasma clot.," *In Vitro Cell. Dev. Biol.*, vol. 26, no. 2, pp. 119–28, Feb. 1990.

[132] R. F. Nicosia, "The aortic ring model of angiogenesis: a quarter century of search and discovery," *J. Cell. Mol. Med.*, vol. 13, no. 10, pp. 4113–4136, Oct. 2009.

[133] M. Baker *et al.*, "Use of the mouse aortic ring assay to study angiogenesis," *Nat. Protoc.*, vol. 7, no. 1, pp. 89–104, Jan. 2012.

[134] W. Song *et al.*, "The fetal mouse metatarsal bone explant as a model of angiogenesis," *Nat. Protoc.*, vol. 10, no. 10, pp. 1459–1473, Sep. 2015.

[135] D. Ribatti, "The chick embryo chorioallantoic membrane (CAM). A multifaceted experimental model," *Mech. Dev.*, vol. 141, pp. 70–77, Aug. 2016.

[136] J. Folkman, "Tumor angiogenesis: therapeutic implications.," *N. Engl. J. Med.*, vol. 285, no. 21, pp. 1182–6, Nov. 1971.

[137] I. Moreno-Jiménez *et al.*, "The chorioallantoic membrane (CAM) assay for the study of human bone regeneration: a refinement animal model for tissue engineering," *Sci. Rep.*, vol. 6, no. 1, p. 32168, Oct. 2016.

[138] N. Mangır, C. J. Hillary, C. R. Chapple, and S. MacNeil, "Oestradiol-releasing Biodegradable Mesh Stimulates Collagen Production and Angiogenesis: An Approach to Improving Biomaterial Integration in Pelvic Floor Repair," *Eur. Urol. Focus*, Jun. 2017.

[139] N. A. Lokman, A. S. F. Elder, C. Ricciardelli, and M. K. Oehler, "Chick chorioallantoic membrane (CAM) assay as an in vivo model to study the effect of newly identified molecules on ovarian cancer invasion and metastasis.," *Int. J. Mol. Sci.*, vol. 13, no. 8, pp. 9959–70, Aug. 2012.

[140] G. Eke, N. Mangir, N. Hasirci, S. MacNeil, and V. Hasirci, "Development of a UV crosslinked biodegradable hydrogel containing adipose derived stem cells to promote vascularization for skin wounds and tissue engineering.," *Biomaterials*, vol. 129, pp. 188–198, Jun. 2017.

[141] N. Mangir, A. Raza, J. W. Haycock, C. Chapple, and S. Macneil, "An improved in vivo methodology to visualise tumour induced changes in vasculature using the chick chorionic allantoic membrane assay," *In Vivo (Brooklyn).*, vol. 32, no. 3, 2018.

[142] I. Moreno-Jiménez, J. M. Kanczler, G. Hulsart-Billstrom, S. Inglis, and R. O. C. Oreffo, "* The Chorioallantoic Membrane Assay for Biomaterial Testing in Tissue Engineering: A Short-Term In Vivo Preclinical Model.," *Tissue Eng. Part C. Methods*, vol. 23, no. 12, pp. 938–952, 2017.

[143] G. Gigliobianco, C. K. Chong, and S. MacNeil, "Simple surface coating of electrospun poly-L-lactic acid scaffolds to induce angiogenesis," *J. Biomater. Appl.*, vol. 30, no. 1, pp. 50–60, Jul. 2015.

[144] R. L. Barnhill and T. J. Ryan, "Biochemical modulation of angiogenesis in the chorioallantoic membrane of the chick embryo.," *J. Invest. Dermatol.*, vol. 81, no. 6, pp. 485–8, Dec. 1983.

[145] T. I. Valdes, D. Kreutzer, and F. Moussy, "The chick chorioallantoic membrane as a novel in vivo model for the testing of biomaterials," *J. Biomed. Mater. Res.*, vol. 62, no. 2, pp. 273–282, Nov. 2002.

[146] S. Haller, S. M. Ametamey, R. Schibli, and C. Müller, "Investigation of the chick embryo as a potential alternative to the mouse for evaluation of radiopharmaceuticals," *Nucl. Med. Biol.*, vol. 42, no. 3, pp. 226–233, Mar. 2015.

[147] E. M. Janse and S. H. Jeurissen, "Ontogeny and function of two non-lymphoid cell populations in the chicken embryo.," *Immunobiology*, vol. 182, no. 5, pp. 472–81, Aug. 1991.

[148] J. V. Friend, R. W. R. Crevel, T. C. Williams, and W. E. Parish, "Immaturity of the inflammatory response of the chick chorioallantoic membrane," *Toxicol. Vitr.*, vol. 4, no. 4–5, pp. 324–326, Jan. 1990.

[149] S. Michael, H. Sorg, C.-T. Peck, K. Reimers, and P. M. Vogt, "The mouse dorsal skin fold chamber as a means for the analysis of tissue engineered skin," *Burns*, vol. 39, no. 1, pp. 82–88, Feb. 2013.

[150] A. M. Weber *et al.*, "Basic science and translational research in female pelvic floor disorders: Proceedings of an NIH-sponsored meeting," *Neurourol. Urodyn.*, vol. 23, no. 4, pp. 288–301, 2004.

[151] E. G. Canty and K. E. Kadler, "Procollagen trafficking, processing and fibrillogenesis," *J. Cell Sci.*, vol. 118, no. 7, pp. 1341–1353, Apr. 2005.

[152] O. Kavitha and R. V. Thampan, "Factors influencing collagen biosynthesis," *J. Cell. Biochem.*, vol. 104, no. 4, pp. 1150–1160, Jul. 2008.

[153] C. Falconer *et al.*, "Different organization of collagen fibrils in stress-incontinent women of fertile age.," *Acta Obstet. Gynecol. Scand.*, vol. 77, no. 1, pp. 87–94, Jan. 1998.

[154] C. Goepel, L. Hefler, H.-D. Methfessel, and H. Koelbl, "Periurethral connective tissue status of postmenopausal women with genital prolapse with and without stress incontinence.," *Acta Obstet. Gynecol. Scand.*, vol. 82, no. 7, pp. 659–64, Jul. 2003.

[155] B. Chen, Y. Wen, H. Wang, and M. L. Polan, "Differences in estrogen modulation of tissue inhibitor of matrix metalloproteinase-1 and matrix metalloproteinase-1 expression in cultured fibroblasts from continent and incontinent women.," *Am. J. Obstet. Gynecol.*, vol. 189, no. 1, pp. 59–65, Jul. 2003.

[156] E. Knuuti, S. Kauppila, V. Kotila, J. Risteli, and R. Nissi, "Genitourinary prolapse and joint hypermobility are associated with altered type I and III collagen metabolism," *Arch. Gynecol. Obstet.*, vol. 283, no. 5, pp. 1081–1085, May 2011.

[157] D. J. Prockop and K. I. Kivirikko, "Collagens: Molecular Biology, Diseases, and Potentials for Therapy," *Annu. Rev. Biochem.*, vol. 64, no. 1, pp. 403–434, Jun. 1995.

[158] K. P. Houglum, D. A. Brenner, and M. Chojkier, "Ascorbic acid stimulation of collagen biosynthesis independent of hydroxylation," *Am. J. Clin. Nutr.*, vol. 54, no. 6, p. 1141S–1143S, Dec. 1991.

[159] S. Kurata, H. Senoo, and R. Hata, "Transcriptional activation of type I collagen genes by ascorbic acid 2-phosphate in human skin fibroblasts and its failure in cells from a patient with alpha 2(I)-chain-defective Ehlers-Danlos syndrome.," *Exp. Cell Res.*, vol. 206, no. 1, pp. 63–71, May 1993.

[160] Y. Kishimoto, N. Saito, K. Kurita, K. Shimokado, N. Maruyama, and A. Ishigami, "Ascorbic acid enhances the expression of type 1 and type 4 collagen and SVCT2 in cultured human skin fibroblasts," *Biochem. Biophys. Res. Commun.*, vol. 430, no. 2, pp. 579–584, Jan. 2013.

[161] V. Ivanov, S. V Ivanova, and A. Niedzwiecki, "Ascorbate Affects Proliferation of Guinea-pig Vascular Smooth Muscle Cells by Direct and Extracellular Matrix-mediated Effects," *J. Mol. Cell. Cardiol.*, vol. 29, no. 12, pp. 3293–3303, Dec. 1997.

[162] N. Utoguchi *et al.*, "Ascorbic acid stimulates barrier function of cultured endothelial cell monolayer," *J. Cell. Physiol.*, vol. 163, no. 2, pp. 393–399, May 1995.

[163] H. Ashino *et al.*, "Novel Function of Ascorbic Acid as an Angiostatic Factor," *Angiogenesis*, vol. 6, no. 4, pp. 259–269, 2003.

[164] U. Stumpf *et al.*, "Selection of proangiogenic ascorbate derivatives and their exploitation in a novel drug-releasing system for wound healing," *Wound Repair Regen.*, vol. 19, no. 5, pp. 597–607, Sep. 2011.

[165] R. B. Findik, F. İlkaya, S. Guresci, H. Guzel, S. Karabulut, and J. Karakaya, "Effect of vitamin C on collagen structure of cardinal and uterosacral ligaments during pregnancy," *Eur. J. Obstet. Gynecol. Reprod. Biol.*, vol. 201, pp. 31–35, Jun. 2016.

[166] M. V. Estanol, C. C. Crisp, S. H. Oakley, S. D. Kleeman, A. N. Fellner, and R. N. Pauls, "Systemic markers of collagen metabolism and vitamin C in smokers and non-smokers with pelvic organ prolapse," *Eur. J. Obstet. Gynecol. Reprod. Biol.*, vol. 184, pp. 58–64, Jan. 2015.

[167] N. N. Maserejian, E. L. Giovannucci, K. T. McVary, and J. B. McKinlay, "Intakes of Vitamins and Minerals in Relation to Urinary Incontinence, Voiding, and Storage Symptoms in Women: A Cross-Sectional Analysis from the Boston Area Community Health Survey," *Eur. Urol.*, vol. 59, no. 6, pp. 1039–1047, Jun. 2011.

[168] C. J. Bates and C. I. Levene, "Growth and macromolecular synthesis in the 3T6 mouse fibroblast. II. The role of serum.," *J. Cell Sci.*, vol. 7, no. 3, pp. 683–93, Nov. 1970.

[169] J. Du, J. J. Cullen, and G. R. Buettner, "Ascorbic acid: Chemistry, biology and the treatment of cancer," *Biochim. Biophys. Acta - Rev. Cancer*, vol. 1826, no. 2, pp. 443–457, Dec. 2012.

[170] R.-I. Hata and H. Senoo, "L-ascorbic acid 2-phosphate stimulates collagen accumulation, cell proliferation, and formation of a three-dimensional tissuelike substance by skin fibroblasts," *J. Cell. Physiol.*, vol. 138, no. 1, pp. 8–16, Jan. 1989.

[171] O. Ishikawa, A. Kondo, K. Okada, Y. Miyachi, and M. Furumura, "Morphological and biochemical analyses on fibroblasts and self-produced collagens in a novel three-dimensional culture.," *Br. J. Dermatol.*, vol. 136, no. 1, pp. 6–11, Jan. 1997.

[172] S. Murad, S. Tajima, G. R. Johnson, S. Sivarajah, and S. R. Pinnell, "Collagen synthesis in cultured human skin fibroblasts: effect of ascorbic acid and its analogs.," *J. Invest. Dermatol.*, vol. 81, no. 2, pp. 158–62, Aug. 1983.

[173] A. G. Clark, A. L. Rohrbaugh, I. Otterness, and V. B. Kraus, "The effects of ascorbic acid on cartilage metabolism in guinea pig articular cartilage explants.," *Matrix Biol.*, vol. 21, no. 2, pp. 175–84, Mar. 2002.

[174] H. Kim, H. W. Kim, and H. Suh, "Sustained release of ascorbate-2-phosphate and dexamethasone from porous PLGA scaffolds for bone tissue engineering using mesenchymal stem cells," *Biomaterials*, vol. 24, no. 25, pp. 4671–4679, Nov. 2003.

[175] T. J. Sill and H. A. von Recum, "Electrospinning: Applications in drug delivery and tissue engineering," *Biomaterials*, vol. 29, no. 13, pp. 1989–2006, May 2008.

[176] S. Sinha-Ray, D. D. Pelot, Z. P. Zhou, A. Rahman, X.-F. Wu, and A. L. Yarin, "Encapsulation of self-healing materials by coelectrospinning, emulsion electrospinning, solution blowing and intercalation," *J. Mater. Chem.*, vol. 22, no. 18, p. 9138, Apr. 2012.

[177] L. Tian, M. P. Prabhakaran, X. Ding, D. Kai, and S. Ramakrishna, "Emulsion electrospun nanofibers as substrates for cardiomyogenic differentiation of mesenchymal stem cells," *J. Mater. Sci. Mater. Med.*, vol. 24, no. 11, pp. 2577–2587, Nov. 2013.

[178] Y. Liao, L. Zhang, Y. Gao, Z.-T. Zhu, and H. Fong, "Preparation, characterization, and encapsulation/release studies of a composite nanofiber mat electrospun from an emulsion containing poly(lactic-co-glycolic acid)," *Polymer (Guildf).*, vol. 49, no. 24, pp. 5294–5299, Nov. 2008.

[179] X. Li, Y. Su, S. Liu, L. Tan, X. Mo, and S. Ramakrishna, "Encapsulation of proteins in poly(l-lactide-co-caprolactone) fibers by emulsion electrospinning," *Colloids Surfaces B Biointerfaces*, vol. 75, no. 2, pp. 418–424, Feb. 2010.

[180] N. Nikmaram *et al.*, "Emulsion-based systems for fabrication of electrospun nanofibers: food, pharmaceutical and biomedical applications," *RSC Adv.*, vol. 7, no. 46, pp. 28951–28964, Jun. 2017.

[181] J. Hu, M. P. Prabhakaran, X. Ding, and S. Ramakrishna, "Emulsion electrospinning of polycaprolactone: influence of surfactant type towards the scaffold properties," *J. Biomater. Sci. Polym. Ed.*, vol. 26, no. 1, pp. 57–75, Jan. 2015.

[182] J. Wang and M. Windbergs, "Controlled dual drug release by coaxial electrospun fibers – Impact of the core fluid on drug encapsulation and release," *Int. J. Pharm.*, vol. 556, pp. 363–371, Feb. 2019.

[183] H. Zhang *et al.*, "Dual-delivery of VEGF and PDGF by double-layered electrospun membranes for blood vessel regeneration," *Biomaterials*, vol. 34, no. 9, pp. 2202–2212, Mar. 2013.

[184] R. Qi *et al.*, "Electrospun poly(lactic-co-glycolic acid)/halloysite nanotube composite nanofibers for drug encapsulation and sustained release," *J. Mater. Chem.*, vol. 20, no. 47, p. 10622, Nov. 2010.

[185] W. Xu, A. Atala, J. J. Yoo, and S. J. Lee, "Controllable dual protein delivery through electrospun fibrous scaffolds with different hydrophilicities," *Biomed. Mater.*, vol. 8, no. 1, p. 014104, Jan. 2013.

[186] Y. Wang *et al.*, "A novel multiple drug release system in vitro based on adjusting swelling core of emulsion electrospun nanofibers with core–sheath structure," *Mater. Sci. Eng. C*, vol. 44, pp. 109–116, Nov. 2014.

[187] X. XU, X. CHEN, P. MA, X. WANG, and X. JING, "The release behavior of doxorubicin hydrochloride from medicated fibers prepared by emulsion-electrospinning," *Eur. J. Pharm. Biopharm.*, vol. 70, no. 1, pp. 165–170, Sep. 2008.

[188] W. L. Miller and R. J. Auchus, "The Molecular Biology, Biochemistry, and Physiology of Human Steroidogenesis and Its Disorders," *Endocr. Rev.*, vol. 32, no. 1, pp. 81–151, Feb. 2011.

[189] E. . Simpson, "Sources of estrogen and their importance," *J. Steroid Biochem. Mol. Biol.*, vol. 86, no. 3–5, pp. 225–230, Sep. 2003.

[190] H.-R. Lee, T.-H. Kim, and K.-C. Choi, "Functions and physiological roles of two types of estrogen receptors, ERα and ERβ, identified by estrogen receptor knockout mouse.," *Lab. Anim. Res.*, vol. 28, no. 2, pp. 71–6, Jun. 2012.

[191] D. J. Chung and S. W. Bai, "Roles of sex steroid receptors and cell cycle regulation in pathogenesis of pelvic organ prolapse," *Curr. Opin. Obstet. Gynecol.*, vol. 18, no. 5, pp. 551–554, Oct. 2006.

[192] W. Zong, H. M. Zyczynski, L. A. Meyn, S. C. Gordy, and P. A. Moalli, "Regulation of MMP-1 by sex steroid hormones in fibroblasts derived from the female pelvic floor," *Am. J. Obstet. Gynecol.*, vol. 196, no. 4, p. 349.e1-349.e11, Apr. 2007.

[193] S. R. Jackson, N. C. Avery, J. F. Tarlton, S. D. Eckford, P. Abrams, and A. J. Bailey, "Changes in metabolism of collagen in genitourinary prolapse.," *Lancet (London, England)*, vol. 347, no. 9016, pp. 1658–61, Jun. 1996.

[194] Y. J. Moon, S. W. Bai, C.-Y. Jung, and C. H. Kim, "Estrogen-related genome-based expression profiling study of uterosacral ligaments in women with pelvic organ prolapse," *Int. Urogynecol. J.*, vol. 24, no. 11, pp. 1961–1967, Nov. 2013.

[195] D. W. Losordo and J. M. Isner, "Estrogen and angiogenesis: A review.," *Arterioscler. Thromb. Vasc. Biol.*, vol. 21, no. 1, pp. 6–12, Jan. 2001.

[196] M. A. Weber, D. M. J. Milstein, C. Ince, and J. P. W. R. Roovers, "Is pelvic organ prolapse associated with altered microcirculation of the vaginal wall?," *Neurourol. Urodyn.*, vol. 35, no. 7, pp. 764–70, Sep. 2016.

[197] M. A. Weber, M. M. E. Lakeman, E. Laan, and J. W. R. Roovers, "The Effects of Vaginal Prolapse Surgery Using Synthetic Mesh on Vaginal Wall Sensibility, Vaginal Vasocongestion, and Sexual Function: A Prospective Single-Center Study," *J. Sex. Med.*, vol. 11, no. 7, pp. 1848–1855, Jul. 2014.

[198] M. Brincat, C. F. Moniz, J. W. Studd, A. J. Darby, A. Magos, and D. Cooper, "Sex hormones and skin collagen content in postmenopausal women.," *Br. Med. J. (Clin. Res. Ed).*, vol. 287, no. 6402, pp. 1337–8, Nov. 1983.

[199] J. Simon, L. Nachtigall, R. Gut, E. Lang, D. F. Archer, and W. Utian, "Effective Treatment of Vaginal Atrophy With an Ultra–Low-Dose Estradiol Vaginal Tablet," *Obstet. Gynecol.*, vol. 112, no. 5, pp. 1053–1060, Nov. 2008.

[200] A. L. Clark, O. D. Slayden, K. Hettrich, and R. M. Brenner, "Estrogen increases collagen I and III mRNA expression in the pelvic support tissues of the rhesus macaque," *Am. J. Obstet. Gynecol.*, vol. 192, no. 5, pp. 1523–1529, May 2005.

[201] T. I. Montoya, P. A. Maldonado, J. F. Acevedo, and R. A. Word, "Effect of vaginal or systemic estrogen on dynamics of collagen assembly in the rat vaginal wall.," *Biol. Reprod.*, vol. 92, no. 2, p. 43, Feb. 2015.

[202] M. A. Weber, M. H. Kleijn, M. Langendam, J. Limpens, M. J. Heineman, and J. P. Roovers, "Local Oestrogen for Pelvic Floor Disorders: A Systematic Review.," *PLoS One*, vol. 10, no. 9, p. e0136265, 2015.

[203] S. I. Ismail, C. Bain, and S. Hagen, "Oestrogens for treatment or prevention of pelvic organ prolapse in postmenopausal women," *Cochrane Database Syst. Rev.*, no. 9, p. CD007063, Sep. 2010.

[204] J. D. Cody, M. L. Jacobs, K. Richardson, B. Moehrer, and A. Hextall, "Oestrogen therapy for urinary incontinence in post-menopausal women," *Cochrane Database Syst. Rev.*, vol. 10, p. CD001405, Oct. 2012.

[205] P. J. Oviedo *et al.*, "Estradiol induces endothelial cell migration and proliferation through estrogen receptor-enhanced RhoA/ROCK pathway," *Mol. Cell. Endocrinol.*, vol. 335, no. 2, pp. 96–103, Mar. 2011.

[206] C. Filipe *et al.*, "Estradiol accelerates endothelial healing through the retrograde commitment of uninjured endothelium," *Am. J. Physiol. Circ. Physiol.*, vol. 294, no. 6, pp. H2822–H2830, Jun. 2008.

[207] H. W. Schnaper, K. A. McGowan, S. Kim-Schulze, and M. C. Cid, "Oestrogen and endothelial

cell angiogenic activity.," *Clin. Exp. Pharmacol. Physiol.*, vol. 23, no. 3, pp. 247–50, Mar. 1996.

[208]   G. M. Rubanyi, A. Johns, and K. Kauser, "Effect of estrogen on endothelial function and angiogenesis.," *Vascul. Pharmacol.*, vol. 38, no. 2, pp. 89–98, Feb. 2002.

[209]   M. D. Mueller, J. L. Vigne, A. Minchenko, D. I. Lebovic, D. C. Leitman, and R. N. Taylor, "Regulation of vascular endothelial growth factor (VEGF) gene transcription by estrogen receptors alpha and beta.," *Proc. Natl. Acad. Sci. U. S. A.*, vol. 97, no. 20, pp. 10972–7, Sep. 2000.

[210]   D. A. Redmer, A. T. Grazul, J. D. Kirsch, and L. P. Reynolds, "Angiogenic activity of bovine corpora lutea at several stages of luteal development.," *J. Reprod. Fertil.*, vol. 82, no. 2, pp. 627–34, Mar. 1988.

[211]   S. Mitsos *et al.*, "Therapeutic angiogenesis for myocardial ischemia revisited: basic biological concepts and focus on latest clinical trials," *Angiogenesis*, vol. 15, no. 1, pp. 1–22, Mar. 2012.

[212]   D. D. Rahn *et al.*, "Vaginal estrogen use in postmenopausal women with pelvic floor disorders: systematic review and practice guidelines," *Int. Urogynecol. J.*, vol. 26, no. 1, pp. 3–13, Jan. 2015.

[213]   J. C. Beldekas, B. Smith, L. C. Gerstenfeld, G. E. Sonenshein, and C. Franzblau, "Effects of 17 beta-estradiol on the biosynthesis of collagen in cultured bovine aortic smooth muscle cells.," *Biochemistry*, vol. 20, no. 8, pp. 2162–7, Apr. 1981.

[214]   G. Kwan *et al.*, "Effects of sex hormones on mesangial cell proliferation and collagen synthesis," *Kidney Int.*, vol. 50, no. 4, pp. 1173–1179, Oct. 1996.

[215]   P. S. Cooke, M. K. Nanjappa, C. Ko, G. S. Prins, and R. A. Hess, "Estrogens in Male Physiology," *Physiol. Rev.*, vol. 97, no. 3, pp. 995–1043, Jul. 2017.

[216]   D. E. Morales *et al.*, "Estrogen promotes angiogenic activity in human umbilical vein endothelial cells in vitro and in a murine model.," *Circulation*, vol. 91, no. 3, pp. 755–63, Feb. 1995.

[217]   P. Concina *et al.*, "The Mitogenic Effect of 17β-Estradiol on in vitro Endothelial Cell Proliferation and on in vivo Reendothelialization Are Both Dependent on Vascular Endothelial Growth Factor," *J. Vasc. Res.*, vol. 37, no. 3, pp. 202–208, 2000.

[218]   H. Liu *et al.*, "17β-Estradiol Promotes Angiogenesis of Rat Cardiac Microvascular Endothelial Cells In Vitro.," *Med. Sci. Monit.*, vol. 24, pp. 2489–2496, Apr. 2018.

[219]   G. E. Milo, W. B. Malarkey, J. E. Powell, J. R. Blakeslee, and D. S. Yohn, "Effects of steroid hormones in fetal bovine serum on plating ang cloning of human cells in vitro.," *In Vitro*, vol. 12, no. 1, pp. 23–30, Jan. 1976.

[220]   M. A. Weber, D. M. J. Milstein, C. Ince, K. O. Rengerink, and J.-P. W. R. Roovers, "Vaginal microcirculation: Non-invasive anatomical examination of the micro-vessel architecture, tortuosity and capillary density," *Neurourol. Urodyn.*, vol. 34, no. 8, pp. 723–729, Nov. 2015.

[221]   A. V Emmanuel, M. A. Kamm, and R. W. Beard, "Reproducible assessment of vaginal and rectal mucosal and skin blood flow: laser doppler fluximetry of the pelvic microcirculation.," *Clin. Sci. (Lond).*, vol. 98, no. 2, pp. 201–7, Feb. 2000.

[222]   A. R. Unnithan *et al.*, "Electrospun polyurethane-dextran nanofiber mats loaded with Estradiol for post-menopausal wound dressing," *Int. J. Biol. Macromol.*, vol. 77, pp. 1–8, Jun. 2015.

[223] J. P. Shepherd, A. J. Feola, S. D. Abramowitch, and P. A. Moalli, "Uniaxial biomechanical properties of seven different vaginally implanted meshes for pelvic organ prolapse," *Int. Urogynecol. J.*, vol. 23, no. 5, pp. 613–620, May 2012.

[224] M. Dominici *et al.*, "Minimal criteria for defining multipotent mesenchymal stromal cells. The International Society for Cellular Therapy position statement," *Cytotherapy*, vol. 8, no. 4, pp. 315–317, 2006.

[225] P. Bianco *et al.*, "The meaning, the sense and the significance: translating the science of mesenchymal stem cells into medicine," *Nat. Med.*, vol. 19, no. 1, pp. 35–42, Jan. 2013.

[226] X. Liang, Y. Ding, Y. Zhang, H.-F. Tse, and Q. Lian, "Paracrine Mechanisms of Mesenchymal Stem Cell-Based Therapy: Current Status and Perspectives," *Cell Transplant.*, vol. 23, no. 9, pp. 1045–1059, Sep. 2014.

[227] H. K. Salem and C. Thiemermann, "Mesenchymal Stromal Cells: Current Understanding and Clinical Status," *Stem Cells*, vol. 28, no. 3, p. N/A-N/A, Mar. 2009.

[228] P. M. Murphy *et al.*, "International union of pharmacology. XXII. Nomenclature for chemokine receptors.," *Pharmacol. Rev.*, vol. 52, no. 1, pp. 145–76, Mar. 2000.

[229] E. Spaeth, A. Klopp, J. Dembinski, M. Andreeff, and F. Marini, "Inflammation and tumor microenvironments: defining the migratory itinerary of mesenchymal stem cells," *Gene Ther.*, vol. 15, no. 10, pp. 730–738, May 2008.

[230] J. F. Ji, B. P. He, S. T. Dheen, and S. S. W. Tay, "Interactions of Chemokines and Chemokine Receptors Mediate the Migration of Mesenchymal Stem Cells to the Impaired Site in the Brain After Hypoglossal Nerve Injury," *Stem Cells*, vol. 22, no. 3, pp. 415–427, May 2004.

[231] J. D. Abbott, Y. Huang, D. Liu, R. Hickey, D. S. Krause, and F. J. Giordano, "Stromal Cell–Derived Factor-1α Plays a Critical Role in Stem Cell Recruitment to the Heart After Myocardial Infarction but Is Not Sufficient to Induce Homing in the Absence of Injury," *Circulation*, vol. 110, no. 21, pp. 3300–3305, Nov. 2004.

[232] Y. Li, X. Yu, S. Lin, X. Li, S. Zhang, and Y.-H. Song, "Insulin-like growth factor 1 enhances the migratory capacity of mesenchymal stem cells," *Biochem. Biophys. Res. Commun.*, vol. 356, no. 3, pp. 780–784, May 2007.

[233] S. J. Baek, S. K. Kang, and J. C. Ra, "*In vitro* migration capacity of human adipose tissue-derived mesenchymal stem cells reflects their expression of receptors for chemokines and growth factors," *Exp. Mol. Med.*, vol. 43, no. 10, p. 596, Oct. 2011.

[234] M. Shi *et al.*, "Regulation of CXCR4 expression in human mesenchymal stem cells by cytokine treatment: role in homing efficiency in NOD/SCID mice.," *Haematologica*, vol. 92, no. 7, pp. 897–904, Jul. 2007.

[235] M. E. Bernardo and W. E. Fibbe, "Mesenchymal Stromal Cells: Sensors and Switchers of Inflammation," *Cell Stem Cell*, vol. 13, no. 4, pp. 392–402, Oct. 2013.

[236] R. S. Waterman, S. L. Tomchuck, S. L. Henkle, and A. M. Betancourt, "A new mesenchymal stem cell (MSC) paradigm: polarization into a pro-inflammatory MSC1 or an Immunosuppressive MSC2 phenotype.," *PLoS One*, vol. 5, no. 4, p. e10088, Apr. 2010.

[237] B. Annabi *et al.*, "Hypoxia Promotes Murine Bone-Marrow-Derived Stromal Cell Migration and Tube Formation," *Stem Cells*, vol. 21, no. 3, pp. 337–347, May 2003.

[238] T. Kinnaird *et al.*, "Marrow-Derived Stromal Cells Express Genes Encoding a Broad Spectrum of

Arteriogenic Cytokines and Promote In Vitro and In Vivo Arteriogenesis Through Paracrine Mechanisms," *Circ. Res.*, vol. 94, no. 5, pp. 678–685, Mar. 2004.

[239] J. Liu *et al.*, "Hypoxia pretreatment of bone marrow mesenchymal stem cells facilitates angiogenesis by improving the function of endothelial cells in diabetic rats with lower ischemia.," *PLoS One*, vol. 10, no. 5, p. e0126715, 2015.

[240] T. Lopatina *et al.*, "Adipose-Derived Stem Cells Stimulate Regeneration of Peripheral Nerves: BDNF Secreted by These Cells Promotes Nerve Healing and Axon Growth De Novo," *PLoS One*, vol. 6, no. 3, p. e17899, Mar. 2011.

[241] M. Kendirci, L. Trost, B. Bakondi, M. J. Whitney, W. J. G. Hellstrom, and J. L. Spees, "Transplantation of Nonhematopoietic Adult Bone Marrow Stem/Progenitor Cells Isolated by p75 Nerve Growth Factor Receptor Into the Penis Rescues Erectile Function in a Rat Model of Cavernous Nerve Injury," *J. Urol.*, vol. 184, no. 4, pp. 1560–1566, Oct. 2010.

[242] A. Cselenyák, E. Pankotai, E. M. Horváth, L. Kiss, and Z. Lacza, "Mesenchymal stem cells rescue cardiomyoblasts from cell death in an in vitro ischemia model via direct cell-to-cell connections," *BMC Cell Biol.*, vol. 11, no. 1, p. 29, Dec. 2010.

[243] F. Tögel, K. Weiss, Y. Yang, Z. Hu, P. Zhang, and C. Westenfelder, "Vasculotropic, paracrine actions of infused mesenchymal stem cells are important to the recovery from acute kidney injury," *Am. J. Physiol. Physiol.*, vol. 292, no. 5, pp. F1626–F1635, May 2007.

[244] B. Parekkadan *et al.*, "Mesenchymal Stem Cell-Derived Molecules Reverse Fulminant Hepatic Failure," *PLoS One*, vol. 2, no. 9, p. e941, Sep. 2007.

[245] L. Timmers *et al.*, "Reduction of myocardial infarct size by human mesenchymal stem cell conditioned medium," *Stem Cell Res.*, vol. 1, no. 2, pp. 129–137, Jun. 2008.

[246] M. K. Haahr *et al.*, "Safety and Potential Effect of a Single Intracavernous Injection of Autologous Adipose-Derived Regenerative Cells in Patients with Erectile Dysfunction Following Radical Prostatectomy: An Open-Label Phase I Clinical Trial," *EBioMedicine*, vol. 5, pp. 204–210, Mar. 2016.

[247] "REGULATION (EC) No 1394/2007 OF THE EUROPEAN PARLIAMENT AND OF THE COUNCIL of 13 November 2007 on advanced therapy medicinal products and amending Directive 2001/83/EC and Regulation (EC) No 726/2004 (Text with EEA relevance)."

[248] S. K. Kang, I. S. Shin, M. S. Ko, J. Y. Jo, and J. C. Ra, "Journey of Mesenchymal Stem Cells for Homing: Strategies to Enhance Efficacy and Safety of Stem Cell Therapy," *Stem Cells Int.*, vol. 2012, pp. 1–11, Jun. 2012.

[249] R. Yiou *et al.*, "Safety of Intracavernous Bone Marrow-Mononuclear Cells for Postradical Prostatectomy Erectile Dysfunction: An Open Dose-Escalation Pilot Study," *Eur. Urol.*, vol. 69, no. 6, pp. 988–991, Jun. 2016.

[250] T. Freyman *et al.*, "A quantitative, randomized study evaluating three methods of mesenchymal stem cell delivery following myocardial infarction," *Eur. Heart J.*, vol. 27, no. 9, pp. 1114–1122, May 2006.

[251] R. Harrison, H. Markides, R. H. Morris, P. Richards, A. J. El Haj, and V. Sottile, "Autonomous magnetic labelling of functional mesenchymal stem cells for improved traceability and spatial control in cell therapy applications," *J. Tissue Eng. Regen. Med.*, vol. 11, no. 8, pp. 2333–2348, Aug. 2017.

[252] H. Markides, O. Kehoe, R. H. Morris, and A. J. El Haj, "Whole body tracking of

superparamagnetic iron oxide nanoparticle-labelled cells – a rheumatoid arthritis mouse model," *Stem Cell Res. Ther.*, vol. 4, no. 5, p. 126, Oct. 2013.

[253] H. Markides *et al.*, "Ex vivo MRI cell tracking of autologous mesenchymal stromal cells in an ovine osteochondral defect model," *Stem Cell Res. Ther.*, vol. 10, no. 1, p. 25, Dec. 2019.

[254] B. B. Chin, Y. Nakamoto, J. W. M. Bulte, M. F. Pittenger, R. Wahl, and D. L. Kraitchman, "111In oxine labelled mesenchymal stem cell SPECT after intravenous administration in myocardial infarction.," *Nucl. Med. Commun.*, vol. 24, no. 11, pp. 1149–54, Nov. 2003.

[255] S. K. Chakraborty *et al.*, "Cholera Toxin B Conjugated Quantum Dots for Live Cell Labeling," *Nano Lett.*, vol. 7, no. 9, pp. 2618–2626, Sep. 2007.

[256] B. N. Brown, D. Mani, A. L. Nolfi, R. Liang, S. D. Abramowitch, and P. A. Moalli, "Characterization of the host inflammatory response following implantation of prolapse mesh in rhesus macaque," *Am. J. Obstet. Gynecol.*, vol. 213, no. 5, p. 668.e1-668.e10, Nov. 2015.

[257] R. Liang *et al.*, "Extracellular matrix regenerative graft attenuates the negative impact of polypropylene prolapse mesh on vagina in rhesus macaque," *Am. J. Obstet. Gynecol.*, vol. 216, no. 2, p. 153.e1-153.e9, Feb. 2017.

[258] M. T. Wolf *et al.*, "Polypropylene surgical mesh coated with extracellular matrix mitigates the host foreign body response," *J. Biomed. Mater. Res. Part A*, vol. 102, no. 1, pp. 234–246, Jan. 2014.

[259] X. Li *et al.*, "Characterizing the ex vivo mechanical properties of synthetic polypropylene surgical mesh.," *J. Mech. Behav. Biomed. Mater.*, vol. 37, pp. 48–55, Sep. 2014.

[260] S. L. Edwards, J. A. Werkmeister, A. Rosamilia, J. A. M. Ramshaw, J. F. White, and C. E. Gargett, "Characterisation of clinical and newly fabricated meshes for pelvic organ prolapse repair," *J. Mech. Behav. Biomed. Mater.*, vol. 23, pp. 53–61, Jul. 2013.

[261] S. Roman, N. Mangir, L. Hympanova, C. R. Chapple, J. Deprest, and S. MacNeil, "Use of a simple in vitro fatigue test to assess materials used in the surgical treatment of stress urinary incontinence and pelvic organ prolapse," *Neurourol. Urodyn.*, Sep. 2018.

[262] M. M. Zimkowski, M. E. Rentschler, J. Schoen, B. A. Rech, N. Mandava, and R. Shandas, "Integrating a novel shape memory polymer into surgical meshes decreases placement time in laparoscopic surgery: An *in vitro* and acute *in vivo* study," *J. Biomed. Mater. Res. Part A*, vol. 101A, no. 9, pp. 2613–2620, Sep. 2013.

[263] S. Velayudhan, D. Martin, and J. Cooper-White, "Evaluation of dynamic creep properties of surgical mesh prostheses--uniaxial fatigue.," *J. Biomed. Mater. Res. B. Appl. Biomater.*, vol. 91, no. 1, pp. 287–96, Oct. 2009.

[264] H. Krause and J. Goh, "Sheep and rabbit genital tracts and abdominal wall as an implantation model for the study of surgical mesh," *J. Obstet. Gynaecol. Res.*, vol. 35, no. 2, pp. 219–224, Apr. 2009.

[265] D. Thomas, M. Demetres, J. T. Anger, and B. Chughtai, "Histologic Inflammatory Response to Transvaginal Polypropylene Mesh: A Systematic Review," *Urology*, vol. 111, pp. 11–22, Jan. 2018.

[266] L. M. Pierce, M. A. Grunlan, Y. Hou, S. S. Baumann, T. J. Kuehl, and T. W. Muir, "Biomechanical properties of synthetic and biologic graft materials following long-term implantation in the rabbit abdomen and vagina," *Am. J. Obstet. Gynecol.*, vol. 200, no. 5, p. 549.e1-549.e8, May 2009.

[267] L. N. Otto, O. D. Slayden, A. L. Clark, and R. M. Brenner, "The rhesus macaque as an animal model for pelvic organ prolapse," *Am. J. Obstet. Gynecol.*, vol. 186, no. 3, pp. 416–421, Mar. 2002.

[268] P. McCulloch, J. Barkun, A. Sedrakyan, and IDEAL Collaboration, "Implantable device regulation in Europe," *Lancet*, vol. 380, no. 9843, p. 729, Aug. 2012.

[269] "Regulatory framework | Internal Market, Industry, Entrepreneurship and SMEs." [Online]. Available: https://ec.europa.eu/growth/sectors/medical-devices/regulatory-framework_en#new_regulations. [Accessed: 06-Feb-2019].

[270] A. Sedrakyan, B. Campbell, J. G. Merino, R. Kuntz, A. Hirst, and P. McCulloch, "IDEAL-D: a rational framework for evaluating and regulating the use of medical devices," *BMJ*, p. i2372, Jun. 2016.

Appendices

Appendix I. Confirmation of PhD scholarship grant

Rosetrees Trust

Supporting the best in medical research

Our Ref: A1073

1 March 2016

Professor Sheila MacNeil
Tissue Engineering Group
The Kroto Research Institute
North Campus
Broad Lane
Sheffield S3 7HQ

By Email

Dear Professor MacNeil

Re: **Research project on developing materials which integrate well into the patient's pelvic floor for stress urinary incontinence and pelvic organ prolapse, by Naside Mangir.**

Thank you for sending the proposal for the above project. I am pleased to inform you that the Trustees have agreed to support this PhD studentship with a grant of £24,500 p.a. for two years, in total £49,000, as requested in your application.

The grant is subject to the Conditions of Grant attached to this letter, and we will need your institution's acceptance of these before the grant can commence. We also require your prior written confirmation that with Rosetrees' commitment the project is fully funded and is ready to start.

Please note the following key information on the separate page overleaf.

Please don't hesitate to contact my colleague Ingrida if you need to discuss anything, otherwise we look forward to your reply.

Yours sincerely

RICHARD MILLER
OPERATIONS MANAGER

Appendix II. Confirmation of research scholarship funding

THE UROLOGY FOUNDATION

Naside Mangir
36 Ashton Point
64 Upper Allen Street
Sheffield
S3 7GN

20 April 2016

Dear Naside,

Re: The Urology Foundation - Research Scholarship Applications 2016/17

Project title: *Developing pelvic floor repair materials which can stimulate ingrowth of new blood vessels after implantation.*

Thank you for your application to The Urology Foundation Research Scholarship Programme for funding for the above research project. This year, once again, the quality of the applications was extremely high. After a review that, for the first time, included your pitch presentation, I am very pleased to advise you that the Scientific and Education Committee recommended your project to the Board of Trustees for funding and received approval. It has been agreed to offer you the funding requested of £48,000.

Please write to The Urology Foundation within 2 weeks to confirm acceptance of the award, email is acceptable. In the acceptance, indicate the date on which the funding period will begin and please supply the requested lay summary. Please also complete and return all of the enclosed forms.

Approximately one month prior to the start date, the Foundation will remit payment (via BACS) to cover the first 9 months of funding i.e. 75% of the total final agreed grant, **subject to receipt of an invoice from your institution.** Payment of the final 25% of the grant will be contingent upon us receiving a satisfactory report (500-1000 words max) on your research project findings and a list of any associated publications where relevant.

Please see the attached document 'The Urology Foundation – Research Scholarship Terms and Conditions' for further conditions that apply.

On behalf of the Scientific and Education Committee and the Board of Trustees I would like to congratulate you on your achievement.

243

Kind regards
Yours sincerely

Professor John D Kelly MD FRCS (Urol)
Chairman Scientific and Education Committee
Copy: Professor John Kelly, UCL
        Louise de Winter, TUF

Enclosures:
- Acceptance of Funding Form
- Funding Payment Details Form
- Terms and Conditions
- Report Template

Appendix III. Other sources of funding

Sheffield Teaching Hospitals **NHS**

NHS Trust

Urology Research, J Floor
Royal Hallamshire Hospital
Glossop Road
Sheffield S10 2JF
Tel/Fax: (0114) 2797841
Email: c.r.chapple@shef.ac.uk

Royal Hallamshire Hospital
Glossop Road
Sheffield S10 2JF

Tel 0114 271 1900 Fax 0114 271 1901

Faculty of Engineering
Human Resources
University of Sheffield
Arts Tower
Western Bank
Sheffield, S10 2 TN

23rd June 2017

To whom it concerns Re: Dr Naside Mangir

I writing to confirm that Naside Mangir is a urologist trained in Turkey who came to work with Prof Sheila MacNeil and myself in 2013 to do laboratory-based research related to the problems of stress urinary incontinence and pelvic organ prolapse.
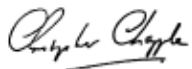She is a very gifted clinician intent on developing an academic career and she obtained funding to do this through the European Urology Association Scholarship Programme. She proved very able and very committed and also undertook her UK clinical registration with the General Medical Council (GMC) in 2016.

She then secured some funding from the Rosetrees foundation to undertake a PhD and she is now registered for a PhD degree with the University of Sheffield under the supervision of Prof Sheila MacNeil and myself.

I can confirm that I fully support her towards completion of her PhD and that I will be providing the extra funds necessary for her to complete her PhD on a staff candidate basis part-time from August 2017 to December 2018.

I am happy to provide any more information that may be required.

With best wishes and kind regards,

Prof Christopher Chapple, BSc, MD, FRCS (Urol), FEBU, DHC
Consultant Urological Surgeon, Royal Hallamshire Hospital
Honorary Professor of Urology, University of Sheffield
Visiting Professor of Urology, Sheffield Hallam University
Secretary General, European Association of Urology